frontiers | Research Topics

Predictive biomarkers for systemic or combination therapy in unresectable hepatocellular carcinoma

Edited by
Xiong Chen, Lujun Shen and Wenyu Lin

Published in
Frontiers in Oncology

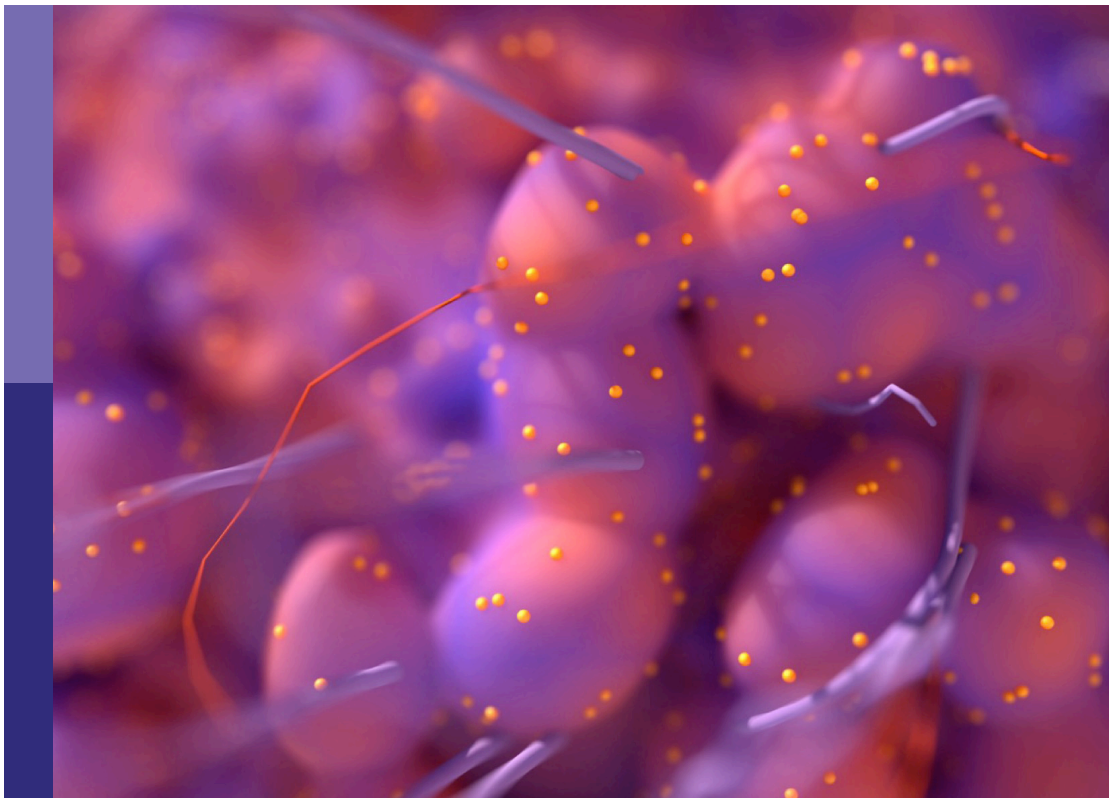

ISSN 1664-8714
ISBN 978-2-8325-3037-5
DOI 10.3389/978-2-8325-3037-5

About Frontiers

Frontiers is more than just an open access publisher of scholarly articles: it is a pioneering approach to the world of academia, radically improving the way scholarly research is managed. The grand vision of Frontiers is a world where all people have an equal opportunity to seek, share and generate knowledge. Frontiers provides immediate and permanent online open access to all its publications, but this alone is not enough to realize our grand goals.

Frontiers journal series

The Frontiers journal series is a multi-tier and interdisciplinary set of open-access, online journals, promising a paradigm shift from the current review, selection and dissemination processes in academic publishing. All Frontiers journals are driven by researchers for researchers; therefore, they constitute a service to the scholarly community. At the same time, the *Frontiers journal series* operates on a revolutionary invention, the tiered publishing system, initially addressing specific communities of scholars, and gradually climbing up to broader public understanding, thus serving the interests of the lay society, too.

Dedication to quality

Each Frontiers article is a landmark of the highest quality, thanks to genuinely collaborative interactions between authors and review editors, who include some of the world's best academicians. Research must be certified by peers before entering a stream of knowledge that may eventually reach the public - and shape society; therefore, Frontiers only applies the most rigorous and unbiased reviews. Frontiers revolutionizes research publishing by freely delivering the most outstanding research, evaluated with no bias from both the academic and social point of view. By applying the most advanced information technologies, Frontiers is catapulting scholarly publishing into a new generation.

What are Frontiers Research Topics?

Frontiers Research Topics are very popular trademarks of the *Frontiers journals series*: they are collections of at least ten articles, all centered on a particular subject. With their unique mix of varied contributions from Original Research to Review Articles, Frontiers Research Topics unify the most influential researchers, the latest key findings and historical advances in a hot research area.

Find out more on how to host your own Frontiers Research Topic or contribute to one as an author by contacting the Frontiers editorial office: frontiersin.org/about/contact

Predictive biomarkers for systemic or combination therapy in unresectable hepatocellular carcinoma

Topic editors

Xiong Chen — Department of Oncology, Nanjing General Hospital of Nanjing Military Command, China

Lujun Shen — Sun Yat-sen University Cancer Center (SYSUCC), China

Wenyu Lin — Massachusetts General Hospital, Harvard Medical School, United States

Citation

Chen, X., Shen, L., Lin, W., eds. (2023). *Predictive biomarkers for systemic or combination therapy in unresectable hepatocellular carcinoma*. Lausanne: Frontiers Media SA. doi: 10.3389/978-2-8325-3037-5

Table of contents

frontiers | Frontiers in Oncology

TYPE Original Research
PUBLISHED 04 January 2023
DOI 10.3389/fonc.2022.1094104

OPEN ACCESS

EDITED BY
Lujun Shen,
Sun Yat-sen University Cancer Center (SYSUCC), China

REVIEWED BY
Mingda Wang,
Eastern Hepatobiliary Surgery Hospital, China
Le-Qun Li,
Guangxi Medical University, China
Cheng-Cheng Zhang,
Army Medical University, China

*CORRESPONDENCE
Nan-Ya Wang
wangny@jlu.edu.cn

†These authors have contributed equally to this work

SPECIALTY SECTION
This article was submitted to Gastrointestinal Cancers: Hepato Pancreatic Biliary Cancers, a section of the journal Frontiers in Oncology

RECEIVED 09 November 2022
ACCEPTED 12 December 2022
PUBLISHED 04 January 2023

CITATION
Hou G, Liu B, Fan Z-Q, Li C, Zhang J-P, Guo Y-H, Zhang R-Y, Zheng Y, Zhu H and Wang N-Y (2023) Association between early response of alpha-fetoprotein and treatment efficacy of systemic therapy for advanced hepatocellular carcinoma: A multicenter cohort study from China. *Front. Oncol.* 12:1094104. doi: 10.3389/fonc.2022.1094104

Association between early response of alpha-fetoprotein and treatment efficacy of systemic therapy for advanced hepatocellular carcinoma: A multicenter cohort study from China

Gang Hou[1†], Bo Liu[1†], Zhong-Qi Fan[2], Chao Li[3], Jian-Ping Zhang[4], Yan-Hui Guo[5], Ru-Yi Zhang[6], Yi Zheng[7], Hong Zhu[8] and Nan-Ya Wang[1*]

[1]Cancer Center, First Hospital of Jilin University, Changchun, Jilin, China, [2]Department of Hepatobiliary and Pancreatic Surgery, General Surgery Center, First Hospital of Jilin University, Changchun, Jilin, China, [3]Department of Hepatobiliary Surgery, Eastern Hepatobiliary Surgery Hospital, Second Military Medical University, Shanghai, China, [4]Health Examination Center, Changchun Central Hospital, Changchun, Jilin, China, [5]Department of hematology and oncology, Meihekou Central Hospital, Meihekou Jilin, China, [6]Department of Medical Oncology, Key Laboratory of Cancer Prevention and Intervention, The First Affiliated Hospital, Zhejiang University School of Medicine, Ministry of Education, Hangzhou, China, [7]Department of Medical Oncology, The First Affiliated Hospital, Zhejiang University School of Medicine, Hangzhou, China, [8]Department of Medical Oncology, The First Affiliated Hospital of Soochow University, Suzhou, Jiangsu, China

Background: Alpha-fetoprotein (AFP) is a well-identified biomarker in hepatocellular carcinoma (HCC). However, only limited AFP-related studies have evaluated its early response to systemic therapy. This study was performed with the aim of assessing the value of early AFP response in predicting overall survival (OS) and progression-free survival (PFS) in advanced HCC patients receiving systemic therapy.

Methods: This cohort study included HCC patients with baseline AFP ≥ 200 ng/ml and no prior treatment history. A > 20% decline in the serum AFP level from baseline to the first follow-up (i.e., 4~6 weeks after treatment) was defined as an early AFP response. Patient demographic information, clinical characteristics, radiological response, and survival rates were compared between patients with early AFP response and patients without early AFP response. We further utilized multivariate Cox regression to seek characteristics related to OS and PFS.

Results: Among 154 patients, 69 patients (44.8%) showed an early AFP response. The disease control rate (76.8 *vs*. 54.1%; P = 0.003) and objective response rate (38.4 *vs*. 11.8%; P = 0.001) were significantly higher in patients

with an early AFP response. By performing multivariate analysis, early AFP response remained a prognostic factor for longer PFS (HR 0.546; 95% CI 0.371-0.804; P = 0.002) and longer OS (HR 0.529; 95% CI 0.335-0.834; P = 0.006).

Conclusion: An early AFP response is correlated with longer overall survival and progression-free survival for advanced HCC patients receiving systemic therapy. Moreover, an early AFP response is an independent prognostic factor for longer OS and PFS.

KEYWORDS

hepatocellular carcinoma, AFP response, systemic therapy, targeted therapy, immune-based combination therapy

1 Introduction

Hepatocellular carcinoma (HCC) is a prevalent malignancy derived from liver cells and poses a tremendous threat to global health (1). Most patients are already in advanced stages when first diagnosed (2). Patients diagnosed with advanced HCC are not eligible for curative surgery. Systemic therapy is the main treatment for patients with advanced HCC. Recently, with the emergence of targeted agents and immune-based combination therapy, the systemic therapeutic options for HCC have expanded (2–5). Sorafenib, lenvatinib, and atezolizumab combined with bevacizumab have been recommended as first-line systemic therapies (6). However, there are several limitations. The clinical benefit varies widely among patients. Some patients have long-term benefits, while others develop primary resistance. Adverse reactions also limit the clinical application. There is an urgent need to find better biomarkers to assess the treatment response in the early stage.

Serum biomarkers are noninvasive, labor-saving, and inexpensive tools for disease prediction, diagnosis, and monitoring. Alpha-fetoprotein (AFP) is a glycoprotein that is widely used in HCC detection, screening, monitoring, and prognosis evaluation (7). Almost 70% of HCC patients show an elevated AFP level in their serum (8). Overexpression of baseline AFP is considered an indicator of poor oncological biology, burden, and survival (9).

In addition to the prognostic impact of baseline biomarker levels, the response of biomarkers to malignant tumors after treatment is increasingly recognized as an effective tool to assess treatment efficacy and predict tumor response (10). Previous studies of patients with HCC have demonstrated early AFP response in transcatheter arterial chemoembolization, chemotherapy, and radiotherapy (3, 11–29). However, due to the limited published data on AFP in newly developed immune-based combination therapy and targeted agents, a small number of studies have assessed the value of early AFP response in advanced HCC patients receiving systemic therapy.

The present study was performed with the aim of investigating whether an early AFP response is associated with systemic therapy in advanced HCC patients by utilizing a multicenter database. We aimed to provide clinicians with data on treatment efficacy monitoring and planning for decision-making.

Abbreviations: HCC, Hepatocellular carcinoma; AFP, Alpha-fetoprotein; ECOG, Eastern Cooperative Oncology Group; ALBI, albumin-bilirubin; CT, Computed tomography; MRI, Magnetic resonance imaging; OS, Overall survival; PFS, progression-free survival; ORR, objective response rate; CR, complete response; PR, partial response; DCR, disease control rate; SD, stable disease; HR, Hazard ratio; 95% CI, 95 percent confidence interval.

2 Patients and methods

2.1 Patient selection

We conducted this multicenter study between May 2018 and May 2021 in seven hospitals. These seven medical centers were the First Hospital of Jilin University, Eastern Hepatobiliary Surgery Hospital, Meihekou Central Hospital, Changchun Central Hospital, The First Affiliated Hospital, Zhejiang University School of Medicine, and the First Affiliated Hospital of Soochow University. We retrospectively analyzed 450 HCC patients receiving lenvatinib, sorafenib, or any immune-based combination therapy (e.g., sintilimab, camrelizumab, toripalimab, et al). Sorafenib, lenvatinib, apatinib, and regorafenib are combined with immunotherapy. We included advanced HCC patients with a baseline AFP level ≥ 200 ng/ml and a duration of medical interventions ≥ 1 month. All patients signed informed consent during hospital admission. The study was conducted in accordance with the Declaration of

Helsinki and the Ethical Guidelines for Clinical Studies. The study was approved by the Institutional Review Board of the First Hospital of Jilin University (IRB number 032-06).

2.2 Baseline characteristics

The baseline characteristics included sex, age, comorbidities, Eastern Cooperative Oncology Group (ECOG) performance status, etiology of liver disease, cirrhosis, portal hypertension, international normalized ratio, total bilirubin, albumin-bilirubin (ALBI) grade, alanine transaminase, aspartate transaminase, albumin, and Child-Pugh grade. Comorbidities included hypertension, diabetes mellitus, cardiovascular disease, chronic obstructive pulmonary disease, and renal dysfunction. Portal hypertension was defined as the presence of either splenomegaly with a decreased platelet count ($\leq 100 \times 10^9$/L) or esophageal varicose veins. Tumor-related characteristics included baseline AFP, maximum tumor size, tumor number, macrovascular invasion, and extrahepatic spread.

2.3 Patient follow-up

The follow-up strategies were consistent in all participating hospitals. Our strategies included detecting the concentration of serum AFP and performing contrast-enhanced computed tomography (CT) or magnetic resonance imaging (MRI) on a regular basis. The first follow-up evaluation was performed 4~6 weeks after treatment. After the first follow-up, the strategies were performed every 2-3 months. As HCC progression was suspected, contrast-enhanced CT or MRI, chest CT, bone scan, or positron emission tomography were performed as clinically indicated. Our last follow-up was concluded on May 30, 2021.

2.4 Biomarker response of serum AFP

Patients with baseline AFP ≥ 200 ng/ml were enrolled in the present study. The first follow-up of AFP was performed 4 to 6 weeks after treatment. In our study, we defined patients with a > 20% decrease in serum AFP level at the first follow-up compared with baseline as having an early AFP response. Correspondingly, patients whose serum AFP levels failed to reach the abovementioned levels were defined as no AFP responders.

2.5 Clinical outcomes

The primary clinical outcomes of this study were overall survival (OS) and progression-free survival (PFS). PFS refers to the time from the start of treatment to tumor progression or death. OS refers to the interval from study initiation to either the date of death or the date of the last follow-up. We used enhanced CT or MRI to perform radiological assessment in accordance with RECIST v1.1 criteria. The objective response rate (ORR) is the total proportion of patients with complete response (CR) or partial response (PR). The disease control rate (DCR) is the sum of CR, PR, and stable disease (SD).

2.6 Statistical analysis

Statistical analyses were performed using SPSS software version 25.0 (SPSS, Chicago, IL, USA). The patient characteristics between the early AFP response and no response groups were compared using the $\chi 2$ test for continuous variables or Fisher's exact test for categorical variables. Early AFP response was defined as a > 20% decrease in serum AFP levels at the first follow-up. Those patients who died before the first follow-up were excluded. The OS and PFS rates were calculated and compared using the Kaplan-Meier method generated by the log-rank test. Univariate and multivariate Cox regression analyses were performed to identify independent predictors associated with poor OS and PFS, with hazard ratios (HRs) and 95 percent confidence interval (95% CIs). Those variables significant at $P < 0.1$ in the univariable analyses were entered into the multivariable competing-risks regression models. A two-tailed P value < 0.05 was considered to be statistically significant.

3 Results

3.1 Clinical characteristics

A total of 450 patients with advanced HCC were screened. We excluded patients whose missing AFP data within 1 week before treatment (n = 32), baseline AFP level < 200 ng/ml (n = 133), death within 30 days after treatment (n = 11), unavailable AFP level results at the first follow-up (n = 21), and missing data on important prognostic variables (n = 5). Ultimately, 154 patients who met the inclusion criteria were enrolled in this retrospective cohort study (Figure 1). According to the definition of early AFP response, we divided all patients into two groups: 69 (44.8%) patients were in the early AFP response group, and 85 (55.2%) were in the no AFP response group. Demographic and tumor-related characteristics were virtually balanced in the two groups. The median follow-up time is 10.7 months (range, 1.9 to 31.6 months). 23 (15.8%) patients had a dose reduction and 9 (6.2%) had a treatment interruption due to AEs. More detailed information is shown in Table 1.

3.2 Correlation of early AFP response with radiologic response

As shown in Table 2, we assessed the treatment efficacy in the two groups by RECIST ver1.1. In patients with an early AFP

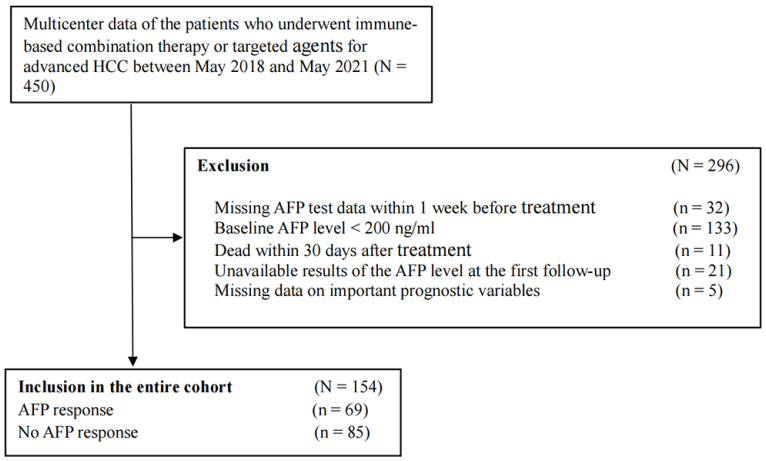

FIGURE 1
Flow chart of the cohort.

response, 1 (1.4%) patient experienced CR, and 23 (33.3%) patients experienced PR. No patients underwent CR and only 10 (11.8%) patients underwent PR in the group without an early AFP response. Regarding the SD rate, a difference between the two groups was not apparent: 42.0% in the group with an early AFP response and 42.4% in the group without an early AFP response. The PD rate in the early AFP response group was 23.2%, which was lower than the 45.9% in the no AFP response group. Of note, patients in the group with an early AFP response had a higher ORR (38.4% *vs*. 11.8%, $P = 0.001$) and DCR (76.8% *vs*. 54.1%, $P = 0.003$) than the group without an early AFP response.

3.3 Survival analyses of OS and PFS

The OS and PFS curves between the entire cohorts of patients with early AFP response and no AFP response are demonstrated in Figures 2 and 3, respectively. Compared with the no AFP response group, the early AFP response group had significantly improved OS ($P < 0.001$) and PFS ($P < 0.001$). Similar results of the OS and PFS rates with a significant difference were shown in the cohorts of patients with the targeted agents (Figures 4A, B, $P = 0.005$ and $P = 0.003$) and immune combination targeted therapy (Figures 4C, D, $P = 0.012$ and $P = 0.019$), respectively.

3.4 Univariate and multivariate analyses of OS and PFS

In univariate analysis of OS, we found that patients with ECOG performance status of 1 or 2 (HR, 1.949; 95% CI, 1.109-3.426; $P = 0.020$), early AFP response (HR, 0.507; 95% CI, 0.322-0.798; $P = 0.003$), aspartate transaminase (AST) > 40 U/L (HR, 1.748; 95% CI, 1.111-2.750; $P = 0.016$), Child-Pugh B (HR, 2.040; 95% CI, 1.173-3.548; $P = 0.012$), and multiple tumors (HR, 1.546; 95% CI, 0.923-2.588; $P = 0.098$) were likely to achieve longer OS. Adjusting for sex, age, comorbidities, and etiology of cancer, the multivariate analysis indicated that early AFP response (HR, 0.490; 95% CI, 0.308-0.780; $P = 0.003$) and ECOG performance status of 1 or 2 (HR, 2.201; 95% CI, 1.240-3.907; $P = 0.007$) were independent prognostic factors associated with longer OS (Table 3).

The univariate analysis of PFS revealed that the odds of longer OS were high in the patients with ECOG performance status of 1 or 2 (HR, 1.554; 95% CI, 1.036-2.330; $P = 0.033$), early AFP response (HR, 0.538; 95% CI, 0.366-0.791; $P = 0.002$), AST > 40 U/L (HR, 1.865; 95% CI, 1.267-2.745; $P = 0.002$), and multiple tumors (HR, 1.432; 95% CI, 0.937-2.188; $P = 0.097$). By adjusting for sex, age, comorbidities, and etiology of cancer, the multivariate analysis indicated that early AFP response (HR, 0.501; 95% CI, 0.339-0.742; $P = 0.001$), ECOG performance status of 1 or 2 (HR, 1.677; 95% CI, 1.100-2.557; $P = 0.016$) and AST > 40 U/L (HR, 1.933; 95% CI, 1.309-2.855; $P = 0.001$) were independent prognostic factors for longer PFS (Table 4).

4 Discussion

With the therapeutic techniques constantly advancing, immune-based combination therapy and targeted agents have attracted increasing attention as effective systemic therapy methods. Further exploration of biomarkers associated with clinical efficacy and survival benefits is urgent. AFP is an available serum biomarker that is routinely used in clinical

TABLE 1 Comparisons of the patients' baseline characteristics.

Variables	Total (N=154)	Early AFP Response (N=69)	No AFP Response (N=85)	*P*
Treatment				
Lenvatinib	64 (41.6)	25 (39.1)	39 (60.9)	0.125
sorafenib	35 (22.7)	12 (34.3)	23 (65.7)	
sintilimab combination therapy	28 (18.2)	17 (60.7)	11 (39.3)	
camrelizumab combination therapy	18 (11.7)	11 (61.1)	7 (38.9)	
toripalimab combination therapy	9 (5.8)	4 (44.4)	5 (55.6)	
Sex, male	136 (88.3)	59 (43.4)	77 (56.6)	0.329
Age > 60 years old	52 (33.8)	24 (46.2)	28 (53.8)	0.810
Comorbidities	32 (20.8)	14 (43.8)	18 (56.2)	0.893
ECOG performance status				
0	48 (31.2)	18 (37.6)	30 (62.4)	0.220
1-2	106 (68.8)	51 (48.1)	55 (51.9)	
Etiology of liver disease				
HBV (+) and/or HCV (+)	109 (70.8)	53 (48.6)	56 (51.4)	0.138
Others	45 (29.2)	16 (35.6)	29 (64.4)	
Cirrhosis	117 (76)	56 (47.9)	61 (52.1)	0.175
Portal hypertension	55 (35.7)	24 (43.6)	31 (56.4)	0.828
Baseline AFP, ng/ml*	1210.0 (668.1,5305.8)	1000.0 (647.7,4651.0)	2000.0 (681.8,10809.9)	0.511
INR,s*	1.04 (0.98,1.12)	1.03 (0.98,1.12)	1.04 (0.99,1.14)	0.921
Total bilirubin, μmol/L*	20.0 (13.0,44.0)	19.0 (11.0,42.0)	20.0 (14.0,45.0)	0.610
Alanine transaminase, U/L*	30.0 (20.6,49.7)	30.0 (21.0,47.9)	32.4 (20.0,53.4)	0.528
Aspartate transaminase, U/L*	42.0 (27.0,66.0)	40.0 (25.6,66.4)	43.5 (28.5,63.8)	0.778
Albumin, g/L*	39.2 (34.8,41.6)	39.6 (36.6,42.1)	38.7 (34.0,40.8)	0.763
ALBI grade				
ALBI grade 1	60 (39.5)	30 (50.0)	30 (50.0)	0.300
ALBI grade 2	94 (61.0)	39 (41.5)	55 (58.5)	
Child-Pugh grade				
Child-Pugh grade A	126 (81.8)	60 (47.6)	66 (52.4)	0.136
Child-Pugh grade B	28 (18.2)	9 (32.1)	19 (67.9)	
Maximum tumor size > 5.0 cm	104 (67.5)	48 (46.2)	56 (53.8)	0.627
Multiple tumors	104 (67.5)	46 (44.2)	58 (55.8)	0.836
Gross vascular invasion	53 (34.4)	24 (45.3)	29 (54.7)	0.931
Extrahepatic spread	78 (50.6)	31 (39.7)	47 (60.3)	0.201

* Values are the median and interquartile range.
Abbreviations: AFP, alpha-fetoprotein; ALBI, albumin-bilirubin; ECOG, Eastern Cooperative Oncology Group; HBV, hepatitis B virus; HCV, hepatitis C virus; INR, international normalized ratio.

10.3389/fonc.2022.1094104

TABLE 2 Comparison of the efficacy between the patients with and without early AFP response.

	Total (N=154)	Early AFP Response (N=69)	No AFP Response (N=85)	*P*
RECIST v1.1				
Complete response (CR)	1 (0.6)	1 (1.4)	0 (0)	0.002
Partial response (PR)	33 (21.4)	23 (33.3)	10 (11.8)	
Stable disease (SD)	65 (42.2)	29 (42.0)	36 (42.4)	
Progressive disease (PD)	55 (35.7)	16 (23.2)	39 (45.9)	
Objective response rate (ORR)	34 (22.0)	24 (38.4)	10 (11.8)	0.001
Disease control rate (DCR)	99 (64.3)	53 (76.8)	46 (54.1)	0.003

practice in many regions of the world for HCC. However, studies utilizing AFP to predict treatment efficacy and survival benefit in systemic treatment for advanced HCC are limited. Our study analyzed advanced HCC patients with high AFP levels receiving systemic therapy. The patients with early AFP response had significantly longer OS ($P < 0.001$) and PFS ($P < 0.001$). By performing multivariate analysis, early AFP response was confirmed as a prognostic factor for both OS and PFS. In the present study, we further verified the role of early AFP response in predicting prognosis for advanced HCC patients receiving systemic therapy, which is consistent with published studies (11, 12, 18, 27).

As a well-identified biomarker, early AFP response has demonstrated incomparable predictive value in both systemic and locoregional therapies for HCC patients. However, these studies assessed early AFP response using different criteria. It is difficult to make a widely recognized, accurate, and clinically significant definition of early AFP response. On the one hand, choosing an appropriate baseline AFP value is crucial for clinicians. Some studies analyzed patients with baseline AFP ≥ 40 ng/ml (30). Some studies chose 20 ng/ml as the baseline (12). This is because AFP is not distinctive and specific for cancer diagnosis: serum AFP may not demonstrate elevated levels in approximately 30-40% of HCC patients, and AFP fluctuations are seen not only in HCC but also in chronic liver diseases caused by cirrhosis or chronic viral hepatitis (7). To rule out the interfering factors mentioned above, our study excluded patients whose AFP levels were positive but low (20-200 ng/mL) and negative (< 20 ng/mL). We also strictly set the baseline AFP level (≥ 200 ng/ml) to ensure higher specificity. For the analysis, a relatively high baseline was chosen to capture real changes related to HCC and minimize the effects of background sources and hospital changes on different tests. On the other hand, selecting a precise time point to measure serum AFP levels is also crucial for clinicians. In a recent study, the first follow-up choice was 7 days after treatment (31). Some studies detected serum AFP levels at 90 days after treatment, and another study was performed at 180 days (32–34). These

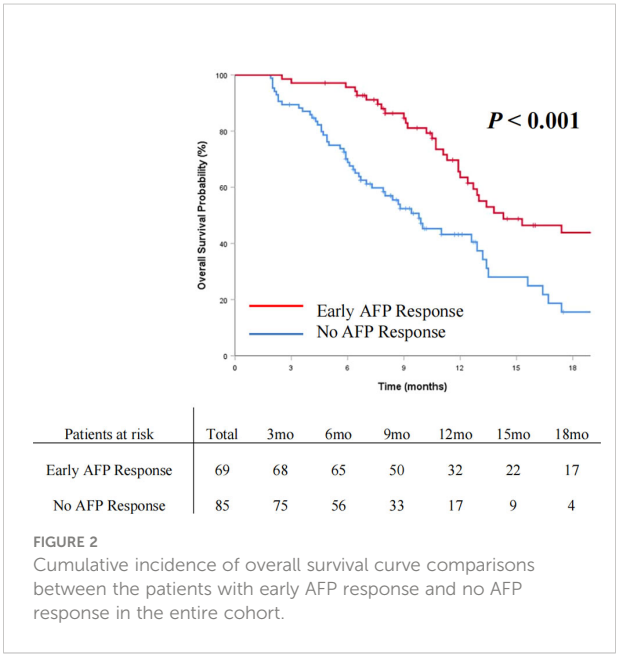

FIGURE 2
Cumulative incidence of overall survival curve comparisons between the patients with early AFP response and no AFP response in the entire cohort.

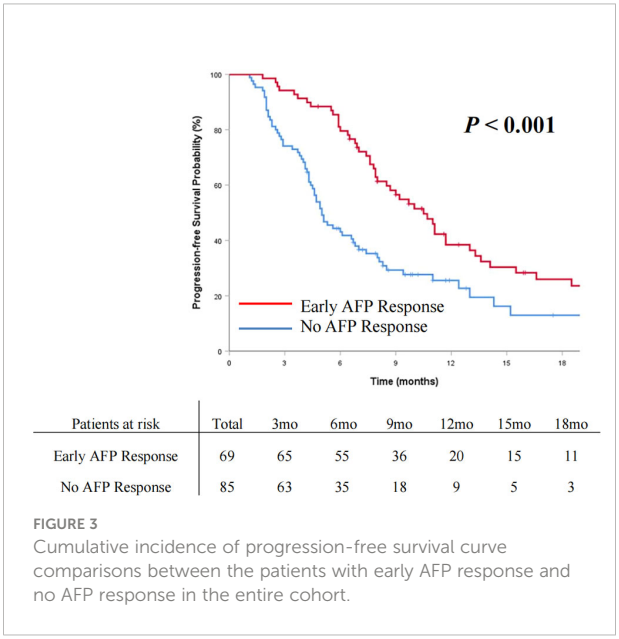

FIGURE 3
Cumulative incidence of progression-free survival curve comparisons between the patients with early AFP response and no AFP response in the entire cohort.

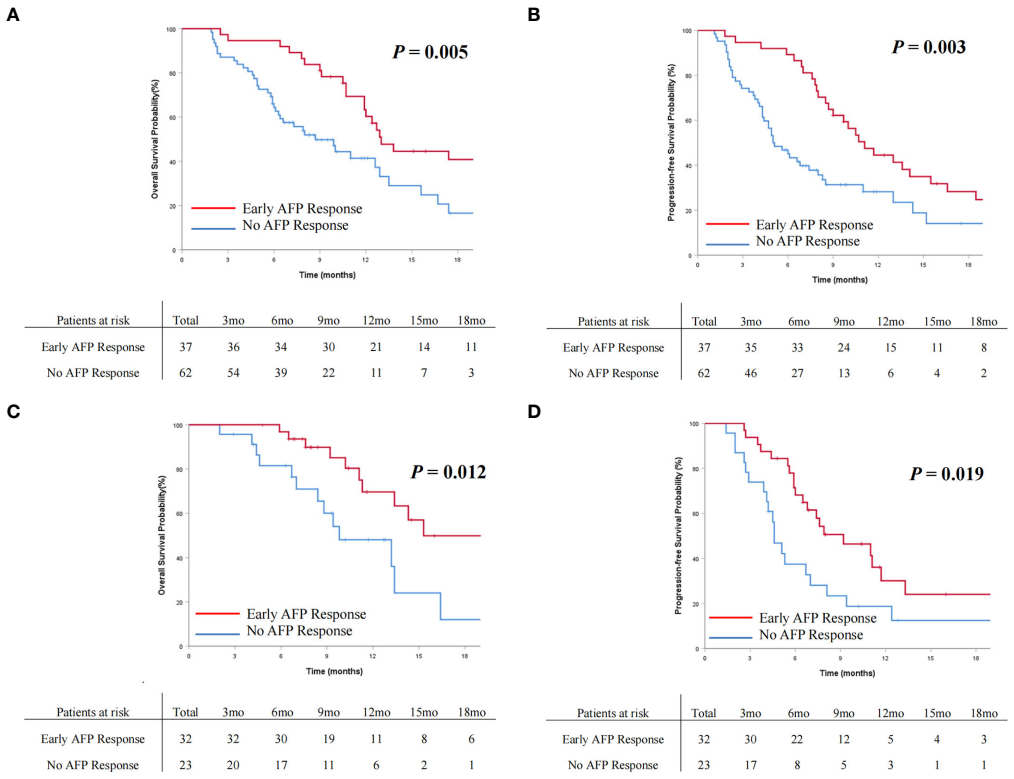

FIGURE 4
Cumulative incidence of overall survival **(A)** and progression-free survival **(B)** curves comparisons between the patients with AFP response and no AFP response in the targeted agents' cohort. Cumulative incidence of overall survival **(C)** and progression-free survival **(D)** curves comparisons between the patients with early AFP response and no AFP response in the immune combination targeted therapy cohort.

TABLE 3 Univariate and multivariate Cox regression analyses predicting overall survival.

Variables	Comparison	Univariable Analyses		Multivariate Analyses	
		HR (95% CI)	*P*	HR (95% CI)	*P*
Sex	Male *vs.* Female	1.366 (0.628-2.969)	0.432		
Age	≤ 60 *vs.* > 60 years	1.402 (0.894-2.199)	0.141		
Comorbidities	Yes *vs.* No	1.119 (0.661-1.896)	0.676		
ECOG performance status	1/2 *vs.* 0	1.949 (1.109-3.426)	0.020*	2.201 (1.240-3.907)	0.007
HBV (+) and/or HCV (+)	Yes *vs.* No	1.487 (0.909-2.434)	0.114		
Cirrhosis	Yes *vs.* No	1.187 (0.676-2.086)	0.550		
Portal hypertension	Yes *vs.* No	1.214 (0.762-1.936)	0.415		
Early AFP Response	Yes *vs.* No	0.507 (0.322-0.798)	0.003*	0.490 (0.308-0.780)	0.003
Baseline AFP	> 1000 *vs.* ≤ 1000 ng/ml	1.365 (0.871-2.139)	0.175		
Alanine transaminase	> 40 *vs.* ≤ 40 U/L	1.401 (0.897-2.187)	0.138		
Aspartate transaminase	> 40 *vs.* ≤ 40 U/L	1.748 (1.111-2.750)	0.016*	1.578 (0.972-2.561)	0.065
Albumin	≤ 35 *vs.* > 35 g/L	1.191 (0.753-1.882)	0.455		
ALBI	2 *vs.* 1	1.228 (0.783-1.824)	0.371		

(Continued)

TABLE 3 Continued

Variables	Comparison	Univariable Analyses		Multivariate Analyses	
		HR (95% CI)	*P*	HR (95% CI)	*P*
Child-Pugh	B *vs.* A	2.040 (1.173-3.548)	0.012*	1.660 (0.921-2.990)	0.092
Maximum tumor size	> 5.0 cm *vs.* ≤ 5.0 cm	1.126 (0.708-1.791)	0.617		
Multiple tumors	Multiple *vs.* Solitary	1.546 (0.923-2.588)	0.098*	1.648 (0.981-2.770)	0.059
Extrahepatic spread	Yes *vs.* No	1.184 (0.764-1.836)	0.450		

*Those variables found significant at P < 0.1 in the univariable analyses were entered into the multivariable Cox regression analyses.
AFP, alpha-fetoprotein; CI, confidence interval; ECOG, Eastern Cooperative Oncology Group; HBV, hepatitis B virus; HCV, hepatitis C virus; HR, hazard ratio; ORR, objective response rate; ALBI, albumin-bilirubin; BCLC, Barcelona Clinic Liver Cancer.

TABLE 4 Univariate and multivariate Cox regression analyses predicting progression-free survival.

Variables	Comparison	Univariable Analyses		Multivariate Analyses	
		HR (95% CI)	*P*	HR (95% CI)	*P*
Sex	Male *vs.* Female	0.954 (0.523-1.742)	0.879		
Age	≤ 60 *vs.* > 60 years	1.180 (0.798-1.743)	0.407		
Comorbidities	Yes *vs.* No	1.245 (0.786-1.974)	0.350		
ECOG performance status	1/2 *vs.* 0	1.554 (1.036-2.330)	0.033*	1.677 (1.100-2.557)	0.016
HBV (+) and/or HCV (+)	Yes *vs.* No	1.353 (0.896-2.043)	0.151		
Cirrhosis	Yes *vs.* No	1.243 (0.790-1.955)	0.346		
Portal hypertension	Yes *vs.* No	1.094 (0.738-1.621)	0.656		
Early AFP Response	Yes *vs.* No	0.538 (0.366-0.791)	0.002*	0.501 (0.339-0.742)	0.001
Baseline AFP	> 1000 *vs.* ≤ 1000 ng/ml	1.246 (0.853-1.821)	0.255		
Alanine transaminase	> 40 *vs.* ≤ 40 U/L	1.302 (0.886-1.195)	0.179		
Aspartate transaminase	> 40 *vs.* ≤ 40 U/L	1.865 (1.267-2.745)	0.002*	1.933 (1.309-2.855)	0.001
Albumin	≤ 35 *vs.* > 35 g/L	1.302 (0.886-1915)	0.179		
ALBI	2 *vs.* 1	1.293 (0.883-1.894)	0.187		
Child-Pugh	B *vs.* A	1.232 (0.754-2.035)	0.416		
Maximum tumor size	> 5.0 cm *vs.* ≤ 5.0 cm	1.111 (0.744-1.658)	0.607		
Multiple tumors	Multiple *vs.* Solitary	1.432 (0.937-2.188)	0.097*	1.409 (0.913-2.175)	0.121
Extrahepatic spread	Yes *vs.* No	1.244 (0.855-1.811)	0.254		

*Those variables found significant at P < 0.1 in the univariable analyses were entered into the multivariable Cox regression analyses.
AFP, alpha-fetoprotein; CI, confidence interval; ECOG, Eastern Cooperative Oncology Group; HBV, hepatitis B virus; HCV, hepatitis C virus; HR, hazard ratio; ORR, objective response rate; ALBI, albumin-bilirubin; BCLC, Barcelona Clinic Liver Cancer.

studies all drew a similar conclusion that early AFP response is independently related to the progression rate and overall survival rate after treatment of HCC. However, considering the half-life of AFP to be 5~7 days, 7 days seems too short, while 90 days or 180 days are too late to start early adjuvant treatments against progression. Therefore, in this analysis, the time period of 4-6 weeks after treatment was selected as the first follow-up.

In the present study, we found that there was a close correlation between early AFP response and imaging findings in most patients. The rates of ORR and DCR in the patients with early AFP response were significantly higher than those in

the patients with no AFP response (38.4% *vs*. 11.8%, $P = 0.001$, and 76.8% *vs*. 54.1%, $P = 0.003$). Our results are consistent with many previous studies. Chan et al. reported on the correlation between AFP response and the achievement of imaging response (12). Another study reported that patients with AFP response versus no response had a significantly higher ORR (68.4% *vs*. 7.1%; $P < 0.001$) and DCR (84.2% *vs*. 36.0%; $P = 0.009$) (35). Early AFP response may be considered a supplement or alternative to RECIST v1.1 to systemic therapy for HCC.

For several years, circulating tumor cells, microRNAs or DNAs have been used to predict accurate prediction and early detection of tumor progression. However, sophisticated technology and expensive costs limit their applicability. High AFP secreted by tumor cells is a feature of HCC. Once the tumor has progressed after treatment, more AFP will be produced, and the serum AFP levels will be elevated. The present study provides further proof of this theory. Clinicians may consider changing treatment regimens when tumor progression occurs.

There are some limitations to the present study. First, as a retrospective study, it has its intrinsic defects. Second, in addition to tumor response, changes in AFP may also be affected by cirrhosis or chronic viral hepatitis. Although we set a stricter baseline AFP level (200 ng/ml) to minimize the effects of background sources, further studies with long-term follow-up are still needed. Third, the generalizability of the study might be restricted to the Chinese population since most HCC patients in the present study had a history of HBV infection and related diseases. In contrast, HCC cases in the United States and Europe are mainly caused by HCV infection and overconsumption of alcohol. The study needs to be verified in different populations.

In conclusion, the present study revealed that an early AFP response may be applied as an indicator to predict survival and surveillance progression in patients with advanced HCC receiving targeted agents or immune-based combination therapy. For HCC patients with high AFP levels, an early AFP response is a noninvasive and practical alternative endpoint to assess the long-term tumor prognosis of patients. If an AFP response is not reached in the first follow-up, it is necessary to actively consider strengthening the frequency of examinations or changing the treatment plan in time.

Data availability statement

The raw data supporting the conclusions of this article will be made available by the authors, without undue reservation.

Ethics statement

The studies involving human participants were reviewed and approved by The Institutional Review Board of the First Hospital of Jilin University. The patients/participants provided their written informed consent to participate in this study.

Author contributions

GH and BL contributed equally to this work. Study design: N-YW, GH, and CL. Data collection and acquisition: GH, BL, Z-QF, CL, J-PZ, R-YZ, YZ, HZ, and N-YW. Manuscript preparation: GH and BL. Critical revision: N-YW. Final approval of manuscript: All authors. All authors contributed to the article and approved the submitted version.

Funding

Scientific Research Fund of Beijing Mutual Care Foundation.

Acknowledgments

The authors acknowledge the First Hospital of Jilin University, Eastern Hepatobiliary Surgery Hospital, Meihekou Central Hospital, Changchun Central Hospital, The First Affiliated Hospital, Zhejiang University School of Medicine, and the First Affiliated Hospital of Soochow University, for their assistance with data collection.

Conflict of interest

The authors declare that the research was conducted in the absence of any commercial or financial relationships that could be construed as a potential conflict of interest.

The reviewer MW declared a shared affiliation with the author CL to the handling editor at the time of the review.

Publisher's note

References

1. Villanueva A. Hepatocellular carcinoma. *N Engl J Med* (2019) 380:1450–62. doi: 10.1056/NEJMra1713263

2. European Association for the Study of the Liver. EASL clinical practice guidelines: Management of hepatocellular carcinoma. *J Hepatol* (2018) 69:182–236. doi: 10.1016/j.jhep.2018.03.019

3. El-Khoueiry AB, Sangro B, Yau T, Crocenzi TS, Kudo M, Hsu C, et al. Nivolumab in patients with advanced hepatocellular carcinoma (CheckMate 040): An open-label, non-comparative, phase 1/2 dose escalation and expansion trial. *Lancet* (2017) 389:2492–502. doi: 10.1016/S0140-6736(17)31046-2

4. Zhu AX, Finn RS, Edeline J, Cattan S, Ogasawara S, Palmer D, et al. Pembrolizumab in patients with advanced hepatocellular carcinoma previously treated with sorafenib (KEYNOTE-224): A non-randomised, open-label phase 2 trial. *Lancet Oncol* (2018) 19:940–52. doi: 10.1016/S1470-2045(18)30351-6

5. Topalian SL, Hodi FS, Brahmer JR, Gettinger SN, Smith DC, McDermott DF, et al. Safety, activity, and immune correlates of anti-PD-1 antibody in cancer. *N Engl J Med* (2012) 366:2443–54. doi: 10.1056/NEJMoa1200690

6. Chen K, Wei W, Liu L, Deng ZJ, Li L, Liang XM, et al. Lenvatinib with or without immune checkpoint inhibitors for patients with unresectable hepatocellular carcinoma in real-world clinical practice. *Cancer Immunol Immunother* (2022) 71:1063–74. doi: 10.1007/s00262-021-03060-w

7. Galle PR, Foerster F, Kudo M, Chan SL, Llovet JM, Qin S, et al. Biology and significance of alpha-fetoprotein in hepatocellular carcinoma. *Liver Int* (2019) 39:2214–29. doi: 10.1111/liv.14223

8. Mitsuhashi N, Kobayashi S, Doki T, Kimura F, Shimizu H, Yoshidome H, et al. Clinical significance of alpha-fetoprotein: Involvement in proliferation, angiogenesis, and apoptosis of hepatocellular carcinoma. *J Gastroenterol Hepatol* (2008) 23:e189–97. doi: 10.1111/j.1440-1746.2008.05340.x

9. Xu XF, Xing H, Han J, Li ZL, Lau WY, Zhou YH, et al. Risk factors, patterns, and outcomes of late recurrence after liver resection for hepatocellular carcinoma: A multicenter study from China. *JAMA Surg* (2019) 154:209–17. doi: 10.1001/jamasurg.2018.4334

10. Nault JC, Villanueva A. Biomarkers for hepatobiliary cancers. *Hepatology* (2021) 73 Suppl 1:115–27. doi: 10.1002/hep.31175

11. Personeni N, Bozzarelli S, Pressiani T, Rimassa L, Tronconi MC, Sclafani F, et al. Usefulness of alpha-fetoprotein response in patients treated with sorafenib for advanced hepatocellular carcinoma. *J Hepatol* (2012) 57:101–7. doi: 10.1016/j.jhep.2012.02.016

12. Chan SL, Mo FK, Johnson PJ, Hui EP, Ma BB, Ho WM, et al. New utility of an old marker: Serial alpha-fetoprotein measurement in predicting radiologic response and survival of patients with hepatocellular carcinoma undergoing systemic chemotherapy. *J Clin Oncol* (2009) 27:446–52. doi: 10.1200/JCO.2008.18.8151

13. Liang L, Wang MD, Zhang YM, Zhang WG, Zhang CW, Lau WY, et al. Association of postoperative biomarker response with recurrence and survival in patients with hepatocellular carcinoma and high alpha-fetoprotein expressions (>400 ng/ml). *J Hepatocell Carcinoma* (2021) 8:103–18. doi: 10.2147/JHC.S289840

14. Riaz A, Ryu RK, Kulik LM, Mulcahy MF, Lewandowski RJ, Minocha J, et al. Alpha-fetoprotein response after locoregional therapy for hepatocellular carcinoma: Oncologic marker of radiologic response, progression, and survival. *J Clin Oncol* (2009) 27:5734–42. doi: 10.1200/JCO.2009.23.1282

15. Xu L, Peng ZW, Chen MS, Shi M, Zhang YJ, Guo RP, et al. Prognostic nomogram for patients with unresectable hepatocellular carcinoma after transcatheter arterial chemoembolization. *J Hepatol* (2015) 63:122–30. doi: 10.1016/j.jhep.2015.02.034

16. Memon K, Kulik L, Lewandowski RJ, Wang E, Ryu RK, Riaz A, et al. Alpha-fetoprotein response correlates with EASL response and survival in solitary hepatocellular carcinoma treated with transarterial therapies: A subgroup analysis. *J Hepatol* (2012) 56:1112–20. doi: 10.1016/j.jhep.2011.11.020

17. Chen M, Cao J, Hu J, Topatana W, Li S, Juengpanich S, et al. Clinical-radiomic analysis for pretreatment prediction of objective response to first transarterial chemoembolization in hepatocellular carcinoma. *Liver Cancer* (2021) 10:38–51. doi: 10.1159/000512028

18. Llovet JM, Ricci S, Mazzaferro V, Hilgard P, Gane E, Blanc JF, et al. Sorafenib in advanced hepatocellular carcinoma. *N Engl J Med* (2008) 359:378–90. doi: 10.1056/NEJMoa0708857

19. de Koning HJ, van der Aalst CM, de Jong PA, Scholten ET, Kristiaan N, Heuvelmans MA, et al. Reduced lung-cancer mortality with volume CT screening in a randomized trial. *New Engl J Med* (2020) 382:2. doi: 10.1056/NEJMoa1911793

20. Finn RS, Qin S, Ikeda M, Galle PR, Ducreux M, Kim TY, et al. Atezolizumab plus bevacizumab in unresectable hepatocellular carcinoma. *N Engl J Med* (2020) 382:1894–905. doi: 10.1056/NEJMoa1915745

21. Forner A, Reig M, Bruix J. Hepatocellular carcinoma. *Lancet* (2018) 391:1301–14. doi: 10.1016/S0140-6736(18)30010-2

22. McInnes M, Moher D, Thombs BD, McGrath TA, Bossuyt PMPRISMA-DTA Group, et al. Preferred reporting items for a systematic review and meta-analysis of diagnostic test accuracy studies: The PRISMA-DTA statement. *JAMA* (2018) 319:388–96. doi: 10.1001/jama.2017.19163

23. Horvath S, Raj K. DNA Methylation-based biomarkers and the epigenetic clock theory of ageing. *Nat Rev Genet* (2018) 19:371–84. doi: 10.1038/s41576-018-0004-3

24. Cohen JD, Li L, Wang Y, Thoburn C, Afsari B, Danilova L, et al. Detection and localization of surgically resectable cancers with a multi-analyte blood test. *Science* (2018) 359:926–30. doi: 10.1126/science.aar3247

25. Forner A, Bruix J. Biomarkers for early diagnosis of hepatocellular carcinoma. *Lancet Oncol* (2012) 13:750–1. doi: 10.1016/S1470-2045(12)70271-1

26. Zhu AX, Kang YK, Yen CJ, Finn RS, Galle PR, Llovet JM, et al. Ramucirumab after sorafenib in patients with advanced hepatocellular carcinoma and increased α-fetoprotein concentrations (REACH-2): A randomised, double-blind, placebo-controlled, phase 3 trial. *Lancet Oncol* (2019) 20:282–96. doi: 10.1016/S1470-2045(18)30937-9

27. Zhu AX, Finn RS, Galle PR, Llovet JM, Kudo M. Ramucirumab in advanced hepatocellular carcinoma in REACH-2: the true value of α-fetoprotein. *Lancet Oncol* (2019) 20:e191. doi: 10.1016/S1470-2045(19)30165-2

28. Chen LT, Shiah HS, Chao Y, Chang JY, Cheng LT, Whang-Peng J. Alpha-fetoprotein response in advanced hepatocellular carcinoma receiving cytostatic agent. *J Clin Oncol* (2009) 27:e271. doi: 10.1200/JCO.2009.23.8311

29. Dresel S, Kirsch CM, Tatsch K, Zachoval R, Hahn K, Goldenberg DM. Detection of hepatocellular carcinoma with a new alpha-fetoprotein antibody imaging kit. *J Clin Oncol* (1997) 15:2683–90. doi: 10.1200/JCO.1997.15.7.2683

30. Zhou PY, Yang CP, Tang Z, Yi Y, Liu WR, Tian MX, et al. Daily decrease of post-operative alpha-fetoprotein by 9% discriminates prognosis of HCC: A multicenter retrospective study. *Aging* (2019) 11:11111–23. doi: 10.18632/aging.102513

31. Li XL, Zhu XD, Cai H, Li Y, Zhou J, Fan J, et al. Postoperative α-fetoprotein response predicts tumor recurrence and survival after hepatectomy for hepatocellular carcinoma: A propensity score matching analysis. *Surgery* (2019) 165:1161–7. doi: 10.1016/j.surg.2019.01.009

32. Shen JY, Li C, Wen TF, Yan LN, Li B, Wang WT, et al. Alpha fetoprotein changes predict hepatocellular carcinoma survival beyond the Milan criteria after hepatectomy. *J Surg Res* (2017) 209:102–11. doi: 10.1016/j.jss.2016.10.005

33. Allard MA, Sa Cunha A, Ruiz A, Vibert E, Sebagh M, Castaing D, et al. The postresection alpha-fetoprotein in cirrhotic patients with hepatocellular carcinoma. an independent predictor of outcome. *J Gastroint Surg* (2014) 18:701–8. doi: 10.1007/s11605-013-2433-9

34. Rungsakulkij N, Suragul W, Mingphruedhi S, Tangtawee P, Muangkaew P, Aeesoa S. Prognostic role of alpha-fetoprotein response after hepatocellular carcinoma resection. *World J Clin cases* (2018) 6:110–20. doi: 10.12998/wjcc.v6.i6.110

35. Saeki I, Yamasaki T, Yamashita S, Hanazono T, Urata Y, Furutani T, et al. Early predictors of objective response in patients with hepatocellular carcinoma undergoing lenvatinib treatment. *Cancers* (2020) 12:9. doi: 10.3390/cancers12040779

frontiers | Frontiers in Oncology

TYPE Original Research
PUBLISHED 09 January 2023
DOI 10.3389/fonc.2022.1081510

OPEN ACCESS

EDITED BY
Wenyu Lin,
Massachusetts General Hospital and Harvard Medical School, United States

REVIEWED BY
Linbin Lu,
Xijing Hospital, China
Xiaoqiong Duan,
Institut National de la Transfusion Sanguine, France

*CORRESPONDENCE
Bianqiao Cheng
cbq751115@sina.com
Yanhua Lai
1379771812@qq.com
Zhixian Wu
zxwu@xmu.edu.cn

†These authors share first authorship

SPECIALTY SECTION
This article was submitted to Gastrointestinal Cancers: Hepato Pancreatic Biliary Cancers, a section of the journal Frontiers in Oncology

RECEIVED 27 October 2022
ACCEPTED 29 November 2022
PUBLISHED 09 January 2023

CITATION
Cui Z, Wang J, Chen G, Li D, Cheng B, Lai Y and Wu Z (2023) The upregulation of *CLGN* in hepatocellular carcinoma is potentially regulated by hsa-miR-194-3p and associated with patient progression. *Front. Oncol.* 12:1081510. doi: 10.3389/fonc.2022.1081510

The upregulation of *CLGN* in hepatocellular carcinoma is potentially regulated by hsa-miR-194-3p and associated with patient progression

Zhongyuan Cui[1†], Jielong Wang[1†], Gang Chen[2], Dongliang Li[1], Bianqiao Cheng[3*], Yanhua Lai[4*] and Zhixian Wu[1*]

[1]Department of Hepatobiliary Disease, Dongfang Hospital, School of Medicine, Xiamen University, Fuzhou, China, [2]Department of Gastroenterology, Liuzhou Workers' Hospital (The Fourth Affiliated Hospital), Guangxi Medical University, Liuzhou, China, [3]Department of Gastroenterology, Fuzhou Second Hospital, Fuzhou, China, [4]Department of Transplantation, People's Hospital of Guangxi Zhuang Autonomous Region, Guangxi, China

Background: Patients with hepatocellular carcinoma (HCC) have poor prognosis, especially in advanced stages. Targeted therapy is the main treatment for advanced HCC patients, but the optimal targets for HCC remain poorly understood. The main purpose of this study was to identify potential novel prognostic markers and therapeutic targets.

Methods: Firstly, differentially expressed genes (DEGs) in HCC were identified from the Gene Expression Omnibus (GEO) database. The expression, significance in prognosis, and potential mechanisms of DEGs were analyzed using GEPIA, TIMER, HPA, Kaplan Meier Plotter, CBioPortal, miRWalk, TargetScan, and ENCORI databases. Immunohistochemical staining was used to determine the protein expression levels of potential candidate genes.

Results: The mRNA levels of *MND1*, *STXBP6*, and *CLGN* were significantly increased in HCC ($p< 0.01$). HCC patients with elevated *CLGN* mRNA levels had poorer overall survival (OS), disease-free survival (DFS), progression-free survival (PFS), and disease-specific survival (DSS) ($p < 0.05$). Higher *MND1* mRNA levels significantly correlated with poorer DFS in HCC patients ($p< 0.05$). However, there was no significant correlation between *STXBP6* expression and prognosis of HCC ($p> 0.05$). Further analysis revealed that patients with elevated *CLGN* mRNA expression in advanced pathology stages had poorer prognosis ($p< 0.01$). In addition, CLGN protein levels were elevated in HCC compared to their levels in normal tissues. The mRNA levels of *CLGN* had no significant correlation with the abundance of six common tumor infiltrating lymphocytes in HCC (COR < 0.5). Moreover, the mutation rate of *CLGN* was less than 1% in HCC patients (10/1089). Finally, the expression level of hsa-miR-194-3p in HCC was significantly lower than that in normal tissues ($p < 0.05$), and prognosis of HCC with low expression of hsa-miR-194 was poor ($p < 0.05$).

Conclusion: The upregulation of *CLGN* in HCC is significantly associated with poor patient prognosis, especially in the advanced stages, and may be regulated by hsa-miR-194-3p. These findings suggest that *CLGN* may be closely related to the progression of HCC, and is a potential therapeutic target and prognostic indicator for patients with advanced HCC.

KEYWORDS

hepatocellular carcinoma (HCC), prognosis, CLGN, MND1, STXBP6, MiR-194-3p

Introduction

Primary liver cancer remains the sixth most common cancer and the third leading cause of cancer-related deaths worldwide in 2020, according to the latest statistics (1). Hepatocellular carcinoma (HCC) encompasses 75% -85% of liver cancer cases (1). Most HCC is in advanced stages at the time of diagnosis and is resistant to conventional cytotoxic drugs. Currently, systemic therapy for patients with advanced HCC includes molecularly targeted agents, immune checkpoint inhibitors, or a combination of both (2–4). However, a substantial proportion of patients have yet to benefit from systemic therapy (5, 6). Recent studies have identified several novel biomarkers that can predict HCC prognosis. Lu et al. showed that serum α-fetoprotein trajectories were associated with overall survival of patients with intermediate-stage HCC after transarterial chemoembolization (7). However, it is imperative to identify the most effective predictive biomarkers to facilitate individualized and targeted treatments. Therefore, it is necessary to screen more biomarkers to improve patient diagnosis, and prognosis and identify therapeutic targets for precision therapy.

In recent years, bioinformatic databases have provided abundant transcriptomic and clinical data (8, 9), which are convenient for the analysis of relevant markers with potential significance (10–12). In this study, we explored several databases for molecular markers of HCC and investigated their expression levels in clinical specimens.

Methods

Screening of DEGs in HCC patients

Tumor and normal tissue Gene expression datasets GSE54236 (https://www.ncbi.nlm.nih.gov/geo/query/acc.cgi?acc=GSE54236) (13) and GSE121248 (https://www.ncbi.nlm.nih.gov/geo/query/acc.cgi?acc=GSE121248) were downloaded from Gene Expression Omnibus (GEO, http://www.ncbi.nlm.nih.gov/geo/) (14). D ifferentially expressed genes (DEGs) were analyzed using the online tool GEO2R. Gene Expression Profiling Interactive Analysis (GEPIA, http://gepia.cancer-pku.cn/) (15) and Tumor Immune Estimation Resource database (TIMER, https://cistrome.shinyapps.io/timer/) (16) were used to further verify the DEGs. A p-value of <0.05 was statistically significant.

The significance of DEGs in the prognosis of HCC

GEPIA was used to analyze the relationship between DEGs and overall survival (OS) and disease-free survival (DFS) in HCC patients. Kaplan Meier Plotter (http://kmplot.com/analysis/index.php?p=service&cancer=liver_rnaseq) (17) was used to verify the relationship between candidate gene expression levels and OS, progression-free survival (PFS), relapse-free survival (RFS), and disease-specific survival (DSS) in HCC patients. Then, Kaplan Meier Plotter was used to explore the relationship between candidate genes and OS in patients with different pathological stages. Patients were trichotomized (T1 vs. T3).

CLGN protein expression in HCC and normal tissues

Ethics Statement: The study was conducted in accordance with the principles of the Declaration of Helsinki (18). The collection of HCC specimens was approved by the Ethics Committee of Liuzhou Workers' Hospital (No.KY2022051).

Immunohistochemical Staining: Samples from 24 HCC patients who underwent surgical resection at Liuzhou Workers' Hospital were collected. The acquisition of specimens was approved by the Ethics Committee of Liuzhou Workers' Hospital.

Five-micrometer sections were obtained from paraffin-embedded tumor and non-tumor specimens. All sections were

dewaxed in xylene and rehydrated in alcohol, followed by wet autoclave pretreatment in citrate buffer for antigen retrieval (10 min at 120°C, pH=6.0) and then rinsed with phosphate buffer saline. Immunohistochemical staining with antibody to *CLGN* (Anti-Calmegin/CLGN Antibody, Rabbit: A05261-1, Boster Biological Technology Co. Ltd.) was performed using the avidin-biotin- peroxidase complex method. The primary antibody (1:200 dilution for *CLGN*) was applied to the sections and allowed to bind for 1 h at room temperature. The sections were then incubated with biotinylated anti-mouse/rabbit antibody for 30 min and an avidin-biotin-peroxidase reagent for 10 min. After color development with diaminobenzidine, the sections were counterstained with hematoxylin.

In addition, PATHOLOGY module in HPA (https://www.proteinatlas.org/) database was used to verify the expression of CLGN protein in HCC patient specimens and normal liver tissue.

Analysis of mutation and immune cell infiltration levels

The CBioportal database (https://www.cbioportal.org/) (19) was used to analyze the mutation of *CLGN* in HCC patients. The relationships between the expression levels of *CLGN* and six immune cells (B cells, CD4+ T cells, CD8+ T cells, neutrophils, macrophages, and dendritic cells) in HCC were estimated using the TIMER algorithm. Statistical significance was set at p values of <0.05 and correlation coefficients (COR) of ≥ 0.5.

Screening of regulating microRNAs

MiRWalk (http://mirwalk.umm.uni-heidelberg.de/) (20) and TargetScan (http://www.targetscan.org/vert_72) (21) databases were used to predict microRNAs (miRNAs) that regulate *CLGN* mRNA expression. The Encyclopedia of RNA Interactomes (ENCORI, http://rna.sysu.edu.cn/encori/mirTarPathways.php) (22) database was used to analyze the expression levels of candidate miRNAs in HCC and normal tissues. Kaplan Meier Plotter was used to analyze the relationship between the levels of candidate miRNAs and prognosis of HCC. A p value of <0.05 was considered statistically significant.

Data processing and visualization

Gene expression data were cleaned and visualized using R (Version 3.6.3) and the R packages ggplot2 and VennDiagram. The cleaning algorithm for the gene expression data included removal of non-coding genes, miRNA, and blank probes; FDR ≤0.05 and FC ≥2; retaining one level from one gene that had several high or, consistently, low expression levels in different specimens. We removed genes that had both high expression and low expression in different specimens. Cytoscape (Version: 3.7.2) and cytoHubba plugin were used to analyze miRNAs with the potential to regulate *CLGN* mRNA expression.

Results

Significant DEGs in HCC

The DEG analysis revealed 290 genes with significantly high expression and 518 genes with significantly low expression in the GSE54236 (G1) dataset (Figures 1A, C). In the GSE121248 (G2) dataset, 319 genes were significantly upregulated, and 611 genes were significantly under-expressed (Figures 1B, C). There were 121 genes with high expression and 249 genes with low

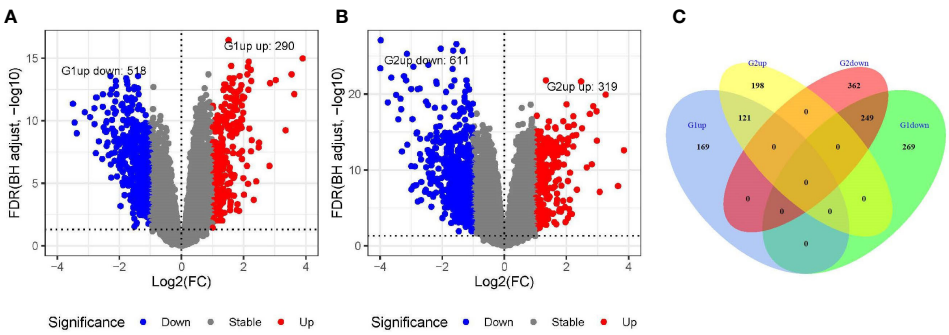

FIGURE 1
Screening of differentially expressed genes in GSE54236 (G1) and GSE121248 (G2) datasets. **(A, B)** Gene expression levels in GSE54236 (G1) and GSE121248 (G2) datasets, with blue dots indicating significantly low expression and red dots indicating significantly high expression. **(C)** The number of genes with high or low expression in both datasets.

expression in both the datasets (Figure 1C). After removing the genes that have been reported, we found that the expression levels of *MND1*, *STXBP6*, and *CLGN* in HCC were significantly higher than those in normal tissues.

The expression levels of *MND1*, *STXBP6*, and *CLGN* mRNA in HCC w ere verified. The results showed that the *MND1*, *STXBP6*, and *CLGN* mRNA levels in HCC were significantly higher than those in normal tissues ($p < 0.01$, Figures 2A-C). In addition, the mRNA expression of *CLGN* was high in breast invasive carcinoma, kidney chromophobe, kidney renal papillary cell carcinoma, lung adenocarcinoma, lung squamous cell carcinoma prostate adenocarcinoma, and uterine corpus endometrial carcinoma ($p < 0.01$, Figure 3).

Relationship between DEGs and prognosis of HCC

The prognostic value of *MND1*, *STXBP6*, and *CLGN* in HCC patients was explored. HCC patients with higher mRNA levels of *CLGN* had poorer OS and DFS ($p< 0.05$, Figures 4A, B). There was no significant correlation between *MND1* mRNA levels and OS ($p> 0.05$; Figure 4C), and patients with higher *MND1* mRNA levels had poorer DFS ($p< 0.05$, Figure 4D). However, there was no significant correlation between the mRNA levels of *STXBP6* and OS or DFS in HCC patients ($p > 0.05$, Figures 4E, F).

The relationship between *CLGN* mRNA levels and the prognosis of HCC was also investigated. The results showed that the mRNA

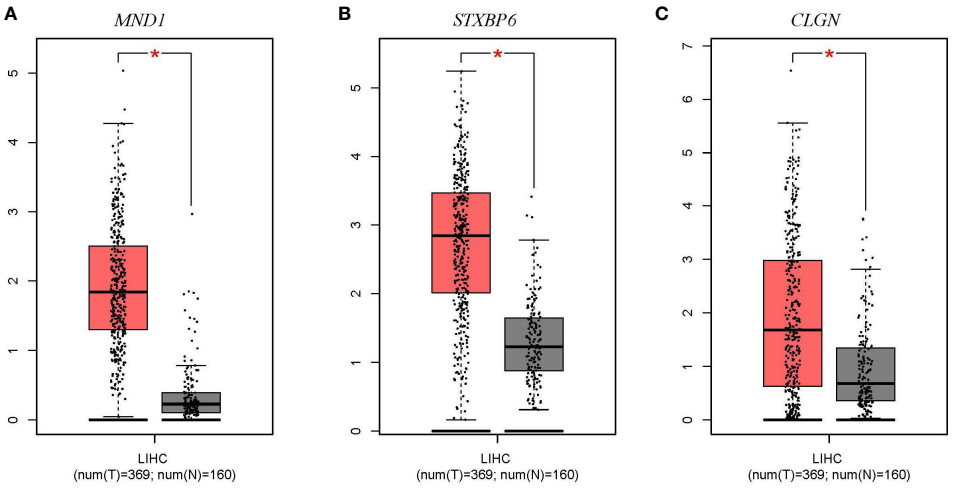

FIGURE 2
The mRNA expression levels of *MND1*, *STXBP6*, and *CLGN* in HCC (GEPIA). **(A-C)** The mRNA expression levels of *MND1*, *STXBP6*, and *CLGN* in HCC were significantly higher than in normal tissue. *$p < 0.01$.

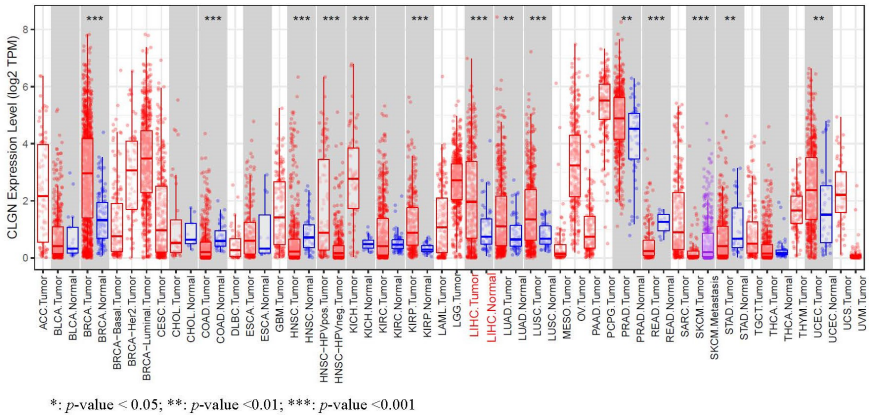

FIGURE 3
The mRNA expression of levels of *CLGN* in several common human tumors. The mRNA of *CLGN* was upregulated in liver and other tumors (TIMER).

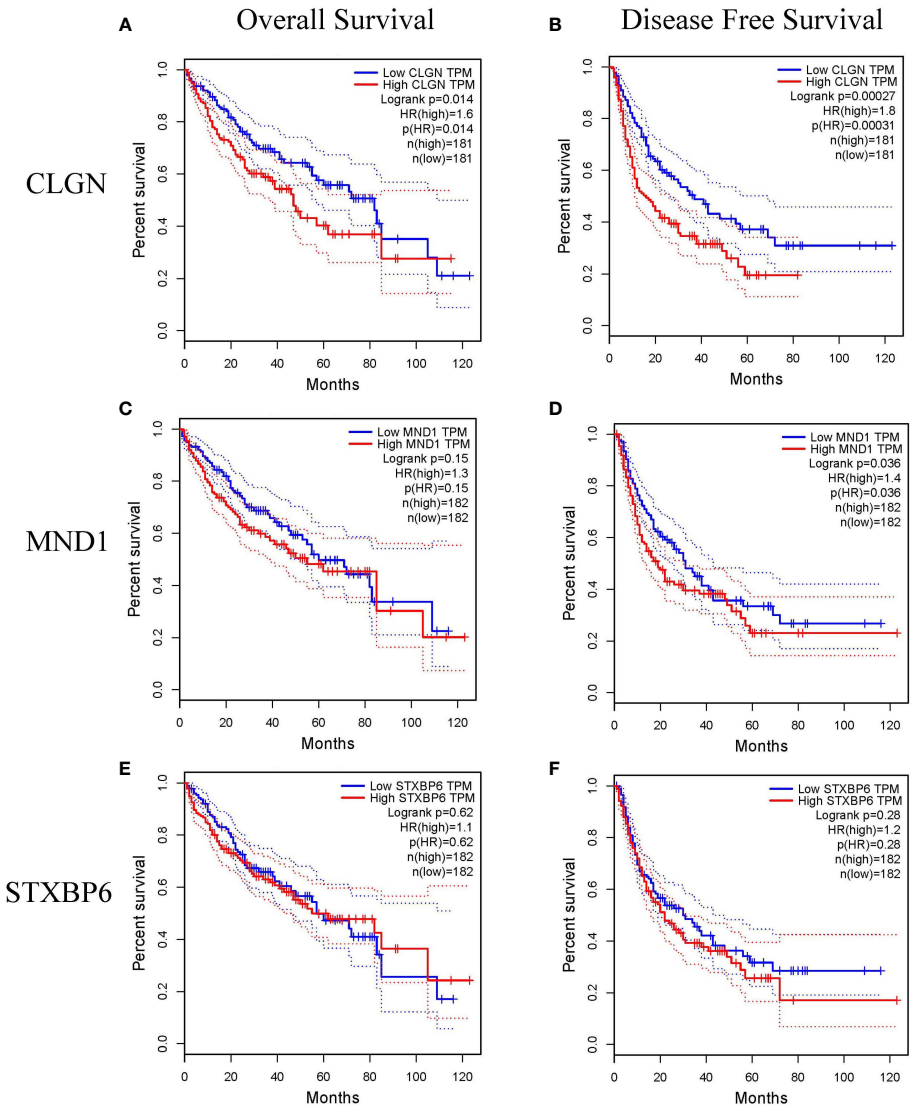

FIGURE 4
The relationship between the mRNA levels of *MND1*, *STXBP6* and *CLGN* and the prognosis of HCC (GEPIA). **(A, B)** HCC patients with higher mRNA levels of *CLGN* had poorer overall survival and disease-free survival ($p < 0.05$). **(C)** No significant relationship between *MND1* mRNA levels and patients' overall survival was observed ($p > 0.05$). **(D)** Patients with higher *MND1* mRNA levels had poorer disease-free survival ($p < 0.05$). **(E, F)** There was no significant correlation between the mRNA levels of *STXBP6* and overall survival and disease-free survival in HCC patients ($p > 0.05$).

levels of *CLGN* were significantly correlated with OS, PFS, and DSS in HCC patients ($p < 0.05$, Figures 5A-C and Table 1). However, there was no significant relationship between *CLGN* mRNA levels and RFS ($p > 0.05$, Figure 5D and Table 1). Furthermore, the mRNA level of *CLGN* was significantly correlated with the OS in different pathology stages in HCC patients. Specifically, HCC patients with higher mRNA expression of *CLGN* in advanced stages (T3, T3+T4) had poorer OS ($p < 0.01$, Figures 6C, D and Table 2). No significant correlation was found between *CLGN* mRNA levels and OS in patients with early-stage HCC (T1-T2) ($p > 0.05$, Figures 6A, B and Table 2).

CLGN protein expression in clinical specimens

The p rotein expression of CLGN in tumor and normal tissues of clinical specimens from patients with HCC was investigated. Immunohistochemical staining showed that the CLGN protein was significantly regulated in HCC compared with normal liver tissues in 58% (14/24) of cases (Figure 7A). The HPA database results also showed that CLGN protein levels were higher in HCC than in non-tumor tissues (Figure 7B).

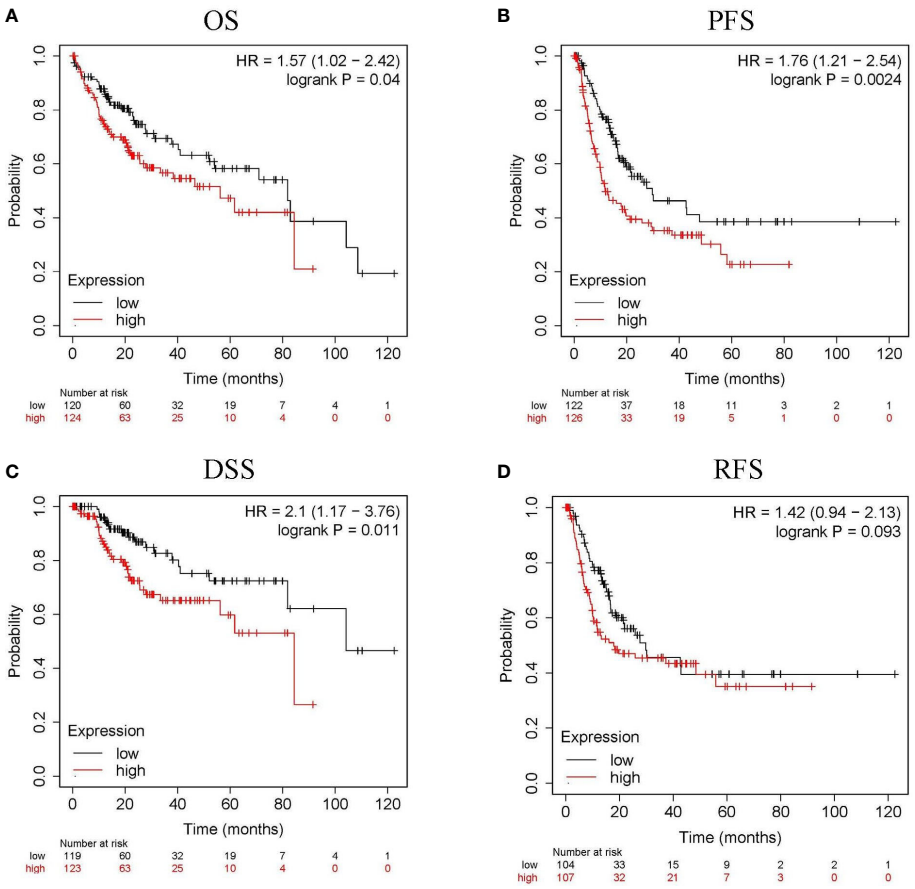

FIGURE 5
The relationship between *CLGN* mRNA and prognosis of HCC (Kaplan Meier Plotter). **(A–C)** HCC patients with higher *CLGN* mRNA expression have poorer OS, PFS, and DSS, $p < 0.05$. **(D)** There was no significant relationship between *CLGN* mRNA level and RFS, $p > 0.05$.

CLGN mutation in HCC and the correlation between *CLGN* expression and tumor infiltrating lymphocytes

CLGN mutations were analyzed in 1089 patients with HCC from six data sources. The results showed that *CLGN* was mutated in < 1% (10/1089) of patients (Figure 8A). Furthermore, there was no significant correlation between *CLGN* expression and the levels of B cells, CD4+ T cells, CD8 + T cells, neutrophils, macrophages, or dendritic cells in HCC (COR < 0.5 (Figure 8B).

miRNAs that regulate *CLGN*

Firstly, 4357 and 634 miRNAs that potentially regulate *CLGN* were predicted in the miRWalk and TargetScan databases, respectively. Duplicate data from the two groups

TABLE 1 Correlation between the *CLGN* mRNA expression and the survival of HCC patients.

Gene	Survival	Patients	HR	*p* Value	Median survival (months)	
					Low	High
CLGN	OS	244	1.57	0.0401	81.9	56.2
	RFS	211	1.42	0.0929	29.77	17.9
	PFS	248	1.76	0.0024	29.77	11.83
	DSS	242	2.10	0.0106	104.17	84.4

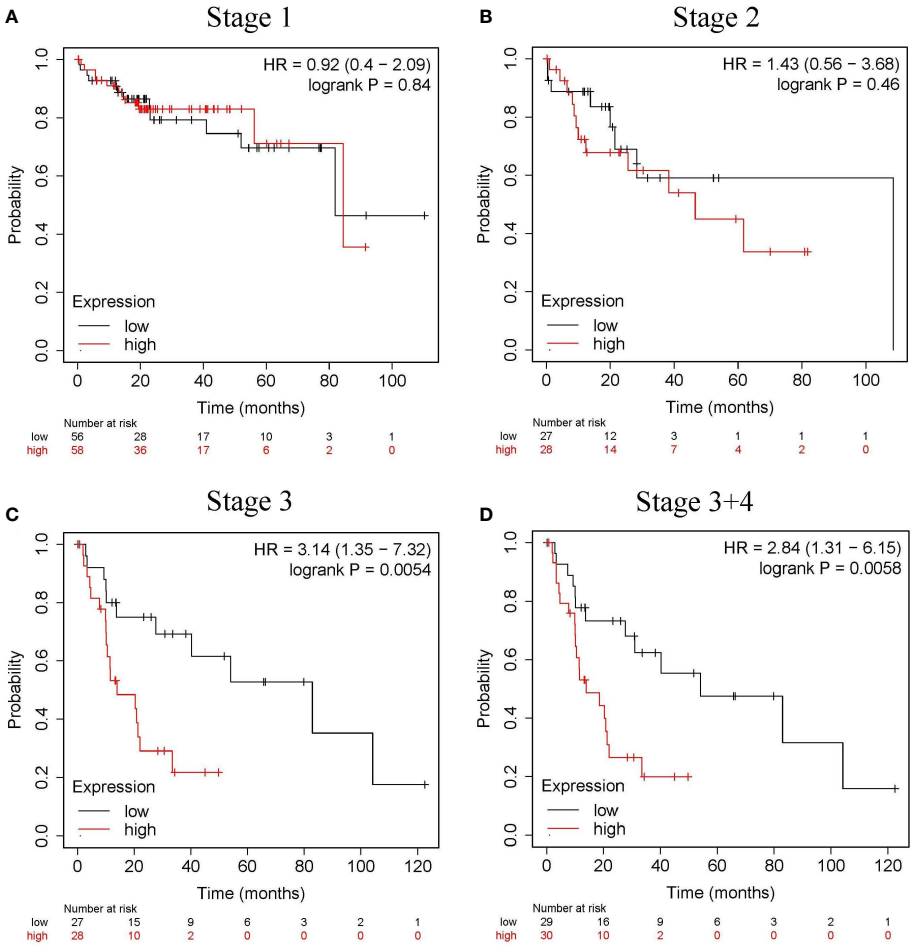

FIGURE 6
The relationship between the *CLGN* mRNA level and the OS in different pathology stages in HCC patients. (Kaplan Meier Plotter). **(A, B)** There was no significant correlation between the *CLGN* mRNA level and the OS in HCC patients in early stages (T1 and T2), $p > 0.05$. **(C, D)** HCC patients in advanced T stages (T3 and T3+T4) have higher *CLGN* mRNA expression and poorer OS, $p < 0.05$.

were removed, and their intersection contained 248 potential miRNAs (Supplementary 1). As calculated with Cytoscape, the top 14 miRNAs that were most likely to regulate *CLGN* mRNA expression were hsa-miR-642b-3p, hsa-miR-7114-5p, hsa-miR-6130, hsa-miR-4738-3p, hsa-miR-520g-3p, hsa-miR-6759-5p, hsa-miR-4446-3p, hsa-miR-6843-3p, hsa-miR-4482-5p, hsa-miR-202-3p, hsa-let-7a-5p, hsa-miR-6080, hsa-miR-2681-5p, and hsa-miR-194-3p (Figure 9A). A further analysis revealed that hsa-miR-194-3p was significantly underexpressed in HCC (Fold Change = 0.72, $p < 2.1e\text{-}5$ and FDR< 0.001, Figure 9B). HCC patients with low hsa-miR-194 expression had poorer OS than those without ($p < 0.001$, Figure 9C).

TABLE 2 Correlation between the *CLGN* mRNA expression and patient OS at different pathological stages.

Stage	Patients	HR	*p* Value	Median survival (months)	
				Low	Low
1	170	0.92	0.84	81.9	84.4
2	83	1.43	0.46	108.6	46.6
1+2	253	1.35	0.34	108.6	84.4
3	83	3.14	0.0054	82.9	14
3+4	87	2.84	0.0058	54.1	14

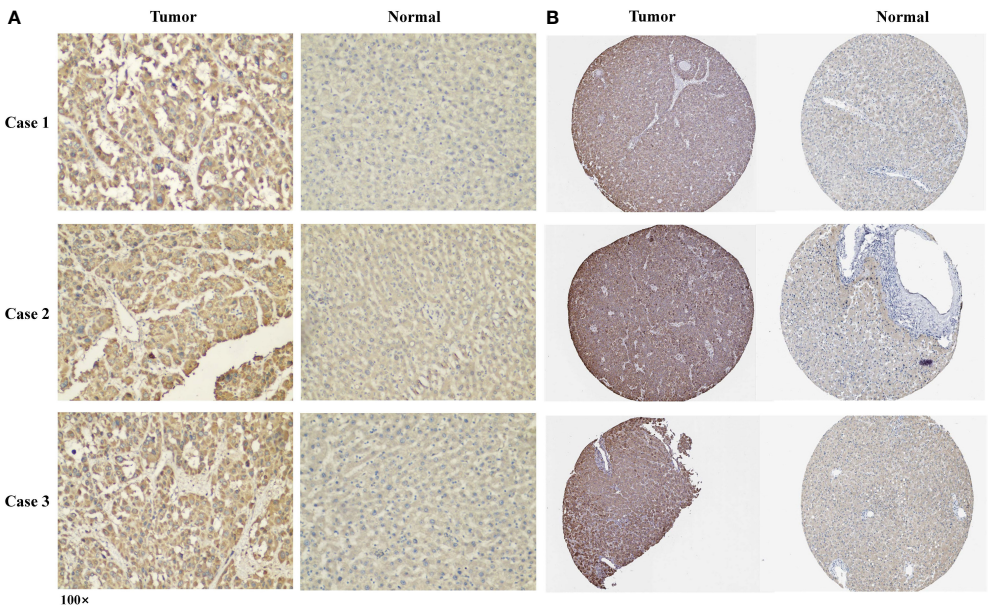

FIGURE 7
The expression of CLGN protein in HCC and adjacent tissues. **(A)** Three typical cases of CLGN protein upregulation in HCC in 24 clinical specimens. **(B)** The expression of CLGN protein in HCC is higher than non-cancerous liver tissue (HPA).

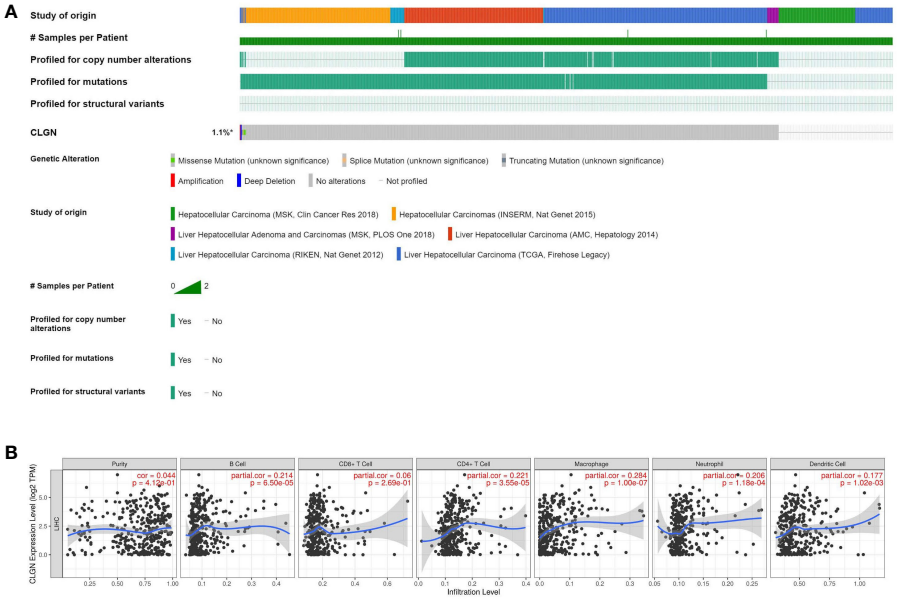

FIGURE 8
CLGN mutations in HCC patients and the correlation between *CLGN* expression and tumor infiltrating lymphocytes. **(A)** *CLGN* mutations occurred in 10 (< 1%) of 1089 patients from six data sources (CBioportal). **(B)** There is no significant correlation between the mRNA of *CLGN* and the infiltrating levels of B cells, CD4+ T cells, CD8+ T cells, neutrophils, macrophages, and dendritic cells in HCC, COR < 0.5 (TIMER).

Discussion

CLGN (Calmegin) is a testis-specific endoplasmic reticulum chaperone protein (23, 24). Previous studies have shown that CLGN acted as a chaperone for one or more sperm surface proteins to mediate the interaction between sperm and eggs during spermatogenesis (23). Therefore, *CLGN* may play an important role in spermatogenesis and infertility. A recent study found that *CLGN* was up-regulated in aldogen-producing adenomas and was related to the generation of aldosterone (25). However, the role of *CLGN* in several malignant tumors, including HCC, remains unclear.

In this study, it was found that the mRNA and protein of *CLGN* were highly expressed in HCC compared with normal liver tissues. Furthermore, patients with higher *CLGN* mRNA levels had poorer prognoses, and *CLGN* mRNA levels were valuable in predicting the prognosis of patients with advanced pathology. These results suggest that *CLGN* is associated with malignant progression in HCC patients. Additionally, *CLGN* was found to be significantly upregulated in invasive breast cancer, chromophobe renal cell carcinoma, papillary renal cell carcinoma lung adenocarcinoma, lung squamous cell carcinoma, prostate adenocarcinoma, and uterine corpus endometrial carcinoma. To the best of our knowledge, no studies have investigated the role of *CLGN* in these tumors, which is worth of further investigation.

However, the relationship between *MND1* and STXBP6 in HCC remains unknown. Notably, Zierhut et al. found that *MND1* was necessary for meiosis homologue repair (26). Zhang et al. found that *MND1* was upregulated in lung adenocarcinoma and was an independent risk factor for overall survival (27). Furthermore, *MND1* was a prognostic biomarker for renal clear cell carcinoma (28). Lenka et al. found that *STXBP6* hypermethylation was associated with adverse clinical outcomes in patients with lung cancer (29). A nother recent study showed that the expression level of *STXBP6* predicted the response to PD-1/PD-L1 immunotherapy in patients with cancer (30). In this study, we found that *MND1* and *STXBP6* were upregulated in HCC, but no significant correlation was found between their expression and patient prognosis .

Gene mutations are a common tumorigenic mechanism in liver cancer (31–34). In this study, it was found that *CLGN* was rarely mutated in HCC patients, which suggests that the pathological effects of *CLGN* may not be exerted through genetic mutations. The immune microenvironment is closely related to tumor progression (35–37). Therefore, we also analyzed the relationship between *CLGN* mRNA levels and the abundance of tumor-infiltrating lymphocytes in HCC; however, no significant correlation was found. Based on this, we hypothesized that *CLGN* might influence the progression of HCC by promoting cell proliferation or inhibiting tumor cell apoptosis, which requires further study in the future.

MicroRNAs (miRNAs) are small non-coding RNAs composed of approximately 20 nucleotides that regulate gene expression by binding to the 3'-UTR of the target mRNA (38). Recent studies have shown that miRNAs were an important regulator of mRNA expression (39–41). hsa-miR-194-3p was significantly underexpressed in HCC, and patients with lower hsa-miR-194 expression had poorer prognosis. A study found that hsa-miR-194-3p might target MECP2 to promote breast cancer progression and reduce sensitivity to rapamycin (42). Recent studies have shown that hsa-miR-194-3p might be associated with colorectal cancer progression (43). However, its specific therapeutic and prognostic value in tumors requires further investigation. In this study, we discovered that hsa-miR-194-3p may also play an important role in HCC progression by regulating *CLGN* expression.

Our findings suggest that *CLGN* is a potential prognostic marker for HCC and is associated with HCC progression,

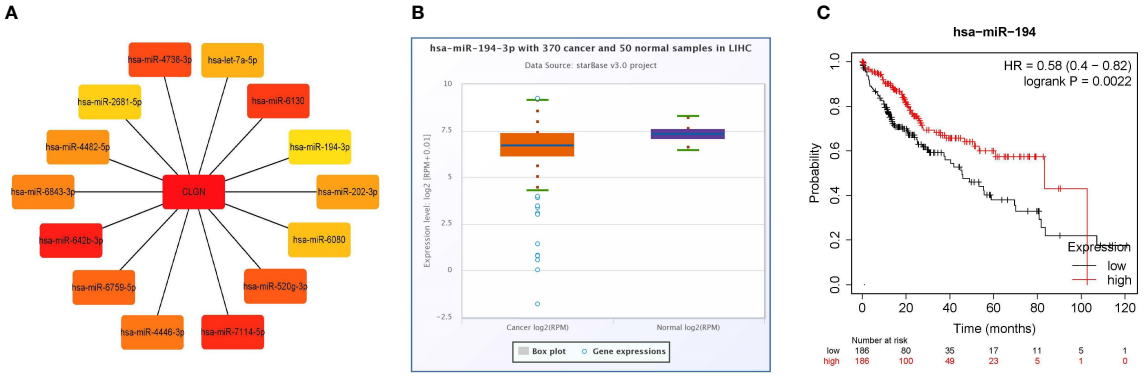

FIGURE 9
miRNAs that likely regulate the expression of *CLGN* mRNA (miRWalk and TargetScan). **(A)** The 14 miRNAs that most closely related to *CLGN* mRNA. **(B)** The expression of hsa-miR-194-3p in HCC is significantly lower than in normal tissue, $p < 0.05$ (ENCORI). **(C)** HCC patients with lower hsa-miR-194 expression have poorer OS than those without, $p < 0.05$ (Kaplan Meier Plotter).

however, several limitations are associated with our study. Specifically, the relationship between *CLGN* expression and patient prognosis has not yet been verified at the center. Additionally, laboratory research on the cancer-promoting mechanisms of *CLGN* were not available, and the sample size used for immunohistochemistry in this study was small. Therefore, a large-scale verification study is required in the future.

Conclusion

CLGN is upregulated in HCC and significantly correlates with patient prognosis, especially in the advanced stages. In addition, the mRNA levels of *CLGN* were found to be potentially regulated by hsa-miR-194-3p. These results suggest that *CLGN* may have important therapeutic and prognostic value in HCC patients.

Data availability statement

The datasets analyzed during the current study are available on Gene Expression Omnibus (GEO) (accession numbers: GSE54236, GSE121248), Gene Expression Profiling Interactive Analysis (GEPIA), Tumor Immune Estimation Resource (TIMER), Kaplan Meier Plotter, The Human Protein Atlas (HPA), cBioPortal, miRWalk, TargetScan, and The Encyclopedia of RNA Interactomes (ENCORI).

Ethics statement

The studies involving human participants were reviewed and approved by Ethics Committee of Liuzhou Workers' Hospital. Written informed consent for participation was not required for this study in accordance with the national legislation and the institutional requirements.

Author contributions

ZC: Data analysis and writing of the first draft. BC, YL and ZW: Data analysis, manuscript editing, review, and approval. JW, ZC, and GC: Data analysis, data collection and experiments. DL: Data analysis, manuscript editing and review. All authors have read and approved the final manuscript.

Funding

This study was supported by the Science and Technology Innovation Joint Fund Project of Fujian Province (No. 2019Y9044) and Natural Science Foundation of Fujian Province (No. 2020J011131).

Acknowledgments

We are grateful to the generous data contributors, developers, and maintainers of the public databases.

Conflict of interest

The authors declare that the research was conducted in the absence of any commercial or financial relationships that could be construed as a potential conflict of interest.

Publisher's note

Supplementary material

The Supplementary Material for this article can be found online at: https://www.frontiersin.org/articles/10.3389/fonc.2022.1081510/full#supplementary-material

References

1. Sung H, Ferlay J, Siegel RL, Laversanne M, Soerjomataram I, Jemal A, et al. Global cancer statistics 2020: GLOBOCAN estimates of incidence and mortality worldwide for 36 cancers in 185 countries. *CA Cancer J Clin* (2021) 71(3):209–49. doi: 10.3322/caac.21660

2. Zhang H, Zhang W, Jiang L, Chen Y. Recent advances in systemic therapy for hepatocellular carcinoma. *biomark Res* (2022) 10(1):3. doi: 10.1186/s40364-021-00350-4

3. Yang JD, Hainaut P, Gores GJ, Amadou A, Plymoth A, Roberts LR. A global view of hepatocellular carcinoma: trends, risk, prevention and management. *Nat Rev Gastroenterol Hepatol* (2019) 16(10):589–604. doi: 10.1038/s41575-019-0186-y

4. Llovet JM, Castet F, Heikenwalder M, Maini MK, Mazzaferro V, Pinato DJ, et al. Immunotherapies for hepatocellular carcinoma. *Nat Rev Clin Oncol* (2022) 19 (3):151–72. doi: 10.1038/s41571-021-00573-2

5. El-Khoueiry AB, Sangro B, Yau T, Crocenzi TS, Kudo M, Hsu C, et al. Nivolumab in patients with advanced hepatocellular carcinoma (CheckMate 040): an open-label, non-comparative, phase 1/2 dose escalation and expansion trial. *Lancet* (2017) 389(10088):2492–502. doi: 10.1016/S0140-6736(17)31046-2

6. Pallozzi M, Di Tommaso N, Maccauro V, Santopaolo F, Gasbarrini A, Ponziani FR, et al. Non-invasive biomarkers for immunotherapy in patients with hepatocellular carcinoma: Current knowledge and future perspectives. *Cancers (Basel)* (2022) 14(19). doi: 10.3390/cancers14194631

7. Lu L, Shen L, Wu Z, Shi Y, Hou P, Xue Z, et al. Trajectories of serum alpha-fetoprotein and intermediate-stage hepatocellular carcinoma outcomes after transarterial chemoembolization: A longitudinal, retrospective, multicentre, cohort study. *E Clin Med* (2022) 47:101391. doi: 10.1016/j.eclinm.2022.101391

8. Hussen BM, Abdullah ST, Salihi A, Sabir DK, Sidiq KR, Rasul MF, et al. The emerging roles of NGS in clinical oncology and personalized medicine. *Pathol Res Pract* (2022) 230:153760. doi: 10.1016/j.prp.2022.153760

9. Morganti S, Tarantino P, Ferraro E, D'Amico P, Viale G, Trapani D, et al. Complexity of genome sequencing and reporting: Next generation sequencing (NGS) technologies and implementation of precision medicine in real life. *Crit Rev Oncol Hematol* (2019) 133:171–82. doi: 10.1016/j.critrevonc.2018.11.008

10. Schmidt B, Hildebrandt A. Deep learning in next-generation sequencing. *Drug Discovery Today* (2021) 26(1):173–80. doi: 10.1016/j.drudis.2020.10.002

11. Zhong Y, Xu F, Wu J, Schubert J, Li MM. Application of next generation sequencing in laboratory medicine. *Ann Lab Med* (2021) 41(1):25–43. doi: 10.3343/alm.2021.41.1.25

12. Chen F, Wang J, Wu Y, Gao Q, Zhang S. Potential biomarkers for liver cancer diagnosis based on multi-omics strategy. *Front Oncol* (2022) 12:822449. doi: 10.3389/fonc.2022.822449

13. Villa E, Critelli R, Lei B, Marzocchi G, Camma C, Giannelli G, et al. Neoangiogenesis-related genes are hallmarks of fast-growing hepatocellular carcinomas and worst survival. results from a prospective study. *Gut* (2016) 65 (5):861–9. doi: 10.1136/gutjnl-2014-308483

14. Wang SM, Ooi LL, Hui KM. Identification and validation of a novel gene signature associated with the recurrence of human hepatocellular carcinoma. *Clin Cancer Res* (2007) 13(21):6275–83. doi: 10.1158/1078-0432.CCR-06-2236

15. Tang Z, Li C, Kang B, Gao G, Li C, Zhang Z. GEPIA: a web server for cancer and normal gene expression profiling and interactive analyses. *Nucleic Acids Res* (2017) 45(W1):W98–W102. doi: 10.1093/nar/gkx247

16. Li T, Fan J, Wang B, Traugh N, Chen Q, Liu JS, et al. TIMER: A web server for comprehensive analysis of tumor-infiltrating immune cells. *Cancer Res* (2017) 77(21):e108–e10. doi: 10.1158/0008-5472.CAN-17-0307

17. Lanczky A, Gyorffy B. Web-based survival analysis tool tailored for medical research (KMplot): Development and implementation. *J Med Internet Res* (2021) 23(7):e27633. doi: 10.2196/27633

18. World Medical A. World medical association declaration of Helsinki: ethical principles for medical research involving human subjects. *JAMA* (2013) 310 (20):2191–4. doi: 10.1001/jama.2013.281053

19. Cerami E, Gao J, Dogrusoz U, Gross BE, Sumer SO, Aksoy BA, et al. The cBio cancer genomics portal: an open platform for exploring multidimensional cancer genomics data. *Cancer Discovery* (2012) 2(5):401–4. doi: 10.1158/2159-8290.CD-12-0095

20. Sticht C, de la Torre C, Parveen A, Gretz N. miRWalk: An online resource for prediction of microRNA binding sites. *PloS One* (2018) 13(10):e0206239. doi: 10.1371/journal.pone.0206239

21. Agarwal V, Bell GW, Nam JW, Bartel DP. Predicting effective microRNA target sites in mammalian mRNAs. *Elife* (2015) 4. doi: 10.7554/eLife.05005

22. Li JH, Liu S, Zhou H, Qu LH, Yang JH. starBase v2.0: decoding miRNA-ceRNA, miRNA-ncRNA and protein-RNA interaction networks from large-scale CLIP-seq data. *Nucleic Acids Res* (2014) 42(Database issue):D92–7. doi: 10.1093/nar/gkt1248

23. Ikawa M, Wada I, Kominami K, Watanabe D, Toshimori K, Nishimune Y, et al. The putative chaperone calmegin is required for sperm fertility. *Nature* (1997) 387(6633):607–11. doi: 10.1038/42484

24. Siep M, Sleddens-Linkels E, Mulders S, van Eenennaam H, Wassenaar E, Van Cappellen WA, et al. Basic helix-loop-helix transcription factor Tcfl5 interacts with the calmegin gene promoter in mouse spermatogenesis. *Nucleic Acids Res* (2004) 32(21):6425–36. doi: 10.1093/nar/gkh979

25. Itcho K, Oki K, Gomez-Sanchez CE, Gomez-Sanchez EP, Ohno H, Kobuke K, et al. Endoplasmic reticulum chaperone calmegin is upregulated in aldosterone-producing adenoma and associates with aldosterone production. *Hypertension* (2020) 75(2):492–9. doi: 10.1161/HYPERTENSIONAHA.119.14062

26. Zierhut C, Berlinger M, Rupp C, Shinohara A, Klein F. Mnd1 is required for meiotic interhomolog repair. *Curr Biol* (2004) 14(9):752–62. doi: 10.1016/j.cub.2004.04.030

27. Zhang Q, Shi R, Bai Y, Meng L, Hu J, Zhu H, et al. Meiotic nuclear divisions 1 (MND1) fuels cell cycle progression by activating a KLF6/E2F1 positive feedback loop in lung adenocarcinoma. *Cancer Commun (Lond)* (2021) 41(6):492–510. doi: 10.1002/cac2.12155

28. Fang J, Zhen J, Gong Y, Ke Y, Fu B, Jiang Y, et al. MND1 functions as a potential prognostic biomarker associated with cell cycle and immune infiltration in kidney renal clear cell carcinoma. *Aging (Albany NY)* (2022) 14(18):7416–42. doi: 10.18632/aging.204280

29. Lenka G, Tsai MH, Lin HC, Hsiao JH, Lee YC, Lu TP, et al. Identification of methylation-driven, differentially expressed STXBP6 as a novel biomarker in lung adenocarcinoma. *Sci Rep* (2017) 7:42573. doi: 10.1038/srep42573

30. Liu Y, Huang Z, Wei Y, Zhang M, Li X, Yang S, et al. Identification of STXBP6-IRF1 positive feedback loop in regulation of PD-L1 in cancer. *Cancer Immunol Immunother* (2021) 70(2):275–87. doi: 10.1007/s00262-020-02678-6

31. Li Y, Li D, Liu Y, Wang S, Sun M, Zhang Z, et al. The positive feedback loop of NHE1-ERK phosphorylation mediated by BRAF(V600E) mutation contributes to tumorigenesis and development of glioblastoma. *Biochem Biophys Res Commun* (2022) 588:1–7. doi: 10.1016/j.bbrc.2021.11.104

32. Vu T, Datta A, Banister C, Jin L, Yuan G, Samuel T, et al. Serine-threonine kinase receptor-associated protein is a critical mediator of APC mutation-induced intestinal tumorigenesis through a feed-forward mechanism. *Gastroenterology* (2022) 162(1):193–208. doi: 10.1053/j.gastro.2021.09.010

33. Wen X, Lu F, Liu S. Prognostic value of p53 mutation for poor outcome of Asian primary liver cancer patients: evidence from a cohort study and meta-analysis of 988 patients. *OncoTargets Ther* (2016) 9:7425–33. doi: 10.2147/OTT.S121594

34. Li J, Yu CP, Li Q, Chang S, Xie LL, Wang S. Large-Scale omics data reveal the cooperation of mutation-circRNA-miRNA-target gene network in liver cancer oncogenesis. *Future Oncol* (2022) 18(2):163–78. doi: 10.2217/fon-2021-0940

35. Chew V, Toh HC, Abastado JP. Immune microenvironment in tumor progression: characteristics and challenges for therapy. *J Oncol* (2012) 2012:608406. doi: 10.1155/2012/608406

36. Makarova-Rusher OV, Medina-Echeverz J, Duffy AG, Greten TF. The yin and yang of evasion and immune activation in HCC. *J hepatol* (2015) 62(6):1420–9. doi: 10.1016/j.jhep.2015.02.038

37. Xing Y, Ruan G, Ni H, Qin H, Chen S, Gu X, et al. Tumor immune microenvironment and its related miRNAs in tumor progression. *Front Immunol* (2021) 12:624725. doi: 10.3389/fimmu.2021.624725

38. Bartel DP. MicroRNAs: genomics, biogenesis, mechanism, and function. *Cell* (2004) 116(2):281–97. doi: 10.1016/S0092-8674(04)00045-5

39. Thomson DW, Dinger ME. Endogenous microRNA sponges: evidence and controversy. *Nat Rev Genet* (2016) 17(5):272–83. doi: 10.1038/nrg.2016.20

40. Friedman RC, Farh KK, Burge CB, Bartel DP. Most mammalian mRNAs are conserved targets of microRNAs. *Genome Res* (2009) 19(1):92–105. doi: 10.1101/gr.082701.108

41. Pan X, Wenzel A, Jensen LJ, Gorodkin J. Genome-wide identification of clusters of predicted microRNA binding sites as microRNA sponge candidates. *PloS One* (2018) 13(8):e0202369. doi: 10.1371/journal.pone.0202369

42. Zhou Q, Guo J, Huang W, Yu X, Xu C, Long X. Linc-ROR promotes the progression of breast cancer and decreases the sensitivity to rapamycin through miR-194-3p targeting MECP2. *Mol Oncol* (2020) 14(9):2231–50. doi: 10.1002/1878-0261.12700

43. Liu T, Fang Y. MiR-194-3p modulates the progression of colorectal cancer by targeting KLK10. *Histol Histopathol* (2021) 18413. doi: 10.14670/HH-18-413

frontiers | Frontiers in Oncology

TYPE Original Research
PUBLISHED 13 January 2023
DOI 10.3389/fonc.2022.1101351

OPEN ACCESS

EDITED BY
Wenyu Lin,
Massachusetts General Hospital and Harvard Medical School, United States

REVIEWED BY
Xingshun Qi,
General Hospital of Shenyang Military Command, China
Yi Li,
Kunming General Hospital of Chengdu Military Command, China

*CORRESPONDENCE
Zhixian Wu
zxwu@xmu.edu.cn
Yonghai Peng
1208852065@qq.com
Yanhua Lai
laiyanhua303@sina.com

†These authors have contributed equally to this work

SPECIALTY SECTION
This article was submitted to Gastrointestinal Cancers: Hepato Pancreatic Biliary Cancers, a section of the journal Frontiers in Oncology

RECEIVED 17 November 2022
ACCEPTED 20 December 2022
PUBLISHED 13 January 2023

CITATION
Zhang X, Cai L, Fang J, Chen F, Pan F, Zhang K, Huang Q, Huang Y, Li D, Lv L, Chen M, Yan R, Lai Y, Peng Y and Wu Z (2023) Efficacy and safety of transarterial chemoembolization plus sorafenib in patients with recurrent hepatocellular carcinoma after liver transplantation. *Front. Oncol.* 12:1101351. doi: 10.3389/fonc.2022.1101351

Efficacy and safety of transarterial chemoembolization plus sorafenib in patients with recurrent hepatocellular carcinoma after liver transplantation

Xia Zhang[1†], Lirong Cai[1†], Jian Fang[2†], Fengsui Chen[1], Fan Pan[3], Kun Zhang[4], Qian Huang[3], Yuju Huang[1], Dongliang Li[1], Lizhi Lv[3], Man Chen[1], Ruiying Yan[1], Yanhua Lai[5*], Yonghai Peng[6*] and Zhixian Wu[1*]

[1]Department of Hepatobiliary Disease, the 900th Hospital of Joint Logistics Support Force, Fujian Medical University, Fuzhou, China, [2]Department of Hepatobiliary Disease, The Third People's Hospital of Fujian University of Traditional Chinese Medicine, Fuzhou, China, [3]Department of Hepatobiliary Surgery, the 900th Hospital of Joint Logistics Support Force, Fujian Medical University, Fuzhou, China, [4]Department of Hepatobiliary Surgery, Xiang'an Hospital, Xiamen University, Xiamen, China, [5]Department of Transplantation, People's Hospital of Guangxi Zhuang Autonomous Region, Nanning, China, [6]Department of Oncology, the 900th Hospital of Joint Logistics Support Force, Fujian Medica University, Fuzhou, China

Objectives: To explore the benefit and safety of transarterial chemoembolization (TACE) in combination with sorafenib in patients with recurrent hepatocellular carcinoma (HCC) after orthotopic liver transplantation (OLT).

Methods: In this multi-center retrospective study, 106 patients with recurrent HCC after OLT were included. Fifty-two patients were treated with TACE plus sorafenib (TS group) and 54 were treated with TACE alone (TC group). Primary and secondary endpoints including overall survival (OS) and progression-free survival (PFS), and safety were assessed.

Results: The median OS (17 vs 10 months, P=0.035) and PFS (12 vs 6 months, P=0.004) in the TS group were longer than those in the TC group. On multivariate analysis, BCLC stage (HR [hazard ratio]=0.73 [95% CI, 0.27–0.99], P=0.036) and sorafenib medication (HR=2.26 [95% CI, 1.35–3.69], P=0.01) were identified as independent prognostic risk factors for OS. No severe adverse events related to sorafenib were noted in the TS group. Four patients discontinued sorafenib due to intolerance.

Conclusion: TACE in combination with sorafenib is a feasible regimen to improve the survival with mild toxicity in patients with recurrent HCC after OLT.

KEYWORDS

hepatocellular carcinoma, sorafenib, transarterial chemoembolization, liver transplantation, overall survival

1 Introduction

Globally, hepatocellular carcinoma (HCC) is the third most common cause of cancer-related deaths (1, 2). According to estimates, China accounts for more than half of all deaths attributable to HCC in the world. Owing to the insidious onset of symptoms, most patients with HCC have medium or advanced-stage disease at the time of diagnosis. The natural survival of HCC patients after diagnosis is typically shorter than 6 months (3, 4).

Orthotopic liver transplantation (OLT) is one of the optimal therapeutic options for end-stage liver disease and transplantable HCC (5). The technological advances in drug development have enabled post-OLT five-year survival rates of >75% (6, 7). However, the risk of HCC recurrence is the major concern in transplanted patients. Prior to the development of sorafenib (the recommended molecular targeted drug for HCC), the primary management of recurrent HCC included surgical resection and transarterial chemoembolization (TACE). Several studies have now demonstrated the survival benefit conferred by sorafenib in patients with post-OLT recurrent HCC (8, 9).

Sorafenib, an oral multiple-tyrosine kinase inhibitor, has been shown to be effective in advanced HCC in randomized clinical trials and several small retrospective studies (10–14). A meta-analysis showed that sorafenib plus TACE improved overall survival (OS), time to progression (TTP), and progression-free survival (PFS) in patients with advanced HCC (15–17). However, whether TACE plus sorafenib is a beneficial therapeutic strategy for patients with post-OLT recurrent HCC is not clear (18–20). In this study, we retrospectively analyzed the efficacy and safety of TACE in combination with sorafenib in patients with post-OLT recurrent HCC.

2 Methods

2.1 Study population

Adult (≥18 years) patients who had undergone liver transplantation (transplantation criteria included Milan and Hangzhou criteria) at the Dongfang Hospital, Xiang'an Hospital, and the People's Hospital of Guangxi Zhuang Autonomous Region between January 2009 and December 2015 were screened for eligibility.

Transplantation criteria and immunosuppressants

Milan criteria (13): tumor diameter ≤ 5 cm in patients with single tumor; ≤ 3 tumor nodules, each ≤ 3 cm in diameter in patients with multiple tumors; no major vascular invasion and distant metastasis. For HCC patients that exceeded the Milan criteria, Hangzhou criteria, a system proposed by China Transplantation Society, was employed (21).

Hangzhou criteria: patients without macrovascular invasion who qualify either of the two: (a) total tumor diameter ≤ 8 cm; (b) total tumor diameter > 8 cm, with histopathologic grade I or II and preoperative alpha fetoprotein (AFP) level ≤ 400 ng/mL.

All operations in this study were OLT. The immunosuppressive regimen was steroid tacrolimus plus sirolimus for 3 months post-transplant followed by low-dose tacrolimus plus sirolimus.

The study inclusion criteria were: (a) patients diagnosed with intrahepatic recurrence after transplantation by medical imaging and serum AFP level; (b) recurrent tumor with at least one measurable intrahepatic lesion; (c) survival time ≥ 12 weeks; (d): Child-Pugh classification: A, B (scores ≤ 7); (e): ECOG score: 0–1; (f): patients who received TACE plus sorafenib after recurrence were included in the TS group. Patients who received only TACE were included in the TC group.

Propensity score matching: To reduce the selection bias, a propensity score analysis was employed to minimize imbalanced distribution of treatments and confounders. The treatments were set as the dependent variable and confounders that potentially affect treatment were set as independent variables; then propensity scores were calculated using the software program. One-to-one matching was performed based on the calculated scores to select a propensity score-matched cohort of patients from both groups to compare the outcomes.

The study procedures conformed to the ethical principles enshrined in the Declaration of Helsinki, and were approved by the ethics committees of all three participating hospitals. Owing to the retrospective study design, the requirement for informed consent of individual patients was waived off.

2.2 TACE and sorafenib treatment

Procedure for TACE: The celiac trunk was cannulated using a standard percutaneous 5 French catheter such as the hepatic duct (Cook, Bloomington, USA). Digital subtraction angiography was performed to ensure complete visualization of all tumor vessels. Selective catheterization of the right or left hepatic artery was achieved using a micro-catheter (Cook, Bloomington, USA). A super-selective approach involving tumor-feeding vessels was utilized to minimize the risk of TACE-induced hepatic failure. Oxaliplatin (50–100 mg) and epirubicin (10–20 mg) mixed with 10–20 mL lipiodol were infused within 10 minutes to minimize the side-effects of nausea, vomiting, pain, ototoxicity, nephrotoxicity, and neurotoxicity. In 5 minutes, fluoroscopy was performed to determine whether full embolization of the tumor was achieved. The patients underwent treatment under conscious sedation.

Sorafenib was prescribed orally starting from day 3 post-TACE at an initial dosage of 400 mg/day. The dosage of sorafenib was adjusted according to the patient's tolerance. The adverse events of sorafenib were graded. If the adverse events were ≥ grade 3 without effective remission, the dosage was reduced to 200 mg/day to relieve the adverse events. The drug

was discontinued if the adverse events (≥ grade 3) did not remit after dose-adjustment.

2.3 Data collection

Data pertaining to the following variables were collected: (a) demographic characteristics; (b) clinicopathological parameters including BCLC stage, the diameter and number of tumors, tumor encapsulation, immunosuppressive regimen, Child-Pugh classification, serum AFP level, infection with hepatitis B virus, cirrhosis, complete blood cell counts, urine test, stool test, and coagulation function. The duration of sorafenib medication, PFS, adherence, and death were recorded.

2.4 Endpoint assessment

The follow-up interval was 1–2 months for patients with unstable conditions (generally for the first 6 months) and 3 months for patients with stable conditions. Patients were evaluated using abdominal ultrasound, computed tomography (CT), and magnetic resonance imaging (MRI). Efficacy was determined using the modified response evaluation criteria in solid tumor (mRECIST). The adverse effects of deranged white blood cell count, neutrophil count, hemoglobin, and platelet count, and the occurrence of hand-foot syndrome, diarrhea, hypertension, and rash were recorded. The adverse events were graded according to the classification criteria for common adverse reactions (CTCAE 3.0) of the National Cancer Institute (NCI).

2.5 Statistical analysis

Baseline characteristics of patients in the two groups were compared using the Chi-squared test or Fisher's exact test. Kaplan-Meier method was used for survival analysis and the between-group differences in OS and PFS were assessed using the log-rank and Breslow test. Multivariate analysis of patient survival was performed using the Cox regression model. *P* values < 0.05 were considered indicative of statistical significance. All statistical analyses were performed using the SPSS 19.0 software (Chicago, USA).

3 Results

A total of 504 patients who had undergone OLT were screened. Of these, 293 patients had preoperative HCC. Among these, 159 had no recurrence or had resectable recurrence, and 134 patients had unresectable intrahepatic and/or extrahepatic recurrence diagnosed based on imaging findings and serum AFP level. Seven patients who received only best supportive care (BSC) and eight patients who received only chemotherapy were excluded. After propensity score matching, a total of 106 patients, including 52 patients treated with TACE plus sorafenib (TS group) and 54 patients treated with TACE alone (TC group) were included in this study. A schematic illustration of the study design and patient grouping are depicted in Figure 1.

3.1 Baseline characteristics

The baseline characteristics are presented in Table 1. There was no significant difference between the TS group and TC group with respect to sex (*P*=0.94), age (*P*=0.59), HBV infection (*P*=0.73), cirrhosis (*P*=0.74), serum levels of alanine aminotransferase (*P*=0.42), total bilirubin (*P*=0.43), white blood cell count (WBC, *P*=0.09), platelet count (*P*=0.13) and AFP (*P*=0.33), transplantation criteria (*P*=0.73), pathological grade (*P*=0.41), number of tumors (*P*=0.52), tumor diameter (*P*=0.32), encapsulation (*P*=0.92), BCLC stage (*P*=0.49), Child-Pugh grade (*P*=0.62), or immunosuppressant treatment (tacrolimus, *P*=0.50; sirolimus, *P*=0.67) (Table 1).

3.2 Efficacy assessment

The median overall survival (mOS) was 17 months in the TS group versus 10 months in the TC group (log rank, *P*=0.035; Breslow, *P*=0.005, Figure 2A). The median PFS (mPFS) in the TS group and TC group were 12 months and 6 months, respectively (log rank, *P*=0.004; Breslow, *P*=0.001, Figure 2B). The 1-, 2-, and 3-year OS rates in the TS group were 68.9%, 48.4%, and 35.2%, respectively. The corresponding rates in the TC group were 44.71%, 42.2%, and 19.5%, respectively.

On univariate analysis, BCLC stage (HR=0.70 [95% CI, 0.16–0.98], *P*=0.022) and sorafenib medication (HR=2.94 [95% CI, 1.75–5.16], *P*=0.007) were identified as significant predictors of OS. On multivariate analysis, BCLC stage (HR=0.73 [95% CI, 0.27–0.99], *P*=0.036) and sorafenib medication (HR=2.26 [95% CI, 1.35–3.69], *P*=0.01) were independent risk factors for OS (Table 2). Age, male sex, AFP level, liver cirrhosis, tumor size, and time to recurrence were not identified as risk factors (*P*>0.05).

3.3 Safety assessment

Adverse events considered to be caused by or related to sorafenib are listed in Table 3. The most common adverse effects were decreased hemoglobin (n=16, 30.8%), hand-foot syndrome (16, 30.8%), and rash (18, 34.6%) (Table 3). Other adverse events of sorafenib were leukopenia (14, 26.9%),

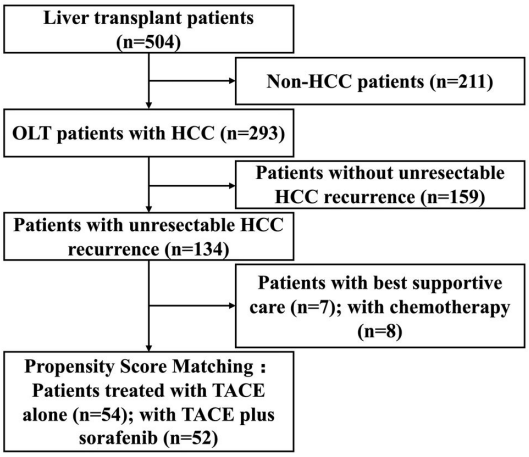

FIGURE 1
Schematic illustration of the study design and patient selection.

thrombocytopenia (15, 28.8%), pruritus (12, 23.1%), hypertension (10, 19.2%), poor appetite (10, 19.2%), paresthesia (10, 19.2%) and alopecia (12, 23.1%). No level 4 adverse effects were observed. Sorafenib was discontinued in four patients.

4 Discussion

Sorafenib alone has been shown to be beneficial in OLT recipients with relapsed HCC (unresectable and not amenable to local treatment). In a retrospective study by Sposito et al., 15 patients with HCC recurrence after liver transplantation received sorafenib, and other 24 patients received BSC (13). The OS and PFS in the sorafenib-treated group were significantly longer than those in the BSC group (OS: 21.3 months vs. 11.8 months, respectively; PFS: 10.6 months vs. 2.2

TABLE 1 Baseline characteristics of patients in the TS and TC groups.

Parameters	TS group (n=52)	TC group (n=54)	*P*
Sex			0.94
Male	46	48	
Female	6	6	
Age			0.59
<60	47	47	
≥60	5	7	
HBV infection			0.73
Yes	43	46	
No	9	8	
Cirrhosis			0.74
Yes	40	43	
No	12	11	
ALT (IU/L)	49.5 ± 11.3	47.8 ± 10.2	0.42
TBil (μmol/L)	13.6 ± 4.8	14.3 ± 4.2	0.43
WBC ($\times10^9$/L)	7.2 ± 1.3	6.8 ± 1.1	0.09
PLT ($\times10^9$/L)	152.8 ± 21.6	159.7 ± 24.3	0.13
Serum AFP (ng/mL)			0.33
≤400	24	30	
>400	28	24	
Transplantation criteria			0.73
Milan	20	19	

(Continued)

TABLE 1 Continued

Parameters	TS group (n=52)	TC group (n=54)	*P*
Hangzhou	32	35	
Pathological grade			0.41
Medium or low	42	40	
High	10	14	
Number of tumors			0.52
1	18	22	
≥2	34	32	
Tumor diameter			0.32
<5 cm	35	41	
≥5 cm	17	13	
Encapsulation			0.92
Yes	41	43	
No	11	11	
BCLC stage			0.49
A	7	5	
B	45	49	
Child-Pugh			0.62
A	35	36	
B	5	7	
Immunosuppressant levels			
Tacrolimus (ng/mL)	4.1 ± 0.7	4.2 ± 0.8	0.50
Sirolimus (ng/mL)	5.1 ± 1.2	5.0 ± 1.2	0.67
Time to recurrence (months)	9 (3–21)	11 (4–25)	0.58

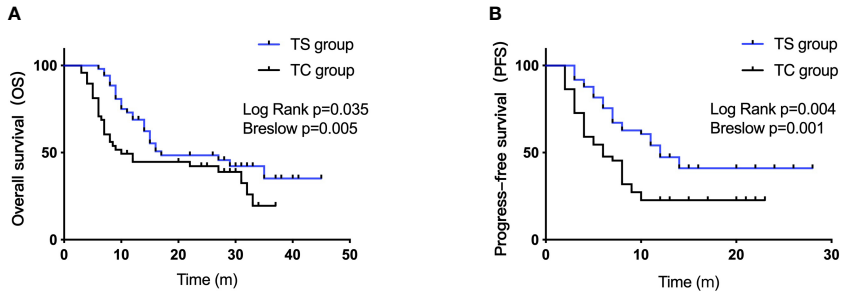

FIGURE 2
OS and PFS in the TS and TC group plotted by Kaplan-Meier method.

TABLE 2 Results of univariate and multivariate analyses showing prognostic factors for OS in patients with post-OLT HCC recurrence.

	Overall survival			
	Univariate		Multivariate	
	HR (95% CI)	*P*	HR (95% CI)	*P*
Age (<60 vs. ≥60)	0.93 (0.82–1.20)	0.65		
Male Sex	0.75 (0.33–1.34)	0.61		
AFP levels (≤400 vs. >400)	0.95 (0.77–2.19)	0.13	0.96 (0.84–2.34)	0.23
Liver cirrhosis	0.92 (0.62–1.82)	0.26		
Tumor size (<5 cm vs. ≥5 cm)	0.63 (0.14–1.41)	0.48		
BCLC stage	0.70 (0.16–0.98)	0.022	0.73 (0.27–0.99)	0.036
Sorafenib	2.94 (1.75–5.16)	0.007	2.26 (1.35–3.69)	0.01

months, respectively). In another retrospective study, patients with untreatable progression (including those who had undergone resection and local-regional treatment) were treated with either sorafenib or BSC; the median survival time in the sorafenib group was longer than that in the BSC group (14.2 vs. 6.8 months, respectively) (22). Additionally, Huang et al. found that in patients with primary hepatic carcinoma exceeding the Milan criteria, sorafenib reduced or delayed tumor recurrence after liver transplantation and improved patient survival with tolerable adverse effects compared with capecitabine (8).

The benefit of TACE plus sorafenib in OLT patients with relapsed HCC amenable to local treatment remains unclear. TACE in combination with sorafenib has been shown to confer a distinct advantage over single therapy in both single-center studies (23) and clinical trials with high level evidence (24–26); therefore, evaluating the efficacy of this therapeutic strategy in the setting of post-OLT HCC recurrence is of much clinical relevance. In this study, the median OS in the TS group was significantly longer than that in the TC group, which demonstrated the benefit of TACE plus sorafenib in this setting. Similar results were observed regarding mPFS. Additionally, there was a marked gap in the 1-, 2-, and 3-year OS rates between the TS group and TC group. Multivariate regression analysis suggested that the sorafenib medication conferred survival benefit. To the best

TABLE 3 Adverse events in the TS group.

Adverse events		Incidence (n, %)			
	Total	Level 0	Level 1	Level 2	Level 3
Leukopenia	14 (26.9%)	1 (1.9%)	5 (9.6%)	5 (9.6%)	3 (5.8%)
Decreased hemoglobin	16 (30.8%)	5 (9.6%)	8 (15.4%)	1 (1.9%)	2 (3.8%)
Thrombocytopenia	15 (28.8%)	8 (15.4%)	4 (7.7%)	2 (3.8%)	1 (1.9%)
Hand-foot syndrome	16 (30.8%)	7 (13.5%)	4 (7.7%)	5 (9.6%)	0 (0%)
Rash	18 (34.6%)	4 (7.7%)	7 (13.5%)	6 (11.5%)	1 (1.9%)
Pruritus	12 (23.1%)	5 (9.6%)	3 (5.8%)	2 (3.8%)	2 (3.8%)
Hypertension	10 (19.2%)	4 (7.7%)	6 (11.5%)	0 (0%)	0 (0%)
Poor appetite	10 (19.2%)	4 (7.7%)	3 (5.8%)	3 (5.8%)	0 (0%)
Nausea	10 (19.2%)	3 (5.8%)	4 (7.7%)	3 (5.8%)	0 (0%)
Vomiting	9 (17.3%)	2 (3.8%)	5 (9.6%)	2 (3.8%)	0 (0%)
Diarrhea	12 (23.1%)	3 (5.8%)	6 (11.5%)	3 (5.8%)	0 (0%)
Paresthesia	10 (19.2%)	4 (7.7%)	3 (5.8%)	3 (5.8%)	0 (0%)
Alopecia	12 (23.1%)	3 (5.8%)	4 (7.7%)	5 (9.6%)	0 (0%)

of our knowledge, this is the first study to demonstrate that TACE plus sorafenib therapy may help improve the outcomes of relapsed HCC after OLT. Our findings suggest the need to conduct larger studies to provide more robust evidence. An accumulating body of evidence has demonstrated the benefit of sorafenib, either as monotherapy or in combination, in patients with recurrent HCC after liver transplantation. Interestingly, preoperative TACE plus sorafenib treatment was found to have a positive effect on the OS of OLT patients with preoperative unresectable HCC compared with TACE alone (27).

The adverse effects of sorafenib call for close monitoring. The major adverse events include myelosuppression, hand-foot syndrome, hypertension, gastrointestinal toxicity, and rash (11, 12). In the TS group, neutropenia, decreased hemoglobin, and thrombocytopenia were frequent. Symptomatic treatment has been shown to relieve the patient's bone marrow suppression (12). Hand-foot syndrome, rash, pruritus, and hypertension were mild and were promptly relieved. In a study of 65 patients with recurrent HCC after liver transplantation, Kang et al. showed that 45 patients treated with sorafenib had longer survival compared to those treated with BSC, and that the toxicity was tolerable. Therefore, despite the adverse effects, sorafenib is recommended in this population and adverse events should be closely observed.

This was a retrospective study with a moderate sample size, which may have introduced confounders that resulted in bias. However, we performed propensity score matching to minimize bias caused by confounding variables. Because of the low incidence of post-OLT HCC recurrence, multi-center, prospective cohort studies are needed to investigate this issue more in depth.

5 Conclusions

In this study, patients treated with TACE plus sorafenib gained therapeutic benefit and exhibited acceptable toxicity. Thus, sorafenib targeted therapy provides an add-on alternative for patients with post-OLT recurrent HCC. A large randomized controlled trial is required to verify these findings.

Data availability statement

The original contributions presented in the study are included in the article/supplementary material. Further inquiries can be directed to the corresponding authors.

Ethics statement

The studies involving human participants were reviewed and approved by the Dongfang Hospital, Xiang'an Hospital, and the People's Hospital of Guangxi Zhuang Autonomous Region. Written informed consent for participation was not required for this study in accordance with the national legislation and the institutional requirements.

Author contributions

Conceptualization XZ, JF, LC, FC. Methodology FP, KZ. Validation QH, DL, LL. Formal analysis MC, RY. Investigation YL. Resources ZW. Data curation YP, YH. Writing—original draft preparation. ZW, XZ. Writing—review and editing ZW, XZ. Project administration FP, JF, KZ. All authors contributed to the article and approved the submitted version.

Funding

The authors are grateful for the support of the Fujian Provincial Social Development Guiding Key Project (2016Y0068); the Science and Technology Innovation Joint Fund Project of Fujian (2019Y9044); the Natural Science Fund of Fujian Province (2020J011131); Hospital-Level Funds of 900th Hospital (2018Q07); the National Natural Science Foundation of China (81572452); the Gandanxiangzhao Fund of the Henan Provincial Charity Federation.

Conflict of interest

The authors declare that the research was conducted in the absence of any commercial or financial relationships that could be construed as a potential conflict of interest.

Publisher's note

References

1. Zeng HM, Cao MM, Zheng RS, Zhangs SW, Cai JQ, Qu CF, et al. [Trend analysis of age of diagnosis for liver cancer in cancer registry areas of China, 2000-2014]. *Zhonghua Yu Fang Yi Xue Za Zhi* (2018) 52(6):573–8. doi: 10.3760/cma.j.issn.0253-9624.2018.06.004

2. Siegel R, Ma J, Zou Z, Jemal A. Cancer statistics, 2014. *CA Cancer J Clin* (2014) 64(1):9–29. doi: 10.3322/caac.21208

3. Zheng R, Peng X, Zeng H, Zhang S, Chen T, Wang H, et al. Incidence, mortality and survival of childhood cancer in China during 2000-2010 period: A population-based study. *Cancer Lett* (2015) 363(2):176–80. doi: 10.1016/j.canlet.2015.04.021

4. Gish RG, Marrero JA, Benson AB. A multidisciplinary approach to the management of hepatocellular carcinoma. *Gastroenterol Hepatol (N Y)* (2010) 6(3 Suppl 6):1–16.

5. Cillo U, Vitale A, Volk ML, Frigo AC, Grigoletto F, Brolese A, et al. The survival benefit of liver transplantation in hepatocellular carcinoma patients. *Dig Liver Dis* (2010) 42(9):642–9. doi: 10.1016/j.dld.2010.02.010

6. Song P, Gao J, Inagaki Y, Kokudo N, Hasegawa K, Sugawara Y, et al. Biomarkers: evaluation of screening for and early diagnosis of hepatocellular carcinoma in Japan and china. *Liver Cancer* (2013) 2(1):31–9. doi: 10.1159/000346220

7. Song P. Standardizing management of hepatocellular carcinoma in China: devising evidence-based clinical practice guidelines. *Biosci Trends* (2013) 7(5):250–2. doi: 10.5582/bst.2013.v7.5.250

8. Huang L, Li GM, Zhu JY, Li Z, Li T, Leng XS. Efficacy of sorafenib after liver transplantation in patients with primary hepatic carcinoma exceeding the Milan criteria: A preliminary study. *Onco Targets Ther* (2012) 5:457–62. doi: 10.2147/OTT.S31387

9. Zhang Q, Chen H, Li Q, Zang Y, Chen X, Zou W, et al. Combination adjuvant chemotherapy with oxaliplatin, 5-fluorouracil and leucovorin after liver transplantation for hepatocellular carcinoma: A preliminary open-label study. *Invest New Drugs* (2011) 29(6):1360–9. doi: 10.1007/s10637-011-9726-1

10. Estfan B, Byrne M, Kim R. Sorafenib in advanced hepatocellular carcinoma: hypertension as a potential surrogate marker for efficacy. *Am J Clin Oncol* (2013) 36(4):319–24. doi: 10.1097/COC.0b013e3182468039

11. Llovet JM, Ricci S, Mazzaferro V, Hilgard P, Gane E, Blanc JF, et al. Sorafenib in advanced hepatocellular carcinoma. *N Engl J Med* (2008) 359(4):378–90. doi: 10.1056/NEJMoa0708857

12. Cheng AL, Kang YK, Chen Z, Tsao CJ, Qin S, Kim JS, et al. Efficacy and safety of sorafenib in patients in the Asia-pacific region with advanced hepatocellular carcinoma: A phase III randomised, double-blind, placebo-controlled trial. *Lancet Oncol* (2009) 10(1):25–34. doi: 10.1016/S1470-2045(08)70285-7

13. Sposito C, Mariani L, Germini A, Flores Reyes M, Bongini M, Grossi G, et al. Comparative efficacy of sorafenib versus best supportive care in recurrent hepatocellular carcinoma after liver transplantation: A case-control study. *J Hepatol* (2013) 59(1):59–66. doi: 10.1016/j.jhep.2013.02.026

14. Waidmann O, Hofmann WP, Zeuzem S, Trojan J. mTOR inhibitors and sorafenib for recurrent heptocellular carcinoma after orthotopic liver transplantation. *J Hepatol* (2011) 54(2):396–8. doi: 10.1016/j.jhep.2010.08.038

15. Zhang L, Hu P, Chen X, Bie P. Transarterial chemoembolization (TACE) plus sorafenib versus TACE for intermediate or advanced stage hepatocellular carcinoma: A meta-analysis. *PloS One* (2014) 9(6):e100305. doi: 10.1371/journal.pone.0100305

16. Wang SN, Chuang SC, Lee KT. Efficacy of sorafenib as adjuvant therapy to prevent early recurrence of hepatocellular carcinoma after curative surgery: A pilot study. *Hepatol Res* (2014) 44(5):523–31. doi: 10.1111/hepr.12159

17. Mazzaferro V, Bhoori S, Sposito C, Bongini M, Langer M, Miceli R, et al. Milan Criteria in liver transplantation for hepatocellular carcinoma: An evidence-based analysis of 15 years of experience. *Liver Transpl* (2011) 17 Suppl 2:S44–57. doi: 10.1002/lt.22365

18. Wilhelm SM, Carter C, Tang L, Wilkie D, McNabola A, Rong H, et al. BAY 43-9006 exhibits broad spectrum oral antitumor activity and targets the RAF/MEK/ERK pathway and receptor tyrosine kinases involved in tumor progression and angiogenesis. *Cancer Res* (2004) 64(19):7099–109. doi: 10.1158/0008-5472.CAN-04-1443

19. Di Marco V, De Vita F, Koskinas J, Semela D, Toniutto P, Verslype C. Sorafenib: from literature to clinical practice. *Ann Oncol* (2013) 24 Suppl 2:ii30–37. doi: 10.1093/annonc/mdt055

20. Iavarone M, Cabibbo G, Piscaglia F, Zavaglia C, Grieco A, Villa E, et al. Field-practice study of sorafenib therapy for hepatocellular carcinoma: A prospective multicenter study in Italy. *Hepatology* (2011) 54(6):2055–63. doi: 10.1002/hep.24644

21. Chen J, Xu X, Wu J, Ling Q, Wang K, Wang W, et al. The stratifying value of hangzhou criteria in liver transplantation for hepatocellular carcinoma. *PloS One* (2014) 9(3):e93128. doi: 10.1371/journal.pone.0093128

22. Kang SH, Cho H, Cho EJ, Lee J-H, Yu SJ, Kim YJ, et al. Efficacy of sorafenib for the treatment of post-transplant hepatocellular carcinoma recurrence. *J Korean Med Sci* (2018) 33(45):e283. doi: 10.3346/jkms.2018.33.e283

23. Varghese J, Kedarisetty C, Venkataraman J, Srinivasan V, Deepashree T, Uthappa M, et al. Combination of TACE and sorafenib improves outcomes in BCLC stages B/C of hepatocellular carcinoma: A single centre experience. *Ann Hepatol* (2017) 16(2):247–54. doi: 10.5604/16652681.1231583

24. Lencioni R, Llovet JM, Han G, Tak WY, Yang J, Guglielmi A, et al. Sorafenib or placebo plus TACE with doxorubicin-eluting beads for intermediate stage HCC: The SPACE trial. *J Hepatol* (2016) 64(5):1090–8. doi: 10.1016/j.jhep.2016.01.012

25. Kudo M, Ueshima K, Ikeda M, Torimura T, Tanabe N, Aikata H, et al. Randomised, multicentre prospective trial of transarterial chemoembolisation (TACE) plus sorafenib as compared with TACE alone in patients with hepatocellular carcinoma: TACTICS trial. *Gut* (2020) 69(8):1492–501. doi: 10.1136/gutjnl-2019-318934

26. Yang M, Yuan JQ, Bai M, Han GH. Transarterial chemoembolization combined with sorafenib for unresectable hepatocellular carcinoma: A systematic review and meta-analysis. *Mol Biol Rep* (2014) 41(10):6575–82. doi: 10.1007/s11033-014-3541-7

27. Abdelrahim M, Victor D, Esmail A, Kodali S, Graviss EA, Nguyen DT, et al. Transarterial chemoembolization (TACE) plus sorafenib compared to TACE alone in transplant recipients with hepatocellular carcinoma: An institution experience. *Cancers (Basel)* (2022) 14(3):650. doi: 10.3390/cancers14030650

frontiers | Frontiers in Oncology

TYPE Review
PUBLISHED 16 January 2023
DOI 10.3389/fonc.2022.1091088

OPEN ACCESS

EDITED BY
Xiong Chen,
Nanjing General Hospital of Nanjing Military Command, China

REVIEWED BY
Eleonora Lai,
University Hospital and University of Cagliari, Italy
Fucun Xie,
Peking Union Medical College Hospital (CAMS), China

*CORRESPONDENCE
Aiping Zhou
aiping_zhou@yeah.net

SPECIALTY SECTION
This article was submitted to Gastrointestinal Cancers: Hepato Pancreatic Biliary Cancers, a section of the journal Frontiers in Oncology

RECEIVED 06 November 2022
ACCEPTED 20 December 2022
PUBLISHED 16 January 2023

CITATION
Peng X, Gong C, Zhang W and Zhou A (2023) Advanced development of biomarkers for immunotherapy in hepatocellular carcinoma. *Front. Oncol.* 12:1091088. doi: 10.3389/fonc.2022.1091088

Advanced development of biomarkers for immunotherapy in hepatocellular carcinoma

Xuenan Peng, Caifeng Gong, Wen Zhang and Aiping Zhou*

Department of Medical Oncology, National Cancer Center/National Clinical Research Center for Cancer/Cancer Hospital, Chinese Academy of Medical Sciences and Peking Union Medical College, Beijing, China

Hepatocellular carcinoma (HCC) is the most common liver cancer and one of the leading causes of cancer-related deaths in the world. Mono-immunotherapy and combination therapy with immune checkpoint inhibitors (ICIs) and multitargeted tyrosine kinase inhibitors (TKIs) or anti-vascular endothelial growth factor (anti-VEGF) inhibitors have become new standard therapies in advanced HCC (aHCC). However, the clinical benefit of these treatments is still limited. Thus, proper biomarkers which can predict treatment response to immunotherapy to maximize clinical benefit while sparing unnecessary toxicity are urgently needed. Contrary to other malignancies, up until now, no acknowledged biomarkers are available to predict resistance or response to immunotherapy for HCC patients. Furthermore, biomarkers, which are established in other cancer types, such as programmed death ligand 1 (PD-L1) expression and tumor mutational burden (TMB), have no stable predictive effect in HCC. Thus, plenty of research focusing on biomarkers for HCC is under exploration. In this review, we summarize the predictive and prognostic biomarkers as well as the potential predictive mechanism in order to guide future research direction for biomarker exploration and clinical treatment options in HCC.

KEYWORDS

hepatocellular carcinoma, immunotherapy, combination therapy, biomarker, tumor immune microenvironment

Introduction

Hepatocellular carcinoma (HCC) is the most common primary liver cancer and mostly develops on a background of chronic liver disease (1). Most patients were diagnosed at an advanced stage and/or had underlying chronic liver disease, with no opportunity to receive liver resection and transplantation. Moreover, even diagnosed at an early stage, the recurrence rates remain at about 70% in 5 years after surgery (2). Systemic treatment options for advanced HCC (aHCC) by multitargeted tyrosine kinase

inhibitors (TKIs) of sorafenib, lenvatinib, regorafenib, cabozantinib, and ramucirumab have improved aHCC patients' survival in a certain degree. However, the overall survival (OS) is merely 10.7-13.6 months (3–7), far from clinical expectation. In recent years, immune checkpoint inhibitors (ICIs) including nivolumab and pembrolizumab have shown survival benefits and have been approved by the United States Food and Drug Administration (FDA) for aHCC treatment (8, 9). Since 2020, anti-programmed death 1 (anti-PD-1) antibodies such as camrelizumab and tislelizumab have been successively approved by National Medical Products Administration (NMPA) as second-line treatment regimens for HCC patients (10, 11). The IMbrave150 trial achieved an improvement in OS of up to 19.2 months with atezolizumab and bevacizumab combination therapy, making it the standard first-line treatment for aHCC (12, 13). Regrettably, the objective response rate (ORR) of combination therapy was only about 30% (14). In addition, approximately 5%–30% of patients develop ≥ grade 3 immune-related adverse events (irAEs) (14). Therefore, proper biomarkers used to predict patient clinical response and spare unnecessary toxicity are urgently needed. Although no widely accepted biomarkers have been identified currently, multidimensional analyses of potential biomarkers for immunotherapy of HCC have been under exploration. In this review, we aim to summarize the predictive and prognostic biomarkers from multiple dimensions to guide future biomarker exploration in HCC (Figure 1).

Circulating biomarkers in peripheral blood

NLR and PLR

Human neutrophils and platelets produce a host of cytokines and growth factors relevant to tumor growth and progression (15–25). Neutrophil-to-lymphocyte ratio (NLR) and platelet-to-lymphocyte ratio (PLR) have been reported as predictive factors in several cancer types (26–34). Elevated NLR and PLR were also found to be associated with poor response to transarterial chemoembolization (TACE) and sorafenib treatment in HCC (35–41). As for immunotherapy in HCC, the same predictive effect has also been reported. In a subcohort of 242 patients in the CheckMate 040 trial, patients with NLR in the low tertile showed better OS than those with medium or high tertile (p = 0.015) (42). A similar result was observed in PLR (p = 1.38e−07). Patients with complete response or partial response (CR/PR) had lower PLR than those with progressive disease (PD) (p = 0.05). In another cohort of 194 aHCC patients treated with nivolumab, those with baseline NLR ≥3 presented poorer progression-free survival (PFS) [11.0 vs. 7.1 weeks; HR = 1.52 (95% CI 1.11–2.07), p = 0.01] and OS [61.3 vs. 21.0 weeks; HR = 2.72 (95% CI 1.86–3.99), p < 0.001]. Moreover, a dynamic increase of NLR at 4 weeks was associated with an increased risk of death [HR = 1.79, 95% CI (1.19–2.68)]. Interestingly, in this study, NLR increased at 4 weeks also had a role in predicting hyperprogressive disease (HPD), which may guide treatment plan in an early phase (43). In a cohort of 362 HCC patients treated with mono or combination immunotherapy, patients with higher NLR and PLR at baseline were reported to have a higher incidence of portal vein thrombosis (PVT), higher Eastern Cooperative Oncology Group (ECOG) performance status, and more advanced Barcelona Clinic Liver Cancer (BCLC) stage. Significantly shorter OS and PFS were observed in patients with NLR ≥5 (OS: 7.7 vs. 17.6 months, p < 0.0001; PFS: 2.1 vs. 3.8 months, p = 0.03) and PLR ≥300 (OS: 6.7 vs.16.5 months, p < 0.0001; PFS: 1.8 vs. 3.7 months, p = 0.0006) (44). On the basis of the independent predictive role for OS of NLR and PLR, Schobert et al. found that the combination of high NLR and PLR was associated with an eightfold increased risk of death (40).

In conclusion, several analyses in different trials have demonstrated the strong survival predictive power of NLR and PLR in HCC immunotherapy and their predictive trend in treatment response. As for potential mechanisms, some reported that IL-8 and other tumor growth factors secreted by tumors may promote neutrophil recruitment (45). The increasing circulating and intratumoral neutrophils can further secrete vascular endothelial growth factor (VEGF), thereby causing higher levels of VEGF in the tumors (46) and promoting angiogenesis.

AFP and CRP

Alpha-fetoprotein (AFP) is widely used for the surveillance, diagnosis, and prognostication of HCC. In recent decades, several studies have been conducted to explore its additional roles, such as being employed for defining HCC molecular classes or as biomarkers for HCC treatment (47–51). In a cohort of 99 patients who received nivolumab or pembrolizumab, those with AFP <400 μg/L at the beginning of ICI treatment were more likely to achieve a higher rate of CR or PR than those with AFP ≥400 μg/L (24% vs. 13%). Patients with baseline serum AFP <400 μg/L presented longer PFS (5.4 vs. 2.6 months, p < 0.05) and OS (21.8 vs. 8.7 months, p < 0.0001) (52). Moreover, a simple and easily applicable score called C-reactive protein (CRP) and AFP in Immunotherapy (CRAFITY) constructed by the analysis of 190 aHCC patients who received mono or combination immunotherapy based on CRP and AFP was recently reported (53). In this score, AFP ≥100 ng/ml and CRP ≥1 mg/dl were both assigned 1 point. Patients could achieve either 0, 1, or 2 points depending on the level of these two variables. Results showed that baseline serum AFP ≥100 ng/ml and CRP ≥1 mg/dl were independently associated with worse

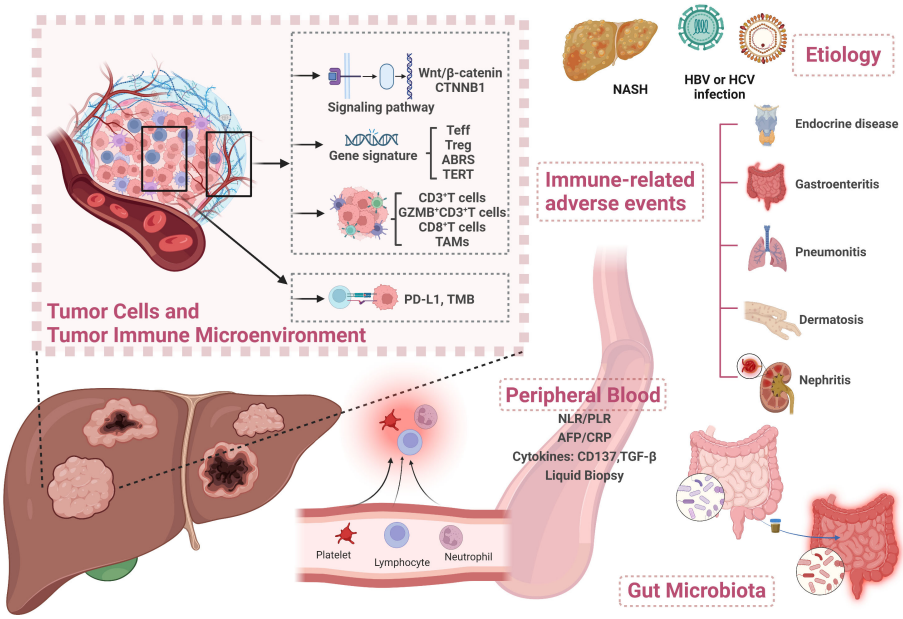

FIGURE 1
Overview of biomarkers for predicting treatment response to immunotherapy in HCC. Created with BioRender.com. Teff, T effector; ABRS, atezolizumab + bevacizumab response signature; TAM, tumor-associated macrophage; PD-L1, programmed death ligand 1; TMB, tumor mutational burden; NLR, neutrophil-to-lymphocyte ratio; PLR, platelet-to-lymphocyte ratio; AFP, alpha-fetoprotein; CRP, C-reactive protein; TGF-β, transforming growth factor-β; HBV, hepatitis B virus; HCV, hepatitis C virus; NASH, non-alcoholic steatohepatitis.

OS in ICI-treated patients with HCC. The median OS of patients with 0 points (CRAFITY - low) (n = 53), 1 point (CRAFITY - intermediate) (n = 75), and 2 points (CRAFITY - high) (n = 62) were 27.6 vs. 11.3 vs. 6.4 months ($p < 0.001$). In addition, a high CRAFITY score also predicted a worse radiological response, and the disease control rate (DCR) was 80% vs. 64% vs. 39% for a score of 0, 1, and 2, respectively ($p < 0.001$). Yang et al. further verified the CRAFITY score in TKI plus immunotherapy and lenvatinib monotherapy cohorts. A high score successfully predicts worse OS and a trend toward worse ORR and DCR (54). This simple prognostic score facilitates early survival evaluation of immunotherapy treatment and is promising to be adopted in clinical application. However, CRP is an acute-phase protein which may increase after injury or infection. Diseases which may increase CRP levels should be considered before score application.

Cytokines

Transforming growth factor-β

Transforming growth factor-β (TGF-β) is known as an immunosuppressive and fibrotic cytokine. Approximately 38% of HCC patients have somatic mutations in the TGF-β pathway (55). High TGF-β levels present more aggressive tumor characteristics and may also cause T-cell exhaustion by upregulating PD-1 signaling in HCC, which demonstrates a specific immunosuppressive role of TGF-β in mediating immunotherapy resistance (56–59). Feun et al. conducted a phase 2 study of pembrolizumab in 29 patients (24 provided plasma samples) with aHCC. In the biomarker analyses, plasma TGF-β levels in responders [those with CR/PR/stable disease (SD)] were lower than those in non-responders (141.9 vs. 1,071.8 pg/ml, p = 0.004). Survival analysis showed that patients with plasma TGF-β ≥200 pg/ml had significantly shorter PFS (2 vs. over 25 months, p = 0.008) and OS (7 vs. over 25 months, p = 0.005), indicating that higher TGF-β levels were associated with poor treatment outcomes (60). This suggests that high plasma TGF-β may be a potential biomarker for poor treatment response and outcome to immunotherapy, which may be related to the tumor microenvironment of decreased T-cell infiltration in tumors shaped by TGF-β (61). However, the role of TGF-β in HCC is still in the exploratory stage, and its predictive value needs to be further confirmed in large-scale studies.

CD137

CD137, also known as 4-1BB or TNF receptor superfamily member 9 (TNFRSF9), is a member of the tumor necrosis factor family and an important costimulatory molecule in the process of T-cell activation, which can enhance the antitumor effects of T cells (62). CD137 is mainly expressed by activated $CD4^+$ and $CD8^+$ T cells (63), it is also found on the surfaces of NK cells, neutrophils, dendritic cells, and monocytes (64, 65). The

expression of CD137 in HCC was higher than that in other types of cancer (e.g., small cell lung cancer and colorectal cancer) and was found to be expressed predominantly on exhausted PD-$1^{high}CD8^+$ T cells (66), as well as activated T cells in peripheral blood samples (67, 68). Preclinical studies have found a synergistic antitumor activity between PD-1/programmed death ligand 1 (PD-L1) inhibitors and activation of the CD137 signaling pathway (69). The increased number of $CD137^+CD8^+$ T cells in peripheral blood was correlated with longer disease-free survival (DFS) in patients with melanoma who were treated with ipilimumab plus nivolumab (70). A study recently conducted on 50 aHCC patients who received sintilimab (a PD-1 inhibitor) plus IBI305 reported the potential predictive role of serum CD137. Among 33 patients with serum CD137 detected, the CD137 concentration was significantly higher in patients with clinical benefit (CB, patients with CR/PR, or SD ≥12 weeks) than in those with non-CB (patients with PD or SD <12 weeks) (32.8 vs. 19.8 pg/ml, $p = 0.034$). Markedly longer PFS (14.2 vs. 4.1 months, $p < 0.001$) and OS (undefined vs. 15.6 months, $p = 0.023$) were observed in patients with high CD137 concentrations (71). However, relevant studies are mainly small sample research. Its predictive role remains to be further explored.

Liquid biopsy

HCC exhibits significant heterogeneity from genetic aberrations and transcriptional and epigenetic dysregulation. A single biopsy specimen containing a small amount of tumor tissue may not be representative of the whole tumor (72). In recent years, liquid biopsy techniques have been developed to collect samples from patients' body fluids to obtain phenotypic, genetic, and transcriptomic information about the primary tumor (73). The primary forms of liquid biopsy include circulating tumor cells (CTCs), circulating tumor DNA (ctDNA), microRNA, and extracellular vesicles (74–77).

Circulating tumor cells

CTCs are malignant cells derived from either the primary or metastasis tumor that migrate into the systemic circulation, which represents a heterogeneous population of cells from the tumor. CTCs have been shown to be a reliable predictor of metastatic prostate cancer and breast cancer (78–81). A recent study conducted on HCC patients, of which 10 patients received anti-PD-1 therapy (9 with nivolumab and 1 with pembrolizumab), reported that all patients ($n = 4$) who did not have PD-L1+CTCs were non-responders (patients with PD or died within 6 months from initiating treatment). Meanwhile, all responders (patients with PR/SD) had PD-L1+CTCs detected at baseline. A longer OS was also found in PD-L1+CTC patients even after controlling for other factors [HR = 3.22 (95%CI 1.33-7.79), $p = 0.01$] (82). However, in a study of 47 HCC patients receiving a PD-1 inhibitor in combination with antiangiogenic therapy and radiotherapy, patients with low PD-L1+CTCs at baseline had a higher ORR (56.5% vs. 16.7%, $p = 0.007$) and longer OS (not reached vs. 10.8 months, $p = 0.001$) than those with high PD-L1+CTCs (83), indicating that CTC is still a controversial biomarker for predicting the treatment response to immunotherapy in HCC. As a result, larger sample studies are required to further explore its predictive value. Meanwhile, an extremely rare frequency of CTCs has been found in the circulation. All of these reasons make the detection of CTCs in the early stage of disease challenging (84).

Circulating tumor DNA

Circulating tumor DNA (ctDNA) can arise in the bloodstream of cancer patients as a result of tumor cell apoptosis or necrosis (85). ctDNA contains cancer-associated molecular characteristics, which allow its discrimination from total normal circulating cellular free DNA (86–88). In a subset of GO30140 arm A of 45 patients, higher ctDNA levels at baseline were associated with an increased baseline tumor burden ($p < 0.03$). After 3 cycles of treatment, ctDNA turned negative in 70% (CR), 27% (PR), 9% (SD), and 0% (PD) of patients, respectively. Patients with ctDNA cleared after 3 cycles of treatment showed longer PFS compared with those still present (6.5 vs. not reached months, $p < 0.00029$) (89). Patients with lower copy number variations (CNVs) in cell-free DNA risk score were also found to have longer OS and PFS in the ICI-treated cohort (90). Moreover, tumor mutational burden (TMB) evaluated by ctDNA was reported to be highly consistent with TMB detected by tissues (91), suggesting that ctDNA analysis could be an alternative option to evaluate TMB prior to immunotherapy in aHCC patients to whom tissue biopsy was not recommended if necessary. Table 1 provides a brief overview of the biomarkers in peripheral blood for HCC immunotherapy.

Tumor tissue-related biomarkers

Tumor immune microenvironment

The HCC tumor immune microenvironment (TiME) is acknowledged for its immunosuppressive character. The crosstalk between tumor cells and the immune microenvironment promotes tumor proliferation, invasion, and metastasis (92). Recent advances in basic and translational research have shown that the different manifestations of the tumor microenvironment are closely related to the efficacy of immunotherapy, revealing that the TiME profile may be a valuable potential biomarker of immunotherapy (14).

Analyses of patients treated with atezolizumab plus bevacizumab in the GO30140 arm A cohort showed that responders (CR/PR) had a higher density of infiltrating $CD8^+$ T cells, $CD3^+$ T cells, and $GZMB^+CD3^+$ T cells in tumor areas than

non-responders (SD/PD) (p = 0.007, p = 0.039, and p = 0.044, respectively). The high presence of several immune subsets, including CD8 and CD4 T cells, Tregs, B cells, and dendritic cells, also seemed to be associated with better response and longer PFS (93). In the IMbrave150 cohort, patients with a high density of intratumoral $CD8^+$ T cells showed longer OS [HR = 0.29 (95% CI 0.14–0.61), p = 0.001] and PFS [HR = 0.54 (95% CI 0.29–1.00), p = 0.053] in atezolizumab plus bevacizumab compared with sorafenib. The reason may be that blockade of the PD-1/PD-L1 axis could restore the antitumor immunity induced by $CD8^+$ lymphocytes in tumors (94). The results above demonstrated that patients with pre-existing immunity seemed to possess improved clinical outcomes to combination therapy. An exploratory research in CheckMate 040 analyzed the levels of multiple inflammation biomarkers and their association between treatment response and survival to nivolumab in patients previously treated with or without sorafenib (42). The results showed that patients with CR/PR had higher $CD3^+$ T cells compared with those with SD (p = 0.03). Those with higher tumor-infiltrating $CD3^+$ and $CD8^+$ T cells showed a trend toward improved OS (both p = 0.08).

Macrophages are major components of the TiME, which can be classified into two main subtypes: the classically activated macrophages (M1 macrophages) with pro-inflammatory functions and the alternatively activated macrophages (M2 macrophages) with immunosuppressive functions (95). Several tumor-promoting roles, such as immune suppression, cancer invasion and metastasis, angiogenesis, maintenance of cancer cell stemness, and drug resistance, have been attributed to these tumor-associated macrophages (TAMs), especially M2 macrophages (96, 97). A previous study had shown that high levels of M2 macrophages have been associated with poor prognosis in patients with HCC (98). Although the expression of $CD68^+$ and $CD163^+$ (M2 macrophages) cells has no association with either treatment response or OS in the CheckMate 040 subgroup (42), the other study reported that a higher density of M1 macrophages ($CD68^+CD163^-$) in the stroma was associated with better efficacy and longer PFS (M1 macrophages low vs. high: 11.4 vs. 3.0 months, p = 0.024) and OS (M1 macrophages low vs. high: undefined vs. 17.5 months, p = 0.046) (71). Therefore, a better understanding of the mechanisms underlying the function of TAMs is necessary for the development of novel TAM-targeting immunological interventions, which may provide promising therapeutic approaches for HCC patients. Collectively, immunocytes with different functions can directly reflect tumor immune status. This advantage makes it become the main research direction at present. More mechanistic research is expected to be further carried out.

Signaling pathway and gene signature

As important regulatory factors in tumor progression and the immune environment, the correlation between molecular features and treatment efficacy has become the focus of recent research. In the GO30140 group A cohort, pathways and immune subsets were identified by genome-wide differentially expressed genes (DEGs), gene set enrichment analysis (GSEA), and xCell analyses. An atezolizumab + bevacizumab response signature (ABRS) consisting of the top 10 genes from the DEG analyses (namely, *CXCR2P1*, *ICOS*, *TIMD4*, *CTLA4*, *PAX5*, *KLRC3*, *FCRL3*, *AIM2*, *GBP5*, and *CCL4*) was found consistently higher in patients with CR/PR than in those with SD/PD, as well as the T effector (Teff) signature (*CXCL9*, *PRF1*, and *GZMB*). Patients with a high expression of these markers had longer PFS than those with low expression [ABRS: HR = 0.51 (95% CI 0.30–0.87), p = 0.013; Teff signature: HR = 0.46 (95% CI 0.27–0.78), p = 0.0035], which was further validated in the IMbrave150 cohort. Patients with high ABRS or the Teff signature showed improved PFS [ABRS: HR = 0.49 (95% CI 0.25–0.97), p = 0.041; Teff signature: HR = 0.52 (95% CI 0.28–0.99), p = 0.047] and OS [ABRS: HR = 0.26 (95% CI 0.11–0.58), p = 0.0012; Teff signature: HR = 0.24 (95% CI 0.11–0.5), p = 0.0002] when treated with atezolizumab + bevacizumab compared with sorafenib. Signature analysis in IMbrave150 revealed that a low ratio of Treg/Teff signatures was associated with improved PFS [HR = 0.42 (95% CI 0.22–0.79), p = 0.007] and OS [HR = 0.24 (95% CI 0.11–0.54), p = 0.0006] when treated with atezolizumab + bevacizumab compared with sorafenib. As for the mutation landscape, *TERT* promoter mutations were observed in 56.2% of patients in the IMbrave150 trial. The benefit of atezolizumab + bevacizumab was more pronounced in patients with *TERT*-mutant than in the sorafenib group [PFS: HR = 0.61 (95% CI 0.33–1.10), p = 0.047; OS: HR = 0.38 (95% CI 0.16–0.89), $p = 7.8 \times 10^{-5}$] (93).

Hyperactive Wnt/β-catenin signaling is implicated in the initiation and progression of various types of cancer, which may be related to the exclusion of $CD8^+$ cells in tumor tissues in melanoma cases (99). *CTNNB1* which is involved in the Wnt/β-catenin signaling pathway is a prevalent mutation gene in HCC (100). Approximately 11%–41% of liver malignancies harbor *CTNNB1*-activating mutations (93, 101–104). Several studies have shown that β-catenin signaling may mediate the immune escape of cancer cells and the resistance to ICIs (99, 105, 106). In the IMbrave150 trial, patients with wild-type *CTNNB1* showed greater treatment effect with atezolizumab + bevacizumab than sorafenib [PFS: HR = 0.45 (95% CI 0.27–0.86), p = 0.0086; OS: HR = 0.42 (95% CI 0.19–0.91), $p = 3 \times 10^{-4}$) (93). A small sample cohort of 34 patients who were treated with anti-PD-1 monotherapy with or without previous treatment with sorafenib found that although patients with negative Wnt/β-catenin activation, high $CD8^+$ TIL infiltration, and high PD-L1-CPS showed higher DCR, PFS, and OS in the univariate analysis, no significant difference was presented after the multivariate analysis. However, the combination of these factors well stratified the survival in both PFS ($p < 0.0001$) and OS (p = 0.0048), suggesting that in patients lacking β-catenin activation, blockade of the PD-1/PD-L1 axis might overcome the presence

TABLE 1 Predictive or prognostic biomarkers in peripheral blood for HCC immunotherapy.

Biomarkers	Treatment	Line of treatment	Number of detected patients	Cutoff value	Outcomes	Year	Ref.
NLR and PLR	Nivolumab (CheckMate 459: NCT02576509)	First-line or previously treated with sorafenib	NLR (*N* = 242); PLR (*N* = 243)	Tertile	Baseline lower NLR and PLR were associated with CR/PR and better OS	2020	(42)
	Nivolumab	Second-line (*N* = 129); third- or later-line (*N* = 65)	Baseline NLR (*N* = 194); dynamic NLR (*N* = 194)	NLR = 3	Patients with baseline NLR ≥3 had poorer PFS and OS; NLR increased rapidly in patients developing HPD; NLR increase at 4 weeks was associated with an increased risk of death, especially among patients with baseline NLR ≥3	2021	(43)
	Mono-immunotherapy and combination therapy	49% of patients with second-line therapy	Monotherapy (*N* = 310); combination therapy (*N* = 52)	NLR = 5; PLR = 300	Patients with higher NLR (≥5) and PLR (≥300) at baseline were reported having a higher incidence of PVT, higher ECOG performance status, more advanced BCLC stage, and shorter PFS and OS	2022	(44)
	Nivolumab	First-line (*N* = 66); subsequent-line (*N* = 37)	*N* = 103	NLR = 5; PLR tertiles	The combination of high NLR and PLR was found associated with an eightfold increased risk of death	2020	(40)
AFP and CRP	Nivolumab (*N* = 67); pembrolizumab (*N* = 32)	First-line (*N* = 13); subsequent-line (*N* = 86)	*N* = 99	AFP = 400 μg/L	Baseline AFP <400 μg/L was associated with better treatment response and longer PFS	2020	(52)
	Mono-immunotherapy and combined therapy	Training cohort: first-line (*N* = 82), subsequent-line (*N* = 108) Validation cohort: first-line (*N* = 35), subsequent-line (*N* = 67)	Training cohort (*N* = 190); validation cohort (*N* = 102)	AFP ≥100 ng/ml; CRP ≥1 mg/dl	Baseline serum AFP ≥100 ng/ml and CRP ≥1 mg/dl were independently associated with worse DCR and OS	2022	(53)
	TKI plus immunotherapy combination and lenvatinib monotherapy	Unknown	Combination cohort (*N* = 108); lenvatinib-treated cohort (*N* = 72)	AFP ≥100 ng/ml; CRP ≥1 mg/dl	Patients with baseline serum AFP ≥100 ng/ml and CRP ≥1 mg/dl showed worse OS and a trend toward lower ORR and DCR in the combination and the lenvatinib-treated cohorts	2022	(54)
TGF-β	Combination of TGF-β inhibition and immunotherapy	Unknown	Transcriptomic analyses (*N* = 193); pathway analyses (*N* = 70)	Unknown	A highly activated TGF-β signature was significantly associated with fibrosis and activated stromal signatures; TGF-β signature subtypes were significantly associated with immune cell infiltration and T-cell exhaustion	2020	(59)
	Pembrolizumab (NCT02658019)	Second-line	*N* = 24	TGF-β = 200 pg/ml	Patients with baseline TGF-β <200 pg/ml presented higher OS and PFS	2019	(60)
CD137	Sintilimab plus IBI305 (NCT04072679)	First-line	*N* = 33	CD137 = 31.8 pg/ml	CD137 concentration was significantly higher in patients with CB than in patients with non-CB	2022	(71)
CTC	Nivolumab (*N* = 9); pembrolizumab (*N* = 1)	First-line and	*N* = 10	Unknown	All patients (*n* = 4) who did not have PD-L1+CTCs were non-responders; meanwhile, all responders had PD-L1+CTCs detected at baseline; PD-L1+CTCs	2020	(82)

(Continued)

TABLE 1 Continued

Biomarkers	Treatment	Line of treatment	Number of detected patients	Cutoff value	Outcomes	Year	Ref.
		subsequent-line			patients had longer OS after controlling for other factors		
	PD-1 inhibitor combined with radiotherapy and antiangiogenic therapy	First-line and subsequent-line	*N* = 47	2 PD-L1 +CTCs	Patients with low PD-L1+CTCs at baseline had a higher ORR and longer OS than those with high PD-L1+CTCs	2022	(83)
ctDNA	Atezolizumab plus bevacizumab	First-line	*N* = 45	70.6 mean tumor molecules/ml of plasma (MTM/ml)	Higher ctDNA levels at baseline were associated with an increased baseline tumor burden; patients with ctDNA that cleared after 3 cycles of treatment showed longer PFS	2020	(89)
	Combination therapy of PD-1 inhibitor with lenvatinib and immune monotherapy	First-line and subsequent-line	Combination therapy (*N* = 43); immune monotherapy (*N* = 108)	CNV risk score: 15.68	Patients with lower CNVs had longer OS and PFS in the immunotherapy cohort	2021	(90)

HCC, hepatocellular carcinoma; NLR, neutrophil-to-lymphocyte ratio; PLR, platelet-to-lymphocyte ratio; CR, complete response; PR, partial response; OS, overall survival; ORR, objective response rate; HPD, hyperprogressive disease; PVT, portal vein thrombosis; ECOG, Eastern Cooperative Oncology Group; BCLC, Barcelona Clinic Liver Cancer; AFP, alpha-fetoprotein; CRP, C-reactive protein; DCR, disease control rate; TKI, multitargeted tyrosine kinase inhibitor; CBR, clinical benefit response; CTC, circulating tumor cell; ctDNA, circulating tumor DNA; PD-1, programmed cell death protein 1; CNV, copy number variation.

of exhausted TILs (107). Harding et al. (108) studied 27 HCC patients treated with ICIs (both monotherapy and combination therapy). The results showed that all patients with Wnt pathway alterations had PD at the first interval scan, whereas 9 of 17 non-Wnt pathway-altered patients had durable disease (SD ≥4 months) or better as the best response ($p < 0.009$). Wnt-activated patients presented shorter mPFS (2.0 vs. 7.4 months, $p < 0.0001$) and numerically shorter OS (9.1 vs. 15.2 months, $p = 0.11$). Lin et al. analyzed the same cohort and verified the results (109). The role of Wnt/β-catenin signaling as a biomarker has been verified in a number of studies, which can be further explored as a powerful factor in a prospective prediction model.

PD-L1 expression and tumor mutational burden

PD-L1 has been reported as an indicator of anti-PD-1/PD-L1 treatment in several cancer types (110–112). However, the predictive role of PD-L1 expression in HCC immunotherapy remains controversial. In the KEYNOTE-224 trial, PD-L1 expression calculated by the combined positive score (CPS, cutoff = 1) was found to be associated with improved ORR and PFS in responders (CR/PR), whereas PD-L1 expression calculated by the tumor proportion score (TPS, cutoff = 1%) has no predictive value as CPS (8). In the CheckMate 459 trial, although patients with baseline PD-L1 expression ≥1% had higher ORR in the nivolumab group (28% vs. 12%), no difference was observed in PFS and OS (113). In the dose-escalation and dose-expansion cohort of Checkmate 040, TPS did not have an apparent predictive effect on the response rate (9). The same result was found in the nivolumab and ipilimumab combined cohort of CheckMate 040 (114). When PD-L1 was detected by the expression of CD274 (PD-L1 messenger RNA) in the G030140 arm A group and in the IMbrave150 trial, it was found to be higher in patients with CR/PR than in patients with SD/PD. Patients with high levels of CD274 also showed longer PFS than those with low expression [HR = 0.42 (95% CI 0.25–0.72), $p = 0.0011$] (93). Patients with high expression of CD274 showed improved PFS and OS in the combination therapy group than in the sorafenib group. In conclusion, the predictive value of PD-L1 is limited in HCC immunotherapy.

Previous studies in melanoma and NSCLC showed that higher TMB was associated with higher tumor responsiveness to PD-1/PD-L1 immunotherapy (115–117). Nonetheless, the value of TMB as an objective biomarker in immunotherapy in HCC remains indefinite. Xie et al. analyzed the HCC cohort with immunotherapy from The Cancer Genome Atlas and found that higher TMB was associated with the immune microenvironment diversification and worse prognosis (118). In the GO30140 biomarker exploration study, ORR was found to be higher in patients with high TMB than in those with median or low levels

in 76 patients in arm A (56% vs. 17% vs. 35%), while PFS has no difference in all the groups (high vs. median vs. low = 13.6 vs. 5.9 vs. 7.9 months). However, no association between TMB and treatment response or survival was found in the combination therapy group in the IMbrave150 cohort (93). The same result was found in another anti-PD-1 treatment cohort (52). The potential reason may be attributed to the generally low level of TMB in HCC (median TMB in HCC was only 4.08) (108). Table 2 provides a brief overview of the biomarkers in tumor tissues for HCC immunotherapy.

Gut microbiota

The gut microbiota is known to influence immune responses and even promote carcinogenesis, which supports its potential role as a biomarker in immunotherapy. Accumulated evidence has shown that the gut microbiota may predict immunotherapy efficacy in various cancer types (119–123). Several mechanisms have been reported such as modulating DNA damage, influencing oncogenesis or tumor suppression by metabolic processes (124), and inducing regulatory T-cell expansion and $CD8^+$ T-cell attenuation (125). The above mechanisms finally inhibit antitumor immunity through mediating immune cells and cytokine production (126–130). Several studies have been conducted to explore the role of the gut microbiome in HCC immunotherapy in recent years. Zheng et al. (131) found that fecal samples from HCC patients treated with camrelizumab showed higher taxa richness and more gene counts of gut microbiome species, such as *Akkermansia* and *Ruminococcaceae*, than from non-responders. Meanwhile, the dissimilarity of beta diversity became prominent as early as 6 weeks, which indicated that the gut microbiome might be used for early prediction for anti-PD-1 immunotherapy after treatment initiation. However, only 8 patients were enrolled in this study. Zhao et al. (132) conducted an analysis of 65 patients with advanced hepatobiliary cancer receiving anti-PD-1 treatment to explore the potential mechanism. The results showed that the clinical benefit response (CBR) group (patients with CR, PR, or SD ≥6 months) had more taxa enrichment than the non-clinical benefit (NCB) group (patients with SD <6 months or PD). *Lachnospiraceae bacterium-GAM79* and *Alistipes spMarseille-P5997* were significantly enriched in the CBR group (74 vs. 40 taxa). Patients with a higher abundance of *Ruminococcus calidus* and *Erysipelotichaceae bacterium-GAM147* presented longer PFS and OS. During treatment, the gut microbiome composition in the CBR group remained stable, while in the NCB group, the microbial diversity seemed to decrease. Fecal microbiota transplantation (FMT) from donors who achieved CR/PR for a long duration treated with anti-PD-1 therapy to patients who were refractory to immunotherapy was reported to increase intratumor lymphocyte infiltration in patients with poor efficacy in melanoma (133, 134). A study conducted in a mouse model showed that FMT could significantly enhance the therapeutic efficacy of ICIs in syngeneic tumor models by increasing tumor-infiltrating IFN-γ^+CD8^+ T cells and the tumor suppression effect (135). All these findings demonstrated that the gut microbiome might be an effective biomarker to predict the clinical response and survival benefit of immunotherapy in HCC. Its predictive prospect is worth anticipating.

Immune-related adverse events

Immunotherapy will inevitably result in irAEs, which are defined as side effects with potential immunological basis and require more frequent monitoring and possible treatment with systemic steroids (136). Mono-immunotherapy conducted by nivolumab in CheckMate 040 and CheckMate 459 resulted in 22%–25% grade 3–5 AEs (9, 137). For pembrolizumab in KEYNOTE-240 and KEYNOTE-224, grade 3–5 AEs were about 52% and 26% (8, 138). As for the combination of immune and targeted therapy, grade 3–5 AEs were about 50%–60% in IMbrave150, GO30140, and ORIENT-32 (12, 139, 140). Several studies conducted in solid malignancies have demonstrated a positive association between irAEs with improved clinical outcomes, such as melanoma, urothelial cancer, renal cell carcinoma, NSCLC, and gastric cancer (141–146). A consistent result was found in a retrospective cohort study of 168 patients with aHCC. In this study, patients with grade ≥3 irAEs demonstrated improved ORR and DCR than those with no irAEs (ORR: 50% vs. 11.3%, $p = 0.002$; DCR: 87.5% vs. 28.2%, $p < 0.001$). The median PFS and OS in patients with grade ≥3 irAEs and grade 1–2 irAEs were significantly longer than in patients with no irAEs (PFS: 8.5 vs. 3.6 vs. 1.3 months, $p < 0.001$; OS: 26.9 vs. 14.0 vs. 4.6 months, $p < 0.001$). Patients with more severe and multisystem (two or more systems) irAEs have a better prognosis (147). The mechanisms are still unclear. Possibly, patients who experience more serious irAEs could have higher T-cell activity and experience better antitumor outcomes. Other possible mechanisms may rely on the potential similar pathway shared by adverse events and the ICIs. Thus, the occurrence of adverse events may reflect that the relative pathway has been inhibited at a high level, which certainly led to better efficacy (148).

The etiology of hepatocellular carcinoma

Over 90% of HCC cases occur in the setting of chronic liver disease. The major risk factors for HCC are chronic infection with hepatitis B virus (HBV) or hepatitis C virus (HCV), heavy

TABLE 2 Predictive or prognostic biomarkers in tumor tissues for HCC immunotherapy.

Biomarker	Treatment	Line of treatment	Number of detected patients	Outcome	Year	Ref.
$SCD8^+$ T cells, $CD3^+$ T cells, and $GZMB^+CD3^+$ T cells	Atezolizumab plus bevacizumab (GO30140: NCT02715531)	First-line	*N* = 61	Responders (CR/PR) had a higher density of infiltrating $CD8^+$ T cells, $CD3^+$ T cells, and $GZMB^+CD3^+$ T cells in tumor areas than non-responders (SD/PD)	2022	(93)
Immune subsets	Atezolizumab plus bevacizumab (GO30140: NCT02715531)	First-line	*N* = 90	High presence of several immune subsets, including $CD8^+$ and $CD4^+$ T cells, Tregs, B cells, and dendritic cells, associated with better response and longer PFS		
Intratumoral $CD8^+$ T cells	Atezolizumab plus bevacizumab vs. sorafenib (IMbrave150: NCT03434379)	First-line	Atezolizumab plus bevacizumab (*N* = 119); sorafenib (*N* = 58)	Patients with a high density of intratumoral $CD8^+$ T cells showed longer OS and PFS with atezolizumab plus bevacizumab compared with sorafenib		
$CD3^+$ T cells and $CD8^+$ T cells	Nivolumab (CheckMate 459: NCT02576509)	First-line or previously treated with sorafenib	$CD3^+$ T cells (*N* = 189), $CD8^+$ T cells (*N* = 192)	Higher $CD3^+$ T cells were associated with patients with CR/PR compared with patients with SD Patients with higher tumor-infiltrating $CD3^+$ T cells and $CD8^+$ T cells showed an improved OS trend	2022	(42)
$CD68^+$ and $CD163^+$ (M2 macrophages)	Nivolumab (CheckMate 459: NCT02576509)	First-line or previously treated with sorafenib	*N* = 135	$CD68^+$ and $CD163^+$ cells have no association with either response or OS	2021	
$CD68^+$ and $CD163^-$ (M1 macrophages)	Sintilimab plus IBI305 (NCT04072679)	First-line	*N* = 33	Higher density of M1 macrophages ($CD68^+CD163^+$) in the stroma is associated with better efficacy and longer PFS and OS	2022	(71)
ARBS and Teff	Atezolizumab plus bevacizumab and atezolizumab plus bevacizumab vs. sorafenib (GO30140: NCT02715531; IMbrave150: NCT03434379)	First-line	GO30140 (*N* = 90); IMbrave150 (atezolizumab plus bevacizumab, *N* = 119; sorafenib, *N* = 58)	Higher expression of ABRS and Teff had better treatment response and longer PFS High expression of ABRS or the Teff signature showed improved PFS and OS when treated with atezolizumab + bevacizumab vs. sorafenib	2022	(93)
Treg/Teff	Atezolizumab plus bevacizumab and atezolizumab plus bevacizumab vs. sorafenib (GO30140: NCT02715531; IMbrave150: NCT03434379)	First-line	GO30140 (*N* = 90); IMbrave150 (atezolizumab plus bevacizumab, *N* = 119; sorafenib, *N* = 58)	Low ratio of Treg/Teff signatures was associated with improved PFS and OS with atezolizumab + bevacizumab vs. sorafenib		
TERT promoter mutation	Atezolizumab plus bevacizumab vs. sorafenib	First-line	IMbrave150 (atezolizumab plus bevacizumab, *N* =	Patients with *TERT*-mutant tumors showed longer PFS and OS in the atezolizumab + bevacizumab group than in the sorafenib group		

(Continued)

TABLE 2 Continued

Biomarker	Treatment	Line of treatment	Number of detected patients	Outcome	Year	Ref.
	(IMbrave150: NCT03434379)		85; sorafenib, *N* = 45)			
Wnt/β-catenin	Atezolizumab plus bevacizumab vs. sorafenib (IMbrave150: NCT03434379)	First-line	IMbrave150 (atezolizumab plus bevacizumab, *N* = 85; sorafenib, *N* = 45)	Patients with wild-type *CTNNB1* showed greater treatment effects from atezolizumab + bevacizumab vs. sorafenib than those with *CTNNB1* mutations		
	Anti-PD-1 monotherapy	First-line or previously treated with sorafenib	*N* = 34	The combination of Wnt/β-catenin activation, high $CD8^+$ TIL infiltration and high PD-L1-CPS well stratified the survival of the patients in both PFS and OS	2021	(107)
	Mono-immunotherapy and combination therapy (NCT01775072)	First-line or previously treated with sorafenib	*N* = 27	Patients with Wnt pathway alterations had worse treatment response, shorter mPFS, and numerically shorter OS	2019	(108)
PD-L1	Pembrolizumab (KEYNOTE-224: NCT02702414)	Second-line	*N* = 52	CPS was associated with improved ORR and PFS in responders (CR/PR), whereas TPS has no predictive value	2018	(8)
	Nivolumab or nivolumab plus ipilimumab (CheckMate 040: NCT01658878)	First- or second-line (dose-escalation and dose-expansion phase)	Dose-escalation phase (*N* = 44); dose-expansion phase (*N* = 174)	Baseline tumor cell PD-1 status has no apparent effect on the response rate	2017	(9)
		Second-line (nivolumab plus ipilimumab cohort)	*N* = 148	Responses occurred regardless of PD-L1 expression	2022	(114)
	Nivolumab (CheckMate 459: NCT02576509)	First-line	Nivolumab (*N* = 366); sorafenib (*N* = 364)	Patients with baseline PD-L1 expression ≥1% had higher ORR in the nivolumab group	2021	(113)
	Atezolizumab plus bevacizumab and atezolizumab plus bevacizumab vs. sorafenib (GO30140: NCT02715531; IMbrave150: NCT03434379)	First-line	GO30140 (*N* = 90); Imbrave150 (atezolizumab plus bevacizumab, *N* = 119; sorafenib, *N* = 58)	PD-L1 detected by CD274 (PD-L1 messenger RNA) was higher in patients with CR/PR than SD/PD; patients with high expression of CD274 showed longer PFS in the combination therapy group. High expression of CD274 showed improved PFS and OS when treated with atezolizumab + bevacizumab vs. sorafenib	2022	(93)
TMB	Immunotherapy	Unknown	*N* = 377	Higher TMB was associated with the immune microenvironment diversification and a worse prognosis	2020	(118)
	Atezolizumab plus	First-line	GO30140 (*N* = 76); IMbrave150		2022	(93)

(Continued)

TABLE 2 Continued

Biomarker	Treatment	Line of treatment	Number of detected patients	Outcome	Year	Ref.
	bevacizumab and atezolizumab plus bevacizumab vs. sorafenib (GO30140: NCT02715531; IMbrave150: NCT03434379)		(atezolizumab plus bevacizumab, *N* = 119; sorafenib, *N* = 58)	ORR was found higher in patients with high TMB than in those with median or low level in the GO30140 arm A; no association was found in the other analysis		
	Nivolumab or pembrolizumab	First-line or subsequent-line	*N* = 15	TMB could not predict treatment response and PFS	2020	(52)

HCC, hepatocellular carcinoma; ARBS, atezolizumab + bevacizumab response signature (including *CXCR2P1*, *ICOS*, *TIMD4*, *CTLA4*, *PAX5*, *KLRC3*, *FCRL3*, *AIM2*, *GBP5*, and *CCL4*); Teff, T effector (including *CXCL9*, *PRF1*, and *GZMB*); CR, complete response; PR, partial response; SD, stable disease; PD, progressive disease; OS, overall survival; PFS, progression-free survival; PD-L1, programmed death ligand 1; CPS, combined positive score; TPS, tumor proportion score; ORR, objective response rate; PD-1, programmed death 1; TMB, tumor mutational burden.

alcohol intake, excess body weight, diabetes, or non-alcoholic fatty liver disease (NAFLD) (1).

The response of HCC induced by various etiologies to immunotherapy may differ. Chun et al. reported that Treg and $CD8^+$ resident memory T cells (TRM) were enriched in HBV-related HCC. Treg and TRM from HBV-related HCC expressed more PD-1 and were functionally more suppressive and exhausted than those from non-viral-related HCC, which could be reversed by anti-PD-1 blockade (149). A meta-analysis included eight systemic therapies cohorts to evaluate the impact of targeted and immune therapies according to different HCC etiologies. Among them, five were TKI/anti-VEGF cohorts (REACH, REACH-2, METIV-HCC, CELESTIAL, and JET-HCC) and three were immunotherapy cohorts (Checkmate 459, IMbrave150, and KEYNOTE-240). Patients with viral-related HCC presented significantly better OS than those with non-viral-related HCC ($p = 0.0259$) in immunotherapy. Efficacy was similar in HBV- and HCV-related HCC [HR = 0.64 (95% CI 0.49–0.83) vs. HR = 0.68 (95% CI 0.47–0.98)]. No impact of etiology was observed in TKI/anti-VEGF therapies (150). In another meta-analysis, the presence of viral infection had a significant interaction with the ICI efficacy in HBV-infected HCC ($p_{interaction} = 0.016$) but not in HCV-infected HCC ($p_{interaction} = 0.081$) (151). The potential reason may be that patients with HCV–HCC were rich in Tregs and M2 macrophages and had an upregulated expression of CTLA4 and other immunosuppressive molecules (152–154), and the expression of negative co-stimulatory signals may contribute to treatment resistance. Meanwhile, unlike HBV-related HCC, the function of HCV-specific $CD8^+$ T cells did not recover after PD-1/PD-L1 blockade (155). However, contrary to the above results, Ho et al. found that the ORR between viral-infected and uninfected patients showed no clinical difference when treated with PD-1/PD-L1 inhibitors, which means that viral status is not suitable to be used as a criterion to select patients for immunotherapy (156). Considering that the meta-analyses were not based on individual patient's data and the trials included were heterogeneous in terms of treatment line and control arm, whether patients with viral infection respond better to immunotherapy than those without infection requires further research.

NAFLD has become an emerging risk factor for HCC over the past decade (157). In a retrospective study with 79 patients [15 patients in the non-alcoholic steatohepatitis (NASH) cirrhosis-related HCC group and 64 patients in the HCC group without NASH cirrhosis], there were significantly higher rates of PD as the best response to immunotherapy in patients with HCC and NASH cirrhosis compared with those without NASH cirrhosis (46.7% vs. 10.9%, $p = 0.004$) (158). A relevant mechanism research found that the exhausted, unconventionally activated $CD8^+PD1^+$ T cells progressively accumulated in NASH-affected livers. However, in mice with NASH but without HCC, preventive $CD8^+$ T-cell depletion significantly decreased the incidence of HCC. Meanwhile, preventive anti-PD-1 treatment in NASH mice increased $CD8^+PD1^+$ T cells and also caused a marked increase in cancer incidence, which means $CD8^+PD1^+$ T cells from patients with NAFLD or NASH might help induce NASH–HCC, rather than invigorating or executing immune surveillance (159). Collectively, NASH–HCC might be less responsive to immunotherapy, probably owing to NASH-related aberrant T-cell activation causing tissue damage that leads to impaired

immune surveillance. Table 3 provides a brief overview of the biomarkers of other types for HCC immunotherapy.

Conclusion

We have concluded an exploratory research on biomarkers as immunotherapy for HCC. As biomarkers detected from peripheral blood, NLR, PLR, and CRAFITY (CRP and AFP in Immunotherapy) score, which are not only easy to be collected but also with high prognostic value supported by a large sample research, are of great significance in the future construction of predictive models. The gene signature and the tumor immune microenvironment have the ability to precisely reflect the pre-existing immunity in baseline tumor tissues, which have shown potential predictive value to drive the clinical activity of immunotherapy in aHCC in the IMbrave150 trial. The gut microbiota and irAEs which were found to be potential biomarkers in immunotherapy are now being further analyzed and are expected to be explored in the future. Fecal microbiota transplantation has been even developed into a combination treatment method and has shown great promise to increase immunotherapy efficacy. CD137 and other cytokines are potential predictive factors that need to be verified in large

TABLE 3 Predictive or prognostic biomarkers of other types for HCC immunotherapy.

Biomarker	Treatment	Line of treatment	Number of detected patients	Outcome	Year	Ref.
Gut microbiota	Anti-PD-1-based systemic therapy (NCT03892577) (NCT03895970) (NCT04010071)	Not mentioned	HCC (N = 30)	Baseline gut microbiome diversity is associated with a favorable response to anti-PD-1 treatment; higher diversity and relative abundance of taxa might be a protective factor against irAEs	2021	(132)
	SHR-1210 (NCT02989922)	Second-line	N = 8	Responders showed higher taxa richness and more gene counts of gut microbiome species than non-responders	2019	(131)
irAEs	Monotherapy and combination therapy	First-line or subsequent-line	N = 168	Patients with more severe irAEs and multisystem (two or more systems) involvement have a better prognosis	2021	(147)
Etiology	CheckMate 459 (NCT02576509) IMbrave150 (NCT03434379) KEYNOTE-240 (NCT02702401)	First-line or second-line	N = 1,656 Meta-analysis	Immunotherapy is less effective in non-viral etiologies than in viral-related HCC. The effect of ICIs was remarkably similar in HBV- and HCV-related HCC	2021	(150)
	CheckMate 459 (NCT02576509) IMbrave150 (NCT03434379) KEYNOTE-240 (NCT02702401)	First-line or second-line	N = 1,656 Meta-analysis	The presence of viral infection had a significant interaction with the ICI efficacy in HBV-infected but not in HCV-infected patients	2021	(151)
	Monotherapy and combination therapy	First-line or second-line	N = 567 Meta-analysis	ORR between virally infected and uninfected patients showed no clinically meaningful difference	2020	(156)
	Atezolizumab, nivolumab, pembrolizumab	Unknown	N = 79	NASH-related HCC patients showed significantly higher rates of disease progression as the best response to immunotherapy compared with those without NASH cirrhosis	2022	(158)
	Monotherapy and combination therapy	First-line or subsequent-line	N = 248 (118 patients in the validation cohort)	NAFLD is associated with a worse outcome in patients with HCC treated with PD(L)1-targeted immunotherapy	2021	(159)

HCC, hepatocellular carcinoma; PD-1, programmed death 1; irAEs, immune-related adverse events; HBV, hepatitis B virus; HCV, hepatitis C virus; NASH, non-alcoholic steatohepatitis; NAFLD, non-alcoholic fatty liver disease.

sample cohorts. Integrative multiparametric approaches that combine peripheral markers, the tumor microenvironment, and immune signatures appear to be the most comprehensive way to assess treatment outcomes and seem to be promising in the future.

Author contributions

XP: conceptualization, data curation, figure preparation, and writing—original draft preparation. CG: writing—review and editing. WZ: writing—review and editing, project administration, and funding acquisition. AZ: conceptualization, writing—original draft preparation, writing—review and editing, project administration, and funding acquisition. All authors contributed to the article and approved the submitted version.

Funding

This research was funded by the CAMS Innovation Fund for Medical Sciences (CIFMS, Grant No. 2021-I2M-1-066) and the Translational Research Project of Medical Oncology Key Foundation of Cancer Hospital Chinese Academy of Medical Sciences (CICAMS-MOTRP, Grant No. 2022005).

Conflict of interest

The authors declare that the research was conducted in the absence of any commercial or financial relationships that could be construed as a potential conflict of interest.

Publisher's note

All claims expressed in this article are solely those of the authors and do not necessarily represent those of their affiliated organizations, or those of the publisher, the editors and the reviewers. Any product that may be evaluated in this article, or claim that may be made by its manufacturer, is not guaranteed or endorsed by the publisher.

References

1. Llovet JM, Kelley RK, Villanueva A, Singal AG, Pikarsky E, Roayaie S, et al. Hepatocellular carcinoma. *Nat Rev Dis Primers* (2021) 7(1):6. doi: 10.1038/s41572-020-00240-3

2. Roayaie S, Obeidat K, Sposito C, Mariani L, Bhoori S, Pellegrinelli A, et al. Resection of hepatocellular cancer ≤ 2 cm: results from two Western centers. *Hepatology* (2013) 57(4):1426–35. doi: 10.1002/hep.25832

3. Llovet JM, Ricci S, Mazzaferro V, Hilgard P, Gane E, Blanc JF, et al. Sorafenib in advanced hepatocellular carcinoma. *N Engl J Med* (2008) 359(4):378–90. doi: 10.1056/NEJMoa0708857

4. Kudo M, Finn RS, Qin S, Han KH, Ikeda K, Piscaglia F, et al. Lenvatinib versus sorafenib in first-line treatment of patients with unresectable hepatocellular carcinoma: a randomised phase 3 non-inferiority trial. *Lancet* (2018) 391 (10126):1163–73. doi: 10.1016/s0140-6736(18)30207-1

5. Bruix J, Qin S, Merle P, Granito A, Huang YH, Bodoky G, et al. Regorafenib for patients with hepatocellular carcinoma who progressed on sorafenib treatment (RESORCE): A randomised, double-blind, placebo-controlled, phase 3 trial. *Lancet* (2017) 389(10064):56–66. doi: 10.1016/s0140-6736(16)32453-9

6. Abou-Alfa GK, Meyer T, Cheng AL, El-Khoueiry AB, Rimassa L, Ryoo BY, et al. Cabozantinib in patients with advanced and progressing hepatocellular carcinoma. *N Engl J Med* (2018) 379(1):54–63. doi: 10.1056/NEJMoa1717002

7. Zhu AX, Kang YK, Yen CJ, Finn RS, Galle PR, Llovet JM, et al. Ramucirumab after sorafenib in patients with advanced hepatocellular carcinoma and increased α-fetoprotein concentrations (REACH-2): a randomised, double-blind, placebo-controlled, phase 3 trial. *Lancet Oncol* (2019) 20(2):282–96. doi: 10.1016/s1470-2045(18)30937-9

8. Zhu AX, Finn RS, Edeline J, Cattan S, Ogasawara S, Palmer D, et al. Pembrolizumab in patients with advanced hepatocellular carcinoma previously treated with sorafenib (KEYNOTE-224): a non-randomised, open-label phase 2 trial. *Lancet Oncol* (2018) 19(7):940–52. doi: 10.1016/s1470-2045(18)30351-6

9. El-Khoueiry AB, Sangro B, Yau T, Crocenzi TS, Kudo M, Hsu C, et al. Nivolumab in patients with advanced hepatocellular carcinoma (CheckMate 040): an open-label, non-comparative, phase 1/2 dose escalation and expansion trial. *Lancet* (2017) 389(10088):2492–502. doi: 10.1016/s0140-6736(17)31046-2

10. Qin S, Ren Z, Meng Z, Chen Z, Chai X, Xiong J, et al. Camrelizumab in patients with previously treated advanced hepatocellular carcinoma: a multicentre, open-label, parallel-group, randomised, phase 2 trial. *Lancet Oncol* (2020) 21 (4):571–80. doi: 10.1016/s1470-2045(20)30011-5

11. Ducreux M, Abou-Alfa G, Ren Z, Edeline J, Li Z, Assenat E, et al. Results from a global phase 2 study of tislelizumab, an investigational PD-1 antibody, in patients with unresectable hepatocellular carcinoma. *Ann Oncol* (2021) 32:S217. doi: 10.1016/j.annonc.2021.05.005

12. Finn RS, Qin S, Ikeda M, Galle PR, Ducreux M, Kim TY, et al. Atezolizumab plus bevacizumab in unresectable hepatocellular carcinoma. *N Engl J Med* (2020) 382(20):1894–905. doi: 10.1056/NEJMoa1915745

13. Finn RS, Qin S, Ikeda M, Galle PR, Ducreux M, Kim T-Y, et al. IMbrave150: Updated overall survival (OS) data from a global, randomized, open-label phase III study of atezolizumab (atezo) + bevacizumab (bev) versus sorafenib (sor) in patients (pts) with unresectable hepatocellular carcinoma (HCC). *J Clin Oncol* (2021) 39(3_suppl):267. doi: 10.1200/JCO.2021.39.3_suppl.267

14. Llovet JM, Castet F, Heikenwalder M, Maini MK, Mazzaferro V, Pinato DJ, et al. Immunotherapies for hepatocellular carcinoma. *Nat Rev Clin Oncol* (2022) 19 (3):151–72. doi: 10.1038/s41571-021-00573-2

15. Jaillon S, Ponzetta A, Di Mitri D, Santoni A, Bonecchi R, Mantovani A. Neutrophil diversity and plasticity in tumour progression and therapy. *Nat Rev Cancer* (2020) 20(9):485–503. doi: 10.1038/s41568-020-0281-y

16. Jensen HK, Donskov F, Marcussen N, Nordsmark M, Lundbeck F, von der Maase H. Presence of intratumoral neutrophils is an independent prognostic factor in localized renal cell carcinoma. *J Clin Oncol* (2009) 27(28):4709–17. doi: 10.1200/jco.2008.18.9498

17. Kuang DM, Zhao Q, Wu Y, Peng C, Wang J, Xu Z, et al. Peritumoral neutrophils link inflammatory response to disease progression by fostering angiogenesis in hepatocellular carcinoma. *J Hepatol* (2011) 54(5):948–55. doi: 10.1016/j.jhep.2010.08.041

18. Gkolfinopoulos S, Jones RL, Constantinidou A. The emerging role of platelets in the formation of the micrometastatic niche: Current evidence and future perspectives. *Front Oncol* (2020) 10:374. doi: 10.3389/fonc.2020.00374

19. Durán-Saenz NZ, Serrano-Puente A, Gallegos-Flores PI, Mendoza-Almanza BD, Esparza-Ibarra EL, Godina-González S, et al. Platelet membrane: An outstanding factor in cancer metastasis. *Membranes (Basel)* (2022) 12(2):182. doi: 10.3390/membranes12020182

20. Haemmerle M, Taylor ML, Gutschner T, Pradeep S, Cho MS, Sheng J, et al. Platelets reduce anoikis and promote metastasis by activating YAP1 signaling. *Nat Commun* (2017) 8(1):310. doi: 10.1038/s41467-017-00411-z

21. Mendoza-Almanza G, Burciaga-Hernández L, Maldonado V, Melendez-Zajgla J, Olmos J. Role of platelets and breast cancer stem cells in metastasis. *World J Stem Cells* (2020) 12(11):1237–54. doi: 10.4252/wjsc.v12.i11.1237

22. Labelle M, Begum S, Hynes RO. Direct signaling between platelets and cancer cells induces an epithelial-mesenchymal-like transition and promotes metastasis. *Cancer Cell* (2011) 20(5):576–90. doi: 10.1016/j.ccr.2011.09.009

23. Wang Y, Yao R, Zhang D, Chen R, Ren Z, Zhang L. Circulating neutrophils predict poor survival for HCC and promote HCC progression through p53 and STAT3 signaling pathway. *J Cancer* (2020) 11(13):3736–44. doi: 10.7150/jca.42953

24. Li XF, Chen DP, Ouyang FZ, Chen MM, Wu Y, Kuang DM, et al. Increased autophagy sustains the survival and pro-tumourigenic effects of neutrophils in human hepatocellular carcinoma. *J Hepatol* (2015) 62(1):131–9. doi: 10.1016/j.jhep.2014.08.023

25. Geh D, Leslie J, Rumney R, Reeves HL, Bird TG, Mann DA. Neutrophils as potential therapeutic targets in hepatocellular carcinoma. *Nat Rev Gastroenterol Hepatol* (2022) 19(4):257–73. doi: 10.1038/s41575-021-00568-5

26. Grenader T, Nash S, Adams R, Kaplan R, Fisher D, Maughan T, et al. Derived neutrophil lymphocyte ratio is predictive of survival from intermittent therapy in advanced colorectal cancer: a *post hoc* analysis of the MRC COIN study. *Br J Cancer* (2016) 114(6):612–5. doi: 10.1038/bjc.2016.23

27. Gu X, Gao X, Li X, Qi X, Ma M, Qin S, et al. Prognostic significance of neutrophil-to-lymphocyte ratio in prostate cancer: evidence from 16,266 patients. *Sci Rep* (2016) 6:22089. doi: 10.1038/srep22089

28. Lin G, Liu Y, Li S, Mao Y, Wang J, Shuang Z, et al. Elevated neutrophil-to-lymphocyte ratio is an independent poor prognostic factor in patients with intrahepatic cholangiocarcinoma. *Oncotarget* (2016) 7(32):50963–71. doi: 10.18632/oncotarget.7680

29. Sun HL, Pan YQ, He BS, Nie ZL, Lin K, Peng HX, et al. Prognostic performance of lymphocyte-to-monocyte ratio in diffuse large b-cell lymphoma: an updated meta-analysis of eleven reports. *Onco Targets Ther* (2016) 9:3017–23. doi: 10.2147/ott.S96910

30. Diem S, Schmid S, Krapf M, Flatz L, Born D, Jochum W, et al. Neutrophil-to-Lymphocyte ratio (NLR) and platelet-to-Lymphocyte ratio (PLR) as prognostic markers in patients with non-small cell lung cancer (NSCLC) treated with nivolumab. *Lung Cancer* (2017) 111:176–81. doi: 10.1016/j.lungcan.2017.07.024

31. Thiagarajan S, Tan JW, Zhou S, Tan QX, Hendrikson J, Ng WH, et al. Postoperative inflammatory marker surveillance in colorectal peritoneal carcinomatosis. *Ann Surg Oncol* (2021) 28(11):6625–35. doi: 10.1245/s10434-020-09544-w

32. Templeton AJ, Knox JJ, Lin X, Simantov R, Xie W, Lawrence N, et al. Change in neutrophil-to-lymphocyte ratio in response to targeted therapy for metastatic renal cell carcinoma as a prognosticator and biomarker of efficacy. *Eur Urol* (2016) 70(2):358–64. doi: 10.1016/j.eururo.2016.02.033

33. Mason M, Maurice C, McNamara MG, Tieu MT, Lwin Z, Millar BA, et al. Neutrophil-lymphocyte ratio dynamics during concurrent chemo-radiotherapy for glioblastoma is an independent predictor for overall survival. *J Neurooncol* (2017) 132(3):463–71. doi: 10.1007/s11060-017-2395-y

34. Walsh SR, Cook EJ, Goulder F, Justin TA, Keeling NJ. Neutrophil-lymphocyte ratio as a prognostic factor in colorectal cancer. *J Surg Oncol* (2005) 91(3):181–4. doi: 10.1002/jso.20329

35. Guo L, Ren H, Pu L, Zhu X, Liu Y, Ma X. The prognostic value of inflammation factors in hepatocellular carcinoma patients with hepatic artery interventional treatments: A retrospective study. *Cancer Manag Res* (2020) 12:7173–88. doi: 10.2147/cmar.S257934

36. Limaye AR, Clark V, Soldevila-Pico C, Morelli G, Suman A, Firpi R, et al. Neutrophil-lymphocyte ratio predicts overall and recurrence-free survival after liver transplantation for hepatocellular carcinoma. *Hepatol Res* (2013) 43(7):757–64. doi: 10.1111/hepr.12019

37. McVey JC, Sasaki K, Firl DJ, Fujiki M, Diago-Uso T, Quintini C, et al. Prognostication of inflammatory cells in liver transplantation: Is the waitlist neutrophil-to-lymphocyte ratio really predictive of tumor biology? *Clin Transplant* (2019) 33(12):e13743. doi: 10.1111/ctr.13743

38. Bhatti I, Peacock O, Lloyd G, Larvin M, Hall RI. Preoperative hematologic markers as independent predictors of prognosis in resected pancreatic ductal adenocarcinoma: neutrophil-lymphocyte versus platelet-lymphocyte ratio. *Am J Surg* (2010) 200(2):197–203. doi: 10.1016/j.amjsurg.2009.08.041

39. Okamura Y, Sugiura T, Ito T, Yamamoto Y, Ashida R, Mori K, et al. Neutrophil to lymphocyte ratio as an indicator of the malignant behaviour of hepatocellular carcinoma. *Br J Surg* (2016) 103(7):891–8. doi: 10.1002/bjs.10123

40. Schobert IT, Savic LJ, Chapiro J, Bousabarah K, Chen E, Laage-Gaupp F, et al. Neutrophil-to-lymphocyte and platelet-to-lymphocyte ratios as predictors of tumor response in hepatocellular carcinoma after DEB-TACE. *Eur Radiol* (2020) 30(10):5663–73. doi: 10.1007/s00330-020-06931-5

41. Yuan J, Liang H, Li J, Li M, Tang B, Ma H, et al. Peripheral blood neutrophil count as a prognostic factor for patients with hepatocellular carcinoma treated with sorafenib. *Mol Clin Oncol* (2017) 7(5):837–42. doi: 10.3892/mco.2017.1416

42. Sangro B, Melero I, Wadhawan S, Finn RS, Abou-Alfa GK, Cheng AL, et al. Association of inflammatory biomarkers with clinical outcomes in nivolumab-treated patients with advanced hepatocellular carcinoma. *J Hepatol* (2020) 73(6):1460–9. doi: 10.1016/j.jhep.2020.07.026

43. Choi WM, Kim JY, Choi J, Lee D, Shim JH, Lim YS, et al. Kinetics of the neutrophil-lymphocyte ratio during PD-1 inhibition as a prognostic factor in advanced hepatocellular carcinoma. *Liver Int* (2021) 41(9):2189–99. doi: 10.1111/liv.14932

44. Muhammed A, Fulgenzi CAM, Dharmapuri S, Pinter M, Balcar L, Scheiner B, et al. The systemic inflammatory response identifies patients with adverse clinical outcome from immunotherapy in hepatocellular carcinoma. *Cancers* (2021) 14(1):186. doi: 10.3390/cancers14010186

45. Waugh DJ, Wilson C. The interleukin-8 pathway in cancer. *Clin Cancer Res* (2008) 14(21):6735–41. doi: 10.1158/1078-0432.Ccr-07-4843

46. Motomura T, Shirabe K, Mano Y, Muto J, Toshima T, Umemoto Y, et al. Neutrophil-lymphocyte ratio reflects hepatocellular carcinoma recurrence after liver transplantation *via* inflammatory microenvironment. *J Hepatol* (2013) 58(1):58–64. doi: 10.1016/j.jhep.2012.08.017

47. Calderaro J, Couchy G, Imbeaud S, Amaddeo G, Letouzé E, Blanc JF, et al. Histological subtypes of hepatocellular carcinoma are related to gene mutations and molecular tumour classification. *J Hepatol* (2017) 67(4):727–38. doi: 10.1016/j.jhep.2017.05.014

48. Chan SL, Mo FK, Johnson PJ, Hui EP, Ma BB, Ho WM, et al. New utility of an old marker: serial alpha-fetoprotein measurement in predicting radiologic response and survival of patients with hepatocellular carcinoma undergoing systemic chemotherapy. *J Clin Oncol* (2009) 27(3):446–52. doi: 10.1200/jco.2008.18.8151

49. Vora SR, Zheng H, Stadler ZK, Fuchs CS, Zhu AX. Serum alpha-fetoprotein response as a surrogate for clinical outcome in patients receiving systemic therapy for advanced hepatocellular carcinoma. *Oncologist* (2009) 14(7):717–25. doi: 10.1634/theoncologist.2009-0038

50. Shao YY, Lin ZZ, Hsu C, Shen YC, Hsu CH, Cheng AL. Early alpha-fetoprotein response predicts treatment efficacy of antiangiogenic systemic therapy in patients with advanced hepatocellular carcinoma. *Cancer* (2010) 116(19):4590–6. doi: 10.1002/cncr.25257

51. Hu X, Chen R, Wei Q, Xu X. The landscape of alpha fetoprotein in hepatocellular carcinoma: Where are we? *Int J Biol Sci* (2022) 18(2):536–51. doi: 10.7150/ijbs.64537

52. Spahn S, Roessler D, Pompilia R, Gabernet G, Gladstone BP, Horger M, et al. Clinical and genetic tumor characteristics of responding and non-responding patients to PD-1 inhibition in hepatocellular carcinoma. *Cancers (Basel)* (2020) 12(12):3830. doi: 10.3390/cancers12123830

53. Scheiner B, Pomej K, Kirstein MM, Hucke F, Finkelmeier F, Waidmann O, et al. Prognosis of patients with hepatocellular carcinoma treated with immunotherapy - development and validation of the CRAFITY score. *J Hepatol* (2022) 76(2):353–63. doi: 10.1016/j.jhep.2021.09.035

54. Yang Y, Ouyang J, Zhou Y, Zhou J, Zhao H. The CRAFITY score: A promising prognostic predictor for patients with hepatocellular carcinoma treated with tyrosine kinase inhibitor and immunotherapy combinations. *J Hepatol* (2022) 77(2):574–6. doi: 10.1016/j.jhep.2022.03.018

55. Chen J, Zaidi S, Rao S, Chen JS, Phan L, Farci P, et al. Analysis of genomes and transcriptomes of hepatocellular carcinomas identifies mutations and gene expression changes in the transforming growth factor-β pathway. *Gastroenterology* (2018) 154(1):195–210. doi: 10.1053/j.gastro.2017.09.007

56. Chen J, Gingold JA, Su X. Immunomodulatory TGF-β signaling in hepatocellular carcinoma. *Trends Mol Med* (2019) 25(11):1010–23. doi: 10.1016/j.molmed.2019.06.007

57. Rebouissou S, Nault JC. Advances in molecular classification and precision oncology in hepatocellular carcinoma. *J Hepatol* (2020) 72(2):215–29. doi: 10.1016/j.jhep.2019.08.017

58. Park BV, Freeman ZT, Ghasemzadeh A, Chattergoon MA, Rutebemberwa A, Steigner J, et al. TGFβ1-mediated SMAD3 enhances PD-1 expression on antigen-specific T cells in cancer. *Cancer Discovery* (2016) 6(12):1366–81. doi: 10.1158/2159-8290.Cd-15-1347

59. Chen J, Su X. Abstract 4286: TGF-β signature is a therapeutic biomarker for combination immunotherapy for hepatocellular carcinoma. *Cancer Res* (2020) 80(16_Suppl):4286. doi: 10.1158/1538-7445.Am2020-4286

60. Feun LG, Li YY, Wu C, Wangpaichitr M, Jones PD, Richman SP, et al. Phase 2 study of pembrolizumab and circulating biomarkers to predict anticancer response in advanced, unresectable hepatocellular carcinoma. *Cancer* (2019) 125(20):3603–14. doi: 10.1002/cncr.32339

61. Mariathasan S, Turley SJ, Nickles D, Castiglioni A, Yuen K, Wang Y, et al. TGFβ attenuates tumour response to PD-L1 blockade by contributing to exclusion of T cells. *Nature* (2018) 554(7693):544–8. doi: 10.1038/nature25501

62. Cheuk AT, Mufti GJ, Guinn BA. Role of 4-1BB:4-1BB ligand in cancer immunotherapy. *Cancer Gene Ther* (2004) 11(3):215–26. doi: 10.1038/sj.cgt.7700670

63. Reithofer M, Rosskopf S, Leitner J, Battin C, Bohle B, Steinberger P, et al. 4-1BB costimulation promotes bystander activation of human CD8 T cells. *Eur J Immunol* (2021) 51(3):721–33. doi: 10.1002/eji.202048762

64. Melero I, Johnston JV, Shufford WW, Mittler RS, Chen L. NK1.1 cells express 4-1BB (CDw137) costimulatory molecule and are required for tumor immunity elicited by anti-4-1BB monoclonal antibodies. *Cell Immunol* (1998) 190 (2):167. doi: 10.1006/cimm.1998.1396

65. Heinisch IV, Daigle I, Knöpfli B, Simon HU. CD137 activation abrogates granulocyte-macrophage colony-stimulating factor-mediated anti-apoptosis in neutrophils. *Eur J Immunol* (2000) 30(12):3441–6. doi: 10.1002/1521-4141(2000012)30:12<3441::Aid-immu3441>3.0.Co;2-l

66. Kim HD, Park S, Jeong S, Lee YJ, Lee H, Kim CG, et al. 4-1BB delineates distinct activation status of exhausted tumor-infiltrating CD8(+) T cells in hepatocellular carcinoma. *Hepatology* (2020) 71(3):955–71. doi: 10.1002/hep.30881

67. Michel J, Langstein J, Hofstädter F, Schwarz H. A soluble form of CD137 (ILA/4-1BB), a member of the TNF receptor family, is released by activated lymphocytes and is detectable in sera of patients with rheumatoid arthritis. *Eur J Immunol* (1998) 28(1):290–5. doi: 10.1002/(sici)1521-4141(199801)28:01<290::Aid-immu290>3.0.Co;2-s

68. DSV A, BSK B. Role of 4-1BB in immune responses. *Semin Immunol* (1998) 10(6):481–9. doi: 10.1006/smim.1998.0157

69. Geuijen C, Tacken P, Wang LC, Klooster R, van Loo PF, Zhou J, et al. A human CD137×PD-L1 bispecific antibody promotes anti-tumor immunity *via* context-dependent T cell costimulation and checkpoint blockade. *Nat Commun* (2021) 12(1):4445. doi: 10.1038/s41467-021-24767-5

70. Jacquelot N, Roberti MP, Enot DP, Rusakiewicz S, Ternès N, Jegou S, et al. Predictors of responses to immune checkpoint blockade in advanced melanoma. *Nat Commun* (2017) 8(1):592. doi: 10.1038/s41467-017-00608-2

71. Zhang W, Gong C, Peng X, Bi X, Sun Y, Zhou J, et al. Serum concentration of CD137 and tumor infiltration by M1 macrophages predict the response to sintilimab plus bevacizumab biosimilar in advanced hepatocellular carcinoma patients. *Clin Cancer Res* (2022) 28(16):3499–508. doi: 10.1158/1078-0432.Ccr-21-3972

72. Zhu S, Hoshida Y. Molecular heterogeneity in hepatocellular carcinoma. *Hepat Oncol* (2018) 5(1):Hep10. doi: 10.2217/hep-2018-0005

73. Ye Q, Ling S, Zheng S, Xu X. Liquid biopsy in hepatocellular carcinoma: circulating tumor cells and circulating tumor DNA. *Mol Cancer* (2019) 18(1):114. doi: 10.1186/s12943-019-1043-x

74. Alunni-Fabbroni M, Rönsch K, Huber T, Cyran CC, Seidensticker M, Mayerle J, et al. Circulating DNA as prognostic biomarker in patients with advanced hepatocellular carcinoma: a translational exploratory study from the SORAMIC trial. *J Transl Med* (2019) 17(1):328. doi: 10.1186/s12967-019-2079-9

75. Moshiri F, Salvi A, Gramantieri L, Sangiovanni A, Guerriero P, De Petro G, et al. Circulating miR-106b-3p, miR-101-3p and miR-1246 as diagnostic biomarkers of hepatocellular carcinoma. *Oncotarget* (2018) 9(20):15350–64. doi: 10.18632/oncotarget.24601

76. Kelley RK, Magbanua MJ, Butler TM, Collisson EA, Hwang J, Sidiropoulos N, et al. Circulating tumor cells in hepatocellular carcinoma: a pilot study of detection, enumeration, and next-generation sequencing in cases and controls. *BMC Cancer* (2015) 15:206. doi: 10.1186/s12885-015-1195-z

77. Julich-Haertel H, Urban SK, Krawczyk M, Willms A, Jankowski K, Patkowski W, et al. Cancer-associated circulating large extracellular vesicles in cholangiocarcinoma and hepatocellular carcinoma. *J Hepatol* (2017) 67(2):282–92. doi: 10.1016/j.jhep.2017.02.024

78. Pantel K, Hille C, Scher HI. Circulating tumor cells in prostate cancer: From discovery to clinical utility. *Clin Chem* (2019) 65(1):87–99. doi: 10.1373/clinchem.2018.287102

79. Chen W, Zhang J, Huang L, Chen L, Zhou Y, Tang D, et al. Detection of HER2-positive circulating tumor cells using the LiquidBiopsy system in breast cancer. *Clin Breast Cancer* (2019) 19(1):e239–e46. doi: 10.1016/j.clbc.2018.10.009

80. Ignatiadis M, Sledge GW, Jeffrey SS. Liquid biopsy enters the clinic - implementation issues and future challenges. *Nat Rev Clin Oncol* (2021) 18 (5):297–312. doi: 10.1038/s41571-020-00457-x

81. Munzone E, Botteri E, Sandri MT, Esposito A, Adamoli L, Zorzino L, et al. Prognostic value of circulating tumor cells according to immunohistochemically defined molecular subtypes in advanced breast cancer. *Clin Breast Cancer* (2012) 12 (5):340–6. doi: 10.1016/j.clbc.2012.07.001

82. Winograd P, Hou S, Court CM, Lee YT, Chen PJ, Zhu Y, et al. Hepatocellular carcinoma-circulating tumor cells expressing PD-L1 are prognostic and potentially associated with response to checkpoint inhibitors. *Hepatol Commun* (2020) 4(10):1527–40. doi: 10.1002/hep4.1577

83. Su K, Guo L, He K, Rao M, Zhang J, Yang X, et al. PD-L1 expression on circulating tumor cells can be a predictive biomarker to PD-1 inhibitors combined with radiotherapy and antiangiogenic therapy in advanced hepatocellular carcinoma. *Front Oncol* (2022) 12:873830. doi: 10.3389/fonc.2022.873830

84. Okajima W, Komatsu S, Ichikawa D, Miyamae M, Ohashi T, Imamura T, et al. Liquid biopsy in patients with hepatocellular carcinoma: Circulating tumor cells and cell-free nucleic acids. *World J Gastroenterol* (2017) 23(31):5650–68. doi: 10.3748/wjg.v23.i31.5650

85. Chakrabarti S, Xie H, Urrutia R, Mahipal A. The promise of Circulating Tumor DNA (ctDNA) in the management of early-stage colon cancer: A critical review. *Cancers* (2020) 12(10):2808. doi: 10.3390/cancers12102808

86. von Felden J, Craig AJ, Garcia-Lezana T, Labgaa I, Haber PK, D'Avola D, et al. Mutations in circulating tumor DNA predict primary resistance to systemic therapies in advanced hepatocellular carcinoma. *Oncogene* (2021) 40(1):140–51. doi: 10.1038/s41388-020-01519-1

87. Wu X, Li J, Gassa A, Buchner D, Alakus H, Dong Q, et al. Circulating tumor DNA as an emerging liquid biopsy biomarker for early diagnosis and therapeutic monitoring in hepatocellular carcinoma. *Int J Biol Sci* (2020) 16(9):1551–62. doi: 10.7150/ijbs.44024

88. Kaseb A, Sánchez N, Sen S, Kelley R, Tan B, Bocobo A, et al. Molecular profiling of hepatocellular carcinoma using circulating cell-free DNA. *Clin Cancer Res* (2019) 25(20):6107–18. doi: 10.1158/1078-0432.CCR-18-3341. clincanres.3341.2018.

89. Hsu C-H, Lu S, Abbas A, Guan Y, Zhu AX, Aleshin A, et al. Longitudinal and personalized detection of circulating tumor DNA (ctDNA) for monitoring efficacy of atezolizumab plus bevacizumab in patients with unresectable hepatocellular carcinoma (HCC). *J Clin Oncol* (2020) 38(15_suppl):3531. doi: 10.1200/JCO.2020.38.15_suppl.3531

90. Yang X, Hu Y, Yang K, Wang D, Lin J, Long J, et al. Cell-free DNA copy number variations predict efficacy of immune checkpoint inhibitor-based therapy in hepatobiliary cancers. *J Immunother Cancer* (2021) 9(5):e001942. doi: 10.1136/jitc-2020-001942

91. Zhao W, Qiu L, Liu H, Xu Y, Zhan M, Zhang W, et al. Circulating tumor DNA as a potential prognostic and predictive biomarker during interventional therapy of unresectable primary liver cancer. *J Gastrointest Oncol* (2020) 11 (5):1065–77. doi: 10.21037/jgo-20-409

92. Santhakumar C, Gane EJ, Liu K, McCaughan GW. Current perspectives on the tumor microenvironment in hepatocellular carcinoma. *Hepatol Int* (2020) 14 (6):947–57. doi: 10.1007/s12072-020-10104-3

93. Zhu AX, Abbas AR, de Galarreta MR, Guan Y, Lu S, Koeppen H, et al. Molecular correlates of clinical response and resistance to atezolizumab in combination with bevacizumab in advanced hepatocellular carcinoma. *Nat Med* (2022) 28(8):1599–611. doi: 10.1038/s41591-022-01868-2

94. Nishida N, Sakai K, Morita M, Aoki T, Takita M, Hagiwara S, et al. Association between genetic and immunological background of hepatocellular carcinoma and expression of programmed cell death-1. *Liver Cancer* (2020) 9 (4):426–39. doi: 10.1159/000506352

95. Tian Z, Hou X, Liu W, Han Z, Wei L. Macrophages and hepatocellular carcinoma. *Cell Biosci* (2019) 9:79. doi: 10.1186/s13578-019-0342-7

96. Cassetta L, Pollard JW. Targeting macrophages: therapeutic approaches in cancer. *Nat Rev Drug Discovery* (2018) 17(12):887–904. doi: 10.1038/nrd.2018.169

97. Lin Y, Xu J, Lan H. Tumor-associated macrophages in tumor metastasis: biological roles and clinical therapeutic applications. *J Hematol Oncol* (2019) 12 (1):76. doi: 10.1186/s13045-019-0760-3

98. Dong N, Shi X, Wang S, Gao Y, Kuang Z, Xie Q, et al. M2 macrophages mediate sorafenib resistance by secreting HGF in a feed-forward manner in hepatocellular carcinoma. *Br J Cancer* (2019) 121(1):22–33. doi: 10.1038/s41416-019-0482-x

99. Spranger S, Bao R, Gajewski TF. Melanoma-intrinsic β-catenin signalling prevents anti-tumour immunity. *Nature* (2015) 523(7559):231–5. doi: 10.1038/nature14404

100. Zucman-Rossi J, Villanueva A, Nault JC, Llovet JM. Genetic landscape and biomarkers of hepatocellular carcinoma. *Gastroenterology* (2015) 149(5):1226–39.e4. doi: 10.1053/j.gastro.2015.05.061

101. Guichard C, Amaddeo G, Imbeaud S, Ladeiro Y, Pelletier L, Maad IB, et al. Integrated analysis of somatic mutations and focal copy-number changes identifies key genes and pathways in hepatocellular carcinoma. *Nat Genet* (2012) 44(6):694–8. doi: 10.1038/ng.2256

102. Takai A, Dang HT, Wang XW. Identification of drivers from cancer genome diversity in hepatocellular carcinoma. *Int J Mol Sci* (2014) 15(6):11142–60. doi: 10.3390/ijms150611142

103. Comprehensive and integrative genomic characterization of hepatocellular carcinoma. *Cell* (2017) 169(7):1327–41.e23. doi: 10.1016/j.cell.2017.05.046

104. Schulze K, Imbeaud S, Letouzé E, Alexandrov LB, Calderaro J, Rebouissou S, et al. Exome sequencing of hepatocellular carcinomas identifies new mutational signatures and potential therapeutic targets. *Nat Genet* (2015) 47(5):505–11. doi: 10.1038/ng.3252

105. Ruiz de Galarreta M, Bresnahan E, Molina-Sánchez P, Lindblad KE, Maier B, Sia D, et al. β-catenin activation promotes immune escape and resistance to anti-PD-1 therapy in hepatocellular carcinoma. *Cancer Discovery* (2019) 9(8):1124–41. doi: 10.1158/2159-8290.Cd-19-0074

106. Waaler J, Mygland L, Tveita A, Strand MF, Solberg NT, Olsen PA, et al. Tankyrase inhibition sensitizes melanoma to PD-1 immune checkpoint blockade in syngeneic mouse models. *Commun Biol* (2020) 3(1):196. doi: 10.1038/s42003-020-0916-2

107. Morita M, Nishida N, Sakai K, Aoki T, Chishina H, Takita M, et al. Immunological microenvironment predicts the survival of the patients with hepatocellular carcinoma treated with anti-PD-1 antibody. *Liver Cancer* (2021) 10(4):380–93. doi: 10.1159/000516899

108. Harding JJ, Nandakumar S, Armenia J, Khalil DN, Albano M, Ly M, et al. Prospective genotyping of hepatocellular carcinoma: Clinical implications of next-generation sequencing for matching patients to targeted and immune therapies. *Clin Cancer Res* (2019) 25(7):2116–26. doi: 10.1158/1078-0432.Ccr-18-2293

109. Chen L, Zhou Q, Liu J, Zhang W. CTNNB1 alternation is a potential biomarker for immunotherapy prognosis in patients with hepatocellular carcinoma. *Front Immunol* (2021) 12:759565. doi: 10.3389/fimmu.2021.759565

110. Mok TSK, Wu YL, Kudaba I, Kowalski DM, Cho BC, Turna HZ, et al. Pembrolizumab versus chemotherapy for previously untreated, PD-L1-expressing, locally advanced or metastatic non-small-cell lung cancer (KEYNOTE-042): a randomised, open-label, controlled, phase 3 trial. *Lancet* (2019) 393(10183):1819–30. doi: 10.1016/s0140-6736(18)32409-7

111. Rini BI, Powles T, Atkins MB, Escudier B, McDermott DF, Suarez C, et al. Atezolizumab plus bevacizumab versus sunitinib in patients with previously untreated metastatic renal cell carcinoma (IMmotion151): a multicentre, open-label, phase 3, randomised controlled trial. *Lancet* (2019) 393(10189):2404–15. doi: 10.1016/s0140-6736(19)30723-8

112. Abdel-Rahman O. PD-L1 expression and outcome of advanced melanoma patients treated with anti-PD-1/PD-L1 agents: a meta-analysis. *Immunotherapy* (2016) 8(9):1081–9. doi: 10.2217/imt-2016-0025

113. Yau T, Park JW, Finn RS, Cheng AL, Mathurin P, Edeline J, et al. Nivolumab versus sorafenib in advanced hepatocellular carcinoma (CheckMate 459): a randomised, multicentre, open-label, phase 3 trial. *Lancet Oncol* (2022) 23 (1):77–90. doi: 10.1016/s1470-2045(21)00604-5

114. Yau T, Kang YK, Kim TY, El-Khoueiry AB, Santoro A, Sangro B, et al. Efficacy and safety of nivolumab plus ipilimumab in patients with advanced hepatocellular carcinoma previously treated with sorafenib: The CheckMate 040 randomized clinical trial. *JAMA Oncol* (2020) 6(11):e204564. doi: 10.1001/jamaoncol.2020.4564

115. Chan TA, Wolchok JD, Snyder A. Genetic basis for clinical response to CTLA-4 blockade in melanoma. *N Engl J Med* (2015) 373(20):1984. doi: 10.1056/NEJMc1508163

116. Rizvi NA, Hellmann MD, Snyder A, Kvistborg P, Makarov V, Havel JJ, et al. Cancer immunology. mutational landscape determines sensitivity to PD-1 blockade in non-small cell lung cancer. *Science* (2015) 348(6230):124–8. doi: 10.1126/science.aaa1348

117. Riaz N, Havel JJ, Makarov V, Desrichard A, Urba WJ, Sims JS, et al. Tumor and microenvironment evolution during immunotherapy with nivolumab. *Cell* (2017) 171(4):934–49.e16. doi: 10.1016/j.cell.2017.09.028

118. Xie F, Bai Y, Yang X, Long J, Mao J, Lin J, et al. Comprehensive analysis of tumour mutation burden and the immune microenvironment in hepatocellular carcinoma. *Int Immunopharmacol* (2020) 89(Pt A):107135. doi: 10.1016/j.intimp.2020.107135

119. Dubin K, Callahan MK, Ren B, Khanin R, Viale A, Ling L, et al. Intestinal microbiome analyses identify melanoma patients at risk for checkpoint-blockade-induced colitis. *Nat Commun* (2016) 7:10391. doi: 10.1038/ncomms10391

120. Havel JJ, Chowell D, Chan TA. The evolving landscape of biomarkers for checkpoint inhibitor immunotherapy. *Nat Rev Cancer* (2019) 19(3):133–50. doi: 10.1038/s41568-019-0116-x

121. Matson V, Fessler J, Bao R, Chongsuwat T, Zha Y, Alegre ML, et al. The commensal microbiome is associated with anti-PD-1 efficacy in metastatic melanoma patients. *Science* (2018) 359(6371):104–8. doi: 10.1126/science.aao3290

122. Vétizou M, Pitt JM, Daillère R, Lepage P, Waldschmitt N, Flament C, et al. Anticancer immunotherapy by CTLA-4 blockade relies on the gut microbiota. *Science* (2015) 350(6264):1079–84. doi: 10.1126/science.aad1329

123. Peng Z, Cheng S, Kou Y, Wang Z, Jin R, Hu H, et al. The gut microbiome is associated with clinical response to anti-PD-1/PD-L1 immunotherapy in gastrointestinal cancer. *Cancer Immunol Res* (2020) 8(10):1251–61. doi: 10.1158/2326-6066.Cir-19-1014

124. Schwabe RF, Jobin C. The microbiome and cancer. *Nat Rev Cancer* (2013) 13(11):800–12. doi: 10.1038/nrc3610

125. Behary J, Amorim N, Jiang XT, Raposo A, Gong L, McGovern E, et al. Gut microbiota impact on the peripheral immune response in non-alcoholic fatty liver disease related hepatocellular carcinoma. *Nat Commun* (2021) 12(1):187. doi: 10.1038/s41467-020-20422-7

126. Sepich-Poore GD, Zitvogel L, Straussman R, Hasty J, Wargo JA, Knight R. The microbiome and human cancer. *Science* (2021) 371(6536):eabc4552. doi: 10.1126/science.abc4552

127. Cullin N, Azevedo Antunes C, Straussman R, Stein-Thoeringer CK, Elinav E. Microbiome and cancer. *Cancer Cell* (2021) 39(10):1317–41. doi: 10.1016/j.ccell.2021.08.006

128. Skelly AN, Sato Y, Kearney S, Honda K. Mining the microbiota for microbial and metabolite-based immunotherapies. *Nat Rev Immunol* (2019) 19 (5):305–23. doi: 10.1038/s41577-019-0144-5

129. Gopalakrishnan V, Helmink BA, Spencer CN, Reuben A, Wargo JA. The influence of the gut microbiome on cancer, immunity, and cancer immunotherapy. *Cancer Cell* (2018) 33(4):570–80. doi: 10.1016/j.ccell.2018.03.015

130. Matson V, Chervin CS, Gajewski TF. Cancer and the microbiome-influence of the commensal microbiota on cancer, immune responses, and immunotherapy. *Gastroenterology* (2021) 160(2):600–13. doi: 10.1053/j.gastro.2020.11.041

131. Zheng Y, Wang T, Tu X, Huang Y, Zhang H, Tan D, et al. Gut microbiome affects the response to anti-PD-1 immunotherapy in patients with hepatocellular carcinoma. *J Immunother Cancer* (2019) 7(1):193. doi: 10.1186/s40425-019-0650-9

132. Mao J, Wang D, Long J, Yang X, Lin J, Song Y, et al. Gut microbiome is associated with the clinical response to anti-PD-1 based immunotherapy in hepatobiliary cancers. *J Immunother Cancer* (2021) 9(12):e003334. doi: 10.1136/jitc-2021-003334

133. Baruch EN, Youngster I, Ben-Betzalel G, Ortenberg R, Lahat A, Katz L, et al. Fecal microbiota transplant promotes response in immunotherapy-refractory melanoma patients. *Science* (2021) 371(6529):602–9. doi: 10.1126/science.abb5920

134. Davar D, Dzutsev AK, McCulloch JA, Rodrigues RR, Chauvin JM, Morrison RM, et al. Fecal microbiota transplant overcomes resistance to anti-PD-1 therapy in melanoma patients. *Science* (2021) 371(6529):595–602. doi: 10.1126/science.abf3363

135. Tanoue T, Morita S, Plichta DR, Skelly AN, Suda W, Sugiura Y, et al. A defined commensal consortium elicits CD8 T cells and anti-cancer immunity. *Nature* (2019) 565(7741):600–5. doi: 10.1038/s41586-019-0878-z

136. Postow MA, Sidlow R, Hellmann MD. Immune-related adverse events associated with immune checkpoint blockade. *N Engl J Med* (2018) 378(2):158–68. doi: 10.1056/NEJMra1703481

137. Yau T, Park JW, Finn RS, Cheng AL, Mathurin P, Edeline J, et al. CheckMate 459: A randomized, multi-center phase III study of nivolumab (NIVO) vs sorafenib (SOR) as first-line (1L) treatment in patients (pts) with advanced hepatocellular carcinoma (aHCC). *Ann Oncol* (2019) 30:v874–v5. doi: 10.1093/annonc/mdz394

138. Finn RS, Ryoo BY, Merle P, Kudo M, Bouattour M, Lim HY, et al. Pembrolizumab as second-line therapy in patients with advanced hepatocellular carcinoma in KEYNOTE-240: A randomized, double-blind, phase III trial. *J Clin Oncol* (2020) 38(3):193–202. doi: 10.1200/jco.19.01307

139. Ren Z, Xu J, Bai Y, Xu A, Cang S, Du C, et al. Sintilimab plus a bevacizumab biosimilar (IBI305) versus sorafenib in unresectable hepatocellular carcinoma (ORIENT-32): a randomised, open-label, phase 2-3 study. *Lancet Oncol* (2021) 22(7):977–90. doi: 10.1016/s1470-2045(21)00252-7

140. Lee MS, Ryoo BY, Hsu CH, Numata K, Stein S, Verret W, et al. Atezolizumab with or without bevacizumab in unresectable hepatocellular carcinoma (GO30140): an open-label, multicentre, phase 1b study. *Lancet Oncol* (2020) 21(6):808–20. doi: 10.1016/s1470-2045(20)30156-x

141. Indini A, Di Guardo L, Cimminiello C, Prisciandaro M, Randon G, De Braud F, et al. Immune-related adverse events correlate with improved survival in patients undergoing anti-PD1 immunotherapy for metastatic melanoma. *J Cancer Res Clin Oncol* (2019) 145(2):511–21. doi: 10.1007/s00432-018-2819-x

142. Maher VE, Fernandes LL, Weinstock C, Tang S, Agarwal S, Brave M, et al. Analysis of the association between adverse events and outcome in patients receiving a programmed death protein 1 or programmed death ligand 1 antibody. *J Clin Oncol* (2019) 37(30):2730–7. doi: 10.1200/jco.19.00318

143. Ishihara H, Takagi T, Kondo T, Homma C, Tachibana H, Fukuda H, et al. Association between immune-related adverse events and prognosis in patients with metastatic renal cell carcinoma treated with nivolumab. *Urol Oncol* (2019) 37 (6):355.e21–.e29. doi: 10.1016/j.urolonc.2019.03.003

144. Haratani K, Hayashi H, Chiba Y, Kudo K, Yonesaka K, Kato R, et al. Association of immune-related adverse events with nivolumab efficacy in non-

Small-Cell lung cancer. *JAMA Oncol* (2018) 4(3):374–8. doi: 10.1001/jamaoncol.2017.2925

145. Masuda K, Shoji H, Nagashima K, Yamamoto S, Ishikawa M, Imazeki H, et al. Correlation between immune-related adverse events and prognosis in patients with gastric cancer treated with nivolumab. *BMC Cancer* (2019) 19(1):974. doi: 10.1186/s12885-019-6150-y

146. Shankar B, Zhang J, Naqash AR, Forde PM, Feliciano JL, Marrone KA, et al. Multisystem immune-related adverse events associated with immune checkpoint inhibitors for treatment of non-small cell lung cancer. *JAMA Oncol* (2020) 6(12):1952–6. doi: 10.1001/jamaoncol.2020.5012

147. Ng KYY, Tan SH, Tan JJE, Tay DSH, Lee AWX, Ang AJS, et al. Impact of immune-related adverse events on efficacy of immune checkpoint inhibitors in patients with advanced hepatocellular carcinoma. *Liver Cancer* (2022) 11(1):9–21. doi: 10.1159/000518619

148. Quandt Z, Young A, Anderson M. Immune checkpoint inhibitor diabetes mellitus: a novel form of autoimmune diabetes. *Clin Exp Immunol* (2020) 200 (2):131–40. doi: 10.1111/cei.13424

149. Lim CJ, Lee YH, Pan L, Lai L, Chua C, Wasser M, et al. Multidimensional analyses reveal distinct immune microenvironment in hepatitis b virus-related hepatocellular carcinoma. *Gut* (2019) 68(5):916–27. doi: 10.1136/gutjnl-2018-316510

150. Haber PK, Puigvehí M, Castet F, Lourdusamy V, Montal R, Tabrizian P, et al. Evidence-based management of hepatocellular carcinoma: Systematic review and meta-analysis of randomized controlled trials (2002-2020). *Gastroenterology* (2021) 161(3):879–98. doi: 10.1053/j.gastro.2021.06.008

151. Liu T, Li Q, Lin Z, Wang P, Chen Y, Fu Y, et al. Viral infections and the efficacy of PD-(L)1 inhibitors in virus-related cancers: Head and neck squamous cell carcinoma and hepatocellular carcinoma. *Int Immunopharmacol* (2021) 100:108128. doi: 10.1016/j.intimp.2021.108128

152. De Battista D, Zamboni F, Gerstein H, Sato S, Markowitz TE, Lack J, et al. Molecular signature and immune landscape of HCV-associated hepatocellular carcinoma (HCC): Differences and similarities with HBV-HCC. *J Hepatocellular Carcinoma* (2021) 8:1399–413. doi: 10.2147/jhc.S325959

153. Larrea E, Riezu-Boj JI, Gil-Guerrero L, Casares N, Aldabe R, Sarobe P, et al. Upregulation of indoleamine 2,3-dioxygenase in hepatitis c virus infection. *J Virol* (2007) 81(7):3662–6. doi: 10.1128/jvi.02248-06

154. Riezu-Boj JI, Larrea E, Aldabe R, Guembe L, Casares N, Galeano E, et al. Hepatitis c virus induces the expression of CCL17 and CCL22 chemokines that attract regulatory T cells to the site of infection. *J Hepatol* (2011) 54(3):422–31. doi: 10.1016/j.jhep.2010.07.014

155. Nakamoto N, Kaplan DE, Coleclough J, Li Y, Valiga ME, Kaminski M, et al. Functional restoration of HCV-specific CD8 T cells by PD-1 blockade is defined by PD-1 expression and compartmentalization. *Gastroenterology* (2008) 134(7):1927–37, 37.e1-2. doi: 10.1053/j.gastro.2008.02.033

156. Ho WJ, Danilova L, Lim SJ, Verma R, Xavier S, Leatherman JM, et al. Viral status, immune microenvironment and immunological response to checkpoint inhibitors in hepatocellular carcinoma. *J Immunother Cancer* (2020) 8(1):e000394. doi: 10.1136/jitc-2019-000394

157. Anstee QM, Reeves HL, Kotsiliti E, Govaere O, Heikenwalder M. From NASH to HCC: current concepts and future challenges. *Nat Rev Gastroenterol Hepatol* (2019) 16(7):411–28. doi: 10.1038/s41575-019-0145-7

158. Chang J, Ryan JS, Ajmera V, Ting S, Tamayo P, Burgoyne A. Responses to immunotherapy in hepatocellular carcinoma patients with nonalcoholic steatohepatitis cirrhosis. *J Clin Oncol* (2022) 40(4_suppl):389. doi: 10.1200/JCO.2022.40.4_suppl.389

159. Pfister D, Núñez NG, Pinyol R, Govaere O, Pinter M, Szydlowska M, et al. NASH limits anti-tumour surveillance in immunotherapy-treated HCC. *Nature* (2021) 592(7854):450–6. doi: 10.1038/s41586-021-03362-0

10.3389/fonc.2022.1091088

Glossary

HCC	hepatocellular carcinoma
aHCC	advanced hepatocellular carcinoma
TKIs	multitargeted tyrosine kinase inhibitors
OS	overall survival
ICIs	immune checkpoint inhibitors
FDA	Food and Drug Administration
PD-1	programmed death 1
NMPA	National Medical Products Administration
ORR	objective response rate
irAEs	immune-related adverse effects
NLR	neutrophilto-lymphocyte ratio
PLR	platelet-to-lymphocyte ratio
TACE	transarterial chemoembolization
CR	complete response
PR	partial response
PD	progressive disease
PFS	progression-free survival
HR	hazard ratio
HPD	hyperprogressive disease
PVT	portal vein thrombosis
ECOG	Eastern Cooperative Oncology Group
BCLC	Barcelona Clinic Liver Cancer
VEGF	vascular endothelial growth factor
AFP	alpha-fetoprotein
CRP	C-reactive protein
SD	stable disease
DCR	disease control rate
TGF-β	transforming growth factor-β
TNFRSF9	TNF receptor superfamily member 9
PD-L1	programmed death ligand 1
DFS	disease-free survival
CB	clinical benefit
CTC	circulating tumor cell
ctDNA	circulating tumor DNA
CNV	copy number variation
TiME	tumor immune microenvironment
TAM	tumor-associated macrophage
DEG	differentially expressed gene
GSEA	gene set enrichment analysis
ABRS	atezolizumab + bevacizumab response signature
Teff	T effector
TMB	tumor mutational burden
CPS	combined positive score
TPS	tumor proportion score
CBR	clinical benefit response
NCB	non-clinical benefit
FMT	fecal microbiota transplantation
HBV	hepatitis B virus
HCV	hepatitis C virus
NAFLD	non-alcoholic fatty liver disease
NASH	nonalcoholic steatohepatitis

frontiers | Frontiers in Oncology

TYPE Original Research
PUBLISHED 19 January 2023
DOI 10.3389/fonc.2022.1086095

OPEN ACCESS

EDITED BY
Xiong Chen,
Nanjing General Hospital of Nanjing Military Command, China

REVIEWED BY
Jiaping Zheng,
University of Chinese Academy of Sciences, China
Kangshun Zhu,
The Second Affiliated Hospital of Guangzhou Medical University, China

*CORRESPONDENCE
Zhi-Ping Yan
zhipingyan@fudan.edu.cn
Xu-Dong Qu
qu.xudong@zs-hospital.sh.cn

†These authors have contributed equally to this work

SPECIALTY SECTION
This article was submitted to Gastrointestinal Cancers: Hepato Pancreatic Biliary Cancers, a section of the journal Frontiers in Oncology

RECEIVED 01 November 2022
ACCEPTED 29 December 2022
PUBLISHED 19 January 2023

CITATION
Zhang Z-H, Hou S-N, Yu J-Z, Zhang W, Ma J-Q, Yang M-J, Liu Q-X, Liu L-X, Luo J-J, Qu X-D and Yan Z-P (2023) Combined iodine-125 seed strand, portal vein stent, transarterial chemoembolization, lenvatinib and anti-PD-1 antibodies therapy for hepatocellular carcinoma and Vp4 portal vein tumor thrombus: A propensity-score analysis. *Front. Oncol.* 12:1086095. doi: 10.3389/fonc.2022.1086095

Combined iodine-125 seed strand, portal vein stent, transarterial chemoembolization, lenvatinib and anti-PD-1 antibodies therapy for hepatocellular carcinoma and Vp4 portal vein tumor thrombus: A propensity-score analysis

Zi-Han Zhang[1,2,3†], Si-Nan Hou[1,2,3†], Jia-Ze Yu[1,2,3†], Wen Zhang[1,2,3], Jing-Qin Ma[1,2,3], Min-Jie Yang[1,2,3], Qing-Xin Liu[1,2,3], Ling-Xiao Liu[1,2,3], Jian-Jun Luo[1,2,3], Xu-Dong Qu[1,2,3*] and Zhi-Ping Yan[1,2,3*]

[1]Department of Interveintional Radiology, Zhongshan hospital, Fudan, University, Shanghai, China, [2]Shanghai Institute of Medical Imaging, Fudan University, Shanghai, China, [3]National Clinical Research Center of Interventional Medicine, Zhongshan Hospital, Fudan University, Shanghai, China

Objective: To evaluate the safety and efficacy of interventional therapy (iodine-125 [^{125}I] seed strand and portal vein stent [PVS] implantation plus transarterial chemoembolization [TACE]) combined with systemic therapy (lenvatinib plus anti-PD-1 antibody) as first-line treatment for hepatocellular carcinoma (HCC) patients with Vp4 portal vein tumor thrombus (PVTT).

Patients and methods: From December 2018 to October 2021, 87 HCC patients with Vp4 PVTT were included in this single-center retrospective study. Forty-seven patients underwent interventional therapy combined with lenvatinib and anti-PD-1 antibody (group A), while 40 cases underwent interventional therapy combined with lenvatinib only (group B). Overall response rate (ORR), stent occlusion rates (SOR), median overall survival (OS), median progression-free survival (PFS) and median stent patency time (SPT) were compared between the 2 groups.

Results: The mean intended dose (r = 10 mm; z = 0; 240 days) was 64.9 ± 1.0 Gy and 64.5 ± 1.1 Gy in group A and B, respectively (p = 0.133). ORR and SOR were significantly different between group A and B (ORR, 55.3% vs 17.5%, p < 0.001; SOR, 12.8% vs 35.0%, p = 0.014). In the propensity-score matching (PSM) cohort, the median OS, median PFS and median SPT were significantly longer in group A compared with group B (32 PSM pairs; OS, 17.7 ± 1.7 vs 12.0 ± 0.8 months, p = 0.010; PFS, 17.0 ± 4.3 vs 8.0 ± 0.7 months, p < 0.001; SPT, not-reached vs 12.5 ± 1.1 months, p = 0.028).

Conclusion: This interventional therapy combined with lenvatinib and anti-PD-1 antibody is safe and effective for HCC patients with Vp4 PVTT.

KEYWORDS

hepatocellular carcinoma, portal vein tumor thrombus, iodine-125 seed strand, transarterial chemoembolization, lenvatinib, anti-PD-1 antibody

Introduction

Portal vein tumor thrombus (PVTT), a common pattern in advanced hepatocellular carcinoma (HCC), is found in 10~40% of patients (1). The prognosis of patients with PVTT in the main trunk (Vp4 PVTT) remains poor. The median overall survival (OS) of these patients is only 2.7~4.0 months if untreated (2). The perioperative mortality rate is 0%-28%, with a 5-year OS rate of 0%-26% (3, 4).

Based on the SHARP and REFLECT trials (5, 6), sorafenib and lenvatinib were recommended as first-line systemic therapy for patients with advanced unresectable HCC (7). However, Kaneko et al. reported a median OS of only 5.5 months in patients with Vp3/4 PVTT administered sorafenib and Lenvatinib (8).

Linear iodine-125(^{125}I) seed strand combined with portal vein stent (PVS) implantation plus transarterial chemoembolization (TACE) was proposed by Luo et al. for patients with HCC and Vp4 PVTT (9). Zhang et al. conducted a retrospective study that combined sorafenib with this interventional treatment strategy. This combined therapy prolonged the OS to 12.3 months in these patients (10).

In recent years, immune checkpoint inhibitor (ICI) therapy, particularly applying antibodies targeting the programmed cell death-1 (PD-1)/programmed cell death ligand-1 (PD-L1) pathway, has been a significant component of numerous combination regimens in advanced HCC (11–13).

This study performed to evaluate the safety and efficacy of interventional therapy (^{125}I seed strand and PVS implantation plus TACE) combined with systemic therapy (lenvatinib plus anti-PD-1 antibody) as first-line treatment for HCC patients with Vp4 PVTT.

Materials and methods

Patients

This was a single-center retrospective study. The study was approved by the local institutional review board. Informed consent was waived. We reviewed the electronic medical records of 109 consecutive patients with hepatitis B-related HCC and Vp4 PVTT, who were administered interventional therapy (^{125}I seed strand and PVS implantation plus TACE) combined with systemic therapy (lenvatinib plus anti-PD-1 antibody) (group A) or interventional therapy (^{125}I seed strand and PVS implantation plus TACE) combined with lenvatinib only (group B) from December 2018 to October 2021. Before treatment initiation, the benefits, and potential adverse events (AEs) related to both combination regimens were explained thoroughly to the patients. The final choices were made by the patients. (Figure 1)

Intrahepatic HCC was diagnosed based on the American Association for the Study of Liver Disease guidelines or histology (14). According to the standard recommended by Shah et al. (15), a PVTT was considered to be neoplastic if at least one of the following criteria was met: (a) expansion of the involved vessel (vessel diameter ≥ 1.8 cm for the MPV, ≥ 1.6 cm for the right portal vein (PV), or ≥ 1.8 cm for the left PV; (b) clear evidence of enhancement on dynamic contrast-enhanced CT images during the arterial phase of dynamic imaging, compared with baseline images (≥ 20 HU on CT). Otherwise, the PVTT was bland. The extent of

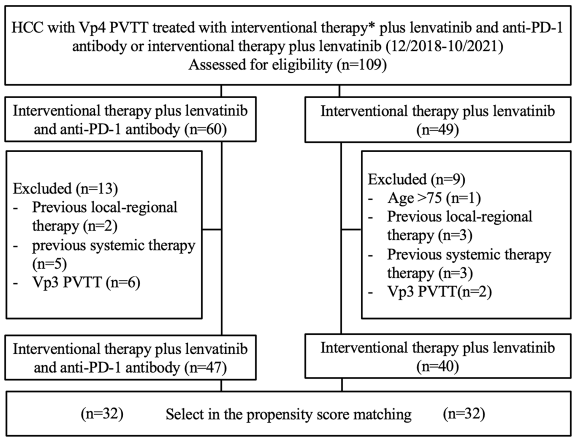

FIGURE 1
Patient selection flow chart. * Interventional therapy = ^{125}I seed strand and PVS implantation plus TACE.

PVTT was classified as follows: Vp0, no PVTT; Vp1, segmental PV invasion; Vp2, right anterior or posterior PV; Vp3, right or left PV; Vp4, main trunk and/or contralateral portal vein branch to the primarily involved lobe (16).

Inclusion criteria were: [1] between 18 and 75 years of age; [2] a single tumor ≥ 5.0 cm or multiple nodular tumors > 3.0 cm; [3] Vp4 PVTT; [4] patent second-order branch of the portal vein prior to PVTT; [5] Child-Pugh class A or B; and [6] an Eastern Cooperative Group performance status (ECOG) score of 0-2. These points represent eligibility criteria for the treatment.

Exclusion criteria were: [1] Vp1-3 PVTT; [2] completely occluded portal vein; [3] hepatic encephalopathy, severe ascites, esophageal, gastric fundal variceal bleeding or other serious medical comorbidities; [4] previous local-regional therapy (radiofrequency ablation [RFA], microwave ablation [MWA], cryoablation, yttrium-90 [90Y] radioembolization, stereotactic body radiotherapy [SBRT], hepatic artery infusion chemotherapy [HAIC], or liver transplantation); [5] previous systemic therapy (tyrosine kinase inhibitors [TKIs], systemic chemotherapy, or immunotherapy); or [6] malignant tumor other than HCC.

Interventional therapy

The protocol for interventional therapy (^{125}I seed strand and PVS implantation plus TACE) was the same in both groups.

^{125}I seed properties

Model 6711 ^{125}I seeds (XinKe; Shanghai, China) were used in this study. The radioactivity of each ^{125}I seed was 25.9 MBq with a half-life of 59.4 days. Principal photon emissions were 27.4 and 35.5 keV X-rays and gamma-rays, respectively. The half-value thickness of the tissue for ^{125}I seed was 17 mm, and the incipient dose rate was 7 cGy/h. The 240-day intended dose at 10 mm from the axis of the ^{125}I seed strand was calculated with a radiation calculation software (version

0.1) based on the American Association of Physicists in Medicine TG43U1 brachytherapy formalism (17). (Figure 2)

The production process of ^{125}I seed strands was as follows: (a) a 4-F flexible compliant cannula (Boston Scientific, Natick, Massachusetts) was sealed at one end with an alcohol lamp; (b) ^{125}I seeds were loaded into the tube linearly, and the number of ^{125}I seeds loaded (N) was determined as N = L/4.5 + 4, where L (mm) is the length of the obstructed PV (9); (c) the other end was cut and sealed.

^{125}I seed strand and PVS implantation

The contralateral secondorder branch was punctured with a 21-gauge Chiba needle (Cook, Bloomington, Indiana) under ultrasound guidance, followed by the insertion of a 0.018-inch wire (Cook) into the MPV. A 6-F NEEF set (Cook) was introduced into the MPV over the wire. Through the outer cannula of the 6-F NEEF set, a 0.035-inch wire (Terumo, Tokyo, Japan) combined with a 4-F Cobra catheter (Cordis, Miami Lakes, Florida) was manipulated across the obstructed MPV into the superior mesenteric vein (SMV). The 4-F Cobra catheter and the 6-F NEEF set were removed, and a 6-F sheath (Cordis) was introduced through the wire. Portography was performed to measure the diameter and length of the obstructed MPV by a 4-F pigtail catheter (Cook) placed in the SMV. Two 0.035-inch stiff wires (Terumo) were inserted into the SMV through the 6F sheath. After the sheath removal, the 6-F NEFF set and a self-expandable stent (Bard, New Jersey, America) of appropriate size were introduced into the MPV over one of the stiff wires, respectively. The stent was deployed from the distal MPV into the contralateral fist-order branch of the portal vein. A ^{125}I seed strand was delivered to the target position *via* the outer cannula of the 6-F NEFF set and released between the stent and the MPV. Portography was repeated through the 4-F pigtail catheter (Cook). The puncture tract was next occluded by 3 × 140 mm Nester coils (Cook).

Then, the ipsilateral second-order portal vein branch was punctured with a 21-gauge Chiba needle (Cook) under ultrasound guidance. With confirmed access, a 0.018-inch wire (Cook) was manipulated to cross the obstructed segment of ipsilateral portal vein branch and positioned into the MPV. A 6-F NEFF set (Cook) was introduced into the ipsilateral portal vein over the 0.018-inch wire. Then, the 0.018-inch wire was replaced by a 0.035-inch wire (Cook). Another ^{125}I seed strand was pushed to the target position of PVTT in ipsilateral portal vein branch by the inner core of the 6-F NEFF set. Then, the outer cannula of the 6-F sheath was retreated slowly until the strand was completely released. The position of the strand should completely cover the macroaxis of PVTT in ipsilateral portal vein branch. Finally, the transhepatic puncture track was occluded by 3 × 140 mm Nester coils (Cook) (Figures 3A-C).

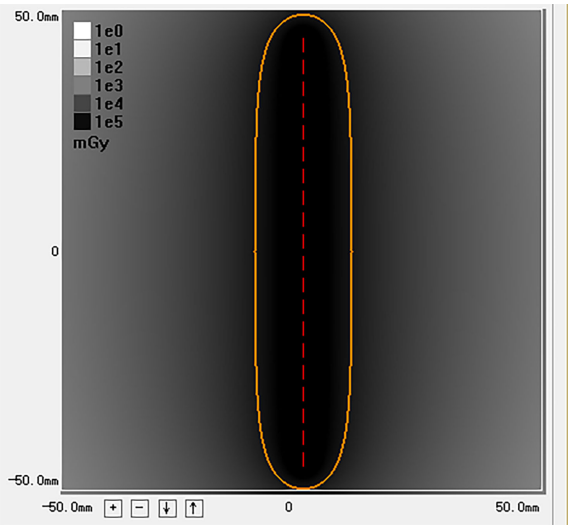

FIGURE 2
This image is the radiation distribution of a strand loaded with 20 ^{125}I seeds simulated by the calculation software. The yellow circle represents a 100% isodose contour (r = 10mm). The 240 days' intended dose of this ^{125}I seed strand is 63.5 Gy.

TACE procedure

TACE was provided after the ^{125}I seed strand and PVS implantation immediately. Hepatic angiography was performed to evaluate tumor vascularity. A chemotherapeutic emulsion consisting of 10-50 mg epirubicin (Pharmorubicin; Pfizer, New York) and 4-10 ml lipiodol (Lipiodol; Guerbet, Roissy, France) was slowly injected at a rate of 0.5-1.0 mL/min under fluoroscopic guidance *via* a 2.4-F microcatheter (Merit Medical, USA) until saturation of the tumor-supplying arteries. The dose of iodized oil was calculated as 1.0-1.5 ml per cm in dimeter of tumor. If the tumor had a rich blood supply, more oil was needed and vice versa. The dose of epirubicin was calculated as 10–50 mg/m^2 of body surface area. Then, 350-560-μm gelatin sponge particles (Jingling, Jiangsu, China) were used to embolize the residual feeding artery of tumor.

Systemic therapy

In both groups, all patients received Lenvatinib (MSD, USA) 3 days after the first interventional procedure. Lenvatinib was orally administered at 8 mg/day in patients weighing <60 kg and at 12 mg/day in those ≥60 kg. In patients developing AEs (grade ≥2), dose reduction or temporary interruption was maintained until the symptoms resolved to grade 0-1. AEs were assessed by the National Cancer Institute (NCI) Common Terminology Criteria for Adverse Events (CTCAE v4.03).

In group A, patients received anti-PD-1 inhibitor injection in 3-7 days after the first interventional procedure. They were monitored regularly, including repeat safety evaluation 2-3 days prior to each anti-PD-1 antibody treatment cycle. Anti-PD-1 antibodies were intravenously administered as follows: nivolumab (Bristol-Myers Squibb, USA) 3 mg/kg or camrelizumab (Hengrui Medicine, China) 200 mg every 2 weeks (18), or pembrolizumab (MSD, USA) 200 mg, sintilimab (Innovent Biologics, China) 200 mg (19) or toripalimab (Junshi Bioscience, China) 240 mg (20), every 3 weeks. In patients developing AEs (grade 2), temporary interruption was maintained until the symptoms resolved to grade 0-1. In patients developing AEs (grade 3-4), anti-PD-1 inhibitor injection was ceased permanently.

Post-procedure management

Single photon-emission computer tomography combined with CT (SPECT/CT) was performed on day 1 to evaluate the location and

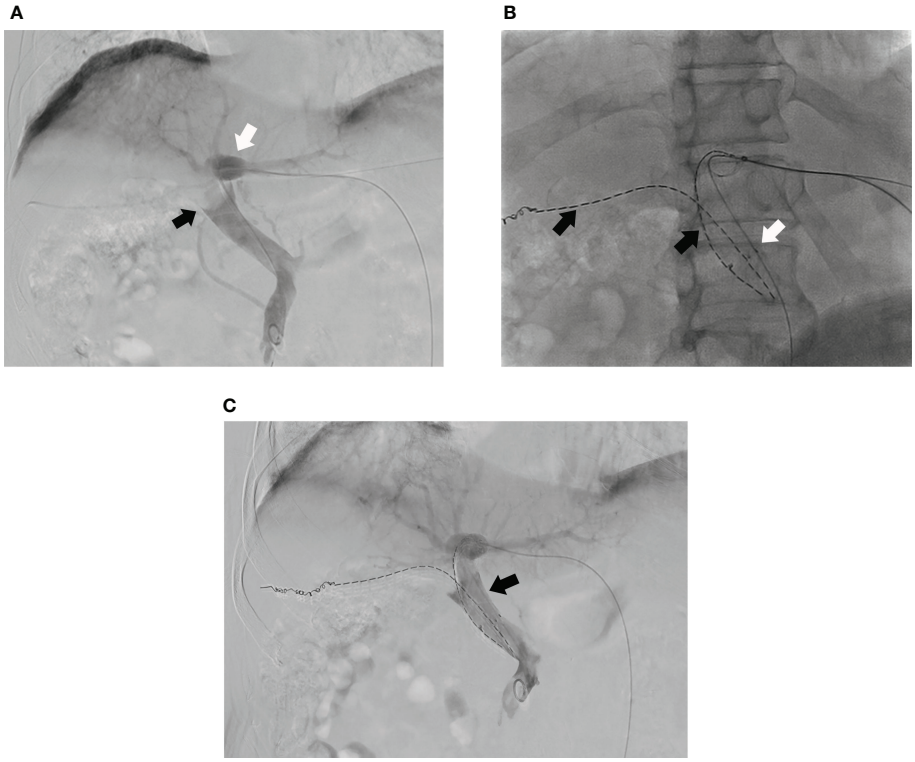

FIGURE 3
(A) Portography of a male patient in group A shows tumor thrombus in MPV (black arrow) and the left portal vein branch is still patent (white arrow) and; **(B)** A ^{125}I seed strand (black arrow) and a stent (white arrow) are placed from left portal vein to MPV and another ^{125}I seed strand is placed into right portal vein (black arrow); **(C)** The portal venography shows the MPV is more patent after the PVS and ^{125}I seed strands implantation (black arrow).

distribution of radiation by the ^{125}I seed strand. Laboratory tests (including hepatic and renal functions, complete blood count, and coagulation parameters) were performed 3-7 days after the initial procedure.

In the first 2 days, 4,100 U of low- molecular-weight heparin (XinYi, Shanghai, China) was injected subcutaneously twice a day. Beginning 3 days after the procedure, warfarin (XinYi, Shanghai, China), starting with 2.5 mg every day, was administered to all patients, and continued for 6 months. The dose of warfarin was adjusted based on the coagulability test (international normalized ratio = 1.8–2.0).

Follow-up and evaluation

The follow-up period was defined as the time from the initial interventional procedure to death or the last follow-up date. Each follow-up session included a detailed medical history, physical examination, laboratory tests, and contrast-enhanced CT or MRI. Follow-up was conducted every 30-45 days after the initial procedure. Patients with residual viable tumors or recurrent tumors in the hepatic parenchyma on CT or MRI images underwent repeated TACE in case the Child-Pugh status remained at class A or B. No other interventional therapy was provided except for TACE. (Figures 4A, B)

The primary endpoint was overall survival (OS, defined as the time from the initial interventional procedure to death from any cause). Secondary endpoint was progression-free survival (PFS, defined as the time from the initial interventional procedure until tumor progression or death from any cause).

Intrahepatic tumor response was classified as complete response (CR), partial response (PR), stable disease (SD), or progressive disease (PD) according to modified Response Evaluation Criteria in Solid Tumor (mRECIST) criteria. Overall response rate (ORR) was defined as the percentage of patients who had a best tumor response rating of CR or PR. Disease control rate (DCR) was defined as the percentage of patients achieving CR, PR or SD as the best tumor response.

PVTT response was evaluated by the rate of stent occlusion and the median stent patency time (SPT). Because PVTT was changed into an irregular shape and positioned between the stent and the portal vein wall after stent implantation, it is hard to calculate the volume of PVTT precisely. Stent occlusion was defined with no contrast medium detected inside the stent on the portal phase of contrast-enhanced CT or contrast-enhanced MRI images, or no blood flow signal detected by color doppler flow imaging (CDFI). SPT was determined from the day of stent placement to stent occlusion or the day of last follow-up.

Statistical analysis

All statistical analysis was performed with SPSS (version 23.0, Chicago, Illinois). Continuous variables were presented as mean ± standard deviation and were compared by independent or paired samples *t* test. Categorical variables were presented as frequency and compared by the Chi-square test. Median PFS, median OS and

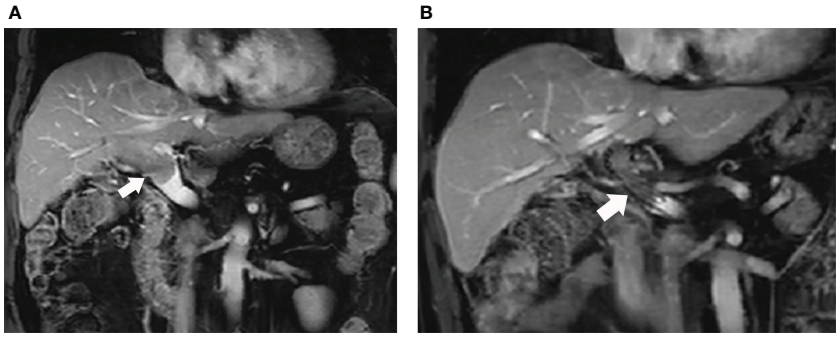

FIGURE 4
(A) The MRI images of this male patient shows the tumor thrombus had invaded into the MPV from right portal vein (white arrow); **(B)** The patient received ^{125}I seed strands and PVS implantation plus TACE combined with lenvatinib and anti-PD-1 antibody therapy. The MRI images performed 11 months after the initial procedure shows the stent is still patent (white arrow).

median SPT were analyzed by the Kaplan-Meier method and the log-rank test. A p-value < 0.05 was considered statistically significant. Factors statistically significant at p-value < 0.05 in univariate analysis were entered a multivariable Cox proportional hazards model.

Sex, age, tumor size, Child-Pugh class, AFP level and extrahepatic metastasis were considered within the propensity-score matching (PSM) model. PSM was performed, with a matching ratio of 1:1 for both groups, using the nearest-neighbor matching method, with a caliper distance of 0.2 without replacement. OS, PFS, SPT and multivariate analysis were compared between the matched groups.

Results

Patients

According to the inclusion and exclusion criteria, 87 patients were included in this study (Group A, n=47; and Group B, n=40). Baseline characteristics are presented in (Table 1). After the PSM, 32 pairs were matched.

Technical success

The technique was performed successfully in all patients. The mean number of ^{125}I seeds loaded were 38.0 ± 13.5 (range, 20-60) and 33.4 ± 14.7 (range, 16-60) in groups A and B, respectively (p = 0.136). The mean intended doses were 64.9 ± 1.0 Gy (range, 63.5-66.5 Gy) and 64.5 ± 1.1 Gy (range, 63.2-66.5 Gy) in groups A and B, respectively (p = 0.133). No dislodge of ^{125}I seed strand was observed in SPETCT/CT and CT images. Totally 87 patients in both groups received a total of 296 TACE procedures (154 and 142 in groups A and B, respectively). Mean 3.3 ± 1.9 (range 1-9) and 3.6 ± 1.6 (range 1-8) TACE procedures were performed in groups A and B, respectively (p = 0.476).

Tumor response

Treatment response for intrahepatic tumors in all patients is presented in (Table 2). ORR and DCR were significantly higher in group A compared with group B (ORR, 55.3% vs 17.5%, p < 0.001; DCR, 70.2 vs 30.0, p < 0.001).

Stent occlusion by tumor invasion was observed in 6 (12.8%) group A and 14 (35.0%) group B patients (p = 0.014). The cumulative stent patency rates at 3-, 6-, 9- and 12-months were 97.8%, 93.3%, 88.7% and 88.7% in group A, and 100.0%, 89.5%, 81.6% and 76.3% in group B, respectively (p = 0.003).

In group A, 2 patients with PR tumor response were administered liver transplantation at 11 and 11.5 months after the initial interventional therapy, respectively. One patient in group A with PR tumor responses was administered surgical resection of intrahepatic tumor at 11.7 months after the initial interventional therapy. No patient received surgical resection or liver transplantation in group B.

Survival

The mean follow-up times were 14.2 ± 5.1 and 11.0 ± 5.0 months in groups A and B, respectively. During the follow-up period, 25 (53.2%) and 34 (85.0%) patients died in groups A and B, respectively (p = 0.002). Overall survival rates at 3-, 6-, 9- and 12-months were 93.6%, 89.4%, 80.9% and 76.6% in group A, and 92.5%, 85.0%, 65.0% and 43.7% in group B, respectively (p < 0.001). The causes of death are presented in (Table 3).

In PSM cohorts, median OS, median PFS, median SPT and multivariate analysis were compared between the 2 groups. The median OS was 17.7 ± 1.7 months (95%CI, 14.3-21.0 months) in group A and 12.0 ± 0.8 months in group B (95%CI, 10.4-13.6 months) (p = 0.010) (Figure 5A). Meanwhile, the median PFS was 17.0 ± 4.3 (95%CI, 8.5-25.5) and 8.0 ± 0.7 (95%CI, 6.6-9.3) months in groups A and B, respectively (p < 0.001) (Figure 5B). The median SPT was not reached in group A and was 12.5 ± 1.1 months in group B (95%CI, 10.3-14.7 months; p = 0.028). (Figure 5C)

In univariate analysis, treatment regimen and sex statistically significant at p < 0.05 and they were entered a multivariable Cox proportional hazards model. Multivariate analysis found that the treatment regimen and sex were two independent prognostic factors of OS. (Table 4)

In group A, 10 patients received pembrolizumab injection (median OS, 16.8 ± 3.7 months; median PFS, 16.8 ± 4.5 months), 9

TABLE 1 Baseline characteristics of the 2 groups before and after propensity score matching.

	Before propensity score matching			After propensity score matching		
Characteristic	Group A (n=47)	Group B (n=40)	*p*-value	Group A (n=32)	Group B (n=32)	*p*-value
Sex			1.000			1.000
Male	42 (89.4)	36 (90.0)		29 (90.6)	30 (93.8)	
Female	5 (10.6)	4 (10.0)		3 (9.4)	2 (6.3)	
Age			0.425			0.448
≥55y	23 (48.9)	23 (57.5)		17 (53.1)	20 (62.5)	
<55y	24 (51.1)	17 (42.5)		15 (46.9)	12 (37.5)	
Tumor size *(mm)			0.446			1.000
≥10cm	22 (46.8)	22 (55.0)		16 (50.0)	16 (50.0)	
<10cm	25 (53.2)	18 (45.0)		16 (50.0)	16 (50.0)	
Extrahepatic metastasis			0.786			1.000
Yes	5 (10.6)	5 (12.5)		3 (9.4)	2 (6.3)	
No	42 (89.4)	35 (87.5)		29 (90.6)	30 (93.8)	
Child-Pugh class			1.000			1.000
A	44 (93.6)	38 (95.0)		30 (93.8)	30 (93.8)	
B	3 (6.4)	2 (5.0)		2 (6.3)	2 (6.3)	
ECOG performance status			0.658			0.238
0/1	45 (95.7)	37 (92.5)		32 (100.0)	29 (90.6)	
2	2 (4.3)	3 (7.5)		0 (0.0)	3 (9.4)	
Serum AFP level			0.064			0.784
≥400	25 (53.2)	29 (72.5)		23 (71.9)	22 (68.8)	
<400	22 (46.8)	11 (27.5)		9 (28.1)	10 (31.3)	

Values in parentheses are percentages.
AFP, α-fetoprotein; ECOG, Eastern Cooperative Oncology Group.
*Tumor size, the maximum diameter of the largest target index lesion.

received toripalimab injection (median OS, 20.0 ± 3.5 months; median PFS, 14.1 ± 3.1 months), 12 received sintilimab injection (median OS, 17.7 ± 2.3 months; median PFS, 17.0 ± 0.0 months), 9 received camrelizumab injection (median OS, 18.0 ± 5.1 months; median PFS, 18.0 ± 6.1 months), and 7 received nivolumab injection (median OS, 19.2 ± 0.4 months; median PFS, 17.6 ± 7.1 months).

Safety

No serious complications related to interventional treatment, including acute hepatic failure, liver abscess, intraperitoneal bleeding, and radiation hepatitis was observed. The incidence rates of fever, vomiting and upper-abdominal pain were 23.4%, 29.8% and

TABLE 2 Response of intrahepatic HCC.

	Group A n=47	Group B n=40	*P*-value
CR	2	0	
PR	24	7	
SD	7	5	
PD	14	28	
ORR (%)	55.3	17.5	<0.001
DCR (%)	70.2	30.0	<0.000

CR, complete response; DCR, disease control rate; PD, progressive disease; PR, partial response; SD, stable disease.
ORR = (CR + PR)/n.
DCR = (CR + PR + SD)/n.

TABLE 3 The causes of death in 2 groups.

Causes of death	Group A (n=25)	Group B (n=34)	*p*-value
Tumor progression	7(28.0)	19(55.9)	0.033
hepatic failure	7(28.0)	7(20.6)	0.508
Variceal bleeding	6(24.0)	5(14.7)	0.365
Hepatic encephalopathy	1(4.1)	1(2.9)	1.000
Liver abscess	0(0.0)	1(2.9)	1.000
Respiratory failure	1(4.1)	1(2.9)	1.000
Myocardial infarction	2(8.0)	0(0.0)	0.175
Cerebral hemorrhage	1(4.1)	0(0.0)	0.424

Values in parentheses are percentages.

53.2% in group A, and 27.5%, 22.5% and 60.0% in group B, respectively. They were all resolved after symptomatic treatment.

In 2 groups, all recorded AEs related to systemic treatment are shown in (Table 5). Eight (17.0%) and 12 (25.5%) patients occurred 11 and 15 AEs related lenvatinib in group A and B, respectively (p = 0.152). Grade 3 diarrhea and hypertension occurred in 1 patient each and led to lenvatinib dose reduction. In group A, 5 (10.6%) patients occurred 5 anti-PD-1 antibody related AEs. Grade 3 immunological enteritis and immunological myocarditis occurred in 1 patient each, and anti-PD-1 antibody injection was ceased permanently.

These patients were all relieved by symptomatic treatment (grade 1AEs) and lenvatinib dose reduction and/or anti-PD-1 antibody cease (grade ≥2 AEs). No grade 4 AE occurred, and no patient died of AEs in this study.

Discussion

This study demonstrated that interventional therapy (^{125}I seed strand and PVS implantation plus TACE) combined with systemic therapy (lenvatinib plus anti-PD-1 antibody) is a safe and effective treatment strategy for HCC patients with Vp4 PVTT.

The prognosis of advanced HCC remains poor, especially for patients with PVTT. Furthermore, OS is shorter in patients with Vp4 PVTT than in those with Vp0-3 PVTT (21, 22). The main reason for the poor prognosis is MPV occlusion, which is associated with increased risk of tumor spread, elevated portal venous pressure causing variceal hemorrhage, and decreased portal flow resulting in ascites, jaundice, hepatic encephalopathy, and liver failure (9). However, without treatment the interval between the formation of

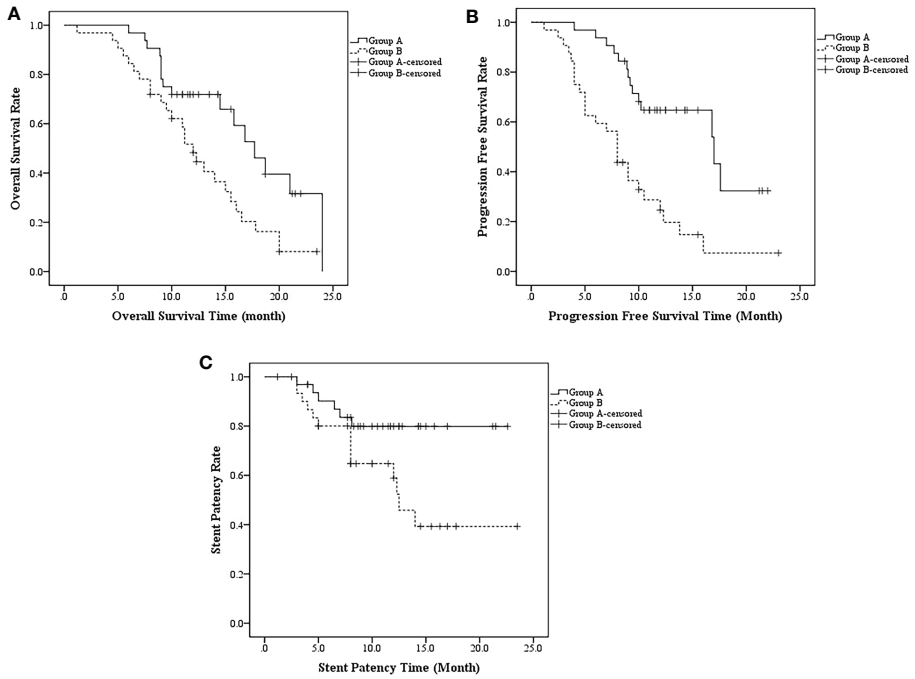

FIGURE 5
(A) The median OS was 17.7 ± 1.7 months (95%CI, 14.3-21.0 months) in group A and 12.0 ± 0.8 months in group B (95%CI, 10.4-13.6 months) (p = 0.010); **(B)** the median PFS was 17.0 ± 4.3 (95%CI, 8.5-25.5) and 8.0 ± 0.7 (95%CI, 6.6-9.3) months in groups A and B, respectively (p < 0.001); **(C)** The median SPT was not reached in group A and was 12.5 ± 1.1 months in group B (95%CI, 10.3-14.7 months; p = 0.028).

TABLE 4 Log-rank test and Cox regression analysis of factors potentially related to OS in PSM cohorts.

	32 PSM pairs (n=64)				
		Log-rank test		Multivariate	
Factors	No. of Patients	Median OS (95%CI)	*p*-value	HR (95%CI)	*p*-value
Sex			0.038		0.035
Male Female	59 5	15.8±1.3 (13.3-18.3) 9.5±0.3 (8.9-10.1)		0.350 (0.132-0.930) 1	
Age			0.120		
≥55y	37	12.0±1.8 (8.4-15.6)			
<55y	27	16.8±2.3 (12.3-21.3)			
Treatment regimen			0.010		0.011
Group A	32	17.7±1.7 (14.4-21.0)		0.434 (0.228-0.823)	
Group B	32	12.0±0.8 (10.4-13.6)		1	
Tumor size *(mm)			0.705		
≥10cm	32	13.0±2.3 (8.6-17.4)			
<10cm	32	15.8±0.7 (14.5-17.1)			
Child-Pugh class			0.330		
A	60	15.0±1.5 (12.1-17.9)			
B	4	10.0±3.7 (2.8-17.2)			
Serum AFP level			0.971		
≥400	45	14.5±2.0 (10.7-18.3)			
<400	19	12.3±4.2 (4.2-20.4)			
Extrahepatic metastasis			0.350		
Yes	5	10.0±2.5 (5.1-14.9)			
No	59	15.0±1.5 (11.9-18.0)			

AFP, α-fetoprotein; CI, confidence interval; HR, hazard ratio.
*Tumor size, the maximum diameter of the largest target index lesion.

segmental PVTT and complete obstruction is <6 weeks (23). These previous studies implied that there are two key points in the treatment strategy for patients with Vp4 PVTT: first, restoring the flow of obstructed portal vein; second, inhibiting intrahepatic tumor and PVTT progression.

Luo et al. proposed PVS and ^{125}I seed strand which implanted from contralateral branch to MPV combined with TACE treatment for HCC patients with Vp4 PVTT (9). Even though, this interventional treatment strategy prolonged the OS to 9.3 months. The PFS was only 1.8 months and stent occlusion by tumor invasion occurred in 68.1% patients. Based on this interventional technique, a new improvement was made in this study: except for the PVS and ^{125}I seed strand which implanted from contralateral branch to MPV, another ^{125}I seed strand was implanted into the ipsilateral branch which inhibited the progression of tumor thrombus in ipsilateral branch and prolonged the stent patency time.

According to BCLC stage, sorafenib and lenvatinib were recommended as first-line systemic therapy for patients with HCC and PVTT (7). Zhang et al. conducted a retrospective study that combined sorafenib with interventional therapy proposed by Luo et al. for treating patients with HCC and Vp4 PVTT (10). The median OS and median time to progression (TTP) were 12.3 and 9.0 months, respectively. In recent years, the approval of lenvatinib has provided a new option for patients in BCLC C stage. According to the REFLECT trial, the ORR of lenvatinib is significantly higher than that of sorafenib (6).

More recently, ICI therapy plus anti-VEGF therapy have been recommended as a new effective systemic treatment strategy for patients with advanced HCC. One of the underlying mechanisms is that anti-VEGF therapies can reduce VEGF therapy-mediated immunosuppression within the tumor and its microenvironment may enhance anti-PD-1/PD-L1 efficacy by reversing VEGF-mediated immunosuppression and promoting tumor T-cell infiltration (24). In the IMbrave150 study, ORRs were 33.2% and 13.3% in the atezolizumab-bevacizumab and sorafenib groups, respectively, and OS was significantly longer with atezolizumab-bevacizumab (25). Huang et al. performed a real-world study that analyzed HCC patients with macrovascular tumor thrombus (MVTT) administered lenvatinib plus anti-PD-1 antibodies as first-line treatment (26). This combination therapy resulted in better tumor responses in MVTT (ORR for MVTT, 54.5%) than in intrahepatic tumor (32.8%) and lung metastases (37.5%). Based on these results, whether combined interventional therapy with ICI therapy and TKIs

10.3389/fonc.2022.1086095

TABLE 5 Adverse events related to systemic therapy in 2 groups.

	Group A (n=47)	Group B (n=40)	*p*-value
Lenvatinib related AEs			
Diarrhea			
Grade 1-2	3 (6.4)	4 (10.0)	0.698
Grade 3-4	1 (2.1)	0 (0.0)	1.000
Hand-foot skin reaction			
Grade 1-2	2 (4.3)	3 (7.5)	0.658
Grade 3-4	0 (0.0)	0 (0.0)	
Hypertension			
Grade 1-2	4 (8.5)	5 (12.5)	0.727
Grade 3-4	0 (0.0)	1 (2.5)	0.460
Duodenal ulcer			
Grade 1-2	1 (2.1)	0 (0.0)	1.000
Grade 3-4	0 (0.0)	0 (0.0)	
Leukopenia and thrombocytopenia			
Grade 1-2	0 (0.0)	2 (5.0)	0.209
Grade 3-4	0 (0.0)	0 (0.0)	
Anti-PD-1 antibody related AEs			
Immunological hypothyroidism			
Grade 1-2	1 (2.1)		
Grade 3-4	0 (0.0)		
Immunological enteritis			
Grade 1-2	0 (0.0)		
Grade 3-4	1 (2.1)		
Immunological myocarditis			
Grade 1-2	0 (0.0)		
Grade 3-4	1 (2.1)		
Immunological pneumonia			
Grade 1-2	2 (2.4)		
Grade 3-4	0 (4.3)		

Values in parentheses are percentages.

could provide more effective tumor control rate and prolong the OS for patients with unresectable HCC and PVTT?

Cao et al. reported TACE combined with lenvatinib and sintilimab for unresectable HCC with a mOS of 23.6 months and ORR of 46.7% (27). Ju et al. reported TACE combined with apatinib and camrelizumab for advanced HCC with a mOS of 24.8 months which longer than apatinib plus camrelizumab (13.1 months) (28). According to these results, TACE combined TKIs and anti-PD-1 antibody might be an effect combined therapy for advanced HCC and PVTT. However, Vp4 PVTT patients were excluded by these studies. Because MPV occlusion is an important factor which affect safety and prognosis for patients who received TACE or TACE plus systemic therapy (23, 29). In our study, the occluded MPV was restored and kept patent by PVS and ^{125}I seed strand. To some extent, based on this interventional treatment regimen, the Vp4 PVTT was down-staged to Vp3. The restoration of MPV provided grantee for normal liver function. Therefore, in our study, TACE combined with lenvatinib and anti-PD-1 antibody could be provided to control tumor progression safely. As a result, patients in group A had significantly better intrahepatic tumor control (55.3% vs 17.5%, $p < 0.001$). And group A patients had significantly longer OS and PFS than group B cases (OS, 17.7 ± 1.7 vs 12.0 ± 0.8 months, $p = 0.010$; PFS, 17.0 ± 4.3 vs 8.0 ± 0.7 months, $p < 0.001$). In group A, 2 patients received liver transplantation and 1 patient received surgical resection. This result implied us that this combined therapy could provide opportunities of surgical treatment for patients with unresectable HCC and Vp4 PVTT.

Furthermore, radiation therapy (RT) has been demonstrated to enhance the priming and effector phases of antitumor-T-cell response, rendering it an attractive therapeutic tool that can be combined with PD-1/PD-L1 inhibitors (30). Two preclinical studies supported the rational combination of RT and PD-1/PD-L1 inhibitors in HCC (31, 32). ^{125}I seed strand implantation is a type of endovascular brachytherapy. X-rays and gamma-rays emitted by ^{125}I seeds could continuously irradiate the PVTT. In the current study, patients in group A who received anti-PD-1 antibody injection had a significantly lower rate of stent occlusion (12.8% vs 35.0%, $p = 0.014$) and significantly longer median stent patency time (not-reached vs 12.5 ± 1.1 months, $p = 0.028$). Therefore, ^{125}I seed may also enhance the therapeutical effect of anti-PD-1 antibodies. More experimental investigations should be conducted to confirm this conclusion.

In addition, 8 (17.0%) and 12 (25.5%) patients occurred 11 and 15 AEs related lenvatinib in group A and B, respectively ($p = 0.152$). The occurrence rate of AEs related to lenvatinib did not increase in patients combined lenvatinib and anti-PD-1 antibodies. No grade 4 AE occurred, and no patient died of AE in this study. Hence, this combined treatment regimen in group A is safe for patients with HCC and Vp4 PVTT.

There were several limitations in the current study. First, this study had a retrospective design, which may affect its generalizability. Second, five different kinds of anti-PD-1 antibody were used in group A, and the sample size was limited, which may affect the survival results. Third, more techniques could be used to evaluate the volume and activity of PVTT more precisely in a future study. Therefore, our next step is to conduct a single-center prospective, randomized, controlled trial to evaluate the long-term efficacy of this encouraging combination therapy in improving survival in HCC patients with Vp4 PVTT.

In conclusion, the interventional therapy (^{125}I seed strand and PVS implantation plus TACE) combined with systemic therapy (lenvatinib plus anti-PD-1 antibody) in patients with HCC and Vp4 PVTT is safe and effective. To our knowledge, this is the first report of patients with HCC and Vp4 PVTT administered this combination therapy as first-line treatment.

Data availability statement

The raw data supporting the conclusions of this article will be made available by the authors, without undue reservation.

Ethics statement

The studies involving human participants were reviewed and approved by Institutional Review Boards of the Zhongshan Hospital, Fudan University. Written informed consent for participation was not required for this study in accordance with the national legislation and the institutional requirements. Written informed consent was obtained from the individual(s) for the publication of any potentially identifiable images or data included in this article.

Author contributions

X-DQ and Z-PY conceived and designed the project. Q-XL, L-XL, and J-JL provided administrative support. WZ, J-QM, and M-JY collected the data. Z-HZ, S-NH, and J-ZY analyzed the data and wrote the manuscript. All authors contributed to the article and approved the submitted version.

Funding

This study has received funding from the project of Shanghai Municipal Heath Bureau (20194Y0154) and Natural Science Foundation of Shanghai (20ZR1452700).

Conflict of interest

The authors declare that the research was conducted in the absence of any commercial or financial relationships that could be construed as a potential conflict of interest.

Publisher's note

References

1. Torre LA, Bray F, Siegel RL, Ferlay J, Lortet-Tieulent J, Jemal A. Global cancer statistics, 2012. *CA Cancer J Clin* (2015) 65(2):87–108. doi: 10.3322/caac.21262

2. Katagiri S, Yamamoto M. Multidisciplinary treatments for hepatocellular carcinoma with major portal vein tumor thrombus. *Surg Today* (2014) 44(2):219–26. doi: 10.1007/s00595-013-0585-6

3. Ikai I, Hatano E, Hasegawa S, Fujii H, Taura K, Uyama N, et al. Prognositic index for patients with hepatocellular carcinoma combined with tumor thrombosis in the major portal vein. *J Am Coll Surg* (2006) 202(3):431–8. doi: 10.1016/j.jamcollsurg.2005.11.012

4. Wu CC, Hsieh SR, Chen JT, Ho WL, Lin MC, Yeh DC, et al. An appraisal of liver and portal vein resection for hepatocellular carcinoma with tumor thrombi extending to portal bifurcation. *Arch Surg* (2000) 135(11):1273–9. doi: 10.1001/archsurg.135.11.1273

5. Llovet JM, Ricci S, Mazzaferro V, Hilgard P, Gane E, Blanc J-F, et al. Sorafenib in advanced hepatocellular carcinoma. *N Engl J Med* (2008) 359(4):378–90. doi: 10.1056/NEJMoa0708857

6. Kudo M, Finn RS, Qin S, Han K-H, Ikeda K, Piscaglia F, et al. Lenvatinib versus sorafenib in first-line treatment of patients with unresectable hepatocellular carcinoma: A randomized phase 3 non-inferiority trial. *Lancet* (2018) 391(10126):1163–73. doi: 10.1016/S0140-6736(18)30207-1

7. Vogel A, Cervantes A, Chau I, Daniele B, Llovet JM, Meyer T, et al. Hepatocellular carcinoma: ESMO clinical practice guidelines for diagnosis, treatment and follow-up. *Ann Oncol* (2018) 29:iv228–55. doi: 10.1093/annonc/mdy308

8. Kaneko S, Tsuchiya K, Yasui Y, Inada K, Kirino S, Yamashita K, et al. Strategy for advanced hepatocellular carcinoma based on liver function and portal vein tumor thrombosis. *Hepatol Res* (2020) 50:1375–85. doi: 10.1111/hepr.13567

9. Luo J-J, Zhang Z-H, Liu Q-X, Zhang W, Wang J-H, Yan Z-P. Endovascular brachytherapy combined with stent placement and TACE for treatment of HCC with main portal vein tumor thrombus. *Hepatol Int* (2016) 10:185–95. doi: 10.1007/s12072-015-9663-8

10. Zhang Z-H, Liu Q-X, Zhang W, Ma J-Q, Wang J-H, Luo J-J, et al. Combined endovascular brachytherapy, sorafenib, and transarterial chemobolization therapy for hepatocellular carcinoma patients with portal vein tumor thrombus. *World J Gastroenterol* (2017) 23(43):7735–45. doi: 10.3748/wjg.v23.i43.7735

11. Rimassa L, Pressiani T, Merle P. Systemic treatment options in hepatocellular carcinoma. *Liver Cancer* (2019) 8(6):427–46. doi: 10.1159/000499765

12. Finn RS, Zhu AX, Farah W, Almasri J, Zaiem F, Prokop LJ, et al. Therapies for advanced stage hepatocellular carcinoma with macrovascular invasion or metastatic disease: A systematic review and meta-analysis. *Hepatology* (2018) 67(1):422–35. doi: 10.1002/hep.29486

13. Brown ZJ, Greten TF, Heinrich B. Adjuvant treatment of hepatocellular carcinoma: prospect of immunotherapy. *Hepatology* (2019) 70(4):1437–42. doi: 10.1002/hep.30633

14. Bruix J, Sherman MPractice Guidelines Committee and American Association for the Study of Liver Disease. Management of hepatocellular carcinoma. *Hepatology* (2005) 42(5):1208–36. doi: 10.1002/hep.20933

15. Shah ZK, McKernan MG, Hahn PF, Sahani DV. Enhancing and expansile portal vein thrombosis: value in the diagnosis of hepatocellular carcinoma in patients with multiple hepatic lesions. *Am J Roentgenol* (2007) 188(5):1320–3. doi: 10.2214/AJR.06.0134

16. Kudo M, Izumi N, Kokudo N, Matsui O, Sakamoto M, Nakashima O, et al. Management of hepatocellular carcinoma in Japan: Consensus-based clinical practice guidelines proposed by the Japan society of hepatology (JSH) 2010 updated version. *Dig Dis* (2011) 29(3):339–64. doi: 10.1159/000327577

17. Yang M, Yan Z, Luo J, Liu Q, Zhang W, Ma J, et al. A pilot study of intraluminal brachytherapy using ^{125}I seed strand for locally advanced pancreatic ductal adenocarcinoma with obstructive jaundice. *Brachytherapy* (2016) 15(6):859–64. doi: 10.1016/j.brachy.2016.05.004

18. Qin S, Ren Z, Meng Z, Chen Z, Chai X, Xiong J, et al. Camrelizumab in patients with previously treated advanced hepatocellular carcinoma: a multicentre, open-label, parallel-group, randomized, phase 2 trial. *Lancet Oncol* (2020) 21(4):571–80. doi: 10.1016/S1470-2045(20)30011-5

19. Hoy SM. Sintilimab: First global approval. *Drugs* (2019) 79(3):341–6. doi: 10.1007/s40265-019-1066-z

20. Keam SJ. Toripalimab: First global approval. *Drugs* (2019) 79(5):573–8. doi: 10.1007/s40265-019-01076-2

21. Minagawa M, Makuuchi M. Treatment of hepatocellular carcinoma accompanied by portal vein tumor thrombus. *World J Gastroenterol* (2006) 12(47):7561–7. doi: 10.3748/wjg.v12.i47.7561

22. Liu L, Zhang C, Zhao Y, Qi X, Chen H, Bai W, et al. Transarterial chemoembolization for the treatment of advanced hepatocellular carcinoma with portal vein tumor thrombosis: prognostic factors in a single-center study of 188 patients. *BioMed Res Int* (2014) 2014:194278. doi: 10.1155/2014/194278

23. Ohnishi K, Okuda K, Ohtsuki T, Nakayama T, Hiyama Y, Iwama S, et al. Formation of hilar collaterals or cavernous transformation after portal vein obstruction by hepatocellular carcinoma. *Gastroenterology* (1984) 87(5):1150–3. doi: 10.1016/S0016-5085(84)80077-3

24. Hegde PS, Wallin JJ, Mancao C. Predictive markers of anti-VEGF and emerging role of angiogenesis inhibitors as immunotherapeutics. *Semin Cancer Biol* (2018) 52(Pt 2):117–24. doi: 10.1016/j.semcancer.2017.12.002

25. Finn RS, Qin S, Ikeda M, Galle PR, Ducreux M, Kim T-K, et al. Atezolizumab plus bevacizumab in unresectable hepatocellular carcinoma. *N Engl J Med* (2020) 382 (20):1894–905. doi: 10.1056/NEJMoa1915745

26. Huang C, Zhu X-D, Shen Y-H, Wu D, Ji Y, Ge N-L, et al. Organ specific responses to first-line lenvatinib plus anti-PD-1 antibodies in patients with unresectable hepatocellular carcinoma: a retrospective analysis. *biomark Res* (2021) 9(1):19. doi: 10.1186/s40364-021-00274-z

27. Cao F, Yang Y, Si T, Luo J, Zeng H, Zhang Z, et al. The efficacy of TACE combined with lenvatinib plus sintilimab in unresectable hepatocellular carcinoma: A multicenter retrospective study. *Front Oncol* (2021) 11:783480. doi: 10.3389/fonc.2021.783480

28. Ju S, Zhou C, Yang C, Wang C, Liu J, Wang Y, et al. Apatinib plus camrelizumab With/Without chemoembolization for hepatocellular carcinoma: A real-world experience of a single center. *Front Oncol* (2022) 11:835889. doi: 10.3389/fonc.2021.835889

29. Zhu K, Chen J, Lai L, Meng X, Zhou B, Huang W, et al. Hepatocellular carcinoma with portal vein tumor thrombus: treatment with transarterial chemoembolization combined with sorafenib–a retrospective controlled study. *Radiology* (2014) 272 (1):284–93. doi: 10.1148/radiol.14131946

30. Jun G, Le TQ, Massarelli E, Hendifar AE, Tuli R. Radiation therapy and PD-1/PD-L1 blockade: the clinical development of an evolving anticancer. *J Immunother Cancer* (2018) 6(1):46. doi: 10.1186/s40425-018-0361-7

31. Friedman D, Baird JR, Young KH, Cottam B, Crittenden MR, Friedman S, et al. Programmed cell death-1 blockade enhanced response to stereotactic radiation in an orthotopic murine model of hepatocellular carcinoma. *Hepatol Res* (2017) 47(7):702–14. doi: 10.1111/hepr.12789

32. Kim K-J, Kim J-H, Lee SJ, Lee E-J, Shin E-C, Seong J. Radiation improves antitumor effect of immune checkpoint inhibitor in murine hepatocellular carcinoma model. *Oncotarget* (2017) 8(25):41242–55. doi: 10.18632/oncotarget.17168

frontiers | Frontiers in Oncology

TYPE Original Research
PUBLISHED 30 January 2023
DOI 10.3389/fonc.2023.1110689

OPEN ACCESS

EDITED BY
Xiong Chen,
Nanjing General Hospital of Nanjing Military Command, China

REVIEWED BY
Chi-Leung Chiang,
The University of Hong Kong, Hong Kong SAR, China
Jaejun Lee,
Catholic University of Korea, Republic of Korea

*CORRESPONDENCE
Lequn Li
li_lequn@263.net
Feixiang Wu
wufeixiang@gxmu.edu.cn

†These authors have contributed equally to this work and share first authorship

SPECIALTY SECTION
This article was submitted to Gastrointestinal Cancers: Hepato Pancreatic Biliary Cancers, a section of the journal Frontiers in Oncology

RECEIVED 29 November 2022
ACCEPTED 17 January 2023
PUBLISHED 30 January 2023

CITATION
Li X, Chen J, Wang X, Bai T, Lu S, Wei T, Tang Z, Huang C, Zhang B, Liu B, Li L and Wu F (2023) Outcomes and prognostic factors in initially unresectable hepatocellular carcinoma treated using conversion therapy with lenvatinib and TACE plus PD-1 inhibitors.
Front. Oncol. 13:1110689.
doi: 10.3389/fonc.2023.1110689

Outcomes and prognostic factors in initially unresectable hepatocellular carcinoma treated using conversion therapy with lenvatinib and TACE plus PD-1 inhibitors

Xingzhi Li[1†], Jie Chen[1†], Xiaobo Wang[1], Tao Bai[1], Shaolong Lu[1], Tao Wei[1], Zhihong Tang[1], Chengwen Huang[1], Bin Zhang[1], Bowen Liu[1], Lequn Li[1*] and Feixiang Wu[1,2*]

[1]Department of Hepatobiliary Surgery, Guangxi Medical University Cancer Hospital, Nanning, China, [2]Key Laboratory of High-Incidence-Tumor Prevention & Treatment, Ministry of Education, Nanning, China

Purpose: To evaluate the outcomes and prognostic factors for patients using conversion therapy with lenvatinib combined with transcatheter arterial chemoembolization (TACE) plus programmed cell death protein-1 (PD-1) inhibitors (LTP) for initially unresectable hepatocellular carcinoma (iuHCC).

Methods: Data on 94 consecutive patients with iuHCC who received LTP conversion therapy from November 2019 to September 2022 were retrospectively analyzed. Early tumor response was reported when patients showed complete or partial response at the time of their first follow-up (4–6 weeks) after initial treatment, in accordance with mRECIST. The endpoints consisted of conversion surgery rate, overall survival (OS), and progression-free survival (PFS).

Results: Early tumor response was found in 68 patients (72.3%) and not in the remaining 26 patients (27.7%) in the entire cohort. Early responders had a significantly higher conversion surgery rate than non-early responders (44.1% vs. 7.7%, p=0.001). Early tumor response was the only factor independently associated with successful conversion resection, as indicated by multivariate analysis (OR=10.296; 95% CI: 2.076–51.063; p=0.004). Survival analysis showed that early responders had longer PFS (15.4 vs. 7.8 months, p=0.005) and OS (23.1 vs. 12.5 months, p=0.004) than non-early responders. Early responders who underwent conversion surgery also had significantly longer median PFS and OS (not reached, not reached) than those who did not (11.2 months, p=0.004; 19.4 months, p<0.001). In multivariate analyses, early tumor response was identified as an independent prognostic factor for longer OS (HR=0.404, 95% CI: 0.171–0.954; p=0.039). Successful conversion surgery was also an independent predictive factor for longer PFS (HR=0.248, 95% CI: 0.099–0.622; p=0.003) and OS (HR=0.147, 95% CI: 0.039–0.554; p=0.005).

Conclusions: Early tumor response is an important predictive marker for successful conversion surgery and prolonged survival in patients with iuHCC treated using LTP conversion therapy. Conversion surgery is necessary to improve survival during conversion therapy, particularly for early responders.

KEYWORDS

conversion therapy, PD-1 inhibitors, initially unresectable hepatocellular carcinoma, transcatheter arterial chemoembolization, lenvatinib

Introduction

Liver cancer is the fourth leading cause of cancer-related mortality (1). Surgical resection can provide a good prognosis for resectable hepatocellular carcinoma (HCC). However, many patients are ineligible for resection because of excessive tumor burden, large vascular invasion, intrahepatic metastases, or external metastases (2). Conversion therapy aims to provide an improved prognosis by converting unresectable hepatocellular carcinoma for a chance to receive curative surgery. In clinical practice, multidrug combination therapy has been explored in intermediate to advanced HCC (3–5). Lenvatinib combined with transcatheter arterial chemoembolization (TACE) plus programmed cell death protein-1 (PD-1) inhibitors (LTP) has shown improved prognosis in initially unresectable hepatocellular carcinoma(iuHCC) (5–7). The objective response rate of LTP are higher than those of TACE alone and TACE combined with lenvatinib (6, 7). Thus, triple-combination therapy can potentially serve as a conversion therapy.

Achieving tumor shrinkage downstaging is an important goal in conversion therapy for the treatment of iuHCC. It provides patients with the opportunity for potential radical resection (2, 8). About 50% of patients have been found to exhibit obvious tumor shrinkage after triple-combination therapy and offered curative conversion resection (9, 10). In this context, early prediction of successful conversion surgery may guide surgical treatment strategies. Moreover, early identification of patients not benefitting from conversion therapy and timely switching to other second-line treatments may improve the prognosis.

Early tumor response could respond to the reduction of tumor burden from radiological evaluation earlier. It has been associated with good prognosis in numerous malignancies (11–17). In HCC patients receiving sorafenib, lenvatinib, and combined therapy, early tumor shrinkage can lead to improved outcomes and extended survival (18–20). However, early tumor response based on the modified Response Evaluation Criteria in Solid Tumors (mRECIST) does not prolong survival in HCC patients receiving PD-1 inhibitors plus bevacizumab (21). Thus, although early tumor response represents a rapid reduction in tumor burden, whether it has a predictive role in patients treated with immune combination therapy, particularly LTP conversion therapy, remains inconclusive.

This retrospective study was aimed at evaluating outcomes and prognostic factors for patients who underwent LTP conversion therapy for iuHCC.

Methods

Study population

Consecutive patients who received LTP conversion therapy from November 2019 to September 2022 for iuHCC were retrospectively analyzed. HCC was diagnosed by clinical assessment or histological examination (22). Tumors were considered unresectable either because of technical unresectability or oncologic unresectability, or both. Technical unresectability is defined in the presence of insufficient future remnant liver volume and lesions assessed by the surgeon as unsuitable for R0 resection. Oncological unresectability is defined as failure to obtain a better prognosis after surgical resection of intermediate-to-advanced HCC, such as major vascular invasion, intrahepatic metastases, and extrahepatic metastases. Other inclusion criteria were as follows: age between 18 and 80 years; Eastern Tumor Collaborative Group physical status (ECOG-PS) score of 0 to 1; Child–Pugh class A or B; adequate organ function; the absence of previous systemic and local treatment history for HCC, and at least one measurable target lesion in accordance with mRECIST. Those who received no radiologic evaluation at the first follow-up 4–6 weeks after the initial treatment for any reason were excluded. The ethics committee at our institution examined and approved the study protocol (LW2022147), and written informed consent was obtained from each patient.

Treatment strategies

Superselective TACE was performed by specialists with extensive surgical experience in the interventional unit (details in supplementary material). Repeat TACE was conducted when the active lesion area exceeded 50% of the baseline while the liver function was reasonable. Lenvatinib (LENVIMA®, Merck Sharp & Dohme, H20180052) and PD-1 inhibitors were given within 1 week after TACE, depending on the general condition and recovery of liver function. Patients were given either 8 mg (weight <60 kg) or 12 mg (weight ≥60 kg) of lenvatinib daily *via* the oral route. PD-1 inhibitors included either 200 mg of camrelizumab (AiRuiKa®, Jiangsu Hengrui Medicine Co. Ltd, S20190027) or 200 mg of sintilimab (Tyvyt®, Innovent Biologics and Eli Lilly and Company, S20180016) *via* intravenous injection every 3 weeks. All patients were treated until

disease progression, intolerable toxicity, death, or withdrawal for any reason.

Hepatectomy was performed if patients met the criteria for resection and informed consent was obtained. The criteria for tumor resectability had to be satisfied, as follows: (1) adequate residual liver volume; (2) adequate cutting edge to achieve R0 resection; (3) tumor response assessment of complete response (CR) or partial response (PR) in accordance with mRECIST criteria, or patients with efficacy assessment of stable disease (SD) and maintenance for more than 8 weeks were considered to have controlled tumor biological behavior; (4) Child–Pugh grade A or B, and no other contraindications to hepatectomy.

Follow-up

The first follow-up was scheduled 4–6 weeks after the initial treatment and then every 2–4 months until October 20, 2022. Each follow-up evaluation includes tumor response and laboratory tests, such as blood tests, liver and kidney function, urine routine, tumor markers, myocardial enzymology examination, and thyroid function. Tumor response was evaluated on contrast-enhanced computed tomography (CE-CT) using mRECIST and RECIST1.1 by two senior hepatobiliary surgeons at our hospital.

Outcome assessments

Early tumor response was defined as patients with CR or PR at the time of the first follow-up (4–6 weeks) after initial treatment using mRECIST, whereas late tumor response was documented after the first follow-up. The non-early response included late tumor response, SD, or progressive disease (PD). Early α-fetoprotein (AFP) response was defined as a reduction of more than 75% in AFP levels following the initial treatment at the first follow-up (23).

We also evaluated the prognostic factors by using inflammatory indexes such as NLR, PLR, and systemic inflammation response index (SIRI). SIRI was calculated as neutrophil count × monocyte count/lymphocyte count (24). These inflammatory indices were split into two groups, based on their median value. Overall survival (OS) was measured from the initiation of the conversion therapy to death from any cause. Progression-free survival (PFS) was calculated from the initiation of the conversion therapy to progression, relapse, or death.

Statistical analysis

The data collected in this study were statistically analyzed using the software SPSS ver. 24.0 (IBM, Armonk, NY, United States) and R ver. 4.1.1 (http://www.R-project.org/). The Mann–Whitney U test or t-test was used to compare continuous variables, represented as median and quartiles or mean ± standard deviation. Categorical variables were presented as the number of cases and percentages by using the χ^2 test or Fisher's exact probability method. Survival analysis was conducted using Kaplan–Meier methods and log-rank tests. The inverse Kaplan–Meier method was conducted to determine the median time of follow-up.

Potential predictive factors of successful conversion surgery were determined using binary logistic regression methods. In multivariate analysis, all factors with $p<0.05$ and clinically important variables in the univariate analyses were included *via* the enter method. Given the clinical correlation between early tumor response and AFP response, two models were used to include early tumor response and AFP response in separate multivariate logistic regression analyses to avoid collinearity. Considering that no patients with distant metastases had successful conversion surgery, we presented a sensitivity binary logistic regression analysis for patients without distant metastases.

Potential prognostic factors for PFS and OS were determined using the Cox proportional-hazards models. All factors with $p<0.05$ and clinically important variables for prognosis were included in the multivariate analysis *via* the enter method. Given the correlation between successful conversion surgery and early tumor response, we included two models in separate multivariate cox regression analyses to avoid collinearity. For all analyses, $p<0.05$ was considered statistically significant.

Results

Patient characteristics

A total of 97 patients who received conversion therapy to treat iuHCC were assessed; 3 patients were subsequently excluded (Figure 1). Among the 94 patients included, 84 (89.4%) had hepatitis B-associated HCC. At baseline, 85 patients (90.4%) were classified as Child–Pugh grade A, and the majority were assigned with an ALBI grade >1 (88.3%). Further, 60 (63.8%) were of Barcelona clinical liver cancer (BCLC) stage C and 19 cases (20.2%) were of BCLC stage B; 56 (59.6%) patients had an initial AFP > 400 ng/mL. In 70.2% of patients, the tumors measured >10 cm in diameter. Multiple tumors were found in 51 patients (54.3%). The laboratory tests were also summarized, including the results for the hepatobiliary enzyme, total bilirubin, NLR, PLR, and SIRI (Table 1). Although adverse events in varying degrees affected all patients, they were within controllable levels (Table S1).

Treatment response and successful conversion surgery

The median follow-up period was 14.4 (10.7–18.2) months. For all patients, the overall response rate was 87.2%, and the disease control rate was 93.6% based on mRECIST (Table 2). Among the patients, 32 (34.0%) underwent conversion surgery. The median time to surgery was 3.8 (3.1–5.4) months. All patients who were successfully converted had no distant metastases. Of the entire cohort, 68 (72.3%) patients showed an early tumor response, and 26 (27.7%) had no early tumor response. The patients who showed early tumor response had a significantly higher conversion surgery rate than those who showed no such response (44.1% vs. 7.7%, p=0.001). The patients with early tumor response had similar baseline characteristics to those with no early tumor response, in addition to the ECOG-PS score (p=0.030) and AST (p=0.020) (Table 1). Representative cases are presented in Supplementary Figure 1.

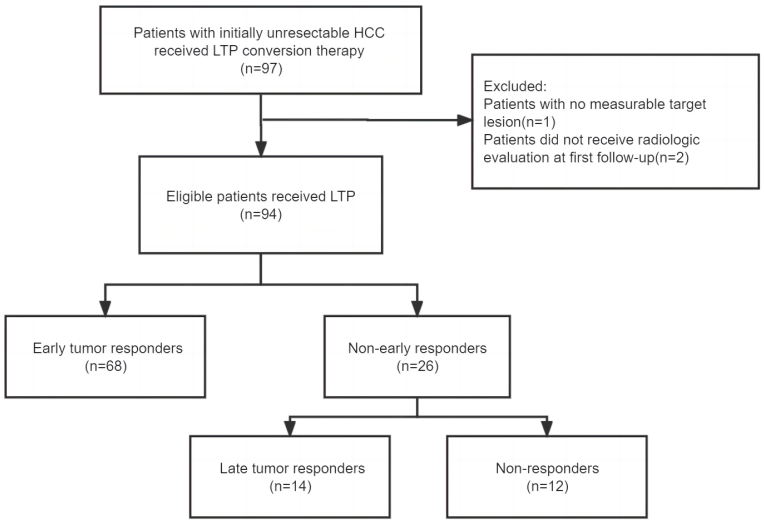

FIGURE 1
Flowchart. LTP, Lenvatinib combined TACE plus PD-1inhibitors.

TABLE 1 Baseline characteristics of 94 patients with initially unresectable HCC.

Variable	Early tumor responders (n=68)	Non-early responders (n=26)	P value
Age (year)			0.344
>60	9 (13.2%)	6 (23.1%)	
≤60	59 (86.8%)	20 (76.9)	
Gender			1.000
Male	64 (94.1%)	25 (96.2%)	
Female	4 (5.9%)	1 (3.8%)	
BCLC stage			0.254
A	12 (17.7%)	3 (11.5%)	
B	16 (23.5%)	3 (11.5%)	
C	40 (58.8%)	20 (77.0%)	
Target tumor size (cm)			0.212
>10	45 (66.2%)	21 (80.8%)	
≤ 10	23 (33.8%)	5 (19.2%)	
Tumor number			0.362
1	29 (42.6%)	14 (53.8%)	
≥2	39 (57.4%)	12 (46.2%)	
Large vascular invasion			0.192
Yes	37 (54.4%)	18 (69.2%)	
No	31 (45.6%)	8 (30.8%)	
PVTT			0.679
Yes	36 (52.9%)	15 (57.7%)	
No	32 (47.1%)	11 (42.3%)	
Extrahepatic metastases			0.066

(Continued)

TABLE 1 Continued

Variable	Early tumor responders (n=68)	Non-early responders (n=26)	P value
Yes	5 (7.4%)	6 (23.1%)	
No	63 (92.6%)	20 (76.9%)	
AFP (ng/mL)			0.810
>400	40 (58.8%)	16 (61.5%)	
≤ 400	28 (41.2%)	10 (38.5%)	
Etiology			0.456
Hepatitis B	62 (91.2%)	22 (84.6%)	
Non−Hepatitis B	6 (8.8%)	4 (15.4%)	
ECOG PS			0.030
0	43 (63.2%)	10 (38.5%)	
1	25 (36.8%)	16 (61.5%)	
Cirrhosis			0.669
Yes	55 (80.9%)	20 (76.9%)	
No	13 (19.1%)	6 (23.1%)	
Ascites			1.000
Yes	10 (14.7%)	3 (11.5%)	
No	58 (85.3%)	23 (88.5%)	
Child-Pugh grade			0.704
A	62 (91.2%)	23 (88.5%)	
B	6 (8.8%)	3 (11.5%)	
ALBI grade			0.739
1	7 (10.3%)	4 (15.4%)	
2	59 (86.8%)	22 (84.6%)	
3	2 (2.9%)	0 (0.0%)	
TBIL (umol/L)	17.5 (11.6-22.4)	15.2 (12.9-18.6)	0.348
ALB (g/L)	37.3 ± 4.3	36.3 ± 4.7	0.310
PT (sec)	12.9 ± 1.6	12.7 ±1.1	0.703
ALT (U/L)	42.5 (31.0-58.5)	49.0 (35.2-75.5)	0.199
AST (U/L)	57.0 (43.5-89.0)	75.5 (61.8-97.8)	0.020
PLT ($\times10^9$/L)	207.5 (164.2-257.5)	216.0 (151.8-288.5)	0.577
NLR			1.000
>2.82	34 (50%)	13 (50%)	
≤2.82	34 (50%)	13 (50%)	
PLR			0.356
>146	32 (47.1%)	15 (57.7%)	
≤146	36 (52.9%)	11 (42.3%)	
SIRI			1.000
>1.38	34 (50%)	13 (50%)	
≤1.38	34 (50%)	13 (50%)	
successful conversion surgery			0.001

(Continued)

TABLE 1 Continued

Variable	Early tumor responders (n=68)	Non-early responders (n=26)	P value
Yes	30 (44.1%)	2 (7.7%)	
No	38 (55.9%)	24 (92.3%)	

ALT, alanine aminotransferase; BCLC, Barcelona Clinic Liver Cancer; ALBI, albumin–bilirubin; HCC, hepatocellular carcinoma; AFP, α-fetoprotein; ECOG PS, Eastern Cooperative Oncology Group performance status; TBIL, Total bilirubin; PT, Prothrombin time; ALB, albumin; PLR, platelet to lymphocyte ratio; SIRI, systemic inflammation response index (neutrophil* monocyte to lymphocyte ratio); NLR, neutrophil to lymphocyte ratio; ALB, albumin; AST, aspartate aminotransferase; PVTT, portal vein tumor thrombosis.

Relationship between early tumor response and conversion resection rate

The first multivariate model incorporated early tumor response in the 94 patients included in the study. The result indicates that the only independent predictive factor for conversion surgery was early tumor response (OR=10.296; 95% CI: 2.076–51.063; p=0.004). Early AFP response was included in the second multivariate model; however, early AFP response was not a predictor of conversion resection (Table 3). The result was confirmed in 83 patients with non-distant metastases (OR=9.659; 95% CI: 1.899–49.125; p=0.006)(Table S2).

Effect of early tumor response on PFS and OS

The median PFS for the patients with early tumor response was 15.4 months, whereas the median PFS with no early tumor response was 7.8 months (p=0.005; Figure 2A). However, early tumor response was not an independent predictive factor of PFS (HR= 0.576, 95% CI: 0.302–1.097; p=0.093) (Table 4, Multivariate model 1). The median OS of the patients with early tumor response was 23.1 months (p=0.004; Figure 2B), whereas that of patients with no early tumor response was 12.5 months. In multivariate analysis, early tumor response was independently correlated with OS (HR= 0.404, 95% CI: 0.171–0.954; p=0.039) and jointly with the following conditions: baseline AFP>400 ng/mL (p=0.020), portal vein tumor thrombosis (PVTT) (p=0.011), and extrahepatic metastasis (p=0.001)(Table 5, Multivariate model 1). The effects of early tumor response on PFS (HR= 0.569, 95% CI: 0.278 – 1.164; p=0.123) and OS (HR= 0.329, 95% CI: 0.119 – 0.910; p=0.032) were confirmed in 83 patients with non-distant metastases (Tables S3, S4, Multivariate model 1).

Given that non-early tumor response was a risk factor for OS, we assigned different scores to each risk factor on the basis of the beta coefficient score in multivariate analysis. We further divided the patients into 4 groups, based on the risk factor. Survival curves showed that the best median OS was in the score 0 group, which declined as the risk factor scores increased (Figure 3).

Relevance of successful conversion surgery for PFS and OS

Median PFS and OS (not reached, not reached) were significantly longer in patients who underwent successful conversion surgery than in those patients who received no such surgery (9.8 months, p<0.001; 14.9 months, p<0.001; Figures 4A, B). We further assessed the role of conversion surgery in patients with early tumor response. Results showed that for patients with early tumor response, those who underwent conversion surgery also had significantly longer median PFS and OS (not reached, not reached) than those who did not undergo conversion resection (11.2 months, p=0.004; 19.4 months, p<0.001; Figures 5A, B). Furthermore, early responders combined with late responders had a similar median OS to that of early responders (p=1.000). Both had significantly longer OS than non-responders (p<0.001, p<0.001; respectively; Supplementary Figure 2A). We further assessed the role of conversion surgery in late tumor responders. The results showed that late responders who underwent conversion surgery had no significantly longer median OS than those who did not (p=0.3; Supplementary Figure 2B).

Multivariate results confirmed that successful conversion surgery (HR=0.248, 95% CI: 0.099–0.622; p=0.003) was independently correlated with PFS (Table 4, Multivariate model 2). In addition, multivariate analysis confirmed that successful conversion surgery was also independently correlated with OS (HR = 0.147, 95% CI: 0.039 – 0.554; p=0.005), in addition to PVTT (p=0.002) and extrahepatic metastasis (p=0.023)(Table 5, Multivariate model 2). The results on the relevance of successful conversion surgery for

TABLE 2 Treatment response to conversion therapy based on mRECIST and RECIST1.1.

Overall response	mRECIST (n=94)	RECIST1.1 (n=94)
Complete response	13 (13.8%)	0
Partial response	69 (73.4%)	25 (26.6%)
Stable disease	6 (6.4%)	63 (67.0%)
Progressive disease	6 (6.4%)	6 (6.4%)
Overall response rate	82 (87.2%)	25 (26.6%)
Disease control rate	88 (93.6%)	88 (93.6%)

TABLE 3 Factors associated with successful conversion surgery in 94 patients who received conversion therapy for initially unresectable HCC.

		Univariate			Multivariate(Model 1)#			Multivariate(Model 2)#		
		OR	95% CI	*P*	OR	95% CI	*P*	OR	95% CI	*P*
Age, y	> 60 vs ≦ 60	0.662	0.193 – 2.274	0.513						
Sex	Male vs Female	2.138	0.229 – 19.968	0.563						
HBsAg-positive	Yes vs No	1.230	0.296 – 5.117	0.776						
Tumor size, cm	> 10 vs ≦ 10	0.375	0.150 – 0.939	0.036	0.495	0.171 – 1.434	0.195	0.436	0.158– 1.198	0.107
Tumor number	multiple vs single	0.637	0.270 – 1.503	0.303						
PVTT	Yes vs No	0.771	0.328– 1.815	0.552						
Macrovascular invasion	Yes vs No	0.590	0.249 – 1.399	0.231						
BCLC stage	Stage C vs A/B	0.409	0.169 – 0.990	0.047	0.538	0.187– 1.548	0.250	0.414	0.153 – 1.120	0.082
AFP, ng/mL	> 400 vs ≦ 400	0.550	0.231 – 1.308	0.176	0.478	0.169 – 1.347	0.163	0.506	0.191 – 1.344	0.172
SIRI	> 1.38 vs ≦ 1.38	0.378	0.156 – 0.918	0.032	0.459	0.165 – 1.276	0.136	0.454	0.168 – 1.229	0.120
Platelet count,×10^9/L	> 100 vs≦ 100	2.719	0.304 – 24.325	0.371						
ALT, U/L	> 40 vs ≦ 40	0.992	0.420 – 2.344	0.985						
AST, U/L	> 40 vs ≦ 40	0.642	0.202 – 2.042	0.453						
Ascites	Yes vs No	0.134	0.017 – 1.085	0.060	0.189	0.020 – 1.767	0.144	0.284	0.031 – 2.566	0.262
NLR	> 2.82 vs ≦ 2.82	0.463	0.193 – 1.109	0.084						
PLR	> 146vs ≦ 146	0.463	0.193 – 1.109	0.084						
ALBI grade	Grade1 vs 2/3	0.698	0.172 – 2.836	0.615						
ECOG PS	0 vs 1	1.790	0.740 – 4.329	0.197						
Early AFP response *	Yes vs No	1.548	0.637 – 3.765	0.335	–	–	–	1.803	0.654 – 4.972	0.255
Early tumor response†	Yes vs No	9.474	2.072– 43.309	0.004	**10.296**	**2.076 – 51.063**	**0.004**	–	–	–

AFP, alpha fetoprotein; HCC, hepatocellular carcinoma; ECOG PS, Eastern Cooperative Oncology Group performance status; ALBI grade, albumin-bilirubin grade; ALT, alanine aminotransferase; NA, not adopted; AST, aspartate aminotransferase; BCLC stage, Barcelona-Clinic liver cancer stage; PLR, platelet to lymphocyte ratio; NLR, neutrophil to lymphocyte ratio; SIRI, systemic inflammation response index; CI, confidence interval; OR, odds ratio; PVTT, portal vein tumor thrombosis.

*Early AFP response: AFP reduced > 75% from baseline serum level at first follow-up.

†Early tumor response: Achievement of complete response (CR) and partial response (PR) using mRECIST at first follow-up.

Model 1 did not include early AFP response into multivariate analysis to avoid collinearity.

Model 2 did not include early tumor response into multivariate analysis to avoid collinearity.

The bold values denote statistically significant results of the multivariate analysis.

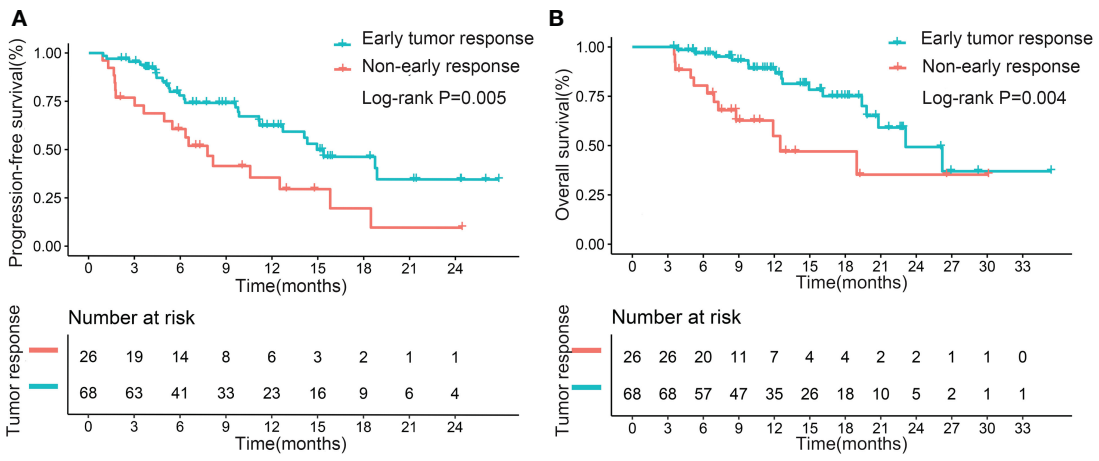

FIGURE 2
Kaplan–Meier curves for progression-free survival **(A)** and overall survival **(B)**, based on early tumor response in the entire cohort.

TABLE 4 Factors associated with progression-free survival in 94 patients who received conversion therapy for initially unresectable HCC.

		Univariate			Multivariate (Model 1)[#]			Multivariate (Model 2)[#]		
		HR	95% CI	*P*	HR	95% CI	*P*	HR	95%CI	*P*
Age, y	> 60 vs ≦ 60	0.677	0.267 – 1.720	0.412						
Sex	Male vs Female	1.934	0.465 – 8.037	0.364						
HBsAg-positive	Yes vs No	1.725	0.534 – 5.568	0.362						
Tumor size, cm	> 10 vs ≦ 10	1.655	0.837 – 3.274	0.148						
Tumor number	multiple vs single	1.440	0.796 – 2.607	0.228						
PVTT	Yes vs No	1.719	0.939 – 3.146	0.079	1.430	0.745 – 2.746	0.282	1.688	0.851 – 3.348	0.134
Macrovascular invasion	Yes vs No	1.645	0.884 – 3.062	0.116						
Extrahepatic metastasis	Yes vs No	4.117	1.975 – 8.580	< 0.001	**3.583**	**1.659 – 7.738**	**0.001**	**2.439**	**1.111 – 5.356**	**0.026**
BCLC stage	Stage C vs A/B	2.202	1.113 – 4.356	0.023			**NA**			**NA**
BCLC stage	Stage A vs B/C	0.673	0.265 – 1.707	0.404						
AFP, ng/mL	> 400 vs ≦ 400	1.057	0.581 – 1.922	0.857						
SIRI	> 1.38 vs ≦ 1.38	1.751	0.968 – 3.170	0.064						
NLR	> 2.82 vs ≦ 2.82	1.515	0.839 – 2.735	0.168						
PLR	> 146vs ≦ 146	1.049	0.584 – 1.883	0.874						
Platelet count,×10^9/L	> 100 vs≦ 100	1.575	0.485 – 5.116	0.450						
ALT, U/L	> 40 vs ≦ 40	0.890	0.493 – 1.606	0.699						
AST, U/L	> 40 vs ≦ 40	1.244	0.553 – 2.796	0.597						
Ascites	Yes vs No	2.779	1.318 – 5.860	0.007			**NA**			**NA**
Child-Pugh class	Class A vs B	0.322	0.134 – 0.775	0.011	0.457	0.172 – 1.212	0.115	0.569	0.218 – 1.488	0.251
ALBI grade	Grade1 vs 2/3	1.011	0.399 – 2.566	0.981						
ECOG PS	0 vs 1	0.525	0.290 – 0.950	0.033	0.770	0.399 – 1.487	0.436	0.724	0.373 – 1.404	0.339
Early AFP response *	Yes vs No	0.378	0.181– 0.789	0.010	–	–	–	0.585	0.270 – 1.268	0.175
Early tumor response†	Yes vs No	0.433	0.237 – 0.789	0.006	0.576	0.302 – 1.097	0.093	–	–	–
Successful conversion surgery	Yes vs No	0.197	0.086 –0.454	<0.001	–	–	–	**0.248**	**0.099– 0.622**	**0.003**

AFP, alpha fetoprotein; HCC, hepatocellular carcinoma; ECOG PS, Eastern Cooperative Oncology Group performance status; ALBI grade, albumin-bilirubin grade; ALT, alanine aminotransferase; NA, not adopted; AST, aspartate aminotransferase; BCLC stage, Barcelona-Clinic liver cancer stage; PLR, platelet to lymphocyte ratio; NLR, neutrophil to lymphocyte ratio; SIRI, systemic inflammation response index; CI, confidence interval; OR, odds ratio; PVTT, portal vein tumor thrombosis.
*Early AFP response: AFP reduced > 75% from baseline serum level at first follow-up.
†Early tumor response: Achievement of complete response (CR) and partial response (PR) using mRECIST at first follow-up.
Model 1 did not include early AFP response, successful conversion surgery, BCLC stage, and ascites into multivariate analysis to avoid collinearity.
Model 2 did not include early tumor response, BCLC stage, and ascites into multivariate analysis to avoid collinearity.
The bold values denote statistically significant results of the multivariate analysis.

PFS (HR= 0.265, 95% CI: 0.105– 0.669; p=0.005) and OS (HR= 0.088, 95% CI: 0.021 – 0.363; p=0.001) were confirmed in 83 patients with non-distant metastases (Table S3, S4, Multivariate model 2).

Discussion

The triple-combination LTP is a trend in conversion therapy for patients with iuHCC (5). However, LTP provides improved treatment outcomes while challenging the prediction of successful conversion surgery and prognosis. We found that early tumor response was independently associated with successful conversion surgery and better survival. Moreover, successful conversion surgery after LTP is essential for a better prognosis, especially early responders.

Some markers might help predict the prognosis of people with liver cancer. NLR is a prognostic factor in iuHCC for patients receiving triple-combination therapy (20). Baseline PLR and SIRI are also associated with the prognosis for HCC (9, 25, 26). In addition, the combination of C-reactive protein (CRP) and AFP showed a prognostic role in HCC patients receiving tyrosine kinase inhibitors (TKIs) combined with immunotherapy (27, 28). However, CRP is not a mandatory test for every patient in our hospital, hence its limited application in current clinical practice. To explore their value in conversion therapy, we chose inflammatory indexes in blood routine,

TABLE 5 Factors associated with overall survival in 94 patients who received conversion therapy for initially unresectable HCC.

		Univariate			Multivariate (Model 1)#			Multivariate (Model 2)#		
		HR	95% CI	*P*	HR	95% CI	*P*	HR	95%CI	*P*
Age, y	> 60 vs ≦ 60	1.162	0.399 – 3.383	0.660						
Sex	Male vs Female	0.990	0.233 – 4.201	0.989						
HBsAg-positive	Yes vs No	3.011	0.408 – 22.202	0.280						
Tumor size, cm	> 10 vs ≦ 10	1.314	0.555 – 3.107	0.535						
Tumor number	multiple vs single	1.375	0.646 – 2.924	0.408						
PVTT	Yes vs No	2.551	1.121 – 5.806	0.026	**3.014**	**1.290 – 7.042**	**0.011**	**4.418**	**1.712 – 11.398**	**0.002**
Macrovascular invasion	Yes vs No	2.410	1.020 – 5.691	0.045			**NA**			**NA**
Extrahepatic metastasis	Yes vs No	4.651	1.918 – 11.275	0.001	**5.068**	**1.897 – 13.534**	**0.001**	**3.189**	**1.172 – 8.678**	**0.023**
BCLC stage	Stage C vs A/B	3.084	1.168 – 8.139	0.023			**NA**			**NA**
BCLC stage	Stage A vs B/C	0.571	0.172 – 1.899	0.361						
AFP, ng/mL	> 400 vs ≦ 400	2.024	0.890 – 4.601	0.092	**3.002**	**1.190 – 7.575**	**0.020**	2.468	0.957 – 6.367	0.062
SIRI	> 1.38 vs ≦ 1.38	2.172	1.006 – 4.688	0.048	2.144	0.900 – 5.110	0.085	2.098	0.844 – 5.214	0.111
NLR	> 2.82 vs ≦ 2.82	1.688	0.796 – 3.580	0.172						
PLR	> 146vs ≦ 146	1.368	0.648 – 2.886	0.411						
Platelet count,×10^9/L	> 100 vs≦ 100	2.990	0.405 – 22.080	0.283						
ALT, U/L	> 40 vs ≦ 40	1.123	0.531 – 2.378	0.761						
AST, U/L	> 40 vs ≦ 40	1.015	0.382 – 2.698	0.977						
Ascites	Yes vs No	2.232	0.831 – 5.998	0.111						
Child-Pugh class	Class A vs B	0.245	0.082 – 0.735	0.012	0.754	0.209 –2.711	0.665	0.880	0.255 – 3.036	0.840
ALBI grade	Grade1 vs 2/3	1.437	0.497 – 4.154	0.503						
ECOG PS	0 vs 1	0.577	0.269 – 1.238	0.158	0.707	0.300 – 1.669	0.429	0.680	0.281 – 1.645	0.392
Early AFP response *	Yes vs No	0.445	0.180– 1.102	0.080	–	–	–	0.580	0.210 – 1.600	0.293
Early tumor response†	Yes vs No	0.348	0.163 – 0.743	0.006	**0.404**	**0.171 – 0.954**	**0.039**	–	–	–
Successful conversion surgery	Yes vs No	0.135	0.044 –0.409	<0.001	–	–	–	**0.147**	**0.039 – 0.554**	**0.005**

AFP, alpha fetoprotein; HCC, hepatocellular carcinoma; ECOG PS, Eastern Cooperative Oncology Group performance status; ALBI grade, albumin-bilirubin grade; ALT, alanine aminotransferase; NA, not adopted; AST, aspartate aminotransferase; BCLC stage, Barcelona-Clinic liver cancer stage; PLR, platelet to lymphocyte ratio; NLR, neutrophil to lymphocyte ratio; SIRI, systemic inflammation response index; CI, confidence interval; OR, odds ratio; PVTT, portal vein tumor thrombosis.

* Early AFP response: AFP reduced > 75% from baseline serum level at first follow-up.

† Early tumor response: Achievement of complete response (CR) and partial response (PR) using mRECIST at first follow-up.

Model 1 did not include successful conversion surgery, early AFP response, macrovascular invasion, and BCLC stage into multivariate analysis to avoid collinearity.

Model 2 did not include early tumor response, macrovascular invasion, and BCLC stage into multivariate analysis to avoid collinearity.

The bold values denote statistically significant results of the multivariate analysis.

such as PLR, NLR, and SIRI substituted for CRP. Further, we used the baseline AFP and early AFP response to explore the potential predictive factor. However, among the aforementioned indicators, only baseline AFP was independently associated with OS. Therefore, the above indicators have a limited role in LTP conversion therapy.

Several studies have been conducted on the prognostic role of early tumor response in iuHCC, but the results have been inconclusive. Earlier studies by Hashi et al. and Öcal et al. evaluated the relationship between survival and early tumor response in patients treated with TKI, in accordance with RECIST and mRECIST, respectively (18, 19). They found that early tumor response was independently associated with prognosis. Current studies recommend mRECIST-based tumor response assessment, given that RECIST is not considered applicable for viable tumors (18, 29, 30). However, a real-world study indicated that early tumor response based on mRECIST was not correlated with prognosis in patients receiving PD-1 inhibitors combined with bevacizumab (21). The study found that the Choi criteria and revised Choi criteria, which consider tumor density on CE-CT, might provide a more suitable evaluation of early tumor response and its correlation with prognosis (21). We considered that applying the Choi criteria and revised Chio criteria is not preferable because of the use of TACE in triple-combination therapy. Therefore, we still chose mRECIST to evaluate early tumor response. We determined that early tumor response was the only factor independently correlated with successful conversion resection. The result is also applicable to

10.3389/fonc.2023.1110689

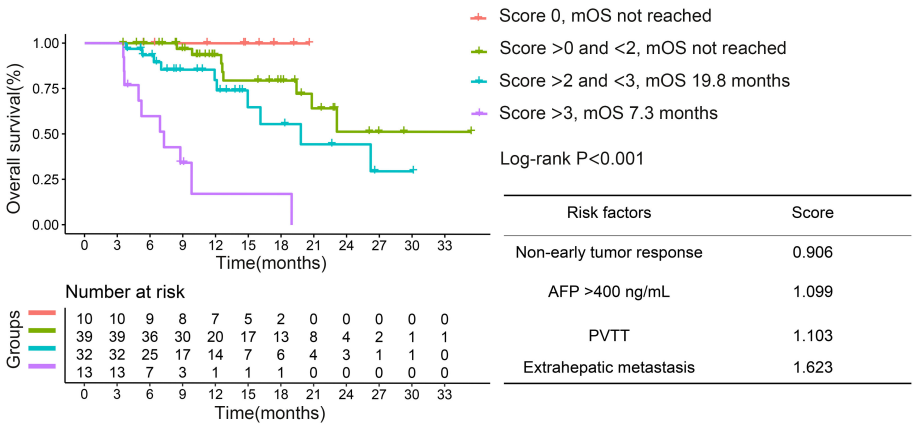

Risk factors	Score
Non-early tumor response	0.906
AFP >400 ng/mL	1.099
PVTT	1.103
Extrahepatic metastasis	1.623

FIGURE 3
Kaplan–Meier curves for overall survival based on different risk factor scores in the entire cohort. PVTT, portal vein tumor thrombosis; AFP, α-fetoprotein; OS, overall survival.

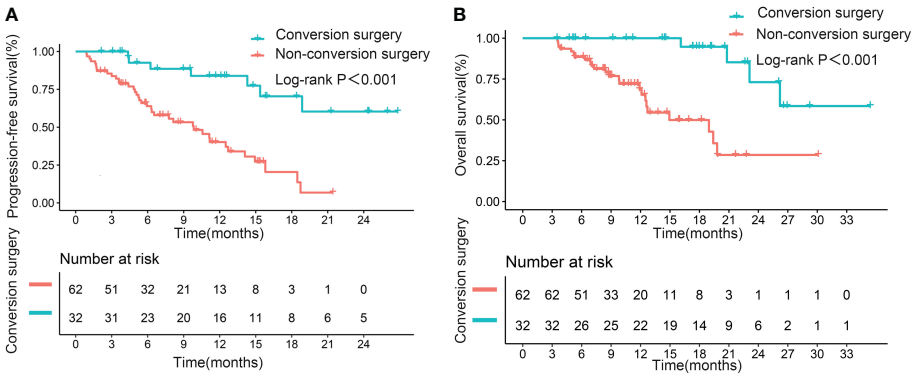

FIGURE 4
Kaplan–Meier curves for progression-free survival **(A)** and overall survival **(B)**, based on successful conversion surgery, in the entire cohort.

patients without distant metastases. A significant association was also found between early tumor response and OS but not between early tumor response and PFS, a finding that is inconsistent with previous results (20). The main reason is that in the previous study, only two patients underwent conversion surgery, whereas in the current study, 34.0% of the patients underwent conversion resection. Therefore, early tumor response is an important impact factor in conversion surgery and the prognosis of patients undergoing LTP conversion therapy. We further included early tumor response for risk stratification and found that OS decreased with increasing risk

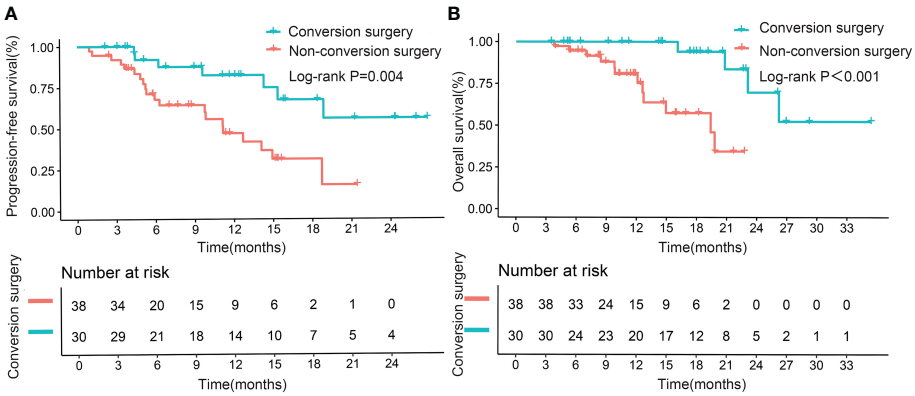

FIGURE 5
Kaplan–Meier curves for progression-free survival **(A)** and overall survival **(B)** in patients with early tumor response, based on successful conversion surgery.

factor scores. It demonstrates the potential clinical value of this stratification that takes into account early tumor response and provides evidence to support the importance of future larger-scale studies.

Conversion resection may be the only means to obtain a cure for patients with iuHCC (2). No more evidence of whether surgical resection should be performed after conversion therapy for the treatment of iuHCC meets the criteria for resectability. In our multivariable prognosis analysis, conversion surgery was an independent predictor of prognosis. This finding suggests that conversion surgery is important and necessary. To further identify the significance of conversion surgery, we compared the survival of patients with early tumor response who received conversion surgery with the survival of patients who were yet to meet the criteria for resectability despite a favorable early tumor response. We also found a better prognosis for patients who had undergone conversion surgery. Therefore, hepatectomy should be performed if patients meet the criteria for resection in early responders. However, late responders only demonstrated a trend toward prolonged OS after conversion surgery, with no significant difference in OS. In addition, late responders had low conversion surgery rate and may be no less effective than early responders. Further sample size expansion is required to confirm this result.Therefore, conversion surgery significantly improved the prognosis in the overall population, but its efficacy in late responders requires further testing.

Several limitations should be noted. First, the small sample size in one hospital prevented us from further exploring the factors influencing the prognosis of patients who received successful conversion surgery. Second, potential selection bias is inevitable because of the retrospective nature of the study. A large sample of prospective studies is necessary to further explore the subject. Third, we used two PD-1 inhibitors. Although no differences in the prognostic impact of these immunotherapeutic drugs were found (data not shown), further studies on the effects of different PD-1 inhibitors on conversion therapy are still needed.

In summary, early tumor response is an important predictive marker for successful conversion surgery and prolonged survival in patients with iuHCC treated using LTP conversion therapy. Conversion surgery is necessary to improve survival during conversion therapy, particularly for early responders.

Data availability statement

The raw data supporting the conclusions of this article will be made available by the authors, without undue reservation.

Ethics statement

The studies involving human participants were reviewed and approved by Ethics Committee of Guangxi Medical University Cancer Hospital(approval number: LW2022147). The patients/participants provided their written informed consent to participate in this study. Written informed consent was obtained from the individual(s) for the publication of any potentially identifiable images or data included in this article.

Author contributions

XL, JC, LL and FW contributed for study concept, design, and finished manuscript writing. XL, JC, XW, TB, and SL performed data analysis and critically revised the article. XL, JC, TW, ZT, CH, BZ, and BL were involved in data collection and verification. All authors contributed to the article and approved the final manuscript.

Funding

This work was supported by the National Natural Science Foundation of China (81860502), Key Laboratory of High-Incidence-Tumor Prevention & Treatment, Ministry of Education (GKE2019-06), Key Laboratory of High-Incidence-Tumor Prevention & Treatment, Ministry of Education(GKE-ZZ202129), Key Laboratory of High-Incidence-Tumor Prevention & Treatment, Ministry of Education(GKE-ZZ202004), and Key Laboratory of Early Prevention and Treatment for Regional High Frequency Tumor, Ministry of Education (GKE-ZZ202216).

Conflict of interest

The authors declare that the research was conducted in the absence of any commercial or financial relationships that could be construed as a potential conflict of interest.

Publisher's note

Supplementary material

The Supplementary Material for this article can be found online at: https://www.frontiersin.org/articles/10.3389/fonc.2023.1110689/full#supplementary-material

References

1. Villanueva A. Hepatocellular carcinoma. *N Engl J Med* (2019) 380(15):1450–62. doi: 10.1056/NEJMra1713263

2. Arita J, Ichida A, Nagata R, Mihara Y, Kawaguchi Y, Ishizawa T, et al. Conversion surgery after preoperative therapy for advanced hepatocellular carcinoma in the era of

molecular targeted therapy and immune checkpoint inhibitors. *J Hepatobiliary Pancreat Sci* (2022) 29:732–40. doi: 10.1002/jhbp.1135

3. Yang F, Xu GL, Huang JT, Yin Y, Xiang W, Zhong BY, et al. Transarterial chemoembolization combined with immune checkpoint inhibitors and tyrosine kinase inhibitors for unresectable hepatocellular carcinoma: Efficacy and systemic immune response. *Front Immunol* (2022) 13:847601. doi: 10.3389/fimmu.2022.847601

4. He MK, Liang RB, Zhao Y, Xu YJ, Chen HW, Zhou YM, et al. Lenvatinib, toripalimab, plus hepatic arterial infusion chemotherapy versus lenvatinib alone for advanced hepatocellular carcinoma. *Ther Adv Med Oncol* (2021) 13:17588359211002720. doi: 10.1177/17588359211002720

5. Ke Q, Xin F, Fang H, Zeng Y, Wang L, Liu J. The significance of transarterial Chemo (Embolization) combined with tyrosine kinase inhibitors and immune checkpoint inhibitors for unresectable hepatocellular carcinoma in the era of systemic therapy: A systematic review. *Front Immunol* (2022) 13:913464. doi: 10.3389/fimmu.2022.913464

6. Qu S, Zhang X, Wu Y, Meng Y, Pan H, Fang Q, et al. Efficacy and safety of tace combined with lenvatinib plus pd-1 inhibitors compared with tace alone for unresectable hepatocellular carcinoma patients: A prospective cohort study. *Front Oncol* (2022) 12:874473. doi: 10.3389/fonc.2022.874473

7. Chen S, Wu Z, Shi F, Mai Q, Wang L, Wang F, et al. Lenvatinib plus tace with or without pembrolizumab for the treatment of initially unresectable hepatocellular carcinoma harbouring pd-L1 expression: A retrospective study. *J Cancer Res Clin Oncol* (2022) 148(8):2115–25. doi: 10.1007/s00432-021-03767-4

8. Zhu XD, Huang C, Shen YH, Ji Y, Ge NL, Qu XD, et al. Downstaging and resection of initially unresectable hepatocellular carcinoma with tyrosine kinase inhibitor and anti-Pd-1 antibody combinations. *Liver Cancer* (2021) 10(4):320–9. doi: 10.1159/000514313

9. Qu WF, Ding ZB, Qu XD, Tang Z, Zhu GQ, Fu XT, et al. Conversion therapy for initially unresectable hepatocellular carcinoma using a combination of toripalimab, lenvatinib plus tace: Real-world study. *BJS Open* (2022) 6(5):zrac114. doi: 10.1093/bjsopen/zrac114

10. Wu JY, Yin ZY, Bai YN, Chen YF, Zhou SQ, Wang SJ, et al. Lenvatinib combined with anti-Pd-1 antibodies plus transcatheter arterial chemoembolization for unresectable hepatocellular carcinoma: A multicenter retrospective study. *J Hepatocell Carcinoma* (2021) 8:1233–40. doi: 10.2147/jhc.S332420

11. Bouchahda M, Boige V, Smith D, Karaboué A, Ducreux M, Hebbar M, et al. Early tumour response as a survival predictor in previously- treated patients receiving triplet hepatic artery infusion and intravenous cetuximab for unresectable liver metastases from wild-type kras colorectal cancer. *Eur J Cancer* (2016) 68:163–72. doi: 10.1016/j.ejca.2016.09.011

12. Cremolini C, Loupakis F, Antoniotti C, Lonardi S, Masi G, Salvatore L, et al. Early tumor shrinkage and depth of response predict long-term outcome in metastatic colorectal cancer patients treated with first-line chemotherapy plus bevacizumab: Results from phase iii tribe trial by the gruppo oncologico del nord ovest. *Ann Oncol* (2015) 26(6):1188–94. doi: 10.1093/annonc/mdv112

13. Piessevaux H, Buyse M, Schlichting M, Van Cutsem E, Bokemeyer C, Heeger S, et al. Use of early tumor shrinkage to predict long-term outcome in metastatic colorectal cancer treated with cetuximab. *J Clin Oncol* (2013) 31(30):3764–75. doi: 10.1200/jco.2012.42.8532

14. Fucà G, Corti F, Ambrosini M, Intini R, Salati M, Fenocchio E, et al. Prognostic impact of early tumor shrinkage and depth of response in patients with microsatellite instability-high metastatic colorectal cancer receiving immune checkpoint inhibitors. *J Immunother Cancer* (2021) 9(4):e002501. doi: 10.1136/jitc-2021-002501

15. Vivaldi C, Fornaro L, Cappelli C, Pecora I, Catanese S, Salani F, et al. Early tumor shrinkage and depth of response evaluation in metastatic pancreatic cancer treated with first line chemotherapy: An observational retrospective cohort study. *Cancers (Basel)* (2019) 11(7):939. doi: 10.3390/cancers11070939

16. Kawachi H, Fujimoto D, Morimoto T, Hosoya K, Sato Y, Kogo M, et al. Early depth of tumor shrinkage and treatment outcomes in non-small cell lung cancer treated using nivolumab. *Invest New Drugs* (2019) 37(6):1257–65. doi: 10.1007/s10637-019-00770-y

17. Miyake H, Miyazaki A, Imai S, Harada K, Fujisawa M. Early tumor shrinkage under treatment with first-line tyrosine kinase inhibitors as a predictor of overall survival in patients with metastatic renal cell carcinoma: A retrospective multi-institutional study in Japan. *Target Oncol* (2016) 11(2):175–82. doi: 10.1007/s11523-015-0385-6

18. Öcal O, Schinner R, Schütte K, de Toni EN, Loewe C, van Delden O, et al. Early tumor shrinkage and response assessment according to mrecist predict overall survival in hepatocellular carcinoma patients under sorafenib. *Cancer Imaging* (2022) 22(1):1. doi: 10.1186/s40644-021-00439-x

19. Takahashi A, Moriguchi M, Seko Y, Shima T, Mitsumoto Y, Takashima H, et al. Early tumor shrinkage as a predictive factor for outcomes in hepatocellular carcinoma patients treated with lenvatinib: A multicenter analysis. *Cancers (Basel)* (2020) 12(3):754. doi: 10.3390/cancers12030754

20. Li X, Fu Z, Chen X, Cao K, Zhong J, Liu L, et al. Efficacy and safety of lenvatinib combined with pd-1 inhibitors plus tace for unresectable hepatocellular carcinoma patients in China real-world. *Front Oncol* (2022) 12:950266. doi: 10.3389/fonc.2022.950266

21. Xu Y, Yang Y, Li L, Zhou A, Zhang H, Ye F, et al. Different radiological criteria for early tumor response evaluation in patients with unresectable hepatocellular carcinoma treated with anti-Pd-1 antibody plus bevacizumab. *Front Oncol* (2022) 12:848129. doi: 10.3389/fonc.2022.848129

22. Zhou J, Sun H, Wang Z, Cong W, Wang J, Zeng M, et al. Guidelines for the diagnosis and treatment of hepatocellular carcinoma (2019 edition). *Liver Cancer* (2020) 9 (6):682–720. doi: 10.1159/000509424

23. Zhu AX, Dayyani F, Yen CJ, Ren Z, Bai Y, Meng Z, et al. Alpha-fetoprotein as a potential surrogate biomarker for atezolizumab + bevacizumab treatment of hepatocellular carcinoma. *Clin Cancer Res* (2022) 28:3537–45. doi: 10.1158/1078-0432.Ccr-21-3275

24. Eissa M, Shaarawy S, Abdellateif MS. The role of different inflammatory indices in the diagnosis of covid-19. *Int J Gen Med* (2021) 14:7843–53. doi: 10.2147/ijgm.S337488

25. Tada T, Kumada T, Hiraoka A, Hirooka M, Kariyama K, Tani J, et al. Neutrophil-lymphocyte ratio predicts early outcomes in patients with unresectable hepatocellular carcinoma treated with atezolizumab plus bevacizumab: A multicenter analysis. *Eur J Gastroenterol Hepatol* (2022) 34(6):698–706. doi: 10.1097/meg.0000000000002356

26. Hong YM, Yoon KT, Cho M. Systemic immune-inflammation index predicts prognosis of sequential therapy with sorafenib and regorafenib in hepatocellular carcinoma. *BMC Cancer* (2021) 21(1):569. doi: 10.1186/s12885-021-08124-9

27. Yang Y, Ouyang J, Zhou Y, Zhou J, Zhao H. The crafity score: A promising prognostic predictor for patients with hepatocellular carcinoma treated with tyrosine kinase inhibitor and immunotherapy combinations. *J Hepatol* (2022) 77:574–6. doi: 10.1016/j.jhep.2022.03.018

28. Scheiner B, Pomej K, Kirstein MM, Hucke F, Finkelmeier F, Waidmann O, et al. Prognosis of patients with hepatocellular carcinoma treated with immunotherapy - development and validation of the crafity score. *J Hepatol* (2022) 76(2):353–63. doi: 10.1016/j.jhep.2021.09.035

29. Lencioni R, Montal R, Torres F, Park JW, Decaens T, Raoul JL, et al. Objective response by mrecist as a predictor and potential surrogate end-point of overall survival in advanced hcc. *J Hepatol* (2017) 66(6):1166–72. doi: 10.1016/j.jhep.2017.01.012

30. Vincenzi B, Di Maio M, Silletta M, D'Onofrio L, Spoto C, Piccirillo MC, et al. Prognostic relevance of objective response according to easl criteria and mrecist criteria in hepatocellular carcinoma patients treated with loco-regional therapies: A literature-based meta-analysis. *PloS One* (2015) 10(7):e0133488. doi: 10.1371/journal.pone.0133488

frontiers | Frontiers in Oncology

TYPE Original Research
PUBLISHED 01 February 2023
DOI 10.3389/fonc.2023.1091132

OPEN ACCESS

EDITED BY
Lujun Shen,
Sun Yat-sen University Cancer Center (SYSUCC), China

REVIEWED BY
Zhenbo Tu,
Beth Israel Deaconess Medical Center, United States
Debanjali Dasgupta,
Mayo Clinic, United States
Wen Chun-yong,
Sun Yat-sen University Cancer Center (SYSUCC), China

*CORRESPONDENCE
Fei Fan
178035587@qq.com
Qian Qian Cai
caiqq@sumhs.edu.cn

SPECIALTY SECTION
This article was submitted to Gastrointestinal Cancers: Hepato Pancreatic Biliary Cancers, a section of the journal Frontiers in Oncology

RECEIVED 06 November 2022
ACCEPTED 18 January 2023
PUBLISHED 01 February 2023

CITATION
Huang XF, Fu LS, Cai QQ and Fan F (2023) Prognostic and immunological role of sulfatide-related lncRNAs in hepatocellular carcinoma. *Front. Oncol.* 13:1091132. doi: 10.3389/fonc.2023.1091132

Prognostic and immunological role of sulfatide-related lncRNAs in hepatocellular carcinoma

Xing Feng Huang[1], Li Sheng Fu[2], Qian Qian Cai[3]* and Fei Fan[4]*

[1]Department of Biliary Tract Surgery, Shanghai Eastern Hepatobiliary Surgery Hospital, Shanghai, China, [2]Department of Biochemistry and Molecular Biology, School of Basic Medical Sciences, Fudan University, Key Lab of Glycoconjugate Research, Ministry of Public Health, Shanghai, China, [3]Shanghai Key Laboratory of Molecular Imaging, Shanghai University of Medicine and Health Sciences, Shanghai, China, [4]Department of The Second Ward of Special Treatment, Shanghai Eastern Hepatobiliary Surgery Hospital, Shanghai, China

Background: Hepatocellular carcinoma (HCC) is the most common primary malignancy of the liver. Long non-coding RNAs (lncRNAs) play important roles in the occurrence and development of HCC through multiple pathways. Our previous study reported the specific molecular mechanism for sulfatide regulation of integrin αV expression and cell adhesion in HCC cells through lncRNA AY927503. Next, it is necessary to identify more sulfatide-related lncRNAs, explore their clinical signifcance, and determine new targeted treatment strategies.

Methods: Microarrays were used to screen a complete set of lncRNAs with different expression profiles in sulfatide-treated cells. Sulfatide-related lncRNAs expression data and corresponding HCC patient survival information were obtained from the The Cancer Genome Atlas (TCGA) database, and the prognosis prediction model was constructed based on Cox regression analysis. Methylated RNA immunoprecipitation with next generation sequencing (MeRIP-seq) was used to detemine the effect of sulfatide on lncRNAs m6A modification. Tumor Immune Estimation Resource (TIMER) and Gene set nnrichment analysis (GSEA) were utilized to enrich the immune and functional pathways of sulfatide-related lncRNAs.

Results: A total of 85 differentially expressed lncRNAs (|Fold Change (FC)|>2, P<0.05) were screened in sulfatide-treated HCC cells. As a result, 24 sulfatide-related lncRNAs were highly expressed in HCC tissues, six of which were associated with poor prognosis in HCC patients. Based on thses data, a sulfatide-related lncRNAs prognosis assessment model for HCC was constructed. According to this risk score analysis, the overall survival (OS) curve showed that the OS of high-risk patients was significantly lower than that of low-risk patients (P<0.05). Notably, the expression difference in sulfatide-related lncRNA NRSN2-AS1 may be related to sulfatide-induced RNA m6A methylation. In addition, the expression level of NRSN2-AS1 was significantly positively correlated with immune cell infiltration in HCC and participated in the peroxisome and Peroxisome proliferator-activated receptor (PPAR) signaling pathways.

Conclusions: In conclusion, sulfatide-related lncRNAs might be promising prognostic and therapeutic targets for HCC.

KEYWORDS

sulfatide, lncRNAs, HCC, prognosis, immune infiltration

Background

Hepatocellular carcinoma (HCC) is the most common liver malignancy worldwide and is one of the top five deadliest cancers, with high morbidity and mortality rates (1). The level of sulfatide, a sulfoglycolipid, is usually elevated in HCC (2). and can protect hepatocytes from ischemia/reperfusion injury (3, 4). We previously reported that sulfatide enhances integrin aV (ITGAV) expression, leading to HCC metastasis (2, 5). Sulfatide is also abnormally expressed in ovarian carcinoma and renal cell carcinoma (6), and can be used as a specific biomarker for these tumors (7, 8). Moreover, direct inhibition of sulfatide biosynthesis by zoledronic acid can significantly inhibit the migration, invasion and lung metastasis of basal-like breast cancer cells (9). In our earlier study, lncRNA AY927503 was identified in sulfatide-treated HCC cells. It promoted HCC metastasis by inducing *ITGAV* transcriptional chromatin modification and was a potential molecular marker of HCC metastasis or poor prognosis (10). Long non-coding RNAs (lncRNAs) are RNA molecules consisting of more than 200 nucleotides with no or limited protein-coding potential, which affect tumor proliferation, migration and metastasis in the process of malignant tumor development (11). Therefore, further research on sulfatide-related lncRNAs will not only expand our understanding of the role of sulfatide in the occurrence and development of HCC, but may also provide potential prognostic biomarkers and individualized therapeutic targets for HCC. The present study sought to determine the role of the sulfatide-related lncRNAs in HCC.

Methods

Cell culture and treatment

SMMC-7721 cells were obtained from Cell Bank of Type Culture Collection of Shanghai Institute of Biochemistry & Cell Biology, Chinese Academy of Science. They were cultured in Dulbecco's Modified Eagle's Medium (Gibco, California, USA) supplemented with 10% fetal bovine serum (FBS) (Gibco). SMMC-7721 cells were identified by their morphological characteristics which were consistent with the establishment report (12). Cells were not contaminated by mycoplasma or infected with bacteria or fungi. All cells were cultured in a humidified incubator with 5% CO_2 at 37°C. For the sulfatide treatment, cells were incubated at the initial density of 0.5×10^5 cells/mL and treated with 2 μM galactocerebroside (GalCer) or sulfatide (Sigma, St. Louis, MO, USA).

Abbreviations: HCC, Hepatocellular Carcinoma; TCGA, The Cancer Genome Atlas; LIHC, Live Hepatocellular Carcinoma; MeRIP-seq, Methylated RNA immunoprecipitation with next generation sequencing; FC, Fold Change; OS, Overall Survival; DSS, Disease-Specific Survival; HR, Hazard Ratios; CI, Confidence Intervals; TIMER, Tumor Immune Estimation Resource; KEGG, Kyoto Encyclopedia of Genes and Genomes; GSEA, Gene Set Enrichment Analysis; NES, normalized enrichment score; NOM P, nominal p value; FDR, false discovery rate; DE-lncRNAs, differentially expressed LncRNAs; ROC, receiver operating characteristic; AUC, area under curve; NKT cells, Natural killer T cells; GSLs, Glycosylsphingolipids; ER, endoplasmic reticulum; TIME, Tumor immune microenvironment; PPARs, Peroxisome proliferator-activated receptors; TDEs, tumor-derived exosomes; FAO, fatty acid oxidation; TIDCs, tumor-infiltrating DCs; ILC2s, group 2 innate lymphoid cells; TAMs, tumor-associated macrophages; GEO, Gene Expression Omnibus

Microarray expression profiling for lncRNA

Microarray profiling was conducted in the laboratory of Aksomics Inc. (Shanghai, China). The microarray was analyzed using the nrStar™ Functional LncRNA PCR chip software, version 1.0 (ArrayStar, Rockville, MD, USA). The hierarchical clustering analysis was carried out using a platform-independent software TBtools (version x64_1_09867) (13).

Assessment of sulfatide-related lncRNAs expression in TCGA-LIHC

The TCGA Liver Cancer project (TCGA-LIHC) (N=423) data were downloaded from the UCSC Xena database (https://xenabrowser.net/) (14). Log2(x+0.001) transformation was used to standardize every gene expression profiles and noncoding genes were identified based on their Ensemble gene IDs.

Survival prognosis analysis

A Cox proportional-hazards regression model was established to analyze the relationship between sulfatide-related lncRNA expression and overall survival (OS) in HCC. The patients were divided into two groups according to the best cutoff value for each sulfatide-related lncRNA, which calculated by the R package maxstat. The OS significance map in HCC was evaluated using the Kaplan-Meier plotter (http://kmplot.com/analysis/) (15).

Prognostic risk score calculation

The least absolute shrinkage and selection operator (LASSO) regression analysis was conducted on the sulfatide-related lncRNAs. The LASSO regression algorithm was used for feature selection with 10-fold cross-validation. The R package glmnet was used for the analysis. For Kaplan-Meier curves, p-values and hazard ratios (HRs) with 95% confidence intervals (CIs) were generated using log-rank tests and univariate Cox proportional -hazards regression. Finally, six sulfatide-related lncRNAs were selected for incorporation into the risk score. The regression coefficient β for multivariate Cox regression model and lncRNA expression were used to construct the risk score formula as follows:

Immune infiltration analysis

The Tumor Immune Estimation Resource (TIMER) database (http://timer.cistrome.org/) (16) analyzes immune cell infiltration in tumor tissues using high-throughput sequencing (RNA-Seq expression profiling) data (16, 17). The B cell, CD4+ T cells, CD8+

T cells, neutrophil, macrophage and dendritic cells infiltration score of HCC are evaluated by the Timer method of IOBR (version 0.99.9) (18), an R software package, based on the expression profile data of TCGA-LIHC. Spearman's correlation coefficient between NRSN2-AS1 and immune cell infiltration score in HCC was calculated using corr.test function of R package psych (version 2.1.6) to determine the significantly correlated immune infiltration score.

m6A-modified RNA immunoprecipitation sequencing

Total RNA samples were extracted, ragmented to 100bp, and immunoprecipitated using anti-m6A antibody (abcam). Then, eluted RNA and MeRIPed RNA were analyzed using deep sequencing with an Illumina Novaseq™ 6000 platform on the CLOUDSEQ Bio-tech Ltd (Shanghai, China) following the vendor's recommended protocol (19)l.

Biological signaling pathway analysis

Pathway enrichment analysis of Kyoto Encyclopedia of Genes and Genomes (KEGG) was performed using the Gene Set Enrichment Analysis (GSEA) database in TCGA-LIHC, which classified the data into high- and low- expression groups based on their *NRSN2-AS1* expression (20). Gene sets with |normalized enrichment score (NES)| >1, nominal p value (NOM *P)* <0.05, and false discovery rate (FDR) *q* <0.25 were considered to have significant enrichment.

Statistical analysis

Differences in the expression of sulfatide-related lncRNAs between normal and tumor samples from each tumor were analyzed for significance using unpaired Wilcoxon rank sum and signed rank tests. Survival curves were statistically tested using the log rank test, where p-values and HRs with 95% CIs were represented *via* Kaplan-Meier plots. The significant correlations between sulfatide-related lncRNAs expression and immune cell infiltration scores in HCC were determined by analyzing Spearman's correlation coefficients. Pearson correlation analysis was performed between the expression level of NRSN2-AS1_ (ENSG00000225377) and gene set expression level of RNA m6A methylation-modifying enzyme. The level of significance was set at $P < 0.05$. The bioinformatics analysis platform Sangerbox, version 3.0 (http://vip.sangerbox.com/) (21), was used for processing of all the statistical analyses.

Results

Sulfatide induced differential expression of multiple lncRNAs in HCC cells

The lncRNA profiles of sulfatide-treated HCC cells were compared to those of control cells using ArrayStar lncRNA microarray V2.0. This comparison identified 85 differentially expressed lncRNAs (DE-lncRNAs) based on their Ensemble IDs (|FC|>2, $P < 0.05$) (Figures 1A, B. Supplementary Table 1). These DE-lncRNAs were further classified by biotype, most of which were lncRNAs as processed transcripts, unclassified processed transcripts, processing/unprocessed pseudogenes, and small amounts of protein coding transcripts or unclassified transcripts (Figure 1C).

Identification of differentially expressed sulfatide-related lncRNAs

The TCGA-LIHC dataset was used to detect the expression of these 85 sulfatide-related lncRNAs in HCC tissues, showing that 24 of them were highly expressed in HCC compared to normal liver tissues (Figure 2A). However, the expression of three sulfatide-related lncRNAs, AP002841.2 (ENST00000504610), RP11-733O18.1 (ENST00000422914) and RP5-885L7.10 (ENST00000412500) were lower in HCC tissues (Figure 2B).

Prognostic value of sulfatide-related lncRNAs

Among the above mentioned 27 sulfatide-related lncRNAs, six lncRNAs were ultimately identified to be related to prognosis (Figure 3A), including RP11-122M14.1 (ENST00000415202), RP11-280O1.2 (also known as LRRC52-AS1; ENST00000438275), AC079354.5 (ENST00000447111), AC005037.3 (ENST00000413848), AC108488.3 (also known as RNASEH1-AS1; ENST00000438436) and RP5-1103G7.4 (also known as NRSN2-AS1; ENST00000442637). Kaplan–Meier survival analysis was utilized to evaluate the significance of lncRNA expression in patient prognosis (Figure 3B). High levels of these sulfatide-related lncRNAs were all correlated with poor prognosis in patients with HCC (Figure 3).

Construction of prognostic signature based on sulfatide-related lncRNAs

Based on the expression of six sulfatide-related lncRNAs and multivariate Cox regression coefficient, the prognosis risk score for sulfatide-related lncRNAs was calculated using the following formula: riskscore (lambda.min=0.0029) = (2.0727) × LRRC52-AS1 + (0.3691) × RNASEH1-AS1 + (0.2646) × NRSN2-AS1 (Figures 4A, B). Subsequently, an X-tile diagram was used to generate the optimal cutoff point for the risk score. The TCGA-LIHC patients were divided into high- and low-risk groups based on this cutoff risk score value. A prognostic curve and a scatter plot were used to indicate the risk score and survival status of each HCC patient (Figures 4C, D). In addition, the heat map of the expression profiles for candidate lncRNAs demonstrated that they were all highly expressed in the high-risk group (Figure 4E). Kaplan-Meier analysis validated that the TCGA-LIHC patients in the high-risk group showed a significantly worse survival than those in the low-risk group at the 10-year time point

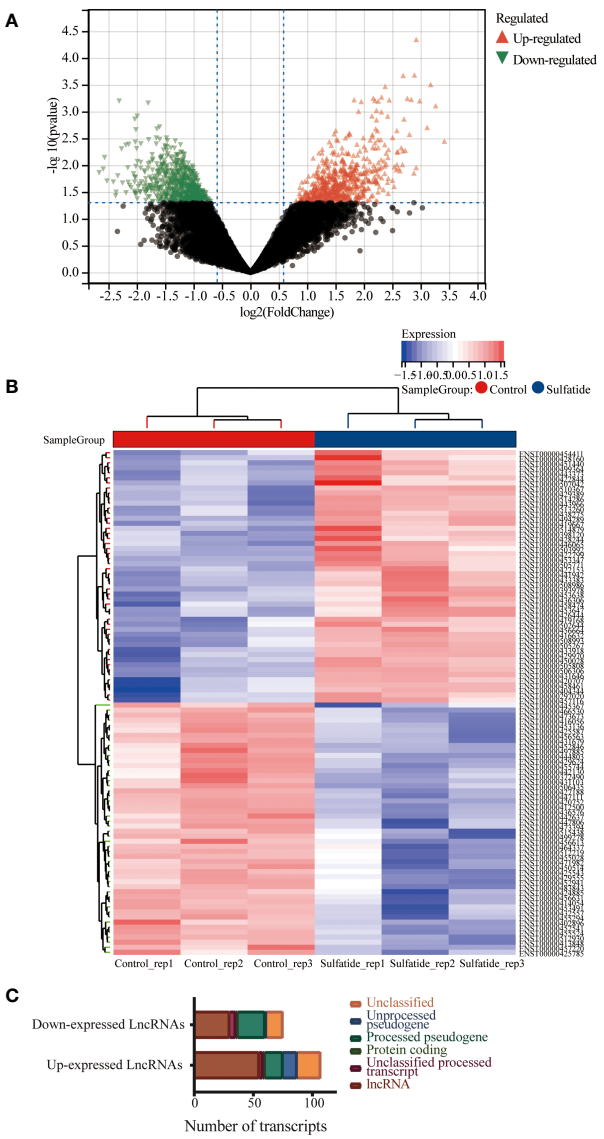

FIGURE 1
Multiple lncRNAs were differentially expressed in HCC cells after sulfatide treatment. **(A)** Volcano plot representing differentially expressed lncRNAs in HCC cells after sulfatide treatment. **(B)** Heat map showing differentially expressed lncRNAs in sulfatide-treated HCC cells and control cells. **(C)** Transcript classification analysis of differentially expressed lncRNAs.

(Figure 4F). Furthermore, the time-dependent receiver operating characteristic (ROC) analyses showed that the area under curve (AUC) for the risk score model was 0.671 at the one-year time point, 0.621 at the three-year time point, and 0.629 at the five-year time point (Figure 4G). Taken together, these findings represented the three sulfatide-related lncRNAs as the prognostic signature for HCC patients.

NRSN2-AS1 expression was associated with RNA m6A methylation

Our previous study reported that sulfatide does not only affect the binding of METTL3 to METTL14 and WTAP by acetylating the METTL3 protein (19), but also inhibits the YTHDF2 expression in HCC cells (22). Next, we investigated whether RNA m6A methylation modification affected sulfatide-related lncRNA expression. The MeRIP-seq experiments were performed, in order to clarify the role of RNA m6A methylation modification. Their results showed that the abundance of m6A in NRSN2-AS1, one of sulfatide-related lncRNAs, was significantly increased in sulfatide-treated HCC cells. This suggested that m6A modification was related to the regulation of NRSN2-AS1 expression (Figure 5A). Furthermore, the relationship between NRSN2-AS1 expression level and a series of m6A-binding proteins (23) was analyzed in TCGA-LIHC samples. The results showed that the expression levels of NRSN2-AS1 were positively correlated with the expression of m6A writer and reader signatures (Figure 5B). In summary, the expression of NRSN2-AS1 in HCC was related to the changes in RNA m6A methylation induced by sulfatide.

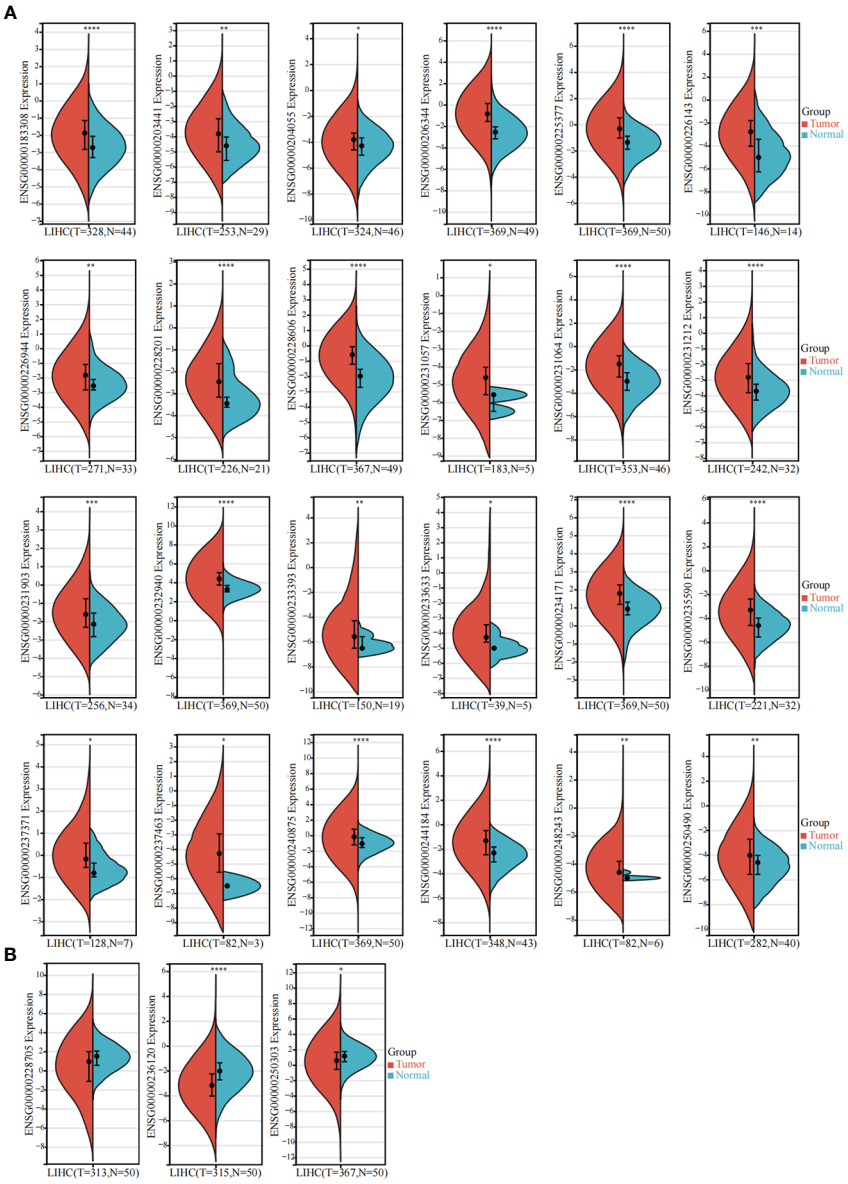

FIGURE 2
Differentially expressed sulfatide-related lncRNAs in TCGA-LIHC. **(A)** Screening of highly expressed sulfatide-related lncRNAs in TCGA-LIHC. **(B)** Sulfatide-related lncRNAs with low expression in TCGA-LIHC. *, p<0.05. **, p<0.01. ***, p<0.001. ****, p<0.0001.

Role of NRSN2-AS1 in HCC immune microenvironment characterization

An increasing number of studies have demonstrated that sulfatide is involved in tumor immunity, where the HIF-1-galactose-3-o-mercaptotransferase 1-sulfide axis enhanced immune escape of renal clear cell carcinoma by increasing tumor cell-platelet binding (24). In addition, a subpopulation of type II Natural killer T cells (NKT cells) characterized by their response to autoglycolipid sulfides was shown to induce a major immunomodulatory mechanism that controls inflammation in anticancer immunity (25). To further examine whether the sulfatide-related lncRNA NRSN2-AS1 can act as an immune indicator, a correlation analysis of NRSN2-AS1 expression with immune infiltration was performed. TIMER data showed that high NRSN2-AS1 expression was significantly associated with six types of immune cells (B cells, CD4+ T cells, CD8+ T cells, macrophages, neutrophils and dendritic cells) in HCC (Figure 6). This result pointed out that NRSN2-AS1 may serve as an indicator in tumor immune microenvironment (TIME) characterization in HCC.

Functional enrichment analysis of NRSN2-AS1 in HCC

To investigate the biological functions and pathways associated with the sulfatide-related lncRNA NRSN2-AS1, the TCGA-LIHC samples were divided into high- and low-expression groups based on their NRSN2-AS1 expression. GSEA was used to evaluate the enrichment of KEGG pathways. The pathways associated with high NRSN2-AS1 expression were enriched in the Cell Cycle pathway

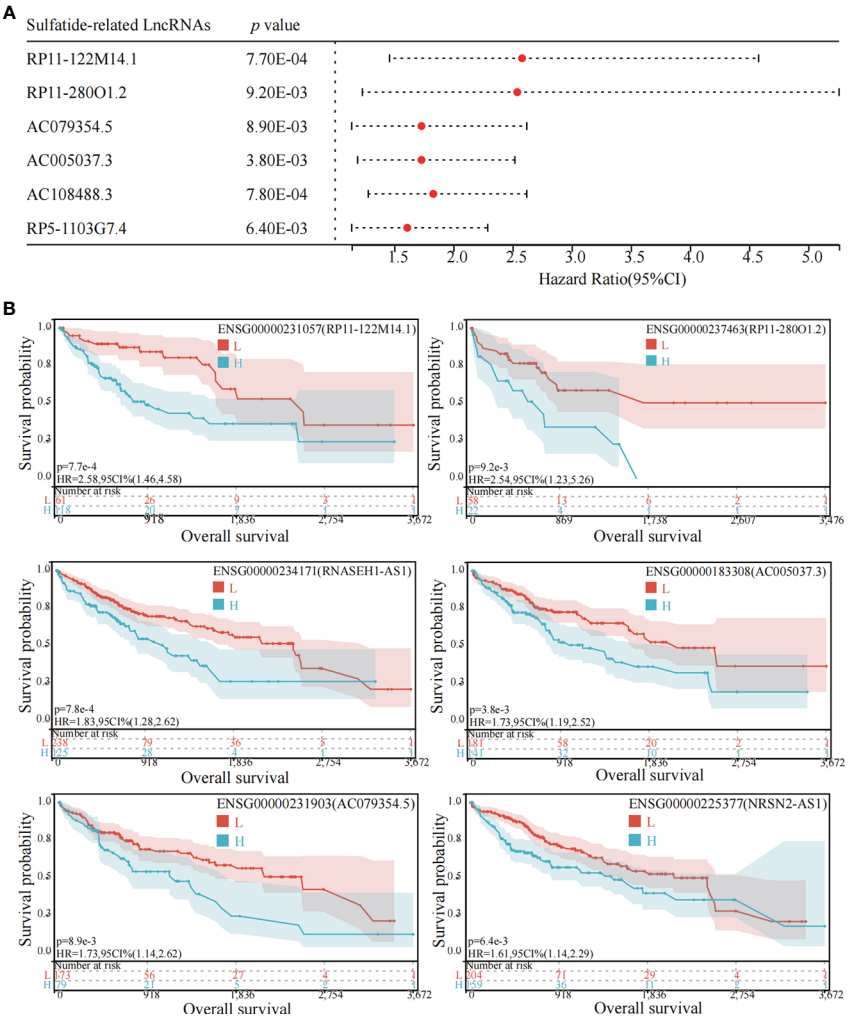

FIGURE 3
Identification of sulfatide-related lncRNAs with prognostic value in HCC patients. **(A)** Univariate Cox regression analysis of six differentially expressed sulfatide-related lncRNAs and risk scores in HCC samples. **(B)** Kaplan-Meier analytical evaluation of prognostic values of six differentially expressed sulfatide-related lncRNAs.

(Figure 7A). The pathways associated with low expression of NRSN2-AS1 were enriched in peroxisome and perxisome proliferator-activated receptor (PPAR) signaling pathways related to immune response (26, 27), as well as a variety of amino acid (tryptophan, arginine, proline, glycine, serine, threonine, tyrosine, and histidine) and lipid (fatty acid and linoleic acid) metabolic pathways (Figures 7B-D).

Discussion

HCC is the most frequently occurring type of primary liver cancer, and its pathogenesis involves a complex transcriptional regulation disorder (28–30) and energy metabolism abnormality (31–33). Therefore, identifying reliable and effective biomarkers for HCC prognosis is of great importance. Glycosylsphingolipids (GSLs) are important components of cell membranes and act as signaling molecules in cellular processes. Similar to GSLs, sulfatide (glycosphingolipid sulfate) is also composed of lipid and sugar components, and its precursor galactosylceramide connects the sulfate ester group to the carbohydrate component in the endoplasmic reticulum (ER) (34). Elevated expression of sulfatide has been found in many human cancer cell lines and tissues, and can be used as a biomarker of some cancers (4, 35, 36). Abundant sulfatide on the surface of cancer cells is a natural ligand of P-selectin ligand that helps to promote tumor metastasis (37, 38). Many lncRNAs are abnormally expressed in various cancers, including HCC, and play a key role in tumorigenesis (39). We previously reported the abundant expression of sulfatide in HCC (5), and investigated the specific molecular mechanism for sulfatide regulation of integrin αV expression and cell adhesion in HCC cells *via* lncRNA AY927503 (10, 22, 40). However, the effect of sulfatide on the expression levels of other lncRNAs in HCC cells and the role of these DE-lncRNAs in prognosis and immunotherapy evaluation require further study.

The present study screened 85 DE-lncRNAs (|FC|>2, P<0.05) in sulfatide-treated HCC cells based on their Ensemble IDs. Tthe TCGA-LIHC database 27 sulfatide-related lncRNAs that were differentially expressed in HCC and adjacent tissues, of which 24 were highly expressed in HCC tissues. RP11-122M14.1, RP11-280O1.2, AC079354.5, AC005037.3, AC108488.3 and RP5-

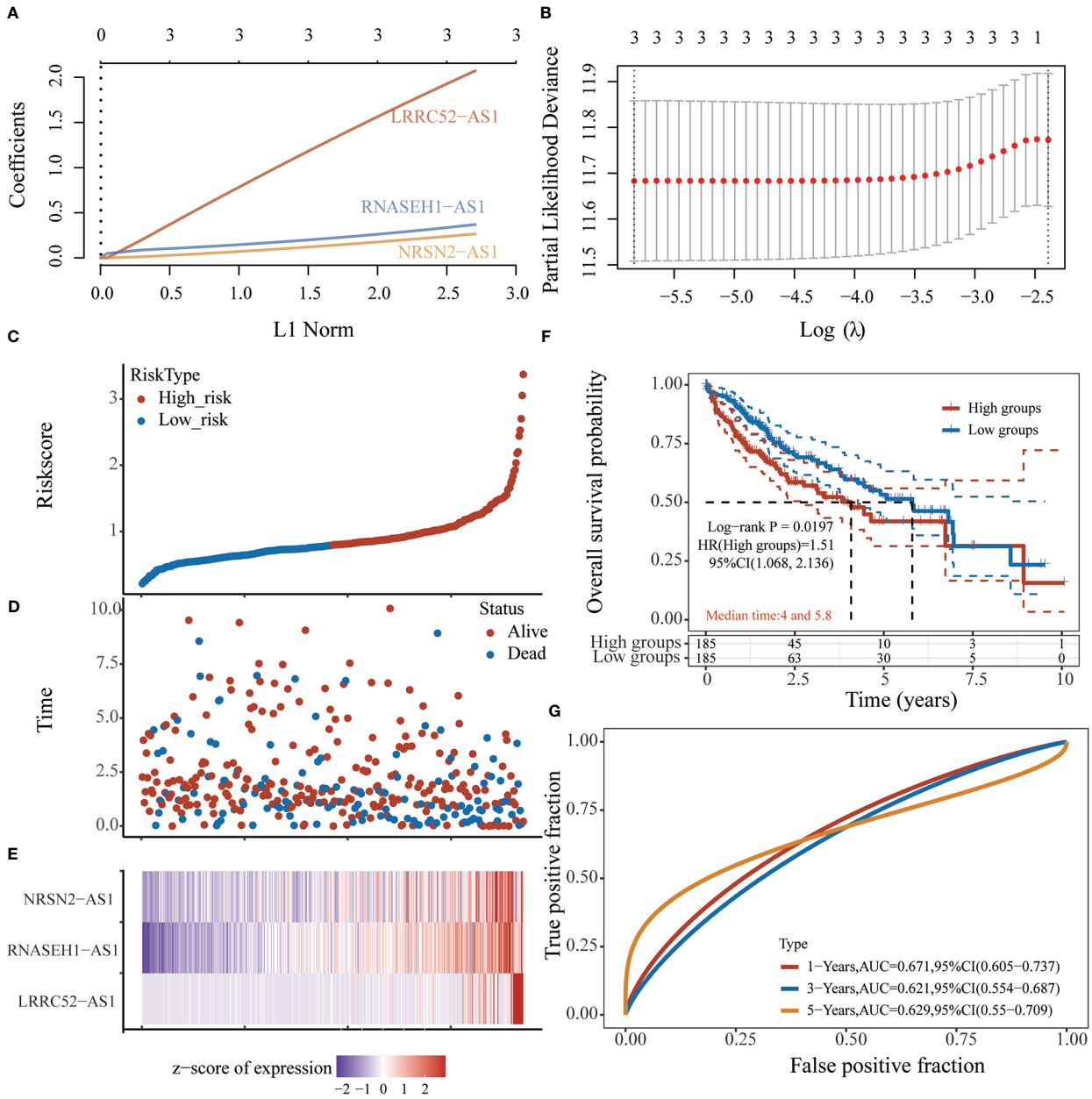

FIGURE 4
Prognostic risk score characteristics of sulfatide-related lncRNAs in HCC. **(A)**, **(B)** LASSO Cox regression with 10-fold cross-validation of the prognostic value of three sulfatide-related lncRNAs, including LRRC52-AS1, RNASEH1-AS1, and NRSN2-AS1. C, **(D)** Risk curve **(C)** and scatter plot **(D)** for the risk score and survival status of each HCC case. Blue and red dots in **(D)** represent death and survival, respectively. **(E)** Heat map showing the expression profiles of three sulfatide-related lncRNAs in the high-risk and low-risk group. **(F)** Kaplan-Meier prognostic prediction analyses of risk score model at 10-year timepoint. **(G)** Time-dependent receiver operating characteristic curves for the prognostic prediction of risk score models at one-, three-, and five-year time points.

1103G7.4 are six sulfatide-related lncRNAs with abnormally high expression that were significantly associated with poor prognosis in HCC patients. When selecting specific variables to build the prognosis evaluation model, overfitting often occurs if too many variables are present (41). Regularization is an important method to solve the overfitting problem (42). LASSO regression constructs a penalty function and adds L1 regularization after the loss function to obtain a more accurate model with fewer variables (43). After the LASSO regression analysis of six lncRNAs, only three were found to be related to the patient prognosis. Based on the risk score results and sulfatide-related lncRNA construction, the OS for high-risk patients was significantly lower than that for low-risk patients (P<0.05).

Sulfatide had been demonstrated to be one of several natural ligands for type II CD1d-restricted NKT cells, which can regulate tumor immunity (36, 44, 45). More and more studies have also found the potential effect of lncRNAs on immune cells infiltration in TIME. For example, lncRNA MIAT is distributed in HCC. It is enriched in FOXP3+CD4+T, PDCD1+CD8+, and GZMK+CD8+T cells, affects the immune microenvironment of HCC by regulating the expression of target genes JAK2, SLC6A6, KCND1, MEIS3, and RIN1, and

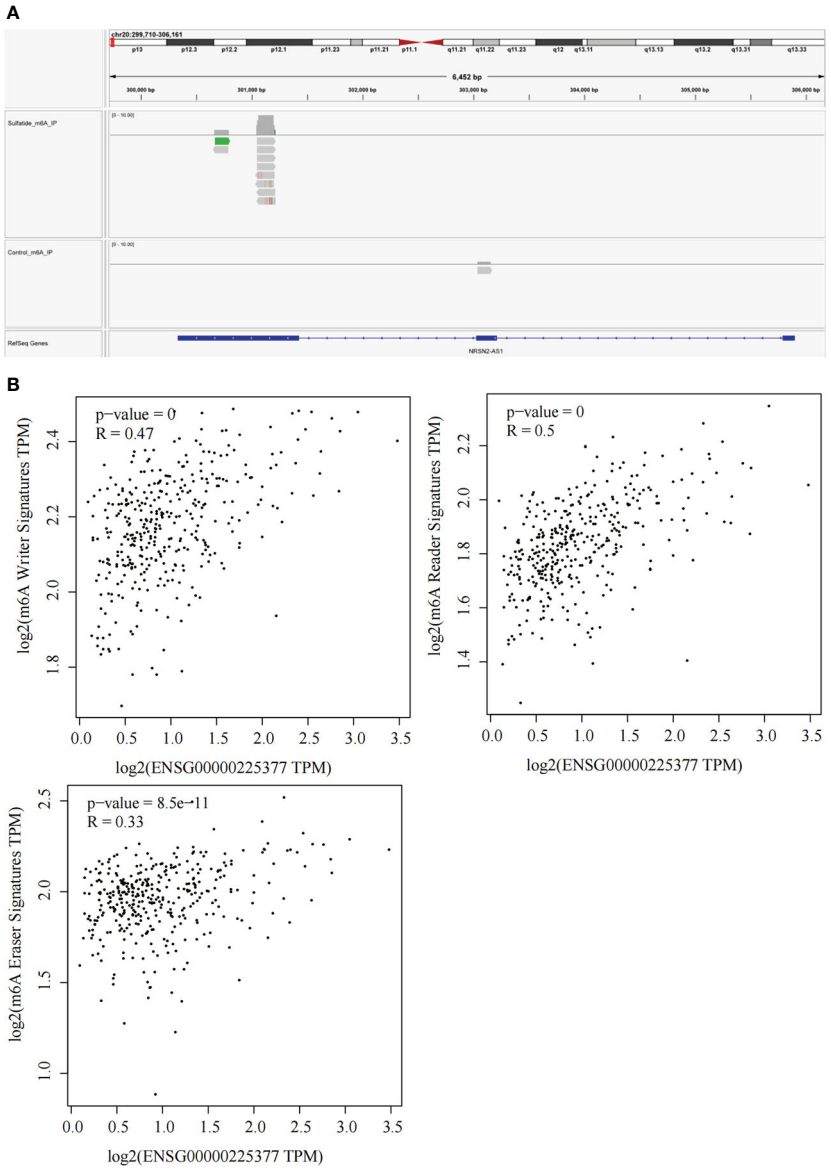

FIGURE 5
Sulfatide affects NRSN2-AS1 expression by regulating the RNA m6A methylation modification. **(A)** Abundances of m6A in NRSN2-AS1 determined by MeRIP-seq. **(B)** Pearson correlation of NRSN2-AS1 expression and m6A writer, reader, and eraser signature expressions.

participates in the immune escape process in HCC (46). The lncRNA MIAT also mediates HCC immune response by targeting the miR-411-5p/STAT3/PD-L1 axis (47). Therefore, we speculated that sulfated-related lncRNAs may also be involved in regulating the HCC TIME. Based on the TIMER database, we confirmed that the high expression of sulfatide-related lncRNA NRSN2-AS1 was significantly related to the infiltration of immune cells, such as macrophages, dendritic cells, neutrophils, B cells, CD4+T cells, and CD8+T cells in HCC. As a newly identified lncRNA, NRSN2-AS1 has not been well studied in cancer. The latest research found that NRSN2-AS1 is significantly overexpressed in ovarian cancer, plays a tumor-promoting role as the sponge of miR-744-5p, and regulates the Wnt/β-catenin signaling pathway *via* the miR-744-5p/PRKX axis (48). It was also found that SOX2 promotes NRSN2-AS1 transcription in esophageal squamous cell carcinoma (ESCC), and that NRSN2-AS1 promotes its progression by regulating the ubiquitin degradation of PGK1 (49). However, the role and mechanism of NRSN2-AS1 in tumor immunity remain unknown.

The GSEA results suggested that the pathways related to the low expression of NRSN2-AS1 are mainly enriched in the peroxisome and PPAR signaling pathways. Peroxisome proliferator-activated receptors (PPARs) belong to the nuclear hormone receptor family. They are divided into α, β, and γ subtypes, and participate in the metabolism of various energy substances and tumor immunity. PPARα was found to respond to the fatty acids delivered by tumor-derived exosomes (TDEs), resulting in excess lipid droplet biogenesis and enhanced fatty acid oxidation (FAO), culminating in a metabolic shift toward mitochondrial oxidative phosphorylation, which drives tumor-infiltrating DCs (TIDCs) immune dysfunction (50). It was reported that CD36 is selectively upregulated in intratumoral Treg

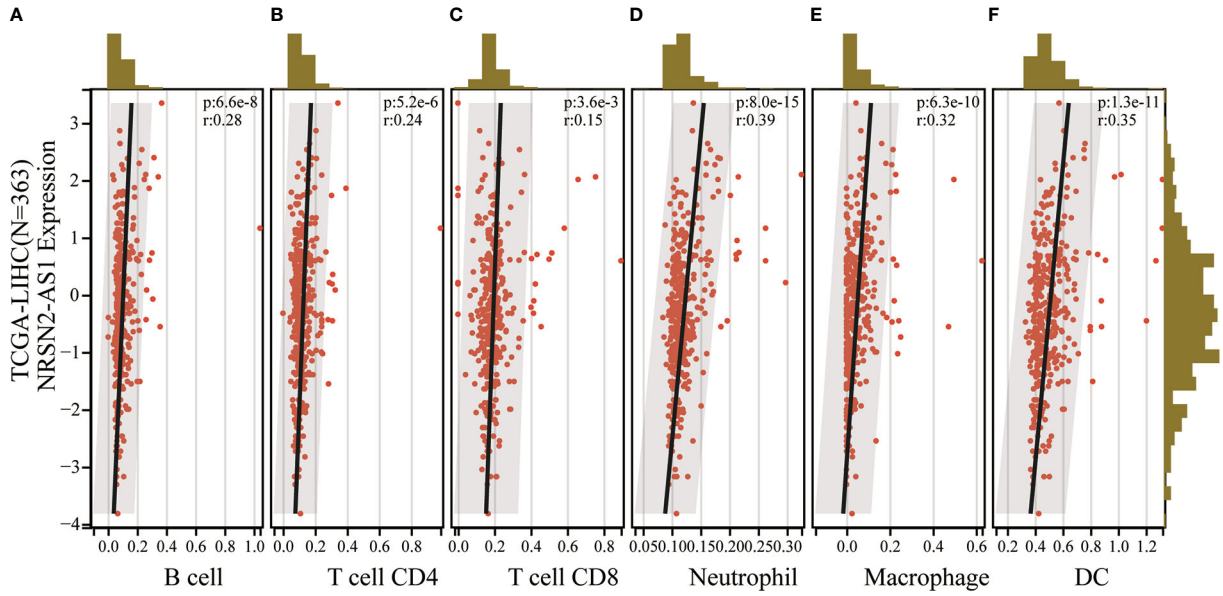

FIGURE 6
Correlation of NRSN2-AS1 in tumor immune microenvironment characterization. **(A–F)**. Correlation between NRSN2-AS1 expression and immune infiltration level of B cells **(A)**, CD4+ T cells **(B)**, CD8+ T cells **(C)**, neutrophils **(D)**, macrophages **(E)**, and dendritic cells **(F)** in HCC.

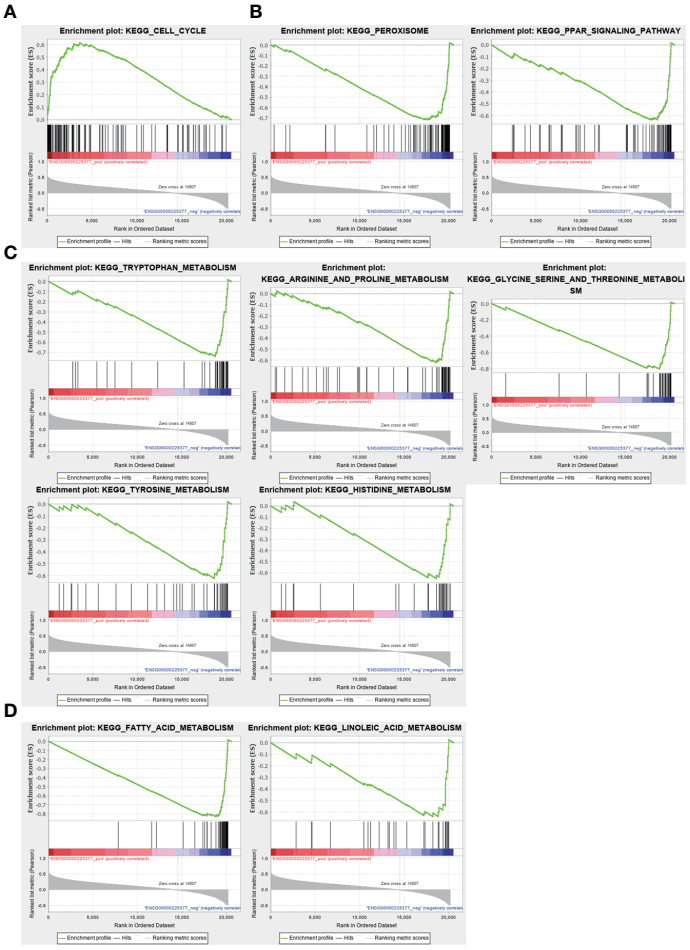

FIGURE 7
Gene set enrichment analysis for NRSN2-AS1. **(A)**. Significantly enriched pathways in patients with high NRSN2-AS1 expression. **(B-D)**. Significantly enriched pathways in patients with low NRSN2-AS1 expression.

cells as a central metabolic modulator activates PPARβ signaling to regulate mitochondrial adaptation, and programs Treg cells to adapt to lactic acid-enriched TME (51). PPARγ is selectively expressed in group 2 innate lymphoid cells (ILC2s) supported the IL-33-dependent tumor promoting effect (27). The PPARγ-dependent upregulation of FAO also mediates the pro-tumor (also known as M2-like) polarization of tumor-associated macrophages (TAMs) (52). Tumor infiltrating T cells have also been found to have a progressive loss of PPAR-gamma coactivator 1α (PGC1α), which programs mitochondrial biogenesis, induced by chronic Akt signaling. This results in continuous loss of mitochondrial function and quality of tumor-specific T cells (53). These results provide a possible direction for further research on the role and mechanism of NRSN2-AS1 in HCC tumor immunity.

Conclusions

In this study, we described the influence of sulfatide on lncRNA expression in HCC cells and found that these sulfatide-related lncRNAs serve as a good prognostic marker for HCC patients. In addition, we showed that NRSN2-AS1 may be an indicator of TIME characterization in HCC. These results help to improve the understanding of the comprehensive characteristics and role of sulfatide in the development and progression of HCC and will help to optimize immunotherapy regimens.

Data availability statement

The datasets presented in this study can be found in online repositories. The names of the repository/repositories and accession number(s) can be found below: https://www.ncbi.nlm.nih.gov/geo/, GSE151111.

Author contributionss

The concept of the project was proposed by FF and QC. XH and QC collected the data from the databases and performed data analysis. The MeRIP-seq cell samples were cultured and prepared by LF. XH wrote the manuscript, and QC and FF contributed to editing and participated in manuscript-related discussions. All authors contributed to the article and approved the submitted version.

Funding

This study was supported by the grants from the Project of Shanghai Health Commission (201940069), National Natural Science Foundation of China (82003101) Shanghai Key Laboratory of Molecular Imaging (18DZ2260400).

Acknowledgments

We are sincerely grateful to organizations responsible for generating and maintaining public databases with free access.

Conflict of interest

The authors declare that the research was conducted in the absence of any commercial or financial relationships that could be construed as a potential conflict of interest.

Publisher's note

Supplementary material

The Supplementary Material for this article can be found online at: https://www.frontiersin.org/articles/10.3389/fonc.2023.1091132/full#supplementary-material

References

1. Sung H, Ferlay J, Siegel RL, Laversanne M, Soerjomataram I, Jemal A, et al. Global cancer statistics 2020: GLOBOCAN estimates of incidence and mortality worldwide for 36 cancers in 185 countries. *CA Cancer J Clin* (2021) 71:209–49. doi: 10.3322/caac.21660

2. Dong YW, Wang R, Cai QQ, Qi B, Wu W, Zhang YH, et al. Sulfatide epigenetically regulates miR-223 and promotes the migration of human hepatocellular carcinoma cells. *J Hepatol* (2014) 60:792–801. doi: 10.1016/j.jhep.2013.12.004

3. Arrenberg P, Maricic I, Kumar V. Sulfatide-mediated activation of type II natural killer T cells prevents hepatic ischemic reperfusion injury in mice. *Gastroenterology* (2011) 140:646–55. doi: 10.1053/j.gastro.2010.10.003

4. Takahashi T, Suzuki T. Role of sulfatide in normal and pathological cells and tissues. *J Lipid Res* (2012) 53:1437–50. doi: 10.1194/jlr.R026682

5. Zhong Wu X, Honke K, Long Zhang Y, Liang Zha X, Taniguchi N. Lactosylsulfatide expression in hepatocellular carcinoma cells enhances cell adhesion to vitronectin and intrahepatic metastasis in nude mice. *Int J Cancer* (2004) 110:504–10. doi: 10.1002/ijc.20127

6. Jirasko R, Holcapek M, Khalikova M, Vrana D, Student V, Prouzova Z, et al. MALDI orbitrap mass spectrometry profiling of dysregulated sulfoglycosphingolipids in renal cell carcinoma tissues. *J Am Soc Mass Spectrom* (2017) 28:1562–74. doi: 10.1007/s13361-017-1644-9

7. Tanaka K, Mikami M, Aoki D, Kiguchi K, Ishiwata I, Iwamori M. Expression of sulfatide and sulfated lactosylceramide among histological types of human ovarian carcinomas. *Hum Cell* (2015) 28:37–43. doi: 10.1007/s13577-014-0100-4

8. Jirasko R, Idkowiak J, Wolrab D, Kvasnicka A, Friedecky D, Polanski K, et al. Urine, and tissue profiles of sulfatides and sphingomyelins in patients with renal cell carcinoma. *Cancers (Basel)* (2022) 14(19):4622. doi: 10.3390/cancers14194622

9. Cao Q, Chen X, Wu X, Liao R, Huang P, Tan Y, et al. Inhibition of UGT8 suppresses basal-like breast cancer progression by attenuating sulfatide-alphaVbeta5 axis. *J Exp Med* (2018) 215:1679–92. doi: 10.1084/jem.20172048

10. Kang CL, Qi B, Cai QQ, Fu LS, Yang Y, Tang C, et al. LncRNA AY promotes hepatocellular carcinoma metastasis by stimulating ITGAV transcription. *Theranostics* (2019) 9:4421–36. doi: 10.7150/thno.32854

11. Quinn JJ, Chang HY. Unique features of long non-coding RNA biogenesis and function. *Nat Rev Genet* (2016) 17:47–62. doi: 10.1038/nrg.2015.10

12. Dong RC ZR, Lv FD, Tao FD. Establishment and biological observation of human hepatocellular carcinoma cell line SMMC-7721. *Bull Second Millitary Med Univ* (1980) 1.

13. Chen C, Chen H, Zhang Y, Thomas HR, Frank MH, He Y, et al. TBtools: An integrative toolkit developed for interactive analyses of big biological data. *Mol Plant* (2020) 13:1194–202. doi: 10.1016/j.molp.2020.06.009

14. Goldman MJ, Craft B, Hastie M, Repecka K, McDade F, Kamath A, et al. Visualizing and interpreting cancer genomics data *via* the xena platform. *Nat Biotechnol* (2020) 38:675–8. doi: 10.1038/s41587-020-0546-8

15. Lanczky A, Gyorffy B. Web-based survival analysis tool tailored for medical research (KMplot): Development and implementation. *J Med Internet Res* (2021) 23: e27633. doi: 10.2196/27633

16. Li T, Fu J, Zeng Z, Cohen D, Li J, Chen Q, et al. TIMER2.0 for analysis of tumor-infiltrating immune cells. *Nucleic Acids Res* (2020) 48:W509–14. doi: 10.1093/nar/gkaa407

17. Li T, Fan J, Wang B, Traugh N, Chen Q, Liu JS, et al. TIMER: A web server for comprehensive analysis of tumor-infiltrating immune cells. *Cancer Res* (2017) 77:e108–10. doi: 10.1158/1538-7445.AM2017-108

18. Zeng D, Ye Z, Shen R, Yu G, Wu J, Xiong Y, et al. IOBR: Multi-omics immuno-oncology biological research to decode tumor microenvironment and signatures. *Front Immunol* (2021) 12:687975. doi: 10.3389/fimmu.2021.687975

19. Yang Y, Qian Cai Q, Sheng Fu L, Wei Dong Y, Fan F, Zhong Wu X. Reduced N6-methyladenosine mediated by METTL3 acetylation promotes MTF1 expression and hepatocellular carcinoma cell growth. *Chem Biodivers* (2022) 19(11):e202200333. doi: 10.1002/cbdv.202200333

20. Subramanian A, Tamayo P, Mootha VK, Mukherjee S, Ebert BL, Gillette MA, et al. Gene set enrichment analysis: a knowledge-based approach for interpreting genome-wide expression profiles. *Proc Natl Acad Sci U.S.A.* (2005) 102:15545–50. doi: 10.1073/pnas.0506580102

21. Shen W, Song Z, Zhong X, Huang M, Shen D, Gao P, et al. Sangerbox: A comprehensive, interaction-friendly clinical bioinformatics analysis platform. *iMeta* (2022) 1:e36. doi: 10.1002/imt2.36

22. Chen MH, Fu LS, Zhang F, Yang Y, Wu XZ. LncAY controls BMI1 expression and activates BMI1/Wnt/beta-catenin signaling axis in hepatocellular carcinoma. *Life Sci* (2021) 280:119748. doi: 10.1016/j.lfs.2021.119748

23. Zhao Y, Shi Y, Shen H, Xie W. m(6)A-binding proteins: the emerging crucial performers in epigenetics. *J Hematol Oncol* (2020) 13:35. doi: 10.1186/s13045-020-00872-8

24. Robinson CM, Poon BPK, Kano Y, Pluthero FG, Kahr WHA, Ohh M. A hypoxia-inducible HIF1-GAL3ST1-Sulfatide axis enhances ccRCC immune evasion *via* increased tumor cell-platelet binding. *Mol Cancer Res* (2019) 17:2306–17. doi: 10.1158/1541-7786.MCR-19-0461

25. Marrero I, Ware R, Kumar V. Type II NKT cells in inflammation, autoimmunity, microbial immunity, and cancer. *Front Immunol* (2015) 6:316. doi: 10.3389/fimmu.2015.00316

26. Christofides A, Konstantinidou E, Jani C, Boussiotis VA. The role of peroxisome proliferator-activated receptors (PPAR) in immune responses. *Metabolism* (2021) 114:154338. doi: 10.1016/j.metabol.2020.154338

27. Ercolano G, Gomez-Cadena A, Dumauthioz N, Vanoni G, Kreutzfeldt M, Wyss T, et al. PPAR drives IL-33-dependent ILC2 pro-tumoral functions. *Nat Commun* (2021) 12:2538. doi: 10.1038/s41467-021-22764-2

28. Rebouissou S, Nault JC. Advances in molecular classification and precision oncology in hepatocellular carcinoma. *J Hepatol* (2020) 72:215–29. doi: 10.1016/j.jhep.2019.08.017

29. Shimada S, Mogushi K, Akiyama Y, Furuyama T, Watanabe S, Ogura T, et al. Comprehensive molecular and immunological characterization of hepatocellular carcinoma. *EBioMedicine* (2019) 40:457–70. doi: 10.1016/j.ebiom.2018.12.058

30. Lee SE, Alcedo KP, Kim HJ, Snider NT. Alternative splicing in hepatocellular carcinoma. *Cell Mol Gastroenterol Hepatol* (2020) 10:699–712. doi: 10.1016/j.jcmgh.2020.04.018

31. Chai F, Li Y, Liu K, Li Q, Sun H. Caveolin enhances hepatocellular carcinoma cell metabolism, migration, and invasion *in vitro via* a hexokinase 2-dependent mechanism. *J Cell Physiol* (2019) 234:1937–46. doi: 10.1002/jcp.27074

32. Hernandez S, Simoni-Nieves A, Gerardo-Ramirez M, Torres S, Fucho R, Gonzalez J, et al. GDF11 restricts aberrant lipogenesis and changes in mitochondrial structure and function in human hepatocellular carcinoma cells. *J Cell Physiol* (2021) 236:4076–90. doi: 10.1002/jcp.30151

33. Yang C, Huang X, Liu Z, Qin W, Wang C. Metabolism-associated molecular classification of hepatocellular carcinoma. *Mol Oncol* (2020) 14:896–913. doi: 10.1002/1878-0261.12639

34. Varki A, Cummings RD, Esko JD, Stanley P, Hart GW, Aebi M, et al. *Essentials of glycobiology*. Cold Spring Harbor (NY) (2015).

35. Liu Y, Chen Y, Momin A, Shaner R, Wang E, Bowen NJ, et al. Elevation of sulfatides in ovarian cancer: an integrated transcriptomic and lipidomic analysis including tissue-imaging mass spectrometry. *Mol Cancer* (2010) 9:186. doi: 10.1186/1476-4598-9-186

36. Byrne FL, Olzomer EM, Lolies N, Hoehn KL, Wegner MS. Update on glycosphingolipids abundance in hepatocellular carcinoma. *Int J Mol Sci* (2022) 23 (9):4477. doi: 10.20944/preprints202203.0309.v1

37. Garcia J, Callewaert N, Borsig L. P-selectin mediates metastatic progression through binding to sulfatides on tumor cells. *Glycobiology* (2007) 17:185–96. doi: 10.1093/glycob/cwl059

38. Simonis D, Schlesinger M, Seelandt C, Borsig L, Bendas G. Analysis of SM4 sulfatide as a p-selectin ligand using model membranes. *Biophys Chem* (2010) 150:98–104. doi: 10.1016/j.bpc.2010.01.007

39. Lim LJ, Wong SYS, Huang F, Lim S, Chong SS, Ooi LL, et al. Roles and regulation of long noncoding RNAs in hepatocellular carcinoma. *Cancer Res* (2019) 79:5131–9. doi: 10.1158/0008-5472.CAN-19-0255

40. Wu W, Dong YW, Shi PC, Yu M, Fu D, Zhang CY, et al. Regulation of integrin alphaV subunit expression by sulfatide in hepatocellular carcinoma cells. *J Lipid Res* (2013) 54:936–52. doi: 10.1194/jlr.M031450

41. Dawes AJ, Sacks GD, Needleman J, Brook RH, Mittman BS, Ko CY, et al. Injury-specific variables improve risk adjustment and hospital quality assessment in severe traumatic brain injury. *J Trauma Acute Care Surg* (2019) 87:386–92. doi: 10.1097/TA.0000000000002297

42. Bejani MM, Ghatee M. Theory of adaptive SVD regularization for deep neural networks. *Neural Netw* (2020) 128:33–46. doi: 10.1016/j.neunet.2020.04.021

43. Vidyasagar M. Identifying predictive features in drug response using machine learning: opportunities and challenges. *Annu Rev Pharmacol Toxicol* (2015) 55:15–34. doi: 10.1146/annurev-pharmtox-010814-124502

44. Blomqvist M, Rhost S, Teneberg S, Lofbom L, Osterbye T, Brigl M, et al. Multiple tissue-specific isoforms of sulfatide activate CD1d-restricted type II NKT cells. *Eur J Immunol* (2009) 39:1726–35. doi: 10.1002/eji.200839001

45. Rhost S, Lofbom L, Rynmark BM, Pei B, Mansson JE, Teneberg S, et al. Identification of novel glycolipid ligands activating a sulfatide-reactive, CD1d-restricted, type II natural killer T lymphocyte. *Eur J Immunol* (2012) 42:2851–60. doi: 10.1002/eji.201142350

46. Peng L, Chen Y, Ou Q, Wang X, Tang N. LncRNA MIAT correlates with immune infiltrates and drug reactions in hepatocellular carcinoma. *Int Immunopharmacol* (2020) 89:107071. doi: 10.1016/j.intimp.2020.107071

47. Zhang X, Pan B, Qiu J, Ke X, Shen S, Wang X, et al. lncRNA MIAT targets miR-411-5p/STAT3/PD-L1 axis mediating hepatocellular carcinoma immune response. *Int J Exp Pathol* (2022) 103:102–11. doi: 10.1111/iep.12440

48. Chen Q, Xie J, Yang Y. Long non-coding RNA NRSN2-AS1 facilitates tumorigenesis and progression of ovarian cancer *via* miR-744-5p/PRKX axis. *Biol Reprod* (2022) 106:526–39. doi: 10.1093/biolre/ioab212

49. Xu T, Yan Z, Lu J, Chen L, Li X, Li Y, et al. Long non-coding RNA NRSN2-AS1, transcribed by SOX2, promotes progression of esophageal squamous cell carcinoma by regulating the ubiquitin-degradation of PGK1. *Clin Exp Metastasis* (2022) 39:757–69. doi: 10.1007/s10585-022-10174-7

50. Yin X, Zeng W, Wu B, Wang L, Wang Z, Tian H, et al. PPARalpha inhibition overcomes tumor-derived exosomal lipid-induced dendritic cell dysfunction. *Cell Rep* (2020) 33:108278. doi: 10.1016/j.celrep.2020.108278

51. Wang H, Franco F, Tsui YC, Xie X, Trefny MP, Zappasodi R, et al. CD36-mediated metabolic adaptation supports regulatory T cell survival and function in tumors. *Nat Immunol* (2020) 21:298–308. doi: 10.1038/s41590-019-0589-5

52. Liu S, Zhang H, Li Y, Zhang Y, Bian Y, Zeng Y, et al. S100A4 enhances protumor macrophage polarization by control of PPAR-gamma-dependent induction of fatty acid oxidation. *J Immunother Cancer* (2021) 9(6):e002548. doi: 10.1136/jitc-2021-002548

53. Scharping NE, Menk AV, Moreci RS, Whetstone RD, Dadey RE, Watkins SC, et al. The tumor microenvironment represses T cell mitochondrial biogenesis to drive intratumoral T cell metabolic insufficiency and dysfunction. *Immunity* (2016) 45:374–88. doi: 10.1016/j.immuni.2016.07.009

frontiers | Frontiers in Oncology

TYPE Original Research
PUBLISHED 09 February 2023
DOI 10.3389/fonc.2023.1096351

OPEN ACCESS

EDITED BY
Lujun Shen,
Sun Yat-sen University Cancer Center (SYSUCC), China

REVIEWED BY
Sandra Lettlova,
University of Zurich, Switzerland
Hao Cheng,
Fudan University, China

*CORRESPONDENCE
Jiong Lu
lujiongmail@163.com
Bei Li
libei@scu.edu.cn

†These authors have contributed equally to this work

SPECIALTY SECTION
This article was submitted to Gastrointestinal Cancers: Hepato Pancreatic Biliary Cancers, a section of the journal Frontiers in Oncology

RECEIVED 12 November 2022
ACCEPTED 09 January 2023
PUBLISHED 09 February 2023

CITATION
Nie G, Peng D, Wen N, Wang Y, Lu J and Li B (2023) Cuproptosis-related genes score: A predictor for hepatocellular carcinoma prognosis, immunotherapy efficacy, and metabolic reprogramming. *Front. Oncol.* 13:1096351. doi: 10.3389/fonc.2023.1096351

Cuproptosis-related genes score: A predictor for hepatocellular carcinoma prognosis, immunotherapy efficacy, and metabolic reprogramming

Guilin Nie[1†], Dingzhong Peng[2†], Ningyuan Wen[1], Yaoqun Wang[1], Jiong Lu[1,3*] and Bei Li[1,3*]

[1]Department of Biliary Surgery, West China Hospital of Sichuan University, Chengdu, China, [2]Department of General Surgury, Division of Hepatobiliopancreatic Surgery, Nanfang Hospital, Southern Medical University, Guangzhou, Guangdong, China, [3]Research Center for Biliary Diseases, West China Hospital, Sichuan University, Chengdu, Sichuan, China

Background: Cuproptosis is a newly identified type of programmed cell death, characterized by aggregation of mitochondrial lipoylated proteins and the destabilization of Fe–S cluster proteins triggered by copper. However, its role in hepatocellular carcinoma (HCC) remains unclear.

Methods: We analyzed the expression and prognostic significance of cuproptosis-related genes using the data obtained from TCGA and ICGC datasets. A cuproptosis-related genes (CRG) score was constructed and validated *via* least absolute shrinkage and selection operator (LASSO) Cox regression, multivariate Cox regression and nomogram model. The metabolic features, immune profile and therapy guidance of CRG-classified HCC patients were processed *via* R packages. The role of kidney-type glutaminase (GLS) in cuproptosis and sorafenib treatment has been confirmed *via* GLS knockdown.

Results: The CRG score and its nomogram model performed well in predicting prognosis of HCC patients based on the TCGA cohort (training set), ICGC cohort and GEO cohort (validation set). The risk score was proved as an independent predictor for overall survival (OS) of HCC. The area under the curves (AUCs) of the model in the training and validation cohorts were all around 0.83 (TCGA, 1- year), 0.73 (TCGA, 3- year), 0.92 (ICGC, 1- year), 0.75 (ICGC, 3- year), 0.77 (GEO, 1- year), 0.76(GEO, 3- year). Expression levels of metabolic genes and subtypes of immune cells, and sorafenib sensitiveness varied significantly between the high-CRG group and low-CRG group. One of the model-included gene, GLS, might be involved in the process of cuproptosis and sorafenib treatment in HCC cell line.

Conclusion: The five cuproptosis-related genes model contributed to prognostic prediction and provided a new sight for cuproptosis-related therapy in HCC.

KEYWORDS

cuproptosis, hepatocellular carcinoma, prognostic model, sorafenib, GLS

Introduction

Several types of regulated programmed cell death have been reported, including apoptosis, pyroptosis, necroptosis, and ferroptosis (1). Ferroptosis, a unique modality of cell death driven by iron-dependent phospholipid peroxidation, is regulated by complex cellular metabolic events, including redox homeostasis, iron handling, mitochondrial activity, and amino acids metabolism, lipid metabolism, sugar metabolism, in addition to numerous signaling pathways relevant to disease (2–4). Similar to iron, copper is a cofactor for essential enzymes and has been recognized to induce the aggregation of lipoylated dihydrolipoamide S-acetyltransferase (DLAT) caused by FDX1. Lipoylated DLAT is associated with the mitochondrial tricarboxylic acid (TCA) cycle, resulting in proteotoxic stress and a novel form of cell death called "cuproptosis" (5). In brief, the copper-induced death was independent of known cell death pathway and relied on mitochondrial metabolism. The new mechanistic information suggests that other trace mentalion-induced forms of cell deaths exist (6). Similar to ferroptosis induction-based cancer therapies in nanoparticle-based gene-target therapies or in combination with other therapeutic approaches (7), curoptosis induction-based treatment provides new therapeutic approaches for cancers with the development of curoptosis-related research.

The role of copper in the development of HCC remains unknown. Otherwise, some studies have proved that copper contributes to hepatocarcinogenesis and its progression. Copper contributes to glycolytic metabolism and the tumorigenic properties of hepatocellular carcinoma (HCC) (8). A copper complex, [Cu(ttpy-tpp)Br^2]Br (referred to as CTB), could induce HCC cells senescence and act as an antitumor compound *via* SLC25A26 and methionine cycle (9). Disulfiram combined with copper inhibits metastasis and epithelial-mesenchymal transition in HCC *via* NF-κB and TGF-β pathways (10). The copper metabolism MURR1 domain 10 (COMMD10) increased intracellular Cu and led to radioresistance of HCC (11). In addition, the increased incidence of HCC in patients and animal models with Wilson disease was found to be associtated with an unknown mechanism promoting the malignant process resulting from copper accumulation (12). The emergence of cuproptosis provides new insights into copper-based therapies for HCC.

This study explored the mechanism of copper-induced cell death underlying HCC. We rescreened the genes involved in copper ionophore-induced death. The data was acquired from the genome-wide CRISPR-Cas9 loss-of-function screens dataset provided by Peter Tsvetkov (5). The association between cuproptosis-related genes and HCC prognosis was explored and the genes were used to establish a prognosis-predicted model, which demonstrated potential in grading HCC in terms of copper-induced cell death.

Materials and methods

Public data acquisition and processing

The cuproptosis-related genes datasets were acquired from the Tsvetkov's study. The gene expression data, phenotype data, and corresponding survival information (if available) of HCC of The Cancer Genome Atlas (TCGA), the liver cancer project (code: LIRI_JP) of the International Cancer Genome Consortium (ICGC), and GSE14520 were downloaded from public databases. The single-cell analysis of GLS, FDX1, and CDKN2A in HCC was conducted in the Tumor Immune Single-Cell Hub (TISCH) database (http://tisch.comp-genomics.org/) and used the data from GSE125449. Additional ethical approval was not required since these data were all publicly available online.

Construction and validation of a cuproptosis-related gene model

OVISE cells were used to screen cuproptosis-related genes. The OVISE-Cas9 cells were then infected with Brunello virus obtained from the Brunello virus library, which contains 76411 sgRNAs targeting 19114 genes. After the primary treatment of 50nM elesclomol-Cu, 200nM Cupric diethyldithiocarbamate (Cu-DDC), or DMSO control to the final dose of 250nM elesclomol-Cu and 700nM Cu-DDC, genomic DNA was isolated and sequenced by the Broad Genetic Perturbation Platform and Broad Genomics Platform for the establishment of gene library (5). The different expression genes were computed and considered as cuproptosis-related genes with an FDR < 0.05. 27 genes were possibly involved in copper ionophore-induced cell death and 25 genes expression levels (AFG3L2, AHR, BRPF1, CAPRIN1, CDKN2A, COQ7, DLAT, DLD, EGLN1, FDX1, GLS, HAUS5, LIAS, LIPT1, MBTPS1, MTF1, OXA1L, PDHA1, PDHB, REXO2, RPL3, SCAP, SLFN11, SOX2, YEATS20) except MCUR1 and MPC1 were detected in the TCGA dataset and put into the LASSO regression *via* the algorithm. We utilized the "glmnet" package (version 2.0-16) to fit the logistic LASSO regression. The optimal penalty coefficient ($\lambda = 0.00542$) in the LASSO regression was identified with the minimum criterion and five genes (FDX1, GLS, CDKN2A, DLAT, and LIAS) were found out as independent risk factors for HCC patients. Ten-fold cross-validation was used to select the penalty term, λ. The binomial deviance was computed for the test data as the measure of the predictive performance of the fitted models. The standard errors of the LASSO coefficients were obtained *via* bootstrapping within the primary sampling unit and strata (13). To performed the HRs of related genes, we showed totally ten HRs of genes included in the LASSO regression.

Gene signature model construction and validation of predictive nomogram

Nomograms are widely used to predict the survival probability of cancer. Clinical characteristic parameters and prognostic signature were adopted to establish a nomogram to quantitatively investigate the probability of 1-, 3-, and 5-year survival of HCC patients. To construct the nomogram, multivariate regression analysis was applied to select the significant predictors of mortality. The nomogram was trained using the TCGA data and externally validated using the ICGC data. Discriminative performance was measured by concordance index (C-index). Calibration plots were used to describe the degree of fit between actual and nomogram-predicted mortality (14).

Enrichment analysis

Gene ontology (GO) annotation and Kyoto Encyclopedia of Genes and Genomes (KEGG) pathway enrichment analyses

between the two groups of patients were performed with the 'clusterProfiler' R package. An FDR <0.05 and |log2FC| ≥1 was set as the cut-off values.

Immune profile analysis

The immune score and stromal score of each sample in the TCGA-LIHC cohort were calculated by the "estimate" package in R. The proportion of immune cells in the tumor microenvironment (TME) of each sample was evaluated *via* the TIMER, CIBERSORT, and CIBERSORT-ABS algorithm in R software. The single-sample gene set enrichment analysis (ssGSEA) with R package GSVA was used to elevate the degree of 16 immune cells infiltration and the activity level of 20 immune-related functions in HCC samples. The differential expression of immune checkpoints between risk groups was analyzed *via* R package limma.

In vitro cell culture, maintenance, and transfection

The human HCC cell lines, PLC/PRF/5, and Huh7 were a gift from Professor Peng Yong (State Key Laboratory of Biotherapy, Sichuan University). Both cell lines were incubated at 37°C with 5% CO2 in Dulbecco's Modified Eagle's Media (DMEM) (Gibco BRL, Grand Island, NY, USA) containing 10% FBS (Gibco, Australia). The cells were transfected with si-RNAs using Lipofectamine™ 3000 (Thermo Fisher Scientific, USA) in accordance with the manufacturer's instructions.

RNA preparation, reverse transcription, and quantitative real-time PCR analysis

Total RNA was extracted using TRIzol Reagent (Invitrogen, Carlsbad, USA), and the concentration and purity of total RNA were determined by Nanodrop 2000 spectrophotometry (Thermo Scientific, USA). Reverse transcriptions were performed using Superscript III transcriptase (Invitrogen, Grand Island, NY). The cDNA amplification was performed using SYBR Green Real-time PCR Master Mix (Roche, Mannheim, Germany). 18S was used as the internal reference gene. The results were analyzed by the $2^{-\Delta\Delta Ct}$ method. The primer and si-RNA sequences were as follows: 5'-TTCCAGAAGGCACAGACATGGTTG-3' (forward) and 5'-GCCAGTGTCGCAGCCATCAC-3' (reverse) for GLS, and si-GLS: 5'-GAUGGACAGAGGCAUUCUA-3' (sense).

Western blot analysis

Protein was extracted from HCC cells using RIPA lysis buffer and quantified using a BCA kit (Thermo, USA). The protein samples were separated by 10% SDS–PAGE and transferred to PVDF membranes (Millipore, USA). After blocking for 1 h in 5% skim milk powder at room temperature, the membranes were incubated with primary antibodies at 4°C overnight, followed by an incubation with an anti-rabbit secondary antibody (1:10000, Abcam, UK) and visualized using Immobilon™ Western Chemiluminescent HRP Substrate (Millipore, USA).

CCK8 assay

The effects of drugs and Copper on HCC cell lines were measured using CCK8 assay. Cells were seeded in 96-well plates at a density of 5×10^3 cells/well, cultured overnight, and subsequently treated with various concentrations of drugs or DMSO. A medium containing CCK8 reagent was added after exposing the cells to drugs, and the optical density (OD) value at 450 nm of each well was measured. Sorafenib was purchased from Selleck Chemicals (USA). Elesclomol was obtained from MCE (USA), $CuCl_2$ was from RHAWN (China).

Immunohistochemistry analysis

The protein expression levels of the selected genes in normal and tumor tissues were confirmed by the Human Protein Atlas database (HPA; https://www.proteinatlas.org/). The relative expression levels of GLS were measured *via* Image J (http://rsb.info.nih.gov).

Statistical analysis

R software (version 4.2.1) with the "ggplot2," "ggforest," "cowplot," "plot3D," "maftools," "VennDiagram," "survminer", "timeROC", and "ggplotify" packages, and GraphPad Prism (version 9.0) were used for statistical analysis and data visualization. For comparison between the two groups in the bioinformatics analysis section, the Wilcoxon test was used for difference analysis to compare the risk scores of the two groups. The Students'-test was used to compare between the two groups in the experimental section like PCR or IHC. Two-way ANOVA was used for the results of CCK. As for more than two groups, the Kruskal-Wallis test was used, like comparing the risk scores of the different pathological stages. Kaplan-Meier survival analysis and log-rank tests were used the survival analysis of the different groups of patients. The univariate and multivariate Cox regression with calculation of hazard ratios (HR) and 95% confidence intervals (CI) was used to evaluate the importance of each parameter to OS. The t-ROC analysis measured the predictive power of the risk model and the predictive power was showed as the area under the curve (AUC). A two-tailed p <0.05 was considered statistically significant.

Results

FDX1, GLS, CKKN2A, DLAT, and LIAS were independent prognostic factors for HCC patients

From the whole-genome CRISPR-Cas9 positive selection screen using two copper ionophores (Cu-DDC and elesclomol-copper) (FDR < 0.05),

we identified 27 genes possibly involved in copper ionophore-induced cell death (Figure 1A) and 25 genes were included in a LASSO regression model. The range of positive and negative standard deviations of log(λ) was identified in the cross-validation plot. A vertical line was drawn at the value selected *via* cross-validation analysis of 10-fold. The function of the analysis to select important variables develops with the increased degree of compression and decreased value of λ (13). The optimal penalty coefficient (λ = 0.00542) in the LASSO regression was identified with the minimum criterion (Figure 1B). The results of survival analysis obtained from TCGA and ICGC datasets showed that FDX1, GLS, CDKN2A, DLAT, and LIAS were independent factors for HCC patients and might contribute to predicting the prognosis of HCC. Meanwhile, they were differentially expressed in HCC tumor and normal tissues (Figures 1C, D). In addition, single-cell sequence indicated that all five genes were included in GSE125449 and were predominantly detected in malignant cells (Figures 1E, S1).

High cuproptosis-related genes risk score predicted the poor outcome of HCC patients

A prediction model was constructed based on the patients' data from TCGA using a LASSO regression model and including the above five genes. The cuproptosis-related genes (CRG) risk scores = 0.53*GLS+0.42*DLAT+ 0.505*CDKN2A-0.135*FDX1-0.491*LIAS.

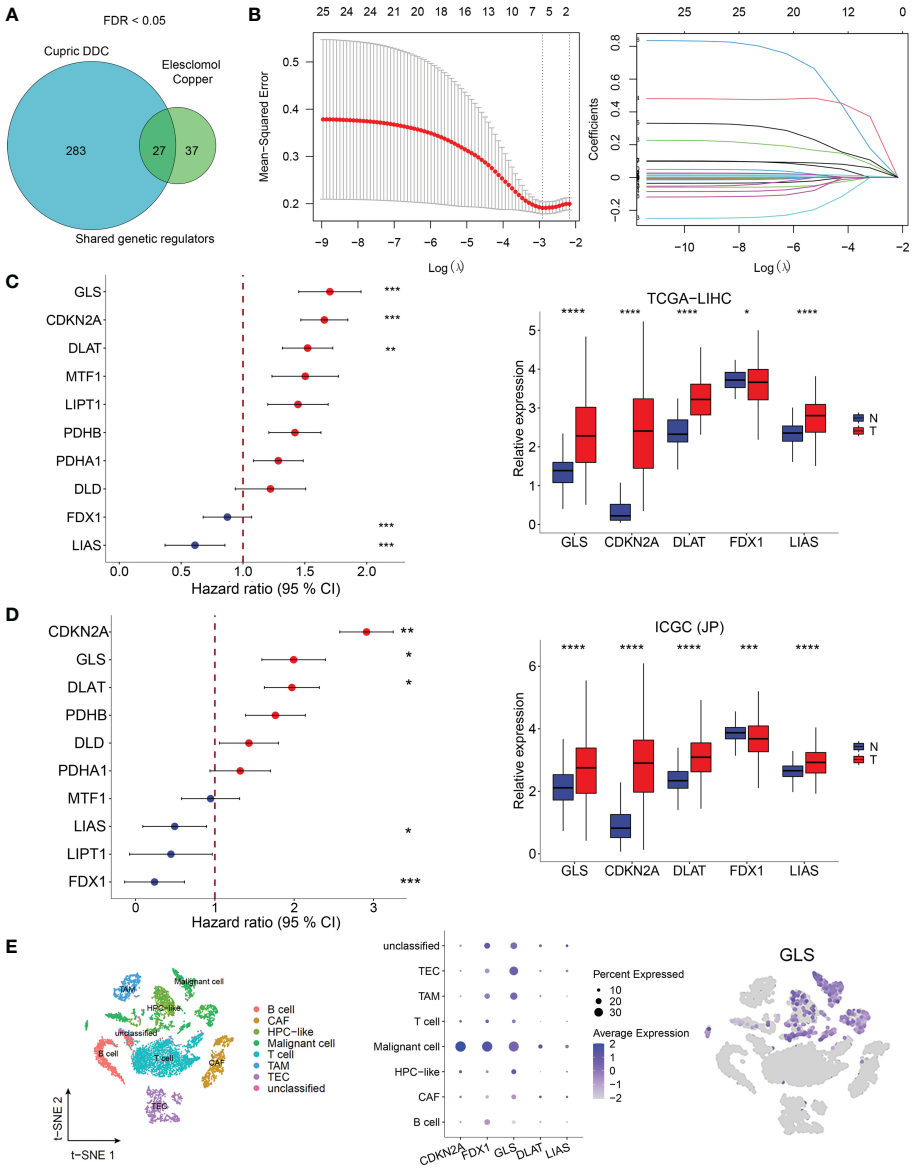

FIGURE 1
Cuproptosis-related genes screening in HCC. **(A)** Identification of cuproptosis-related genes. Whole-genome CRIPSR-Cas9 positive selection screen using two copper ionophores (Cu-DDC and elesclomol-copper). FDR < 0.05. **(B)** Tuning parameter (λ) selection by LASSO Cox regression (left). LASSO coefficient profiles of candidate gene expression (right). Multivariate Cox regression analysis used to screen the independent prognostic genes and relative expression of five genes in normol tissues and HCC tissues in TCGA dataset **(C)** and in ICGC dataset **(D, E)**The expression of CRG-included genes in eight types of cells in the GSE125449 dataset. The left t-SNE subgraph reveals the distribution of eight types of cells from HCC patients (distinguished by colors). The middle showed the relative expression of five genes in eight types of cells. The right subgraph showed the expression of GLS in each cell.

The divided point of high risk and low risk was 4.6 (Figure 2A). The risk score distribution and outcome status showed that more deaths of HCC patients happened in higher risk score groups in our two cohorts (Figure 2B). The high-risk group had a shorter survival time than the low-risk group in the TCGA-LIHC dataset (training cohort, p = 0.033). Similar results were observed in the other two validation cohorts ($p = 8.4x10^{-06}$ in ICGC-JP, p = 0.036 in GSE14520) (Figure 2C). The area under the curve (AUC) of the overall survival (OS) prediction model was 0.83 at one year and 0.73 at three years from TCGA. In the two external validation cohorts, the AUC values of the model in the ICGC-LIRI(JP) dataset were 0.92 at one year and 0.75 at three years, while they were 0.77 at one year and 0.76 at three years in the GSE14520 dataset (Figure 2D).

Development and validation of a comprehensive nomogram based on clinicopathological characteristics and CRG risk score for clinic application

We analyzed the relationship between the model and clinicopathological features of HCC patients. As shown in Figure 3A, age, gender, race, prior malignancy, and radiation therapy were not statistically meaningful for the prediction of prognosis. Otherwise, CRG scores were related to pathologic stage in the TCGA cohort and ICGC cohort (Figures S2A, B). On the other hand, the high score of the CRG model was an independent risk factor of low OS according to the clinical dates from TCGA (HR = 1.5267,

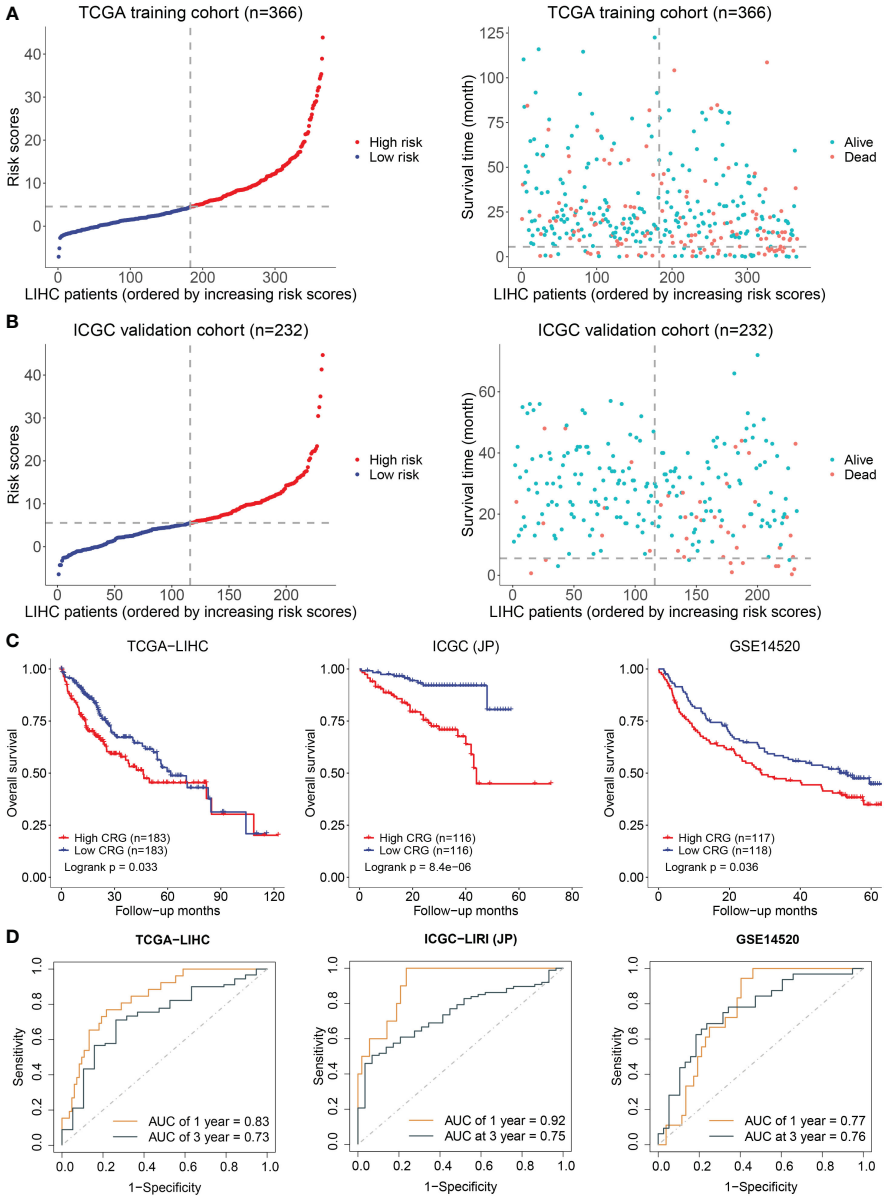

FIGURE 2
Establishment and validation of prediction model. **(A)** The distribution and optimal cutoff value of CRG (left), the OS status of each sample (right) according to TCGA dataset. **(B)** The CRG risk score status (left) and the OS status of each sample (right) according to ICGC dataset. **(C)** The Kaplan–Meier plots of CRG scores in the TCGA, ICGC, and GSE14520 cohorts based on the optimal cutoff value. **(D)** Time-dependent ROC analyses of the CRG for OS prediction in the TCGA, ICGC, and GSE14520 cohorts.

95%CI = 1.0144-2.298, p = 0.04253) (Figure 3A) and ICGC-LIRI(JP) (HR = 3.2132, 95%CI = 1.5607-6.6155, p = 0.00153) (Figure 3B). A nomogram was created to better quantify the predicted value of the risk model for individual HCC patients (Figures 3C, D), and the calibration curves showed the stability and accuracy of the risk model in the training and test cohorts (Figures 3E, F). The C-index was 0.66 in the TCGA group and 0.76 in ICGC-LIRI(JP) group.

The gene signature was closely related to a variety of metabolic characteristics of HCC

Cuproptosis is characterized by the aggregation of lipoylated proteins, which were involved in the process of the TCA cycle occurring in the mitochondria (6). The link between cuproptosis and mitochondrial proteins indicated that the effect of CRG risk score on metabolism in HCC needs to be further clarified. Gene set enrichment analysis (GSEA) based on the TCGA dataset for the two groups showed that HCC patients in the low-CRG group had enrichments in metabolism-related pathways such as pyruvate metabolism, fatty acid metabolism, alanine-aspartate-glutamate metabolism or glutathione metabolism (Figure 4). Specifically, Glutamine is considered as the second important nutrient only to glucose in cancer. Its metabolism begins with the conversion to glutamate by GLS (15). The glutamate could be transferred into mitochondria, transformed to alpha-ketoglutarate and participated in the TCA cycle. As for glutathione (GSH), despite being produced exclusively in the cytosol with the utilization of cysteine, glutamate or glycine, GSH is also abundant in many organelles, including peroxisomes, the nucleus, endoplasmic reticulum and mitochondria (16). The enrichment analysis confirmed that the metabolism-related changes of high-CRG HCC patients centralized in pyrimidine metabolism or purine metabolism. The

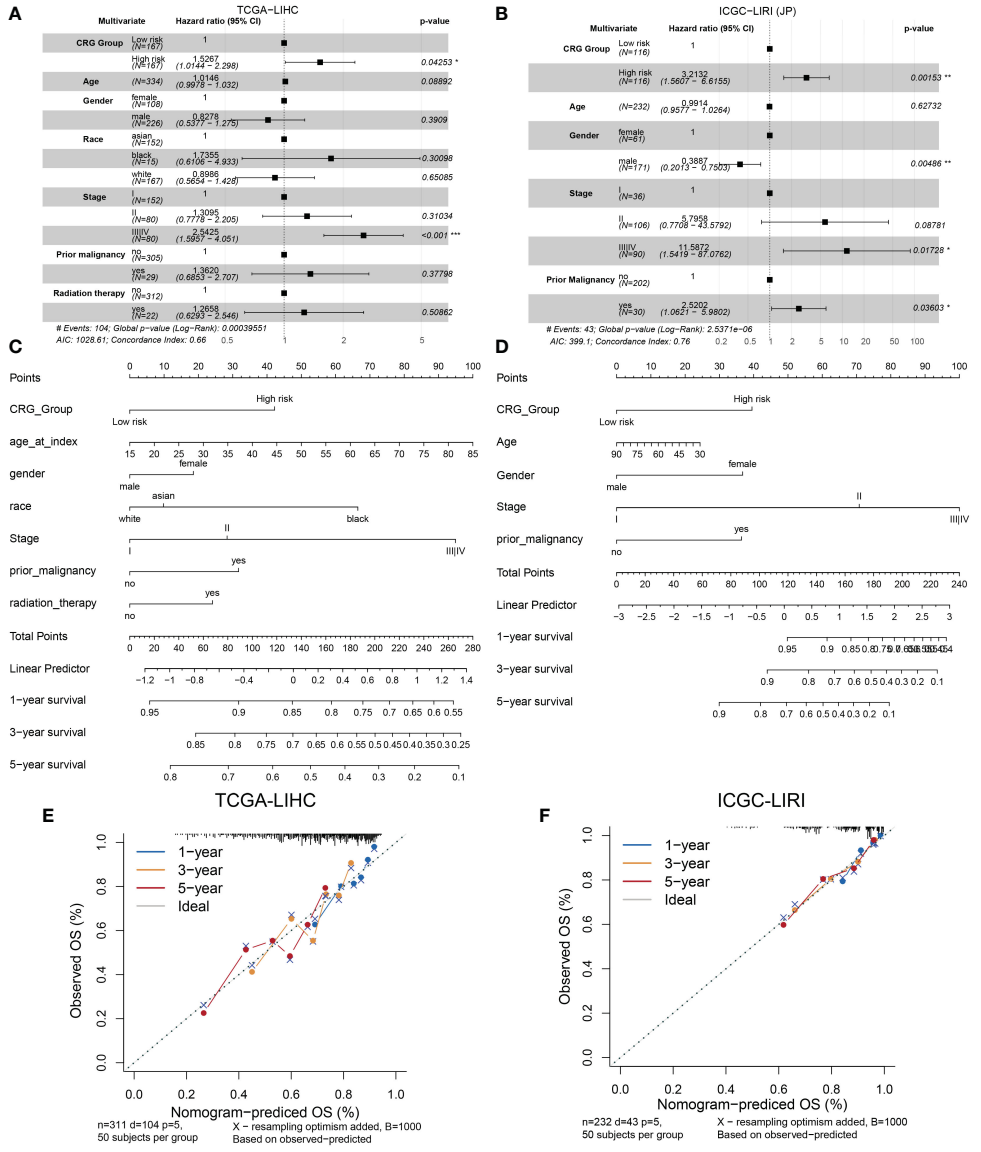

FIGURE 3
Establishment and validation of the model *via* nomogram. **(A)** Multivariate Cox regression analyses of CRG scores for OS in the TCGA cohort. **(B)** the ICGC cohort. **(C)** Nomogram of the clinical characteristic parameters and CRG scores for OS prediction according to the TCGA cohort. **(D)** the ICGC cohort. **(E)** Calibration plots according to the TCGA cohort. **(F)** the ICGC cohort.

pyrimidine metabolism together with purine metabolism, final generates deoxyribonucleoside triphosphates (dNTPs) in the nucleus, cytoplasm and mitochondria for cell proliferation (17) (Figure 4). In our article, we only initially analyzed the varied performance of metabolism-related pathways in two groups. Metabolomics analysis of clinic samples could be used to judge the changes in metabolic substrate and for deeper exploration.

The gene signature served as a valuable marker for immune targets and immunotherapy response

Tumor immunology plays a key role in HCC development and progression (18). We evaluated the immune landscape of CRG and found that high-CRG patients had significantly higher immune scores than low-CRG patients. Besides, using the TIMER algorithm, we initially noticed different scores of macrophages, B cells, CD4+ T cells, and neutrophils in two groups (Figure 5A). According to the results of the CIBERSORT and CIBERSORT-ABS algorithm, more specific features were presented in subtypes of immune cells, such as macrophage M0, M1, and M2 (Figure 5B). Immune infiltration scores of macrophages M0 were higher in the high-risk group in the CIBERSORT, while the other two subtypes showed no statistically significant difference between the two groups. Based on CIBERSORT-ABS, all three subtypes in the high-risk group were higher than the low-risk group ($p < 0.01$) (Figures S3A, B). We performed an ssGSEA analysis to observe immune cell subpopulations, immune functions, and pathways in the high-risk and low-risk groups or risk scores. The results showed that the immune cells including macrophages myeloid DC, Tregs cell, neutrophil and CD4+ Th2 cell were markedly expressed in the high-risk group of the TCGA cohort ($p < 0.05$) (Figure S4). Regarding immune function, the risk levels of lipid mediators, glycogen metabolism, glucose deprivation and TCA cycle were higher in the low-risk group than in the high-risk group, when the functionality of the G1/S and G2/M was opposite to these functions (Figure S5). Immune checkpoints in high- and low-CRG groups relying on TCGA dataset were found to be different, such as BN2A1, BTN2A2, CD276, CD47, CD70, and HLA all highly expressed in high-CRG groups (Figure S6A). Aa for PD-L1, the expression of PD-L1 of high-CRG group was higher in both datasets (Figures S6B, C), which proved the correlation between PD-L1 and cuproptosis.

Sorafenib worked as the first-line treatment for advanced-stage HCC patients (19). Therefore, we evaluated the effect of sorafenib for different CRG risk patients and found that the response of sorafenib treatment followed the relative expression of GLS, DLAT, FDX1, and LIAS and risk scores of CRG (Figures 6A, B) (GSE109211). Patients with a lower score were more sensitive to sorafenib treatment ($p < 0.01$). Similar results were observed in the analysis for transcatheter arterial chemoembolization (TACE) treatment, a widely used therapy for HCC patients at stage BCLC A or B (20). Patients who responded to TACE treatment had significantly variations in expression levels of GLS, CDKN2A, FDX1 and higher values of CRG ($p = 0.0011$) (Figures 6C, D).

GLS was associated with poor prognosis and cuproptosis in HCC

GLS had the highest HR in the multivariate Cox regression analysis and droped our attention. The expression level of GLS was

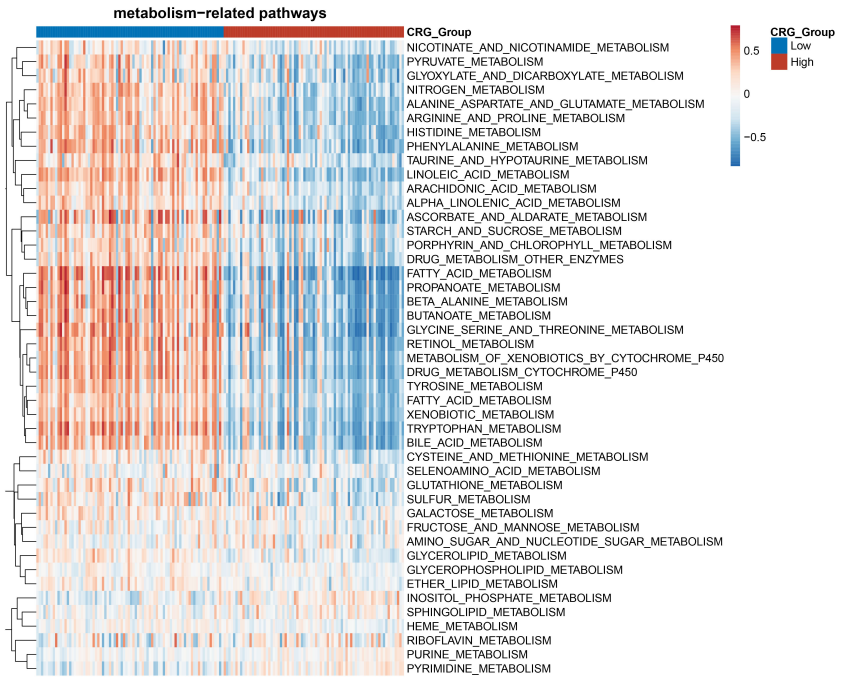

FIGURE 4
Heatmap of the enrichment analysis of metabolism-related pathways in the HCC patients with high- and low- CRG scores.

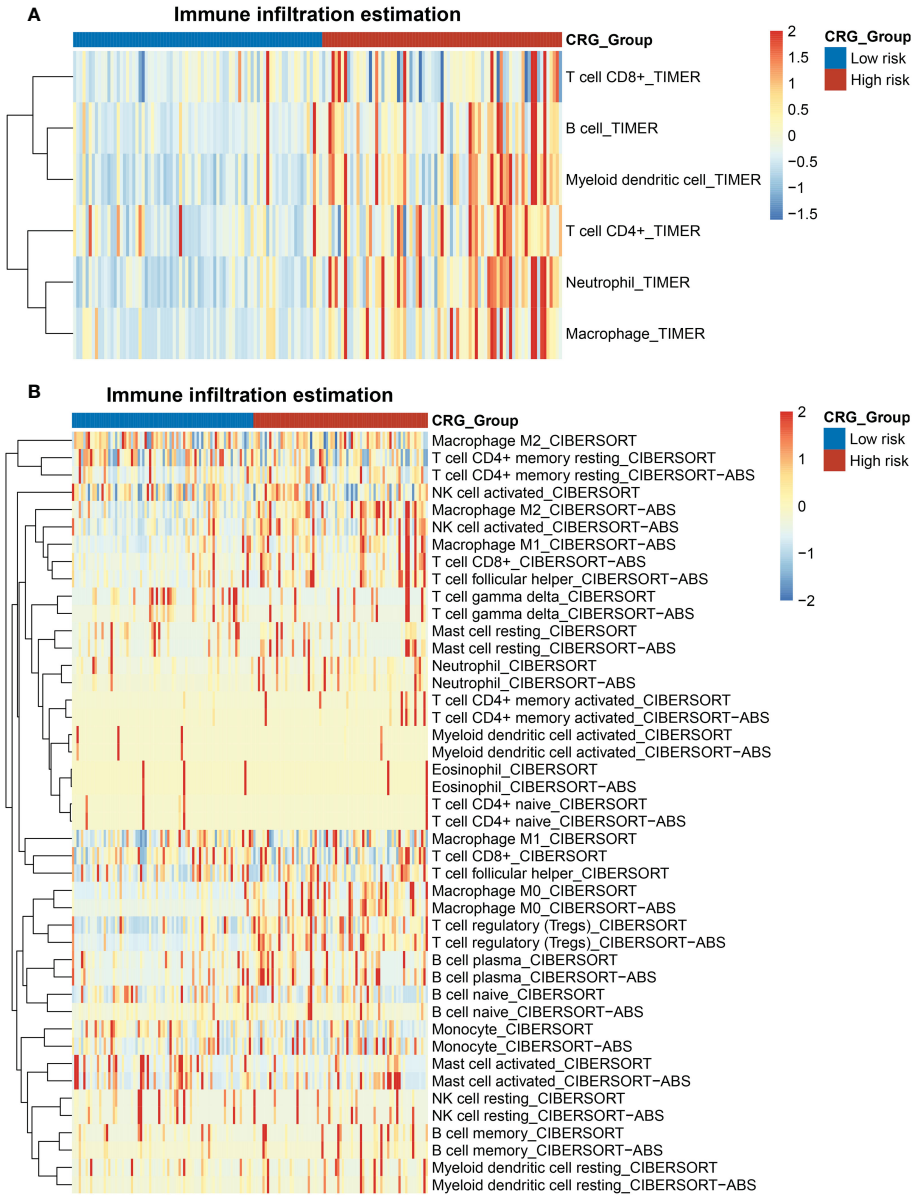

FIGURE 5
Heatmap of the enrichment scores of immune cells in the HCC patients with high- and low- CRG scores. **(A)** TIMER algorithm. **(B)** CIBERSORT and CIBERSORT-ABS algorithm.

related to pathologic stage in the TCGA cohort (Figure S7A). We initially validated the function of $CuCl_2$ in the HCC cell line (PLC and Huh7) related to cuproptosis *via* elesclomol. The results confirmed that the addition of Cu^{2+} enhanced the effect of elesclomol (Figure 7A). The decreased expression of the GLS gene reduced the cell death induced by elesclomol-Cu (Figures 7B, S7B, C). In addition, when the GLS gene was knocked down in PLC and Huh7, they were more sensitive to sorafenib (Figure 7C), corresponding to the previous prediction. The immunohistochemical staining for GLS highlighted its high expression in HCC tissue (Figure 7D). Percentage of positive of HCC group including low positive, positive, high positive, is about 61%. Percentage of positive of non-HCC group is about 24%. After systemically analyzing three databases (Figure 7E), GO analysis showed that they were enriched in actin binding, Ras GTPase binding and so on (Figure 7F). Meanwhile, KEGG analysis indicated that GLS was related to Ras signaling pathway (Figure 7G). In summary, *in vitro*, experimental data suggest that high expression of GLS is related to cuproptosis and poor prognosis in patients with HCC.

Discussion

Traditionally, copper was recognized as an active site cofactor to mediate a variety of essential cellular functions, such as antioxidant defense, biosynthesis of hormones, pigments, neurotransmitters and mitochondrial respiration (21–23). This has been challenged by its newly-discovered role of dynamic signaling metal and metalloallosteric regulator that promote copper-dependent cell proliferation (cuproplasia) and copper-dependent cell death

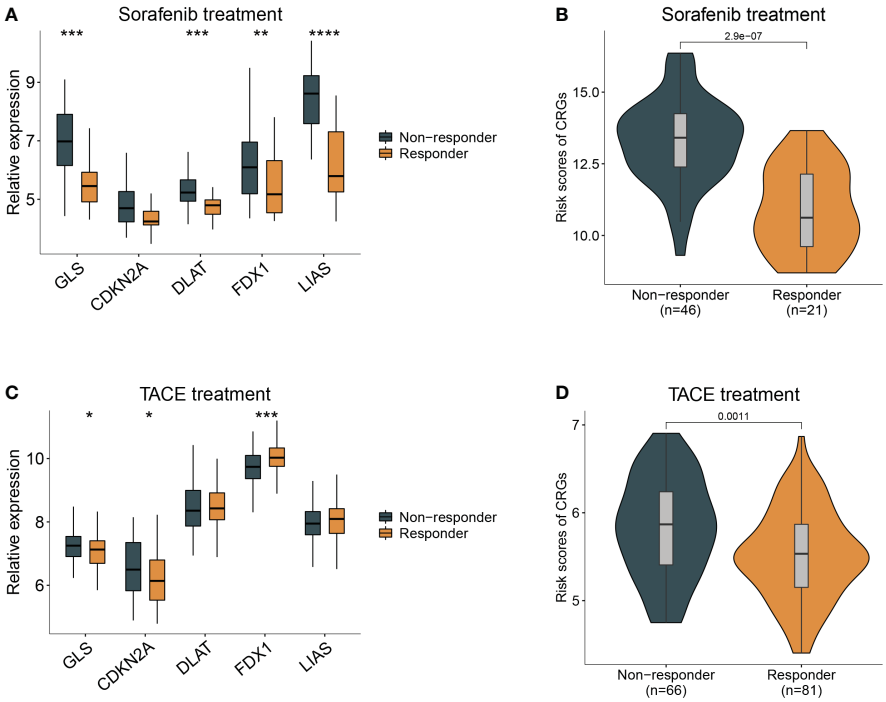

FIGURE 6
Guidance of CRG score in the therapy for HCC patients. **(A)** The different responses to sorafenib in the HCC patients with different expression of cuproptosis-related genes. **(B)**, with high- and low- CRG scores. **(C)** The different responses to TACE treatment in the HCC patients with different expression of cuproptosis-related genes. **(D)**, with high- and low- CRG scores. Wilcoxon test was used for data analyses.

(cuproptosis) (24). According to recent studies, cuproptosis was characterized by the aggregation of mitochondrial lipoylated proteins and the destabilization of Fe–S cluster proteins triggered by copper (6). The liver is a major site of copper storage and removal. Some studies have demonstrated the role of copper in tumorigenesis and the development of HCC (25, 26). The increased incidence of HCC in patients with Wilson disease highlights the unknown mechanism of copper-related malignant transformation (27). In addition, previous studies have established the correlation between serum copper level and overall survival or other prognostic indicators (28, 29). Although decades of studies highlight the interplay between copper and HCC, a systemic molecular explanation of copper does not perform from present researches, and few studies have provided insights into the role of cuproptosis in HCC progression.

Here, we obtained 27 cuproptosis-related genes from a previous study with a FDR score <0.05. The LASSO regression detected that only five (FDX1, GLS, CDKN2A, DLAT, and LIAS) possessed compatible prognostic values considering their expression level and molecular function. The differential expression gene analysis of the TCGA dataset identified all five candidate genes, and FDX1, encoding a small iron-sulfur protein, was recently found to regulate dihydrolipoamide S-acetyltransferase (DLAT) lipoylation and facilitates the oligomerization of lipoylated DLAT (5). The above process attributed to copper-related cell death in a completely different way from apoptosis, pyroptosis, necroptosis, or ferroptosis. GLS encodes a K-type mitochondrial glutaminase, which mainly participates in glutamine metabolism and glutathione (GSH) production (30). GLS could regulate stemness properties of cancer stem cells by increasing ROS accumulation and suppressing the Wnt/β-catenin pathway in HCC (31). CDKN2A (cyclin-dependent kinase inhibitor 2A) is related to three alternatively spliced variants: two kinds of CDK4 kinase or a stabilizer of the tumor suppressor protein p53 (32). CDKN2A was reported to be a tumor suppressor gene. However, it is a highly-expressed gene associated with poor prognosis and immune infiltration in HCC patients (33). As a member of the radical S-adenosylmethionine (SAM), human lipoyl synthase (LIAS) is an enzyme containing two [4Fe–4S] clusters involved in the biosynthesis of the lipoyl cofactor (34). By lipoylation of E2 subunit (dihydrolipoyl succinyltransferase [DLST]) within the mitochondria, LIAS was involved in tricarboxylic acid (TCA) cycle process (35). In addition, the results of the single-cell sequence confirmed that FDX1, GLS, and CDKN2A were predominantly detected in malignant HCC cells, suggesting the involvement of cuproptosis-related genes in the development of HCC.

In the risk genes model, the high-CRG group showed a considerably shorter survival time, and the model performed satisfactorily for prognostic prediction in the training and validation cohorts. The external validation of our model in clinical settings revealed that the prognostic risk score model was an independent prognostic indicator. In addition, a risk-assessment nomogram was used to evaluate the potential clinical application of this model.

We focused on the metabolic and immunological pathways to establish a biological landscape of two groups divided by our five-genes model. The immunologic and metabolic pathways play a leading role in tumorigenesis of HCC, and was chosen as targets of therapeutic researches. Cuproptosis relied on the mitochondrial TCA cycle and was influenced by oxygen concentration (5). The metabolism–related pathways analysis corroborated with previous results. The low-risk group showed

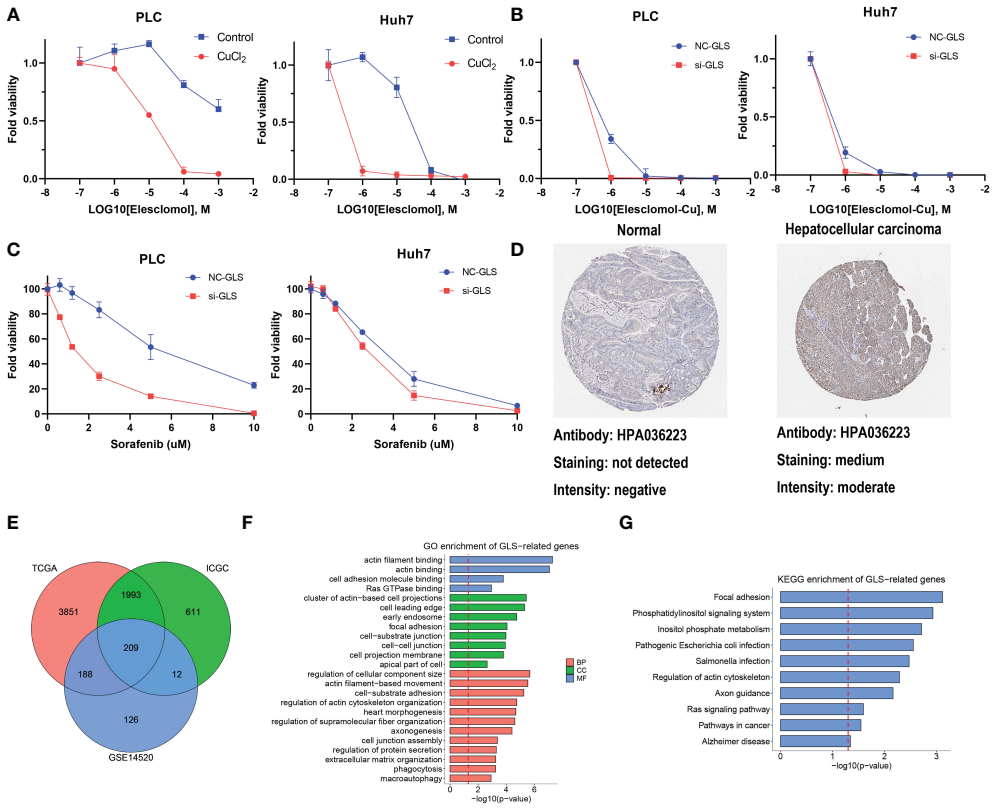

FIGURE 7
The function of GLS in HCC. **(A)** Viability of cells after treatment with elesclomol with or without 1uM of $CuCl_2$. **(B)** Viability of GLS-knockdown or not cells after treatment with elesclomol with 1uM of $CuCl_2$. **(C)** Viability of GLS-knockdown or not cells after treatment with sorafenib. **(D)** The protein expression levels of GLS in Human Protein Atlas database. **(E)** GLS-related genes across TCGA, ICGC and GSE datasets. **(F)** GO enrichment analysis for GLS. **(G)** KEGG pathway enrichment analysis for GLS.

enrichments in mitochondrial metabolism and aerobic glycolysis, such as pyruvate and glutathione metabolism. Otherwise, the low-risk group involved the enrichment of fatty acid metabolism, bile acid metabolism, and amino acid metabolism like alanine, arginine, serine, and glycine, which might be related to oxidative stress. The results of immune infiltration estimation showed the macrophage scores varied in the two groups. The resting macrophages (M0) could be polarized into different phenotypes, pro-inflammatory (M1) or anti-inflammatory (M2) (36). M1 were reported to potentially participate in antitumor immunity. Conversely, M2 could enhance tumor progression by promoting angiogenesis, fibrosis, immunosuppression, lymphocyte exclusion, invasion, and metastasis (37). Nevertheless, how cuproptosis or cuproptosis-inducing drugs affect the function of antitumor immune cells and the metabolic changes remains unclear.

GLS was known as a mitochondrial glutaminase, increasing glutathione and glutamine levels. In a recent study, treatment of HCC cell lines (HCCLM3, SMMC-7721, and Hep3B) with GLS1 inhibitors halted the growth of HCC cell lines (38). As shown in the "Cuproptosis" article, GSH inhibited cuproptosis *via* copper(I), where Chung et al. established the relevance of copper and glutathione in cancer cells. Their work revealed that oncogene-driven changes in the metabolism of glutathione lead to a labile copper(I) deficiency, insinuating that lower GSH/GSSG ratios decreased labile copper(I) availability but did not affect total copper level (39). The theory suggests that copper(I) ion, which is essential for DLAT aggregation and cuproptosis, would prefer forming complexes with "S-ligands" of GSH and protect proteins from copper-induced damage might explain the inhabitation of GSH for cuproptosis (40). In addition, Zuily and collaborators reported that copper toxicity is related to copper-induced protein aggregation, and treatment with copper (I) under anaerobic conditions leads to severe ROS-independent protein aggregation (41). The knockdown of GLS was associated with the exacerbation of copper toxicity with elesclomol. This evidence highlights the role of GLS in HCC copper-related cell death.

Some limitations existed in our study. First, the construction and validation of the prognostic model were based on retrospective public datasets, thus prospective studies are required to verify the accuracy and utility of our model. Second, some environmental and genetic factors closely related to the occurrence of HCC are inevitably missing. Finally, more *in vivo* and *in vitro* experiments regarding the relationships between cuproptosis -related genes and HCC should be further performed.

Conclusion

In conlusion, a novel CRG, based on cuproptosis-related genes, was constructed using the LASSO Cox regression model. HCC patients with a high CRG scores were revealed to be associated with shorter survival time, lower enrichment in metabolic-related pathways, and high infiltration scores of protumor immune cells. In

our model, among all included CRG genes, GLS was marked as a functional gene in the development of HCC, and might be involved in the cuproptosis process in HCC.

Data availability statement

The datasets presented in this study can be found in online repositories. The names of the repository/repositories and accession number(s) can be found in the article/supplementary material.

Author contributions

(i) Conception and design: BL and JL. (ii) Administrative support: BL and JL. (ii) Experiments implementation: DP and NW. (iii) Data analysis and bioinformatics analysis: GN and YW. (iv) Manuscript writing: GN. (v) Final approval of manuscript: All authors. All authors contributed to the article and approved the submitted version.

Funding

Supported by 1·3·5 project for disciplines of excellence–Clinical Research Incubation Project, West China Hospital, Sichuan University (20HXFH021), National Natural Science Foundation of China (Grant No. 82002578).

Conflict of interest

The authors declare that the research was conducted in the absence of any commercial or financial relationships that could be construed as a potential conflict of interest.

Publisher's note

Supplementary material

The Supplementary Material for this article can be found online at: https://www.frontiersin.org/articles/10.3389/fonc.2023.1096351/full#supplementary-material

References

1. Koren E, Fuchs Y. Modes of regulated cell death in cancer. *Cancer Discovery* (2021) 11(2):245–65. doi: 10.1158/2159-8290.Cd-20-0789

2. Jiang X, Stockwell BR, Conrad M. Ferroptosis: Mechanisms, biology and role in disease. *Nat Rev Mol Cell Biol* (2021) 22(4):266–82. doi: 10.1038/s41580-020-00324-8

3. Li D, Li Y. The interaction between ferroptosis and lipid metabolism in cancer. *Signal Transduct Target Ther* (2020) 5(1):108. doi: 10.1038/s41392-020-00216-5

4. Ye Z, Zhuo Q, Hu Q, Xu X, Mengqi L, Zhang Z, et al. Fbw7-Nra41-Scd1 axis synchronously regulates apoptosis and ferroptosis in pancreatic cancer cells. *Redox Biol* (2021) 38:101807. doi: 10.1016/j.redox.2020.101807

5. Tsvetkov P, Coy S, Petrova B, Dreishpoon M, Verma A, Abdusamad M, et al. Copper induces cell death by targeting lipoylated tca cycle proteins. *Science* (2022) 375 (6586):1254–61. doi: 10.1126/science.abf0529

6. Tang D, Chen X, Kroemer G. Cuproptosis: A copper-triggered modality of mitochondrial cell death. *Cell Res* (2022) 32(5):417–8. doi: 10.1038/s41422-022-00653-7

7. Wang Y, Liu T, Li X, Sheng H, Ma X, Hao L. Ferroptosis-inducing nanomedicine for cancer therapy. *Front Pharmacol* (2021) 12:735965. doi: 10.3389/fphar.2021.735965

8. Davis CI, Gu X, Kiefer RM, Ralle M, Gade TP, Brady DC. Altered copper homeostasis underlies sensitivity of hepatocellular carcinoma to copper chelation. *Metallomics* (2020) 12(12):1995–2008. doi: 10.1039/d0mt00156b

9. Jin C, Li Y, Su Y, Guo Z, Wang X, Wang S, et al. Novel copper complex ctb regulates methionine cycle induced tert hypomethylation to promote hcc cells senescence *Via* mitochondrial Slc25a26. *Cell Death Dis* (2020) 11(10):844. doi: 10.1038/s41419-020-03048-x

10. Li Y, Wang LH, Zhang HT, Wang YT, Liu S, Zhou WL, et al. Disulfiram combined with copper inhibits metastasis and epithelial-mesenchymal transition in hepatocellular carcinoma through the nf-κb and tgf-β pathways. *J Cell Mol Med* (2018) 22(1):439–51. doi: 10.1111/jcmm.13334

11. Yang M, Wu X, Hu J, Wang Y, Wang Y, Zhang L, et al. Commd10 inhibits Hif1α/Cp loop to enhance ferroptosis and radiosensitivity by disrupting Cu-fe balance in hepatocellular carcinoma. *J Hepatol* (2022) 76(5):1138–50. doi: 10.1016/j.jhep.2022.01.009

12. Pfeiffenberger J, Mogler C, Gotthardt DN, Schulze-Bergkamen H, Litwin T, Reuner U, et al. Hepatobiliary malignancies in Wilson disease. *Liver Int* (2015) 35(5):1615–22. doi: 10.1111/liv.12727

13. McEligot AJ, Poynor V, Sharma R, Panangadan A. Logistic lasso regression for dietary intakes and breast cancer. *Nutrients* (2020) 12(9):2652. doi: 10.3390/nu12092652

14. Zhang X, Yuan K, Wang H, Gong P, Jiang T, Xie Y, et al. Nomogram to predict mortality of endovascular thrombectomy for ischemic stroke despite successful recanalization. *J Am Heart Assoc* (2020) 9(3):e014899. doi: 10.1161/jaha.119.014899

15. Li Z, Zhang H. Reprogramming of glucose, fatty acid and amino acid metabolism for cancer progression. *Cell Mol Life Sci* (2016) 73(2):377–92. doi: 10.1007/s00018-015-2070-4

16. Wang Y, Yen FS, Zhu XG, Timson RC, Weber R, Xing C, et al. Slc25a39 is necessary for mitochondrial glutathione import in mammalian cells. *Nature* (2021) 599 (7883):136–40. doi: 10.1038/s41586-021-04025-w

17. Siddiqui A, Ceppi P. A non-proliferative role of pyrimidine metabolism in cancer. *Mol Metab* (2020) 35:100962. doi: 10.1016/j.molmet.2020.02.005

18. Ringelhan M, Pfister D, O'Connor T, Pikarsky E, Heikenwalder M. The immunology of hepatocellular carcinoma. *Nat Immunol* (2018) 19(3):222–32. doi: 10.1038/s41590-018-0044-z

19. Tang W, Chen Z, Zhang W, Cheng Y, Zhang B, Wu F, et al. The mechanisms of sorafenib resistance in hepatocellular carcinoma: Theoretical basis and therapeutic aspects. *Signal Transduct Target Ther* (2020) 5(1):87. doi: 10.1038/s41392-020-0187-x

20. Tsurusaki M, Murakami T. Surgical and locoregional therapy of hcc: Tace. *Liver Cancer* (2015) 4(3):165–75. doi: 10.1159/000367739

21. Solomon EI, Sundaram UM, Machonkin TE. Multicopper oxidases and oxygenases. *Chem Rev* (1996) 96(7):2563–606. doi: 10.1021/cr950046o

22. Que EL, Domaille DW, Chang CJ. Metals in neurobiology: Probing their chemistry and biology with molecular imaging. *Chem Rev* (2008) 108(5):1517–49. doi: 10.1021/cr078203u

23. Chang CJ. Searching for harmony in transition-metal signaling. *Nat Chem Biol* (2015) 11(10):744–7. doi: 10.1038/nchembio.1913

24. Ge EJ, Bush AI, Casini A, Cobine PA, Cross JR, DeNicola GM, et al. Connecting copper and cancer: From transition metal signalling to metalloplasia. *Nat Rev Cancer* (2022) 22(2):102–13. doi: 10.1038/s41568-021-00417-2

25. Ren X, Li Y, Zhou Y, Hu W, Yang C, Jing Q, et al. Overcoming the compensatory elevation of Nrf2 renders hepatocellular carcinoma cells more vulnerable to Disulfiram/Copper-induced ferroptosis. *Redox Biol* (2021) 46:102122. doi: 10.1016/j.redox.2021.102122

26. Wachsmann J, Peng F. Molecular imaging and therapy targeting copper metabolism in hepatocellular carcinoma. *World J Gastroenterol* (2016) 22(1):221–31. doi: 10.3748/wjg.v22.i1.221

27. Aggarwal A, Bhatt M. Advances in treatment of Wilson disease. *Tremor Other Hyperkinet Mov (N Y)* (2018) 8:525. doi: 10.7916/d841881d

28. Fang AP, Chen PY, Wang XY, Liu ZY, Zhang DM, Luo Y, et al. Serum copper and zinc levels at diagnosis and hepatocellular carcinoma survival in the guangdong liver cancer cohort. *Int J Cancer* (2019) 144(11):2823–32. doi: 10.1002/ijc.31991

29. Tamai Y, Iwasa M, Eguchi A, Shigefuku R, Sugimoto K, Hasegawa H, et al. Serum copper, zinc and metallothionein serve as potential biomarkers for hepatocellular carcinoma. *PloS One* (2020) 15(8):e0237370. doi: 10.1371/journal.pone.0237370

30. Mukha A, Kahya U, Linge A, Chen O, Löck S, Lukiyanchuk V, et al. Gls-driven glutamine catabolism contributes to prostate cancer radiosensitivity by regulating the redox state, stemness and Atg5-mediated autophagy. *Theranostics* (2021) 11(16):7844–68. doi: 10.7150/thno.58655

31. Li B, Cao Y, Meng G, Qian L, Xu T, Yan C, et al. Targeting glutaminase 1 attenuates stemness properties in hepatocellular carcinoma by increasing reactive oxygen species and suppressing Wnt/Beta-catenin pathway. *EBioMedicine* (2019) 39:239–54. doi: 10.1016/j.ebiom.2018.11.063

32. Foulkes WD, Flanders TY, Pollock PM, Hayward NK. The Cdkn2a (P16) gene and human cancer. *Mol Med* (1997) 3(1):5–20.

33. Luo JP, Wang J, Huang JH. Cdkn2a is a prognostic biomarker and correlated with immune infiltrates in hepatocellular carcinoma. *Biosci Rep* (2021) 41(10):BSR20211103. doi: 10.1042/bsr20211103

34. Saudino G, Ciofi-Baffoni S, Banci L. Protein-interaction affinity gradient drives [4fe-4s] cluster insertion in human lipoyl synthase. *J Am Chem Soc* (2022) 144(13):5713–7. doi: 10.1021/jacs.1c13626

35. Burr SP, Costa AS, Grice GL, Timms RT, Lobb IT, Freisinger P, et al. Mitochondrial protein lipoylation and the 2-oxoglutarate dehydrogenase complex controls Hif1α stability in aerobic conditions. *Cell Metab* (2016) 24(5):740–52. doi: 10.1016/j.cmet.2016.09.015

36. Miao X, Leng X, Zhang Q. The current state of nanoparticle-induced macrophage polarization and reprogramming research. *Int J Mol Sci* (2017) 18(2):336. doi: 10.3390/ijms18020336

37. Italiani P, Boraschi D. From monocytes to M1/M2 macrophages: Phenotypical vs. *Funct Differentiation. Front Immunol* (2014) 5:514. doi: 10.3389/fimmu.2014.00514

38. Wang D, Meng G, Zheng M, Zhang Y, Chen A, Wu J, et al. The glutaminase-1 inhibitor 968 enhances dihydroartemisinin-mediated antitumor efficacy in hepatocellular carcinoma cells. *PloS One* (2016) 11(11):e0166423. doi: 10.1371/journal.pone.0166423

39. Chung CY, Posimo JM, Lee S, Tsang T, Davis JM, Brady DC, et al. Activity-based ratiometric fret probe reveals oncogene-driven changes in labile copper pools induced by altered glutathione metabolism. *Proc Natl Acad Sci U.S.A.* (2019) 116(37):18285–94. doi: 10.1073/pnas.1904610116

40. Kardos J, Héja L, Simon Á, Jablonkai I, Kovács R, Jemnitz K. Copper signalling: Causes and consequences. *Cell Commun Signal* (2018) 16(1):71. doi: 10.1186/s12964-018-0277-3

41. Zuily L, Lahrach N, Fassler R, Genest O, Faller P, Sénèque O, et al. Copper induces protein aggregation, a toxic process compensated by molecular chaperones. *mBio* (2022) 13(2):e0325121. doi: 10.1128/mbio.03251-21

frontiers | Frontiers in Oncology

TYPE Original Research
PUBLISHED 20 February 2023
DOI 10.3389/fonc.2023.1131892

OPEN ACCESS

EDITED BY
Lujun Shen,
Sun Yat-sen University Cancer Center (SYSUCC), China

REVIEWED BY
Jing Zhao,
Brigham and Women's Hospital and Harvard Medical School, United States
Hongwei Cheng,
Xiamen University, China
Mengqian Li,
Kyoto University, Japan

*CORRESPONDENCE
Yu Zhang
zhangyu199831@163.com
Zheping Fang
fangzp@enzemed.com
Shaowei Li
li_shaowei81@hotmail.com

†These authors have contributed equally to this work

SPECIALTY SECTION
This article was submitted to Gastrointestinal Cancers: Hepato Pancreatic Biliary Cancers, a section of the journal Frontiers in Oncology

RECEIVED 26 December 2022
ACCEPTED 07 February 2023
PUBLISHED 20 February 2023

CITATION
Liu L, Wang Q, Zhao X, Huang Y, Feng Y, Zhang Y, Fang Z and Li S (2023) Establishment and validation of nomogram model for the diagnosis of AFP-negative hepatocellular carcinoma. *Front. Oncol.* 13:1131892. doi: 10.3389/fonc.2023.1131892

Establishment and validation of nomogram model for the diagnosis of AFP-negative hepatocellular carcinoma

Long Liu[1†], Qi Wang[2†], Xiaohong Zhao[3], Yuxi Huang[2], Yuyi Feng[5], Yu Zhang[4*], Zheping Fang[1,2*] and Shaowei Li[5*]

[1]Department of Hepatobiliary Surgery, Taizhou Hospital of Zhejiang Province, Zhejiang University, Linhai, Zhejiang, China, [2]Department of Hepatobiliary Surgery, Taizhou Hospital of Zhejiang Province, Wenzhou Medical University, Linhai, Zhejiang, China, [3]Department of Pharmacy, Taizhou Hospital of Zhejiang Province, Zhejiang University, Linhai, Zhejiang, China, [4]Department of Oncology, The First Hospital of the University of Science and Technology of China, Hefei, Anhui, China, [5]Department of Gastroenterology, Taizhou Hospital of Zhejiang Province, Linhai, Zhejiang, China

Introduction: As one of the most common malignant tumors in clinical practice, hepatocellular carcinoma (HCC) is a major threat to human health, where alpha-fetoprotein (AFP) is widely used for early screening and diagnoses. However, the level of AFP would not elevate in about 30-40% of HCC patients, which is clinically referred to as AFP-negative HCC, with small tumors at an early stage and atypical imaging features, making it difficult to distinguish benign from malignant by imaging alone.

Methods: A total of 798 patients, with the majority being HBV-positive, were enrolled in the study and were randomized 2:1 to the training and validation groups. Univariate and multivariate binary logistic regression analyses were used to determine the ability of each parameter to predict HCC. A nomogram model was constructed based on the independent predictors.

Results: A unordered multicategorical logistic regression analyses showed that the age, TBIL, ALT, ALB, PT, GGT and GPR help identify non-hepatic disease, hepatitis, cirrhosis, and hepatocellular carcinoma. A multivariate logistic regression analyses showed that the gender, age, TBIL, GAR, and GPR were independent predictors for the diagnosis of AFP-negative HCC. And an efficient and reliable nomogram model (AUC=0.837) was constructed based on independent predictors.

Discussion: Serum parameters help reveal intrinsic differences between non-hepatic disease, hepatitis, cirrhosis, and HCC. The nomogram based on clinical and serum parameters could be used as a marker for the diagnosis of AFP-negative HCC, providing an objective basis for the early diagnosis and individualized treatment of hepatocellular carcinoma patients.

KEYWORDS

alpha-fetoprotein, AFP-NHCC, nomogram model, early diagnosis, marker

Introduction

Liver cancer is one of the most common malignancies in clinical practice and is a major threat to human health. According to statistics, in 2023, liver cancer became the sixth-most common cancer worldwide and more than 900,000 new cases every year, besides, it is also the third leading cause of cancer-related death (1). In China, the occurrence of liver cancer accounts for half of the global value, with a high incidence and mortality rate (2). According to the pathological type, primary HCC can be divided into HCC, cholangiocellular carcinoma, and mixed HCC accounting for about 91.5% of cases. It is therefore necessary to accurately diagnose and treat HCC.

The levels of AFP, a 70-KD glycoprotein, decline rapidly after birth and remain low throughout the lifespan in normal physiology (3).In the 1960s, alpha-fetoprotein (AFP) was first used for the diagnosis and treatment of HCC (4). Roughly 30% to 40% of all patients with HCC will have negative serum levels of AFP, and 15% to 30% of patients with advanced HCC will initially have elevated serum AFP levels that subsequently return to normal values (5, 6). These factors make the diagnosis of HCC difficult, especially in cases of AFP-negative HCC, so there is an urgent need for more efficient diagnostic indicators to assist in the diagnosis of AFP-negative HCC in clinical practice. Generally, the early screening and diagnosis of AFP-negative HCC patients tend to rely heavily on imaging examinations, such as ultrasound, computed tomography (CT), and magnetic resonance imaging (MRI). Unfortunately, most AFP-negative HCC patients have small tumors at an early stage with atypical imaging features, making it difficult to distinguish benign and malignant nodules by relying on imaging examinations alone. further complicating matters is the fact that AFP-negative HCC lacks ideal biomarkers. Therefore, the misdiagnosis and underdiagnosis rates of AFP-negative HCC are both high (7).

And more importantly, diagnosis of AFP-negative HCC is meanful for clinical practice because the prognosis of these patients is poor than that of AFP-positive patients for poorly differentiated and rapid malignant progression (8–10),therefor, the clinical diagnosis of AFP-negative HCC has become an urgent issue hindering the early treatment and improved prognosis of HCC in general, so we urgently need to find new serum biomarkers other than AFP to facilitate early screening and the early diagnosis of AFP-negative HCC (11). At present, Serum biomarkers are non-invasive, convenient, economical, and reproducible diagnostic tools for oncology with accurate and repeatable measurements and a comparatively fast clinical turnaround time for detecting disease progression. In recent years, with the continuous development of technology, more and more serum biomarkers are used to diagnose AFP-negative HCC. For example, the microRNA miR-21 has higher serum values in patients with HCC compared with healthy subjects, and its positive rate in the AFP-negative HCC group was 77.6%, with a sensitivity of 81.2% and specificity of 83.2% (12). Vitamin K-deficient prothrombin II (PIVKA-II), which is significantly more strongly expressed in early HCC than in chronic hepatitis B, has a sensitivity of 76.3% and a specificity of 89.1% for the diagnosis of AFP-negative HCC, besides, PIVKA-II levels were associated with poor prognosis (13, 14). High-sensitivity AFP-L3%, with a sensitivity of 41.5% and a specificity of 85.1% for the diagnosis of AFP-negative HCC, and its combination with PIVKA-II can effectively improve the diagnostic value of AFP-negative HCC, and in the AFP-negative HCC group, the positive rate of these markers combined to detect early HCC was 81.8%, that to detect small HCC was 86.7%, and that to detect single tumors was 91.7% (15, 16). In addition, it has also been reported that circulating hematopoietic stem cells and cancer stem cells exploring new ideas for the diagnosis of liver cancer (17). Besides, independ on AFP, some other indicators shown outstanding diagnostic value, for example, STC2 was upregulated in both tumors and serum of HCC patients, and has good diagnostic significance and could be used as a co-biomarker for AFP to detect early HCC (18). the positive predictive value (PPV) of APEX1 was significantly higher than that of AFP (67.91% *vs*. 55.22%), and is a better biomarker for HCC diagnosis and prognosis than alpha-fetoprotein (19). However, while these new biomarkers are effective in diagnosing AFP-negative HCC, their expense and complexity make them difficult to employ in clinical practice on a large scale.

In contrast, routine serum tests supply a large source of data containing a great deal of disease-associated information that can provide diagnostic and prognostic decisions for diseases. For example, routine laboratory tests, such as evaluations of serum Prealbumin (PAB), a sensitive indicator of liver impairment and function (20), D-dime r(21), and γ-glutamine transpeptidase (GGT),a surface enzyme involved in glutathione metabolism, (22) and transaminases(ALT/AST) reflected damage of hepatocytes (23) are valuable for the diagnosis of AFP-negative HCC (20, 24). Besides, Due to the lack of diagnostic sensitivity and specificity of a single biomarker for AFP-negative HCC, combinations of multiple biomarkers are often used to effectively improve diagnostic efficiency. Huang et al. found that the fibrinogen/PA ratio and GGT/platelet ratio were much more powerful for the detection of AFP-negative HCC in combination than when applied alone (25). Several studies thus far have investigated the value of inflammatory response markers in the prognosis of HCC, but information on the diagnostic value in patients with AFP-negative HCC is lacking. These drove us to think about whether new meaningful findings could be obtained from the existing examination results. In the present study, we explored the diagnosis of AFP-negative HCC using conventional laboratory examination data in combination with several biomarkers, focusing on γ-glutamine aminotransferase-to-PA ratio (GPR) and γ-glutamine aminotransferase-to-glutathione aminotransferase (GAR), and clinicopathological indicators to assess their feasibility as predictive markers for patients with AFP-negative HCC.

Materials and methods

Collection of clinical specimens

This study collected and retrospectively analyzed 597 patients diagnosed with viral hepatitis B-associated liver disease in Taizhou Hospital, Zhejiang Province between January 2015 and December

2020, including 193 patients (32.3%) in the liver cancer group, 200 patients (33.5%) in the cirrhosis group, and 204 patients (34.2%) in the hepatitis group. In addition, 201 patients who visited the health checkup center during this period but did not suffer from hepatitis B viral hepatitis-associated liver disease were collected, and this group of patients was considered the healthy subject group.

1. Diagnostic criteria for HBV positive hepatitis: (1) positive HBsAg, or abnormal liver biochemistry (predominantly elevated serum alanine aminotransferase (ALT) and aspartate aminotransferase (AST)(WS 299-2008)

2. Diagnostic criteria for cirrhosis: (1) liver histopathology shows diffuse liver fibrosis and pseudolobular formation, (2) if liver histopathological examination is not performed, meet more than 2 of the following 5 and exclude non-cirrhotic portal hypertension can be clinically diagnosed as cirrhosis: (1) gastroscopy shows esophageal and gastric varices; (2) Imaging examination: ultrasound, CT or MRI have imaging features of cirrhosis; (3) Liver elasticity determination: LSM> 13kPa; (4) Decreased liver synthetic function: decreased serum albumin, prothrombin time prolonged; (5) Hypersplenism: platelets, white blood cells or hemoglobin decreased.(2019 Chinese Medical Association Hepatology Branch)

3. Diagnostic criteria for AFP-negative HCC: (1) all patients in the current study had serum AFP <10 ng/ml and were considered AFP-negative. (2) HCC patients were newly diagnosed with HCC, by pathological tests after hepatectomy or liver puncture tissue(26).

The exclusion criteria were as follows: (1) With other digestive system diseases; (2) Those with malignant tumors other than HCC; (3) with hematological or immune-related diseases; (4) recurrence of HCC after the first treatment (including surgical resection, radiofrequency ablation, etc.); (5) cases with incomplete data or missing data.

Data acquisition

This was a retrospective clinical study, and all data were obtained from the electronic medical records of patients in Taizhou Hospital. Collected data included the gender, age, AFP, total bilirubin (TBIL), alanine transaminase (ALT), glutathione transaminase (AST), albumin (ALB), prothrombin time (PT), GGT, and PA values. The tumor size and number were determined by postoperative pathological tests. The liver function was assessed according to the Child-Pugh score standard. CNLC (China liver cancer staging) staging was performed for patients with HCC according to the "Diagnostic and treatment protocol for primary liver cancer (2019 edition) (27). The GPR value was calculated as GGT/PA, and the GAR value was calculated as GGT/AST, and most patients with hepatitis, cirrhosis and liver cancer were HBV-positive.

Statistical analyses

The SPSS 27.0 (SPSS for Windows, version 22.0; SPSS, Inc. Chicago, IL, USA) and R4.1.0(MathSoft.USA) software programs were used for analyses and data processing. (1) Spearman's correlation analysis was used to test the correlation between parameters, and redundant parameters with autocorrelation coefficients >0.7 were excluded. (2) Numerical variables that obeyed a normal distribution were statistically described as the mean ± standard deviation, and a t-test was used for comparisons between two groups, while an analysis of variance was used for comparisons among three or more groups. Non-normally distributed numerical variables were described as the median (interquartile spacing), and the comparisons between two groups was performed by Mann-Whitney U test, while comparisons among three or more groups was performed by Kruskal-Wallis H test. Categorical variables were analyzed using the chi-square test or Fisher exact test.(3) Unordered multicategorical logistic regression analyses were used to further analyze the efficacy of each parameter in identifying patients with non-hepatic and digestive disease, hepatitis, cirrhosis, and HCC. (4) Univariate and multivariate binary logistic regression analyses were used to determine the ability of each parameter to predict HCC. A nomogram model was constructed using by R4.1.0 (rms package) based on the independent predictors from the multivariate logistic regression analyses. (5) The Hosmer-Lemeshow test, calibration curve, decision curve, clinical impact curve, receiver operating characteristic (ROC) curve, and its area under curve (AUC) were used to verify the fit, stability and clinical value of the model. (6) Finally, the model was tested internally using 10-fold cross-validation and brought into the validation group for external testing.

Results

General clinical characteristics of 798 patients

According to the inclusion and exclusion criteria, a total of 798 patients were included in the study, including 193 patients (24.19%) in the liver cancer group, 200 (25.06%) in the cirrhosis group, 204 (25.56%) in the hepatitis group, and 201 (25.19%) in the healthy group. There was no significant difference in the general clinical information between the training group validation groups (P>0.05), indicating that the grouping was randomized and reasonable. More baseline information is shown in Table 1.

Efficacy of serum parameters to discriminate patients with non-liver disease, hepatitis, cirrhosis, and liver cancer

Spearman's correlation analysis showed that the autocorrelation coefficients of ALT and AST, ALB, and PA were all >0.7, so the redundant parameters AST and PA, which had poor discriminatory ability, were excluded. A univariate analysis showed that the gender, age, TBIL, ALT, PT, GGT, ALB, GPR, and GAR values had group

TABLE 1 General clinical characteristics of 798 patients.

Characteristics	Primary Cohort				Validation Cohort				*P value*
	HP (n=129)	CH (n=133)	LC (n=136)	HCC (n=134)	HP (n=64)	CH (n=66)	LC (n=69)	HCC (n=67)	
Gender(male/ female**)**	60/74	96/40	86/47	96/33	29/38	48/21	43/23	48/16	0.938
Age	61(51, 66)	46(39, 54)	58(53, 65)	59(52, 65)	64(51, 72)	49(38, 57)	56(48, 65)	58(50, 66)	0.517
TBIL(μmol/L)	14.9(11.0, 18.8)	14.1(10.5, 17.7)	27.3(16.3, 60.8)	14.5(11.4, 18.8)	14.2(10.6, 18.0)	13.4(10.1, 19.5)	27.1(15.8, 49.6)	13.7(9.6, 17.1)	0.334
ALT(U/L)	20.0(13.8, 26.0)	65.0(27.0, 195, 3)	23.0(17.0, 33.0)	28.0(20.0, 45.0)	18.0(12.0, 25.0)	49.0(21.5, 199.5)	26.0(17.0, 36.0)	27.5(20.0, 43.5)	0.175
AST(U/L)	23.0(20.0, 29.0)	44.5(26.0, 96.0)	36.0(27.0, 56.0)	32.0(25.0, 48.0)	23.0(20.0, 27.0)	38.0(24.0, 90.0)	42.5(26.8, 55.3)	32.5(24.0, 43.0)	0.341
ALB(g/L)	44.9(41.6, 47.1)	42.3(38.9, 45.5)	30.4(25.7, 38.0)	39.8(37.0, 44.1)	44.4(41.2, 47.2)	41.5(39.6, 44.8)	31.7(25.9, 39.5)	39.9(36.9, 43.0)	0.664
PT(s)	13.2(12.3, 13.6)	14.3(13.6, 14.7)	16.6(14.6, 19.9)	14.0(13.3, 14.7)	13.2(11.8, 14.0)	14.3(13.5, 14.8)	16.7(14.4, 19.1)	14.0(13.2, 14.7)	0.827
GGT(U/L)	19.0(15.0, 27.3)	29.0(19.0, 47.8)	25.0(16.0, 41.0)	42.0(27.0, 72.0)	18.0(14.0, 23.0)	29.0(20.0, 50.0)	24.0(15.0, 47.5)	54.5(35.3, 97.8)	0.580
PA(mg/dl)	29.10 ± 6.34	20.31 ± 6.71	10.92 ± 8.03	18.25 ± 6.68	28.68 ± 7.40	19.75 ± 7.43	11.63 ± 7.38	18.88 ± 7.09	0.949
GPR	0.69(0.52, 0.92)	1.43(0.86, 2.59)	3.24(1.85, 5.95)	2.90(1.85, 5.07)	0.61(0.53, 0.81)	1.64(0.91, 2.93)	3.25(1.61, 6.00)	3.67(1.86, 7.20)	0.761
GAR	0.80(0.63, 1.10)	0.65(0.40, 0.91)	0.67(0.43, 1.01)	1.23(0.81, 1.89)	0.78(0.64, 1.00)	0.74(0.44, 1.21)	0.60(0.34, 1.18)	2.00(1.14, 2.63)	0.090

differences, with ALB showing a significant difference among all four groups. The parameters with differences in the univariate analysis were included in the unordered multicategorical logistic regression analysis, and the age, TBIL, ALT, ALB, PT, GGT, and GPR all showed significant differences. Compared to patients with non-liver disease, PT, GGT, and GPR showed significant differences in the hepatitis, cirrhosis, and HCC groups. TBIL showed significant differences in the non-liver disease, hepatitis, and cirrhosis groups compared to patients with liver cancer. This suggests that the age, TBIL, ALT, ALB, PT, GGT, and GPR are useful for identifying patients with AFP-negative non-liver disease, hepatitis, cirrhosis, and HCC but are of limited value (Shown in Table 2).

Nomogram model based on serum parameters for predicting AFP-negative HCC

In the prediction of HCC, PA had greater diagnostic efficacy than ALB, so the redundant parameter excluded was ALB. In the training group, the univariate analysis revealed significant

TABLE 2 Efficacy of serum parameters to discriminate patients with non-liver disease, hepatitis, cirrhosis, and liver cancer.

Characteristics	Univariate χ^2	Univariate *P*	Multivariate χ^2	Multivariate *P*
Sex(male/female**)**	46.44	<0.001	6.61	0.086
Age(year)	132.48	<0.001	36.07	<0.001
TBIL(μmol/L)	152.04	<0.001	10.99	0.012
ALT(U/L)	166.12	<0.001	74.34	<0.001
ALB(g/L)	276.25	<0.001	37.42	<0.001
PT(s)	323.41	<0.001	76.44	<0.001
GGT(U/L)	178.28	<0.001	33.48	<0.001
GPR	378.47	<0.001	136.86	<0.001
GAR	153.80	<0.001	2.93	0.403

TABLE 3 Univariate and multivariate analysis to identify independent influencing factors affecting the diagnosis of AFP-negative hepatocellular carcinoma.

Variables	Univariate analysis			Multivariate analysis		
	OR	95%CI	P	OR	95%CI	P
Gender	1.935	1.243-3.014	0.003	1.682	1.035-2.733	0.036
Age	1.031	1.013-1.049	0.001	1.034	1.014-1.055	0.001
TBIL	0.970	0.952-0.989	0.002	0.959	0.937-0.982	0.001
PA	0.979	0.959-1.000	0.050			
GGT	1.016	1.010-1.022	<0.001			
GPR	1.067	1.026-1.110	0.001	1.096	1.037-1.160	<0.001
GAR	2.561	1.909-3.437	<0.001	1.991	1.466-2.704	0.001

differences in the gender, age, TBIL, PA, GGT, GAR, and GPR between the HCC and non-HCC groups. Further one-way and multi-way logistic regression analyses were performed in which the gender, age, TBIL, GAR, and GPR were independent diagnostic factors for AFP-negative HCC patients (Table 3), resulting in the generation of a nomogram model with an AUC of 0.837. The *P* value of Hosmer-Lemeshow test was 0.120, indicating that the model was not overfitted. Internal validation was performed using 200 ten-fold cross-validation (mean AUC: 0.837) and 1000 resampling Bootstrap tests (mean AUC: 0.838), indicating a more stable model. The model was further brought into the validation group for external testing with an AUC of 0.840, indicating that the model was efficient and reliable. The calibration curve, decision curve, and ROC curve of the model are shown in Figure 1. The nomogram model we establish can efficiently and easily calculate the patient's risk score. By calculating the sum of the scores of the parameters in the model, the patient's cancer risk can be derived. In particular, Figure 1A intuitively shows the parameters and weights in the model, as well as the corresponding liver cancer risk, which provides new ideas and methods for the diagnosis of AFP-negative HCC.

Discussion

In recent years, the diagnosis of hepatitis, cirrhosis and HCC based on haematological parameters, such as γ-glutamyl transpeptidase/platelet ratio predicted liver fibrosis in patients with chronic hepatitis B (28). AST to platelet ratio index for the diagnosis of cirrhosis in patients with autoimmune liver disease (29). There was a significant correlation between serum AFP, GGT and TK1 levels and their clinicopathological and diagnostic value in patients with HCC (30), showing the feasibility of serum indicators in liver disease to play a diagnostic effect, but most of these studies were to study the correlation between healthy people and one of the pathological states in hepatitis, cirrhosis or HCC, clinical diagnosis is actually always a complex group which contained three disease states, our research focuses on the diagnosis of AFP-negative HCC in a mixed population of patients with three liver disease states, which may have a better clinical application.

GGT is widely recognized to play a role in the growth and development as well as the acquisition of resistance to drug toxicity in HCC(31, 32). GGT levels are reportedly elevated in HCC, regardless of AFP levels (33, 34), indicating that GGT levels are not affected by AFP and may thus be a new diagnostic and prognostic predictor of HCC, independent of AFP. This was precisely the reason we chose GGT as the focus of the present study.

However, these previous studies showed that GGT levels were significantly elevated in liver cancer compared to healthy individuals and only predicted the correlation between GGT and the liver cancer prognosis. The studies did not perform an in-depth study analysis of the diagnosis of AFP-negative HCC, so our current study examined the differences in the expression of GGT in diverse populations (healthy individuals, hepatitis, cirrhosis, and HCC). The samples included in our study are more complete than in previous studies, and the error caused by the bias in the population type has been minimized.

PAB was therefore selected as another predictive marker in the present study (35). However, several conditions are known to affect PAB levels, including cirrhosis, viral hepatitis, liver dysfunction, and an abnormal nutritional status. Therefore, even though PAB is useful as a regulatory indicator of hepatocytes, it is limited by its low diagnostic efficacy in detecting HCC.

Previous studies have also used PAB combined with the D-dimer and fibrinogen levels to diagnose AFP-negative HCC(7): PAB (AUC=0.900), PAB+D-dimer (AUC=0.941), and PAB+fibrinogen (AUC=0.901). However, the control group in those studies only included healthy individuals, not taking into account the fact that, in real clinical practice, physicians deal with a diverse group of patients, which can include those with hepatitis and cirrhosis. Therefore, in the present study, we selected a larger sample size, covering a wider range of patients, which better conformed to the actual situation in clinical practice. In the clinical setting, the most difficult part of diagnosing AFP-negative HCC is excluding patients with hepatitis and cirrhosis.

Serum GGT combined with the AST/ALT and GGT/ALT ratios have been shown to be of great value in predicting the prognosis of HCC (34, 36, 37). However, the utility of the GGT/AST for diagnosing AFP-negative HCC patients has not been reported. In our study, significant differences in the GGT/AST

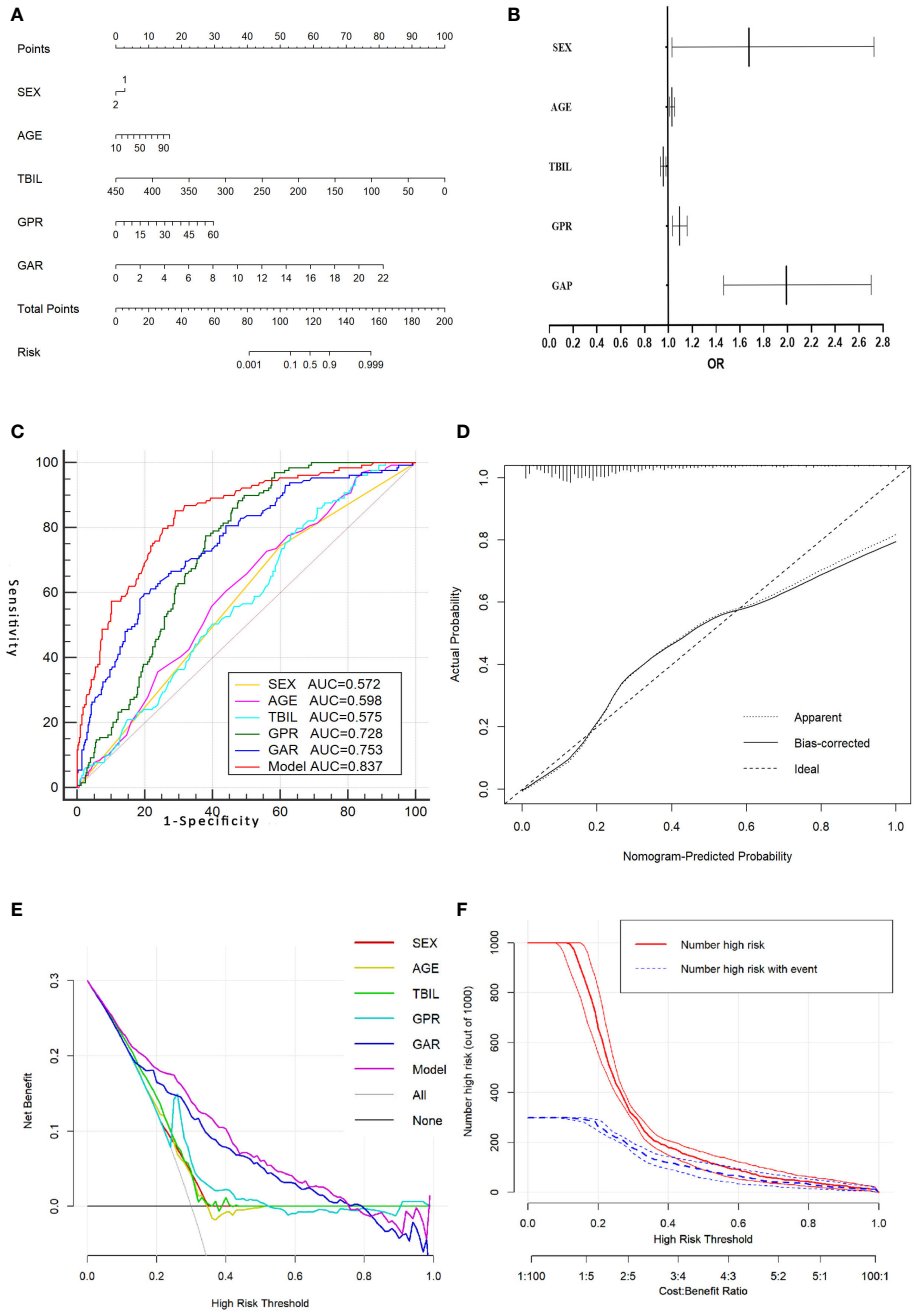

FIGURE 1
Nomogram model for predicting AFP-negative liver cancer and its evaluation curve. **(A)**.Nomogram model for predicting AFP-negative liver cancer. **(B)**. A forest plot of the OR values of each parameter of the Nomogram model. **(C)**. The ROC curve of the Nomogram model and the parameters in the Nomogram model. **(D)**. The calibration curve for the Nomogram model. **(E)**. The decision curve of the Nomogram model. **(F)**. The clinical impact curve of the nomogram model.

were found among healthy individuals and hepatitis, cirrhosis and HCC patients; furthermore, the results of univariate and multifactorial analyses showed that the GGT/AST could be an independent influential factor in the diagnosis of AFP-negative HCC.

In addition, in our present study, we constructed a nomogram model for the diagnosis of AFP-negative HCC by combining the independent influencing factors of gender, age, TBIL, GAR and GPR, which was further refined with univariate and multivariate analyses of each index. Our nomogram model showed a high performance in the diagnosis of AFP-negative HCC in both training (AUC=0.838) and validation (AUC=0.840) sets. Few previous studies have focused on the construction of a nomogram model based on serological indicators for the diagnosis of AFP-negative HCC, with most limited to the analysis of single- or several-factor ROC diagnostic curves showing incomplete consideration of factors and a single study sample of diseases that may bias the results(30, 37, 38).

In recent years, new advances have been made in the diagnosis of HCC and AFP-negative HCC by serological examinations, and new indices, such as, GP73, AFP-L3 and PIVKAII, have been used in clinical practice. According to relevant studies, the AUC values of GP73, AFP-L3 and PIVKAII for differentiating AFP-negative HCC from controls were 0.7811, 0.6094 and 0.856, respectively (13, 39), which were lower or only comparable to our present study model. Another retrospective study showed that the detection rate of the combined PIVKAII and AFP-L3 assay in patients with AFP-negative HCC was only 68.4%(39), which was lower than that of the combined GPR and GAR assay, and the sensitivity was only 40% when the results of the combined AFP-L3 and GP73 assay were used, which was inferior to the combined GPR and GAR. Considering the early occult, insidious nature of AFP-negative HCC and the economic burden of additional marker testing, combined with the present results, the present study model may aid in the preoperative noninvasive diagnosis of AFP-negative HCC and provide an early, effective, noninvasive and simple diagnostic marker for patients with occult HCC. In the clinical setting, it has the advantages of simple operation and economic ease of use.

Several limitations associated with the present study warrant mention. First, this was a single-center retrospective study, and the conclusions drawn need to be validated by multicenter randomized controlled and prospective research trials. Second, the relatively small sample size and the fact that all data originated from a single hospital may have biased the detection of these indicators. In addition, relevant information, such as the family history, was not obtained, and the distribution of different characteristics of patients with HCC increased the heterogeneity, which may have affected the final results. In a subsequent study, we will perform analyses of multiple medical centers on a larger scale, and more detailed information will be obtained to validate these results. In addition, in recent years, Numerous new nanoparticles have been applied to diagnosis and treatment of HCC and demonstrated unique advantages, for example, exosome miR-21 levels in the blood of HCC patients were significantly higher than in chronic hepatitis B (CHB) patients or healthy people and could be used as a potential diagnostic marker for HCC and might later become a non-invasive liquid biopsy marker for HCC(40). Synthetic nanoparticles have also shown outstanding performance in the diagnosis and treatment of HCC, for example, a new material system composed of glucose and TEMPO (2,2,6,6-tetramethylpiperidin-1-yl) oxide was designed to wrap the therapeutic drug CUDC101 and IR780, which play multiple effects such as treatment and multimodal imaging for HCC (41, 42). We consider whether our nomogram model can be combined with these nanoparticles to open up novel and more effective ideas for the diagnosis of AFP-negative HCC.

Conclusions

Serum parameters can reveal, to some extent, intrinsic differences between non-hepatic disease, hepatitis, cirrhosis, and HCC(majority of patients were HBV-positive Chinese). The nomogram model based on clinical and serum parameters can be used as a marker for the diagnosis of AFP-negative HCC, providing an objective basis for the early diagnosis and individualized treatment of HCC patients.

Data availability statement

The original contributions presented in the study are included in the article/supplementary material. Further inquiries can be directed to the corresponding authors.

Ethics statement

The studies involving human participants were reviewed and approved by The Ethics Committee of Taizhou Hospital of Zhejiang Province, approved No.K20210519. The patients/participants provided their written informed consent to participate in this study.

Author contributions

Conceived and designed the research: SL, YZ and ZF. Performed the clinical data collection: LL, QW, XZ. Analyzed the data: LL, YZ. Contributed data analysis: SL, ZF, YZ, YF. Wrote the manuscript: LL, QW. Responsible for the editing: SL and ZF. All authors contributed to the article and approved the submitted version.

Funding

This study was supported by Medical Health Science and Technology Project of Zhejiang Province, No. 2021PY083; Program of Taizhou Science and Technology Grant, No.22ywb09, Major Research Program of Taizhou Enze Medical Center Grant, No. 19EZZDA2. Open Project Program of Key Laboratory of Minimally Invasive Techniques and Rapid Rehabilitation of Digestive System Tumor of Zhejiang Province (21SZDSYS01).

Conflict of interest

The authors declare that the research was conducted in the absence of any commercial or financial relationships that could be construed as a potential conflict of interest.

Publisher's note

References

1. Siegel RL, Miller KD, Wagle NS, Jemal A. 'Cancer statistics 2023. *CA Cancer J Clin* (2023) 73:17–48. doi: 10.3322/caac.21763

2. Chen W, Zheng R, Baade PD, Zhang S, Zeng H, Bray F, et al. 'Cancer statistics in China 2015. *CA Cancer J Clin* (2016) 66:115–32. doi: 10.3322/caac.21338

3. Obiekwe BC, Malek N, Kitau MJ, Chard T. Maternal and fetal alphafetoprotein (AFP) levels at term. relation to sex, weight and gestation of the infant. *Acta Obstet Gynecol Scand* (1985) 64:251–3. doi: 10.3109/00016348509155123

4. Johnson PJ. Role of alpha-fetoprotein in the diagnosis and management of hepatocellular carcinoma. *J Gastroenterol Hepatol* (1999) 14(Suppl):S32–6. doi: 10.1046/j.1440-1746.1999.01873.x

5. Han LL, Lv Y, Guo H, Ruan ZP, Nan KJ. Implications of biomarkers in human hepatocellular carcinoma pathogenesis and therapy. *World J Gastroenterol* (2014) 20:10249–61. doi: 10.3748/wjg.v20.i30.10249

6. Chen S, Chen H, Gao S, Qiu S, Zhou H, Yu M, et al. Differential expression of plasma microRNA-125b in hepatitis b virus-related liver diseases and diagnostic potential for hepatitis b virus-induced hepatocellular carcinoma. *Hepatol Res* (2017) 47:312–20. doi: 10.1111/hepr.12739

7. Jing W, Peng R, Zhu M, Lv S, Jiang S, Ma J, et al. Differential expression and diagnostic significance of pre-albumin, fibrinogen combined with d-dimer in AFP-negative hepatocellular carcinoma. *Pathol Oncol Res* (2020) 26:1669–76. doi: 10.1007/s12253-019-00752-8

8. Farinati F, Marino D, De Giorgio M, Baldan A, Cantarini M, Cursaro C, et al. Diagnostic and prognostic role of alpha-fetoprotein in hepatocellular carcinoma: Both or neither? *Am J Gastroenterol* (2006) 101:524–32. doi: 10.1111/j.1572-0241.2006.00443.x

9. Carr BI, Guerra V. Low alpha-fetoprotein levels are associated with improved survival in hepatocellular carcinoma patients with portal vein thrombosis. *Dig Dis Sci* (2016) 61:937–47. doi: 10.1007/s10620-015-3922-3

10. Bai DS, Zhang C, Chen P, Jin SJ, Jiang GQ. The prognostic correlation of AFP level at diagnosis with pathological grade, progression, and survival of patients with hepatocellular carcinoma. *Sci Rep* (2017) 7:12870. doi: 10.1038/s41598-017-12834-1

11. An SL, Xiao T, Wang LM, Rong WQ, Wu F, Feng L, et al. Prognostic significance of preoperative serum alpha- fetoprotein in hepatocellular carcinoma and correlation with clinicopathological factors: A single-center experience from China. *Asian Pac J Cancer Prev* (2015) 16:4421–7. doi: 10.7314/APJCP.2015.16.10.4421

12. Guo X, Lv X, Lv X, Ma Y, Chen L, Chen Y. Circulating miR-21 serves as a serum biomarker for hepatocellular carcinoma and correlated with distant metastasis. *Oncotarget* (2017) 8:44050–58. doi: 10.18632/oncotarget.17211

13. Ji J, Wang H, Li Y, Zheng L, Yin Y, Zou Z, et al. Diagnostic evaluation of des-Gamma-Carboxy prothrombin versus α-fetoprotein for hepatitis b virus-related hepatocellular carcinoma in China: A Large-scale, multicentre study. *PloS One* (2016) 11:e0153227. doi: 10.1371/journal.pone.0153227

14. Liu Z, Wu M, Lin D, Li N. Des-gamma-carboxyprothrombin is a favorable biomarker for the early diagnosis of alfa-fetoprotein-negative hepatitis b virus-related hepatocellular carcinoma. *J Int Med Res* (2020) 48:300060520902575. doi: 10.1177/0300060520902575

15. Toyoda H, Kumada T, Tada T, Kaneoka Y, Maeda A, Kanke F, et al. Clinical utility of highly sensitive lens culinaris agglutinin-reactive alpha-fetoprotein in hepatocellular carcinoma patients with alpha-fetoprotein <20 ng/mL. *Cancer Sci* (2011) 102:1025–31. doi: 10.1111/j.1349-7006.2011.01875.x

16. Choi JY, Jung SW, Kim HY, Kim M, Kim Y, Kim DG, et al. Diagnostic value of AFP-L3 and PIVKA-II in hepatocellular carcinoma according to total-AFP. *World J Gastroenterol* (2013) 19:339–46. doi: 10.3748/wjg.v19.i3.339

17. Zahran AM, Abdel-Rahim MH, Refaat A, Sayed M, Othman MM, Khalak LMR, et al. Circulating hematopoietic stem cells, endothelial progenitor cells and cancer stem cells in hepatocellular carcinoma patients: Contribution to diagnosis and prognosis. *Acta Oncol* (2020) 59:33–9. doi: 10.1080/0284186X.2019.1657940

18. Wu Z, Cheng H, Liu J, Zhang S, Zhang M, Liu F, et al. The oncogenic and diagnostic potential of stanniocalcin 2 in hepatocellular carcinoma. *J Hepatocell Carcinoma* (2022) 9:141–55. doi: 10.2147/JHC.S351882

19. Cao L, Cheng H, Jiang Q, Li H, Wu Z. APEX1 is a novel diagnostic and prognostic biomarker for hepatocellular carcinoma. *Aging (Albany NY)* (2020) 12:4573–91. doi: 10.18632/aging.102913

20. Qiao W, Leng F, Liu T, Wang X, Wang Y, Chen D, et al. Prognostic value of prealbumin in liver cancer: A systematic review and meta-analysis. *Nutr Cancer* (2020) 72:909–16. doi: 10.1080/01635581.2019.1661501

21. Watanabe A, Araki K, Harimoto N, Kubo N, Igarashi T, Ishii N, et al. D-dimer predicts postoperative recurrence and prognosis in patients with liver metastasis of colorectal cancer. *Int J Clin Oncol* (2018) 23:689–97. doi: 10.1007/s10147-018-1271-x

22. Wang X, Mao M, He Z, Zhang L, Li H, Lin J, et al. Development and validation of a prognostic nomogram in AFP-negative hepatocellular carcinoma. *Int J Biol Sci* (2019) 15:221–28. doi: 10.7150/ijbs.28720

23. Rej R. Measurement of aminotransferases: Part 1. aspartate aminotransferase. *Crit Rev Clin Lab Sci* (1984) 21:99–186. doi: 10.3109/10408368409167137

24. Fang P, Du L, Cai D. Evaluation of plasma d-dimer for the diagnosis in Chinese patients with hepatocellular carcinoma: A meta-analysis. *Med (Baltimore)* (2020) 99:e19461. doi: 10.1097/MD.0000000000019461

25. Huang L, Mo Z, Hu Z, Zhang L, Qin S, Qin X, et al. Diagnostic value of fibrinogen to prealbumin ratio and gamma-glutamyl transpeptidase to platelet ratio in the progression of AFP-negative hepatocellular carcinoma. *Cancer Cell Int* (2020) 20:77. doi: 10.1186/s12935-020-1161-y

26. Zheng M, Ruan Y, Yang M, Guan Y, Wu Z. The comparative study on ultrastructure and immunohistochemistry in AFP negative and positive hepatocellular carcinoma. *J Huazhong Univ Sci Technolog Med Sci* (2004) 24:547–9, 59. doi: 10.1007/BF02911350

27. Xie DY, Ren ZG, Zhou J, Fan J, Gao Q. 2019 Chinese clinical guidelines for the management of hepatocellular carcinoma: Updates and insights. *Hepatob Surg Nutr* (2020) 9:452–63. doi: 10.21037/hbsn-20-480

28. Luo J, Du Z, Liang D, Li M, Yin Y, Chen M, et al. Gamma-glutamyl transpeptidase-to-Platelet ratio predicts liver fibrosis in patients with concomitant chronic hepatitis b and nonalcoholic fatty liver disease. *J Clin Lab Anal* (2022) 36:e24596. doi: 10.1002/jcla.24596

29. Suarez-Quintero CY, Patarroyo Henao O, Muñoz-Velandia O. Concordance between hepatic biopsy and the APRI index (Ast to platelet ratio index) for the diagnosis of cirrhosis in patients with autoimmune liver disease. *Gastroenterol Hepatol* (2021) 44:465–71. doi: 10.1016/j.gastrohep.2020.07.005

30. Gong G, Zheng K, Xue S, Hou J, Zhang Q. Serum AFU, GGT and TK1 levels in PHC patients and their correlation with clinicopathology and diagnostic value. *Cell Mol Biol (Noisy-le-grand)* (2020) 66:111–16. doi: 10.14715/cmb/2020.66.5.20

31. Corti A, Franzini M, Paolicchi A, Pompella A. Gamma-glutamyltransferase of cancer cells at the crossroads of tumor progression, drug resistance and drug targeting. *Anticancer Res* (2010) 30:1169–81.

32. Hanigan MH. Gamma-glutamyl transpeptidase: Redox regulation and drug resistance. *Adv Cancer Res* (2014) 122:103–41. doi: 10.1016/B978-0-12-420117-0.00003-7

33. Ju MJ, Qiu SJ, Fan J, Zhou J, Gao Q, Cai MY, et al. Preoperative serum gamma-glutamyl transferase to alanine aminotransferase ratio is a convenient prognostic marker for child-pugh a hepatocellular carcinoma after operation. *J Gastroenterol* (2009) 44:635–42. doi: 10.1007/s00535-009-0050-x

34. Yang JG, He XF, Huang B, Zhang HA, He YK. Rule of changes in serum GGT levels and GGT/ALT and AST/ALT ratios in primary hepatic carcinoma patients with different AFP levels. *Cancer biomark* (2018) 21:743–46. doi: 10.3233/CBM-170088

35. Goldwasser P, Feldman J. Association of serum albumin and mortality risk. *J Clin Epidemiol* (1997) 50:693–703. doi: 10.1016/S0895-4356(97)00015-2

36. Zhang LX, Lv Y, Xu AM, Wang HZ. The prognostic significance of serum gamma-glutamyltransferase levels and AST/ALT in primary hepatic carcinoma. *BMC Cancer* (2019) 19:841. doi: 10.1186/s12885-019-6011-8

37. Zhang Q, Jiao X. LDH and GGT/ALT ratio as novel prognostic biomarkers in hepatocellular carcinoma patients after liver transplantation. *Comput Math Methods Med* (2021) 2021:9809990. doi: 10.1155/2021/9809990

38. Waidely E, Al-Yuobi AR, Bashammakh AS, El-Shahawi MS, Leblanc RM. Serum protein biomarkers relevant to hepatocellular carcinoma and their detection. *Analyst* (2016) 141:36–44. doi: 10.1039/C5AN01884F

39. Zhang Z, Zhang Y, Wang Y, Xu L, Xu W. Alpha-fetoprotein-L3 and golgi protein 73 may serve as candidate biomarkers for diagnosing alpha-fetoprotein-negative hepatocellular carcinoma. *Onco Targets Ther* (2016) 9:123–9. doi: 10.2147/OTT.S90732

40. Li B, Cao Y, Sun M, Feng H. Expression, regulation, and function of exosome-derived miRNAs in cancer progression and therapy. *FASEB J* (2021) 35:e21916. doi: 10.1096/fj.202100294RR

41. Cao L, Zhu YQ, Wu ZX, Wang GX, Cheng HW. Engineering nanotheranostic strategies for liver cancer. *World J Gastrointest Oncol* (2021) 13:1213–28. doi: 10.4251/wjgo.v13.i10.1213

42. Cheng H, Fan X, Ye E, Chen H, Yang J, Ke L, et al. Dual tumor microenvironment remodeling by glucose-contained radical copolymer for MRI-guided photoimmunotherapy. *Adv Mater* (2022) 34:e2107674. doi: 10.1002/adma.202107674

frontiers | Frontiers in Oncology

TYPE Original Research
PUBLISHED 09 March 2023
DOI 10.3389/fonc.2023.1118152

OPEN ACCESS

EDITED BY
Lujun Shen,
Sun Yat-sen University Cancer Center (SYSUCC), China

REVIEWED BY
Ying Shi,
University of Electronic Science and Technology of China, China
Beili Wang,
Fudan University, China

*CORRESPONDENCE
Yuan Huang
1198736837@qq.com

SPECIALTY SECTION
This article was submitted to Gastrointestinal Cancers: Hepato Pancreatic Biliary Cancers, a section of the journal Frontiers in Oncology

RECEIVED 07 December 2022
ACCEPTED 14 February 2023
PUBLISHED 09 March 2023

CITATION
Gao Y-j, Li S-r and Huang Y (2023) An inflammation-related gene landscape predicts prognosis and response to immunotherapy in virus-associated hepatocellular carcinoma.
Front. Oncol. 13:1118152.
doi: 10.3389/fonc.2023.1118152

An inflammation-related gene landscape predicts prognosis and response to immunotherapy in virus-associated hepatocellular carcinoma

Ying-jie Gao[1], Shi-rong Li[2] and Yuan Huang[1]*

[1]Department of Biochemistry and Molecular Biology, School of Bioscience and Technology, Chengdu Medical College, Chengdu, Sichuan, China, [2]Laboratory of Animal Tumor Models, Frontiers Science Center for Disease-related Molecular Network, State Key Laboratory of Biotherapy and Cancer Center, National Clinical Research Center for Geriatrics, West China Hospital, Sichuan University, Chengdu, Sichuan, China

Background: Due to the viral infection, chronic inflammation significantly increases the likelihood of hepatocellular carcinoma (HCC) development. Nevertheless, an inflammation-based signature aimed to predict the prognosis and therapeutic effect in virus-related HCC has rarely been established.

Method: Based on the integrated analysis, inflammation-associated genes (IRGs) were systematically assessed. We comprehensively investigated the correlation between inflammation and transcriptional profiles, prognosis, and immune cell infiltration. Then, an inflammation-related risk model (IRM) to predict the overall survival (OS) and response to treatment for virus-related HCC patients was constructed and verified. Also, the potential association between IRGs and tumor microenvironment (TME) was investigated. Ultimately, hub genes were validated in plasma samples and cell lines *via* qRT-PCR. After transfection with shCCL20 combined with overSLC7A2, morphological change of SMMC7721 and huh7 cells was observed. Tumorigenicity model in nude mouse was established.

Results: An inflammatory response-related gene signature model, containing *MEP1A*, *CCL20*, *ADORA2B*, *TNFSF9*, *ICAM4*, and *SLC7A2*, was constructed by conjoint analysis of least absolute shrinkage and selection operator (LASSO) Cox regression and gaussian finite mixture model (GMM). Besides, survival analysis attested that higher IRG scores were positively relevant to worse survival outcomes in virus-related HCC patients, which was testified by external validation cohorts (the ICGC cohort and GSE84337 dataset). Univariate and multivariate Cox regression analyses commonly proved that the IRG was an independent prognostic factor for virus-related HCC patients. Thus, a nomogram with clinical factors and IRG was also constructed to superiorly predict the prognosis of patients. Featured with microsatellite instability-high, mutation burden, and immune activation, lower IRG score verified a superior OS for sufferers. Additionally, IRG score was remarkedly correlated with the cancer stem cell index and drug susceptibility. The measurement of plasma samples further validated that CCL20 upexpression and SLC7A2 downexpression were

positively related with virus-related HCC patients, which was in accord with the results in cell lines. Furthermore, CCL20 knockdown combined with SLC7A2 overexpression availably weakened the tumor growth *in vivo*.

Conclusions: Collectively, IRG score, serving as a potential candidate, accurately and stably predicted the prognosis and response to immunotherapy in virus-related HCC patients, which could guide individualized treatment decision-making for the sufferers.

KEYWORDS

hepatocellular carcinoma, virus, inflammation, tumor microenvironment, immune, drug sensitivity

1 Introduction

Considering as the third leading cause of cancer death worldwide, hepatocellular carcinoma (HCC) is the fifth most usual cancer (1). During HCC progression and development, a battery of risk factors, such as genetical (i.e., alteration of tumor suppressors and oncogenes) and environmental factors (i.e., viruses), had been indicated to be involved (2). Thus, comprehensive understanding of risk factors could assist researchists and clinicians to make effective therapeutic options in terms of HCC treatment. As we all know, various viruses, involving hepatitis B virus (HBV) and hepatitis C virus (HCV) targeting several cellular and molecular pathways, could contribute to HCC pathogenesis (3). As we all know, chronic HBV and HCV infections account for probably 60-70% of the leading cause for hepatocarcinogenesis worldwide (4). Especially in Africa and Asia, HBV is the single primary risk factor for liver cancer, whereas HCV infection dominates in Japan, northern Europe and USA (5). Thus, Hepatitis B and C viruses are an universal health issue for the reason of causing acute and chronic infections, which can generate liver cirrhosis and even HCC with significant mortality more than 1.3 million deaths per year (6, 7).

Abbreviations: HCC, hepatocellular carcinoma; HBV, hepatitis B virus; HCV, hepatitis C virus; HCC,Hepatocellular carcinoma; IRGs, inflammation-associated genes; IRM, inflammation-related risk model; OS, overall survival; TME, tumor microenvironment; LASSO, least absolute shrinkage and selection operator; GMM, gaussian finite mixture model; HBV, hepatitis B virus; HCV, hepatitis C virus; mTKIs, multiple tyrosine kinase inhibitors; TCGA, the cancer genome atlas; GEO, gene expression omnibus; t-SNE, t-distributed stochastic neighbor embedding; FDR, false discovery rate; PPI, protein–protein interaction; GO, Gene Ontology; KEGG, Kyoto Encyclopedia of Genes and Genomes; ROC, receiver operating characteristic; AUCs, area under curves; PCA, principal component analysis; TMB, tumor mutation burden; MSI, microsatellite instability; CSC, cancer stem cells; DCA, decision curve analysis; TIDE, Tumor Immune Dysfunction and Exclusion; IPS, immunophenotype score; QC, quality control; ICI, immune cell infiltration; TIME, tumor immune microenvironments; AUC, area under the curve; RNAss, RNA stemness score; MSS, microsatellite stable; scRNA-seq, single-cell RNA sequencing.

Presently for advanced HCC, cure options are finite, among which chemotherapy is one of the most vital treatment patterns (8). Multiple tyrosine kinase inhibitors (mTKIs) such as sorafenib, lenvatinib, cabozantinib, and regorafenib have been used to treat advanced HCC. However, although they show some benefit, it does not significantly alter the course of disease for most patients (9, 10). In addition to standard systemic therapy with mTKIs, recent studies demonstrate the capacity for durable responses from immune checkpoint inhibition in subsets of HCC patients across disease etiologies (11). A majority of HCC derives from the context of chronic inflammation, with a lot of cases relevant with hepatitis virus infections, which are associated with both local and systemic immune deficiency (12). Also, the liver is an immunologic organ to enhance or suppress the immune response to cancer arising within it (13, 14). Therefore, there is an imperative to develop an effective gene signature for risk stratification and guiding clinical treatment, especially involved in targeted therapy and immunotherapy.

Chronic inflammation resulting from viral infection markedly enhances the likelihood of cancer development by activating inflammatory signaling pathways and cytokines, stimulating growth of infected cells and inhibiting apoptosis viruses (15–17). Thus, it attested apparent that inflammation is served as a prime driving force in cancer progression for the close correlation between chronic virus infection and carcinogenesis. When it comes to HCC development, there are approximately 90% of primary liver cancers arising almost exclusively in the setting of inflammation (18, 19). Recently, inflammation inhibition has appeared to be as a conducive therapeutic choice, particularly for tumors where conventional treatment is unavailable (20). Presently, the studies are predominantly concentrated upon figuring out the role of individual inflammation-associated genes on HCC progression and prognosis (21–25). In addition, inflammation-associated genes are often deemed as therapeutic targets for tumors since exploring the relevance between inflammation-associated genes and tumor immune status may conduce to further integration of targeted therapy and immunotherapy (26, 27).

In the present study, we identified IRGs in virus-related HCC and constructed a prognostic signature to accurately predict the clinical outcome of virus-related HCC patients and

immunotherapeutic effect by least absolute shrinkage and selection operator (LASSO) regression analyses as well as Gaussian Mixture Model (GMM) based on The Cancer Genome Atlas (TCGA, https://www.cancer.gov/tcga) and Gene Expression Omnibus (GEO) databases. Also, the prognosis and tumor microenvironmental characteristics of diverse subtypes based on IRGs as well as corresponding responses to therapy were analyzed. Furthermore, we evaluated the molecular features, prognostic significance, and infiltrating immune cell intensities of the IRGs clusters. Our findings verified a potential relationship between inflammation, prognosis, TME, and the response to immunotherapy in virus-related HCC.

2 Materials and methods

2.1 Data acquisition

RNA sequencing data and corresponding clinical information of 179 virus-relevant patients with liver cancer were downloaded from TCGA website (https://portal.gdc.cancer.gov/repository). RNA sequencing data and clinical information of another 260 virus-related HCC samples were obtained from ICGA website (https://dcc.icgc.org/projects/LIRI-JP). Besides, patients from GSE84337 (n=75) in the GEO repository was screened to acquire clinical parameters and normalized gene expression data. Clinical information of virus-related liver cancer patients was shown in Table S2. Samples lacking significant clinicopathological or survival information were excluded from further analysis.

2.2 Curation of inflammation-related genes

200 inflammatory response-related genes were found in the Molecular Signatures database and listed in the Supplementary Table 1. Furthermore, t-distributed Stochastic Neighbor Embedding (t-SNE), a nonparametric and unsupervised algorithm, was employed to sort or condense patients into diverse clusters, based on given signatures or hallmarks by using an R package Seurat (28). According to the OS data, two groups were singled out for comparison to determine the "inflammation^{high}" and "inflammation^{low}" clusters. The limma algorithm was applied to filtrate DEGs between the above two groups, generating genes with false discovery rate (FDR) adjusted p-value<0.05 and absolute value of log2 (fold change)>1 were regarded as inflammation-related DEGs.

2.3 Protein–protein interaction network construction

The STRING database (https://string-db.org/) was used to establish the protein–protein interaction (PPI) network among sufferers with co-expression coefficients >0.4. Also, cytoscape software (version 3.7.2) was exploited to visualize the network. Moreover, the hub genes were screened with the MCC algorithm of the cytoHubba plugin. The correlation between the expression of inflammation-related genes was identified by the "reshape2" R package.

2.4 Enrichment analysis

To explore the potential mechanisms and pathways about inflammation-related genes, the Gene Ontology (GO) and Kyoto Encyclopedia of Genes and Genomes (KEGG) functional enrichment analysis were conducted among IRGs using the R packages "clusterProfiler," "enrichplot," "ggplot2," and "org.Hs.eg.db."

2.5 Consensus clustering analysis of IRGs

Based on the expression of inflammation-related genes (IRGs), we classified distinct inflammation-regulated groups through consensus clustering with the k-means method. The number of patterns and corresponding homologous stability were defined by consensus clustering algorithm using the R package ConsensusClusterPlus with 1,000 repetitions (29).

2.6 Relationship of molecular patterns with TME in virus-related HCC

The immune infiltration characteristics (the immune and stromal scores) of virus-related HCC, based on the RNA-seq dataset of TCGA database LIHC, were evaluated by ESTIMATE algorithm (30). Then, CIBERSORTx was applied to quantify the percentages of 22 immune cell subtypes of each patient in the TME (31). Also, the correlation between the subsets on PD-1, PD-L1, and CTLA-4 expression was assessed.

2.7 Construction and validation of inflammation-related gene score

To define preliminary inflammation-related DEGs that were significantly associated with OS in the training cohort, univariate Cox regression analyses using the R package "survival" were further implemented among favorable and risk DEGs, of which $p<0.05$ were regarded as positive. Also, Least Absolute Shrinkage and Selection Operator (LASSO) regression with 10-fold cross-validation was explored to narrow down the prognosis-related DEGs applying the R package "glmnet" (32). Meanwhile, based on the Gaussian finite mixture model (GMM), classification was conducted with model-based hierarchical agglomerative clustering with the R package "mclust" (33). Afterwards, the clusters made up of DEGs were classified by GMM and logistic regression analysis

was utilized to construct combined models to predict the OS status for patients. Besides, to calculate the predictive value of models, receiver operating characteristic (ROC) curves were established by assessing the area under curves (AUCs). Subsequently, the risk scores of patients were estimated according to the expression level of each inflammatory response-related gene and its relevant regression coefficient. The formula was established as follows: risk score = ∑iCoefficient (mRNAi) × Expression(mRNAi). On the basis of the median risk scores, patients were divided into high- and low-risk clusters among training and validation cohorts. The Kaplan-Meier analysis was applied to compare the OS between the high- and low-risk groups. The predictive value of the prognostic model was assessed on account of ROC analysis. The principal component analysis (PCA), acquiring a low-dimensional cluster distribution from high-dimensional gene sets, was utilized for validating the sectionalization results.

2.8 Clinical significance and classification analysis of the prognostic IRG score

The correlation between IRG score and clinical factors was explored. Univariate Cox and multivariate Cox regression analysis were firstly implemented to prove whether IRG score was an independent prognostic predictor. Ulteriorly, a grouping analysis was conducted to explore whether the IRG score sustained its predictive reliable in disparate subgroups on the basis of multifarious clinical variables. Furthermore, the infiltrating levels of immune cells and immune checkpoint (ICP) were analyzed between the distinct risk subgroups and the relevance between IRG score and tumor mutation burden (TMB) score, microsatellite instability (MSI) score, and cancer stem cells (CSC) score was examined.

2.9 Nomogram and calibration

Nomogram was constructed by the rms R package. Calibration curves and decision curve analysis (DCA) were utilized to quantify the consistency between the predicted and the observed results for 3-, and 5-years survival rates (34).

2.10 Gene mutation analysis

On the basis of the cBioPortal database, genetic alteration data was acquired. And the number and quality of mutations between the two IRG clusters were analyzed using the R "Maftools" package (35). Subsequently, the online database TIDE (Tumor Immune Dysfunction and Exclusion, http://TIDE.dfci.harvard.edu/) and immunophenotype score (IPS) were calculated to execute immune checkpoint inhibitor response of each virus-related HCC patient in the two groups to assess the value of the IRG in terms of prognostic immunotherapy response.

2.11 Prediction of drug susceptibility

The pRRophetic R package was used to predict the half-maximal inhibitory concentration (IC50) value of cancer drugs in diverse risk subgroups, which represented the availability of a substance in inhibiting a particular biological or biochemical process (36, 37).

2.12 Clinical samples

The samples contained 58 blood samples from virus-related HCC patients from West China Guangan Hospital, Sichuan University, between March and November in 2019. The diagnoses of HCC were confirmed by senior pathologist. None of the patients experienced radiotherapy or chemotherapy treatment before samples collection. Also, 50 blood samples from healthy people were considered as the control cluster. Informed consent was obtained from all participants for the use of their blood samples in this study. This project was approved by the Clinical Research Ethics Committee of Chengdu medical college.

2.13 Cell culture

The human cell lines (WLR68, LO2, Huh-7, SMMC7721, HepG2, and HCCLM3) were obtained from the School of Bioscience and Technology, Chengdu Medical College (ChengDu, China). All of them were cultured in DMEM (Gibco) medium, which were supplemented with 10% fetal bovine serum (FBS) at 37 °C with 5% CO_2. In addition, the cells were photographed after treatment with paraformaldehyde.

2.14 Samples processing, RNA extraction, and real-time fluorescence qRT-PCR

Approximately 8 ml of whole blood from participants was gathered in EDTA tube. After centrifuged at 1,2000g at 4°C to spin down the blood cells for 10 min, the supernatant was shifted into microcentrifuge tubes. Afterwards, plasma was aliquoted or stored at −80°C. RNA was isolated from 400 μL plasma with the mirVana PARIS kit (Ambion, USA) abided by the manufacturer's protocol. The PrimeScript™ RT reagent kit (TaKaRa) was further applied for reverse transcriptase reaction. Reverse transcription −quantitative PCR (RTqPCR) were implemented to attest the expression levels of the six hub genes in plasma samples and cell lines. The mRNA expression level of *MEP1A*, *CCL20*, *ADORA2B*, *TNFSF9*, *ICAM4*, and *SLC7A2*, was normalized by GAPDH. Fold differences were calculated for each group with normalized CT values.

2.15 Cell transfection

Full-length SLC7A2 cDNA was synthesized and cloned into the pCS-CG vector (Addgene, Cambridge, MA, USA). shRNA sequences specifically against CCL20 (shCCL20) and control-shRNA against luciferase (shCtrl) were expressed from pLKO.1-puro (Addgene, Cambridge, MA, USA). Production of lentiviral particles using HEK-293T cells and subsequent infection of Huh7 and SMMC7721 cells were performed according to the manual instructions.

2.16 *In vivo* tumorigenicity

14 male nude mice (5-week-old) were purchased from Beijing Vital River Laboratory Animal Technology Co., Ltd. (Beijing, China). SMMC7721 (1×10^7) stably transfected with shCtrl or shCCL20/overSLC7A2 was subcutaneously injected into the right gluteal region of each nide mice (n=7). After tumor formed, the tumor volume was calculated every 3 days on the basis of the formula: volume(mm^3)=width2 (mm^2) *length (mm)/2. All the mice were euthanized and the formed tumors were weighted after 30 days. The animal experiment was approved by the Animal Care Committee of Chengdu Medical College.

2.17 Statistical analysis

All analyses were completed on the strength of R language (Version 4.2.1). Student's t-test, chi-squared test, or Wilcoxon test was applied to compare the differences between groups. Spearman's correlation test was performed to evaluate the correlation between variables. *p*-value of <0.05 was deemed as statistically positive.

3 Results

3.1 Workflow of study

The study flowchart is revealed in Figure 1, which precise procedure is as follows: First, RNA sequencing from the TCGA database for 179 virus-related HCC sufferers was obtained, as well

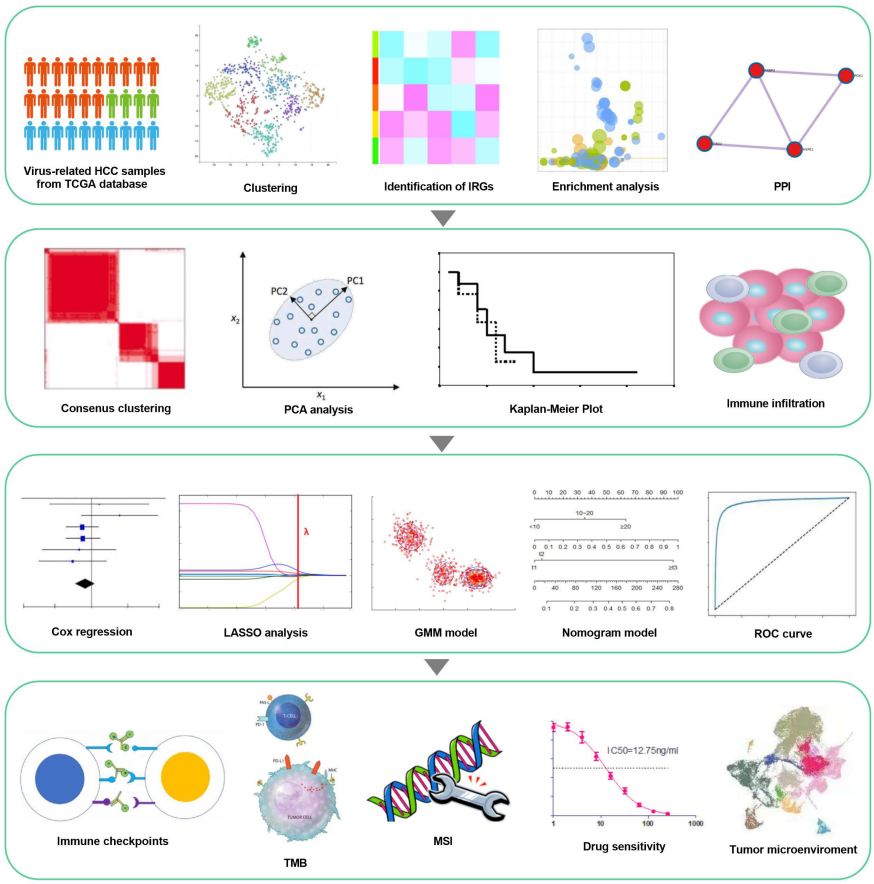

FIGURE 1
workflow of the study. Virus-related HCCs extracted from TCGA database and 200 inflammation-relevant markers from the Molecular Signatures database were analyzed to identify IRG DEGs. Next, consenus clustering was used to classify inflammation subgroups. The prognostic model was constructed and validated in multiple ways and proved to be stable and reliable. Therefore, based on this model, we also performed analysis about immunological characteristics, drug sensitivity and the correlation between IRGs and Tumor Microenvironment.

10.3389/fonc.2023.1118152

as 200 IRGs from the Molecular Signatures database. t-SNE, was applied to sort or condense patients into diverse clusters, based on 200 IRGs and IRG DEGs were identified from survival analysis. Next, consenus clustering was classified inflammation subgroups to analyze immune infiltration. Furthermore, a prognostic inflammation-associated model was established, and its corresponding stability was verified with various methods. Ultimately, immunological characteristics and drug sensitivity analysis extended on the idea of clinical application, while the correlation between IRGs and tumor microenvironment in virus-related HCC was attested.

3.2 Identification and functional enrichment analysis of inflammation-related differentially expressed genes in virus-associated HCC

The expression matrix of 200 IRGs was adopted to compute the euclidean distance between any two patients from 179 virus-related HCCs, and t-SNE algorithm was further condensed the euclidean distance into two-dimensional points. Subsequently, three clusters with virus-related HCC patients were generated and each patient was assigned to its closest (Figure 2A), namely 81, 57, and 41

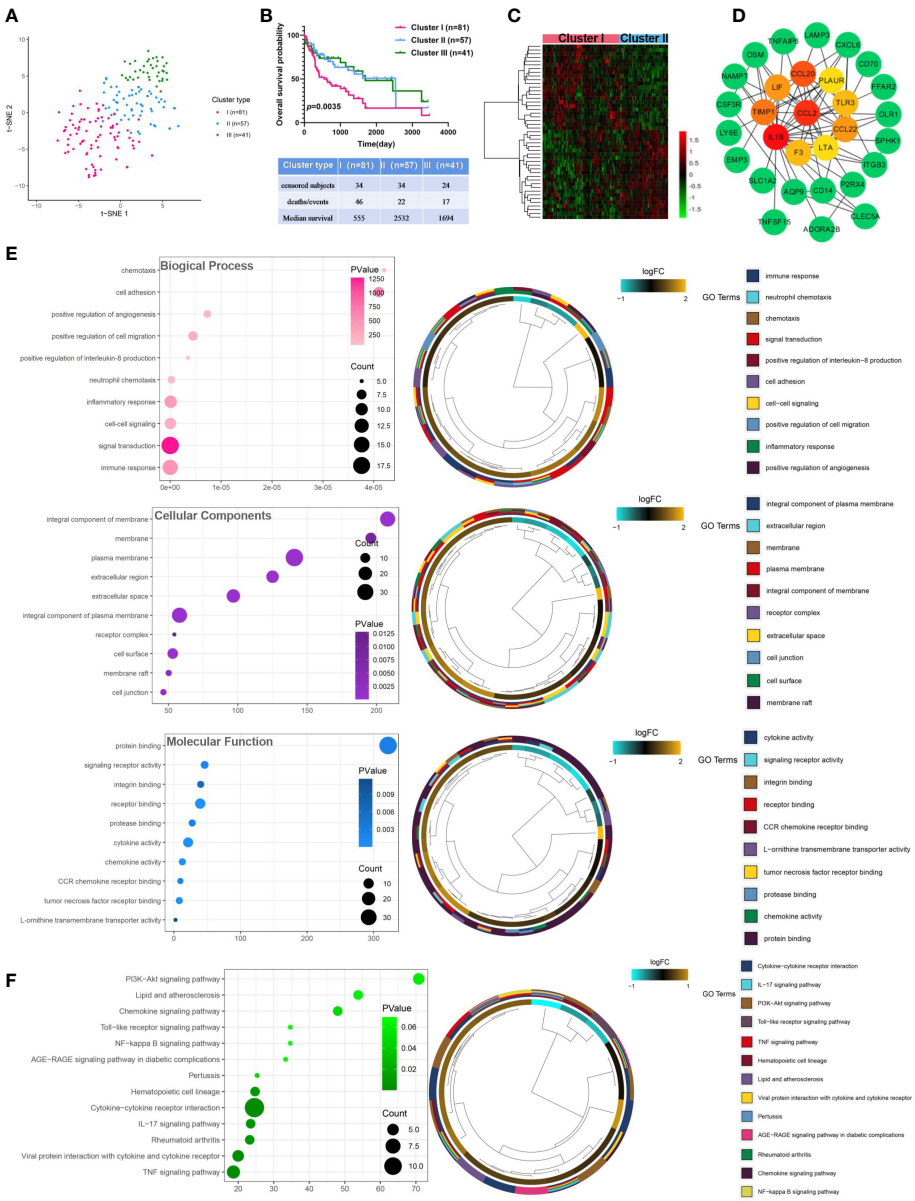

FIGURE 2
Identification and analysis of inflammation-related differentially expressed genes in virus-related HCC. **(A)** Dot plot for three distinct clusters identified by t-SNE algorithm based on 200 inflammation hallmark genes. **(B)** Kaplan-Meier plot of overall survival for patients in three clusters. **(C)** Heatmap showing expression profiles for inflammation-related DEGs with comparison between cluster I (inflammation^{high}) and cluster II (inflammation^{low}) groups. **(D)** The Protein-protein interaction (PPI) network between 47 differentially expressed inflammation-related genes (IRGs). **(E)** Gene Ontology (GO) and **(F)** Kyoto Encyclopedia of Genes and Genomes (KEGG) enrichment analysis for IRGs. Adjusted $p < 0.01$ and $p < 0.05$ were considered significant.

patients in distinct clusters (Cluster I, Cluster II, and Cluster III), respectively. OS analysis displayed that the most significant differences consisted between cluster I and cluster II. Thus, patients in Cluster II yield the best OS while those in Cluster I had the worst prognosis outcome (Figure 2B), indicating that Cluster II and Cluster I might represent the lowest and highest status of inflammation. Accordingly, sufferers in Cluster I and Cluster II were classified into "inflammation^{high}" and "inflammation^{low}" groups, separately. To obtain inflammation-related DEGs, expression profiles were compared between the inflammation^{high} and inflammation^{low} groups, leading to a total of 47 inflammation-related DEGs identified (Figure 2C). Next, A PPI network was constructed, composed of 84 nodes. Among all nodes, 10 hub genes, including CCL20, IL1B, CCL2, CCL22, TIMP1, LIF, TLR3, F3, LTA, and PLAUR were distinguished (Figure 2D). Further research found that the DEGs were mostly enriched in immune response, integral component of membrane, and signaling receptor activity (Figure 2E; Table S3). KEGG analysis also demonstrated that these DEGs were closely related to pathways in inflammation, such as IL-17 signaling pathway, TNF signaling pathway, and NF-kappa B signaling pathway (Figure 2F; Table S3).

3.3 Subtypes classification based on inflammation-related gene signatures

The relevance network of IRGs interactions, regulator relationships, and corresponding survival status in virus-related HCC patients was presented in Figure 3A and Table S4. To further conclude the relation between expression profiles of IRGs and HCC subtypes, a consensus clustering analysis was conducted to separate patients into different gene clusters based on the expression levels of the IRGs (Figure 3B). Three discrepant patterns were determined: 98 cases in Cluster 1, 53 cases in Cluster 2, and 28 cases in Cluster 3 (Figure 3C). Afterwards, OS status of the three patterns was revealed, contributing to a consequential difference observed (Figure 3D). Additionally, the genomic expression and clinicopathological features of three clusters were displayed in Figure 3E, identifying a substantial difference between IRGs expression and clinical characters.

3.4 Discrepancies in TME infiltration for inflammation patterns in virus-related HCCs

The CIBERSORT and ESTIMATE algorithms were implemented to confirm the activity or enrichment levels for immune cells in virus-related HCCs (Table S5). The heatmap of three independent immune cell infiltration (ICI) subtypes was presented in view of 179 tumor samples with matched ICI profiles from TCGA-LIHC (Figure 4A). The expression of three vital ICPs (PD-1, PD-L1, and CTLA-4) was obviously distinct among three clusters. In virtue of the role of TME scores for evaluating the abundance of immune and stromal elements in TME, the ESTIMATE algorithm was further executed to estimate the TME scores, involving stromal score, immune score, and estimate score, in three clusters, the results of which turned out sufferers in cluster 3 yielded superior TME scores (Figures 4B, C). In addition, we explored if the three subclasses generated various tumor immune microenvironments (TIME) (Figure 4D). Indeed, the immune-high subgroup had high infiltration levels of Eosinophils, Macrophages M0, Macrophages M1, and Neutrophils, while the cluster 1 had remarkable enrichment of resting mast cells.

3.5 Development and validation of prognostic IRG score

Firstly, Univariate Cox regression analysis was utilized on the virus-associated HCC groups, demonstrating that 13 prognosis-related IRGs were correlated with OS (Figure 5A; Table S6). To prevent model overfitting, LASSO penalized Cox regression modeling and GMM model were simultaneously conducted to filter the vital DEGs, which were positively associated with the prognosis of HCC patients. With the joint method, a novel prognostic gene model with six hub genes (*ADORA2B*, *CCL20*, *ICAM4*, *MEP1A*, *SLC7A2*, and *TNFSF9*) was constructed (Figures 5B–E). Then, we computed risk score using the following formula: risk score =∑iCoefficient (mRNAi) × Expression(mRNAi), where i, stands for the expression of six key IRGs. In line with the median risk score, samples were clustered into low- and high-risk subgroups. The distribution patterns from PCA analysis illustrated that patients could be distinguished into high- and low-risk classes (Figure 5F). Also, the risk plot of IRG score proved that OS time decreased while mortality rise, as IRG score increased. And survival analysis testified that samples in the low-risk cluster produced significantly longer OS time in comparison with that of the high-risk patients (Figure 5I, $P<0.01$, log-rank test) (Figures 5G–I; Figure S1). Moreover, the expressive relationship among them and heatmap of selected genes were displayed in Figure 5J and Figure 5K, respectively. To comprehend the relationship between immune subtypes and IRG score, an alluvial diagram was drawn for clusters with distinct risk-subgroups, and accompanying survival status (Figure 5L). The outcomes demonstrated that cluster 3 with higher IRG score was most likely associated with death. Whereas the cluster 1 exhibited a lower IRG score and best prognosis status. A time-dependent ROC curve was further performed and the area under the curve (AUC) reached 0.805, 0.7, and 0.718 at 1, 3, and 5 years, respectively (Figure 5M). Besides, the ROC curve explained that the predictive OS accuracy of IRG score was superior to other clinical parameters (Age, gender, Alcohol consumption, Neoplasm histologic grade, and TNM stage and age) (Figure 5N). Tremendous differences in the IRG score of three clusters were discovered (Figure 5O), implying a higher IRG score may be relevant with immune activation-associated features.

10.3389/fonc.2023.1118152

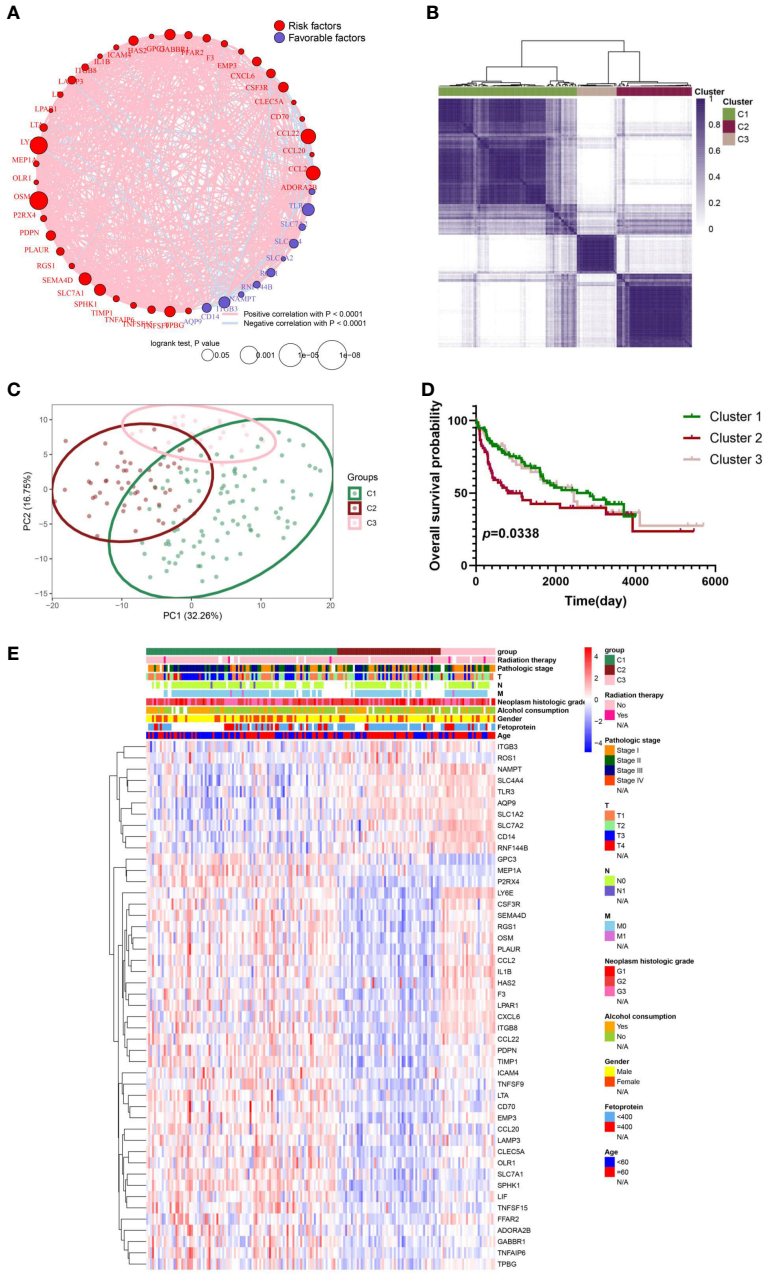

FIGURE 3
IRG subgroups divided by consistent clustering and its corresponding clinicopathological and biological characteristics. **(A)** The correlation in inflammation-related gene expression. **(B)** Consensus clustering of 179 sufferers from virus-related TCGA-LIHC cohorts based on the IRG DEGs. Consensus matrix for optimal k = 3. **(C)** Principal component analysis (PCA) of TCGA database for optimal k = 3. **(D)** Kaplan-Meier analysis for overall survival (OS) curves of patients in distinct clusters. **(E)** Differences in clinicopathologic characteristics and expression levels of IRGs between the three distinct subgroups.

3.6 Independent prognostic value of IRG score

To explore the relation between the IRG score and clinicopathological Characteristics, the interaction between IRG score and multitudinous clinical parameters (Age, Alcohol consumption, gender, TNM stage, Fetoprotein, Radiation therapy and survival status) was discussed (Figures S2A–F). We perceived that IRG scores increased along with the stage III-IV and higher level of fetoprotein. And Univariate and multivariate Cox regression analyses were further conducted to guesstimate the accuracy of the risk model and disclose whether IRG score could be considered as an independent prognostic factor for patients' prognosis. Accordingly, Univariate Cox regression analysis revealed that

10.3389/fonc.2023.1118152

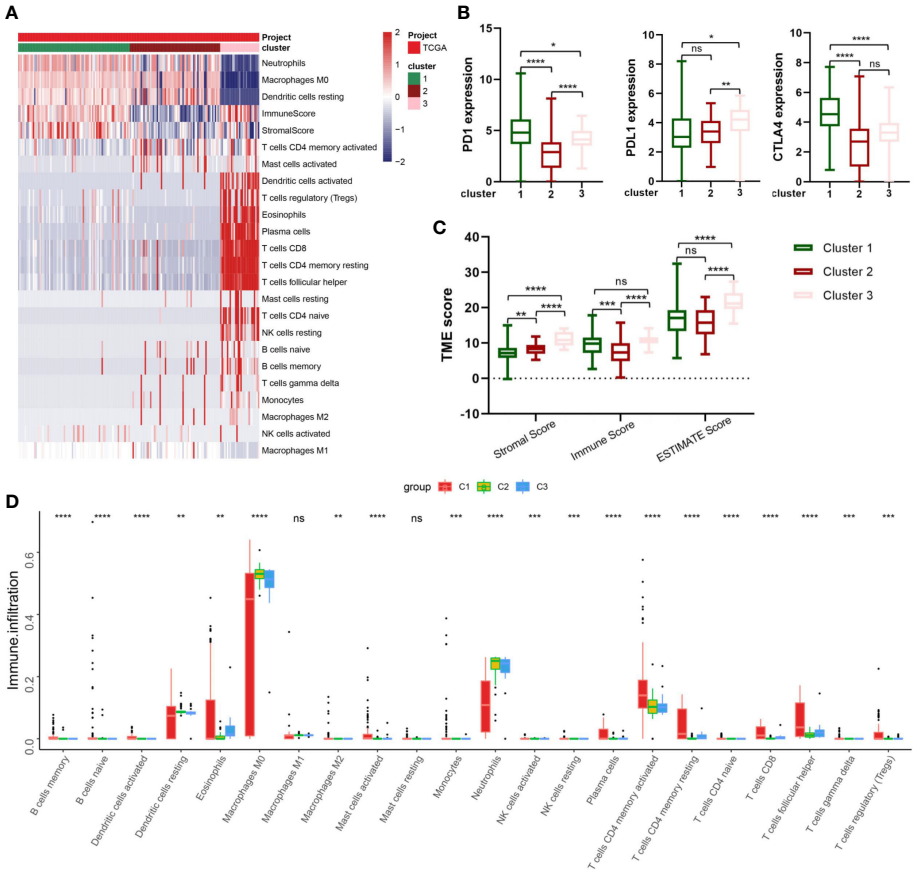

FIGURE 4
Correlation between IRG subgroups and tumor microenvironment in virus-related liver cancer (TCGA cohort). **(A)** heatmap displaying clustering of tumor-infiltrating immune cells in TCGA cohort. Rows represent tumor-infiltrating immune cells, and columns represent samples. **(B)** Expression levels of PD-1, PD-L1, and CTLA-4 in the three virus-related HCC subgroups. **(C)** Comparison of TME scores among IRG subgroups. **(D)** Abundance of 23 infiltrating immune cell types in the three virus-related HCC subgroups. *p<0.05; **p<0.01; ***p<0.001; ****p<0.0001; ns, not significant.

both the IRG score and the stage were significantly correlated with OS of the patient (Table S7). Furthermore, to uncover the prognostic significance of IRG score in virus-related HCC patients, the patients were assigned into different subgroups based on above clinical parameters. Totally, the high-risk patient's survival was generally poorer compared to low-risk patients (Figures S2A–F).

3.7 Establishment of nomogram model

As disclosed in Figure 6A, a nomogram was reciprocally constructed on the foundation of IRG scores, combined with clinical features. Followly, calibration curves defined the reliability and accuracy of nomogram to predict 3-, and 5-year prognosis (Figures 6B–D). As shown in Figures 6E–H, the AUC values were as expected, implying this nomogram had an excellent predictive ability for prognosis. Moreover, we also found that this prognostic model with diverse clinical factors presented more net benefits for predicting the prognosis.

3.8 Estimation of relation between TME and ICPs in inequable sectionalizations

We aimed to assess the relevance between IRG score and immune cells abundance with the CIBERSORT algorithm. As depicted in Figure 7A and Figure S3, the IRG score was significantly associated with the infiltration of B cells memory, Eosinophils, Mast cells activated, Monocytes, Plasma cells, T cells CD4 memory activated, T cells CD4 memory resting, B cells naive, Macrophages M2, Dendritic cells activated, NK cells resting, T cells CD4 naive, T cells gamma delta, T cells CD8, and T cells follicular helper, while the negative performance appeared in relationship with IRG score and Dendritic cells resting, Macrophages M0, and Neutrophils. Then, the correlation between immune cell infiltration and expression status of six genes incorporated with the prognostic model construction was analyzed in Figure 7B. Also, high-risk patients experienced higher EstimateScore and StromalScore levels than those in low-risk group (p<0.05) (Figure 7C). Meanwhile, IRG score was positively associated with the expression of a series of immune checkpoints (such as CD200,

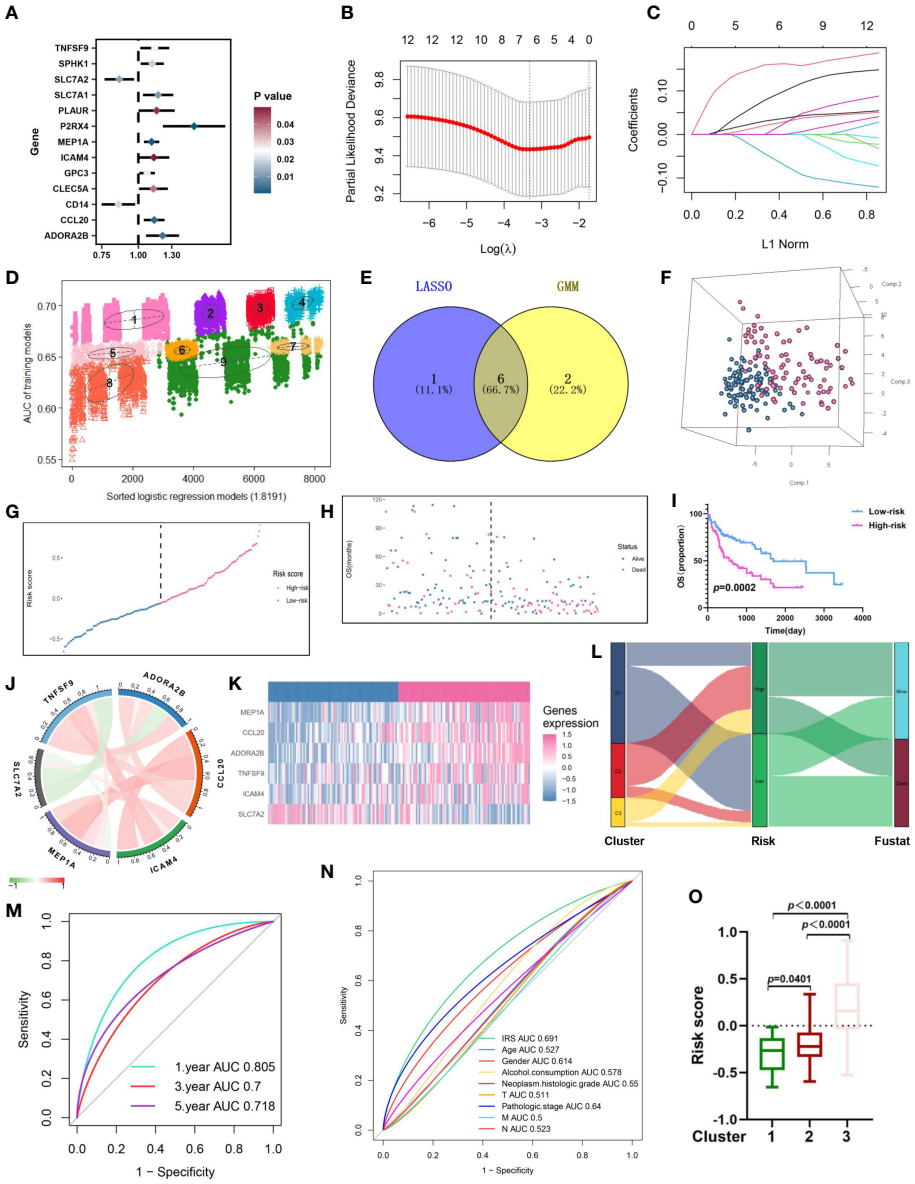

FIGURE 5
Construction of an inflammation-related risk model to predict the OS of virus-related HCC patients. **(A)** 13 prognosis-related IRGs screened by univariate Cox regression analysis (p<0.05). **(B)** The tuning parameter (λ) in the LASSO model is chosen by the minimum criterion. **(C)** LASSO coefficient distribution of 13 inflammation-related IRGs. **(D)** The pattern of the logistic regression model correlated with the AUC scores and was identified by a Gaussian mixture model. There are nine clusters of 8191 combinations. **(E)** Venn diagram of the shared genes by comparing LASSO model to GMM model. **(F-H)** Principal component analysis, risk score distribution, and survival status distribution for virus-related HCCs from TCGA-LIHC database. **(I)** Kaplan-Meier analysis of the OS between the high group and low group. **(J)** Co-expression network of the hub IRGs. **(K)** Expression patterns of 6 hub prognostic IRGs in high- and low-risk groups. **(L)** Alluvial diagram of subgroup distributions in groups with different IRG scores and clinical outcomes. **(M)** ROC curves for 1 year, 3 years and 5 years. **(N)** ROC analysis showed that the predictive accuracy of IRG was superior to other clinical features. **(O)** Differences in IRG score between the three gene clusters.

CD70, and PDCD1) (Figure 7E) and the enrichment scores of immunotherapy response-related gene signatures (Figure 7D). Furthermore, we assessed the relationship between ICPs and risk group, demonstrating that ICPs (PD-1, LAIR1, and VTCN1, et al) were inconsistently distributed in two risk clusters (Figure 7F).

3.9 IRG score-based tumor microenvironment, and stemness analyses

Present studies declared that ICP inhibitors were favorable to populations with increased TMB or higher MSI, uncovering that

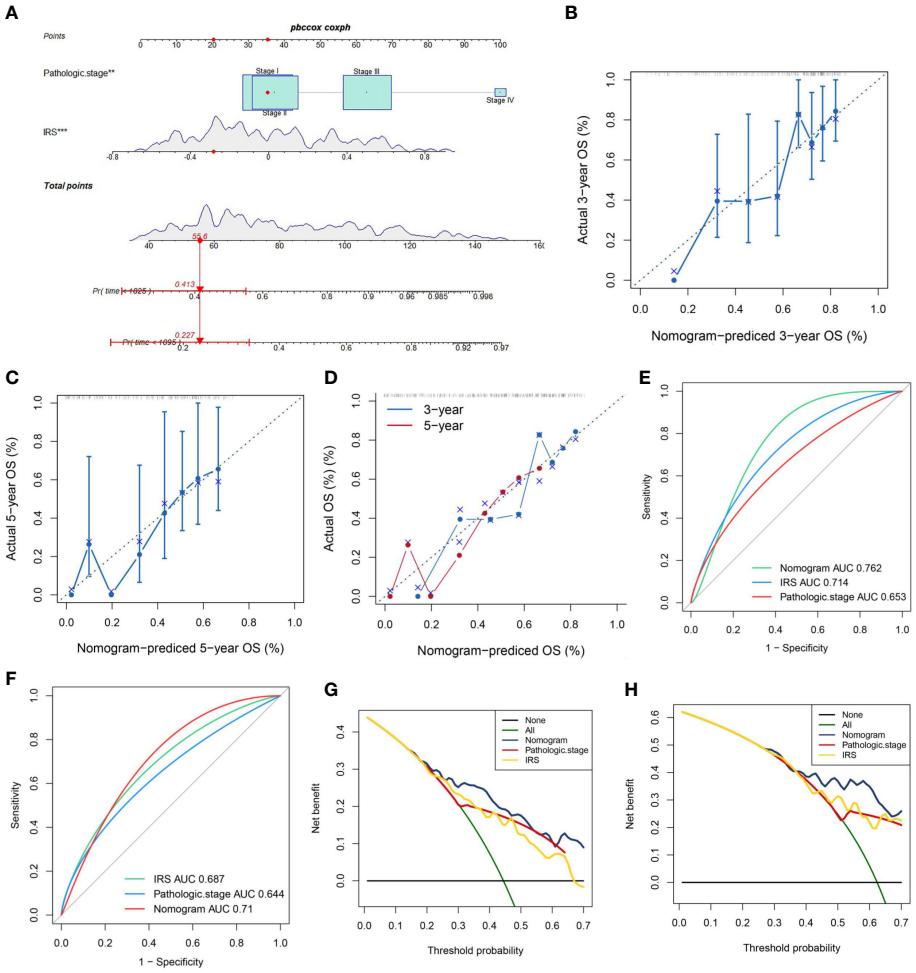

FIGURE 6
A Nomogram model' s Construction. **(A)** Nomogram combining pathological stage and risk score predicts 3-, and 5-years overall survival. **(B–D)** Calibration curves test the agreement between actual and predicted results at 1, 3, and 5 years. **(E, F)** Clinicopathological features and the predictive accuracy of the nomograms compared for 3–, and 5–year OS in virus-related HCC, respectively. **(G, H)** The DCA curves of the nomograms at 3–, and 5–year OS in HCC, separately.

TMB and MSI were both ponderable indexes for predicting tumor immune response (38, 39). As Figure 8A demonstrated, that TMB in the low-risk cluster was higher than high-risk cluster suggested that immunotherapy provided more benefits for patients with high risk. And a negative correlation was drawn between IRG score and TMB in spite of the meaningless value (R=-0.15, p=0.08, Figure 8B). To explore the impact of TMB status on prognosis in virus-related HCC patients, we also conducted survival analysis in various TMB classes. No significant difference of prognosis was revealed between High-TMB patients and low-TMB patients (Figure 8C). However, the survival analysis for combination of TMB and IRG score for virus-related HCC patients drew a conclusion that the prognostic benefit in the high-TMB group was eliminated by IRG score (Figure 8D). The measurement of RNA stemness score (RNAss) could represent cancer stemness, based on mRNA expression (40, 41). The relevance of IRG score and CSC score was presented in Figure 8E. Likewise, lower IRG score was connected with MSI-H pattern, while higher IRG score was linked with the microsatellite stable (MSS) pattern (Figure 8F), which also illustrated that low-risk patients may be more susceptive to immunotherapy. Meanwhile, genomic alterations in high and low groups were further analyzed. A rough similarity in the kinds of the top 30 genes with the highest mutation frequency between the low and high groups emerged (Figures 8G, H).

3.10 Drug sensitivity analysis

TIDE scores and IPS scores were conducted to make prediction for sufferers' responsiveness for appraising the immune response of virus-related HCC patients. Analysis results in Figures 9A,B revealed that patients at low-risk generated a lower TIDE score and a higher IPS score, which demonstrated that they may suffer more sensitivity from immunotherapy (42, 43). In the following, aimed at analyzing the clinical application of IRG model, we calculated the alterations in terms of drug sensitivity between diverse risk clusters, reflecting that 5-fluorouracil, AZ628, AZD7762, Bortezomib, Camptothecin, Cisplatin, Cyclopamine,

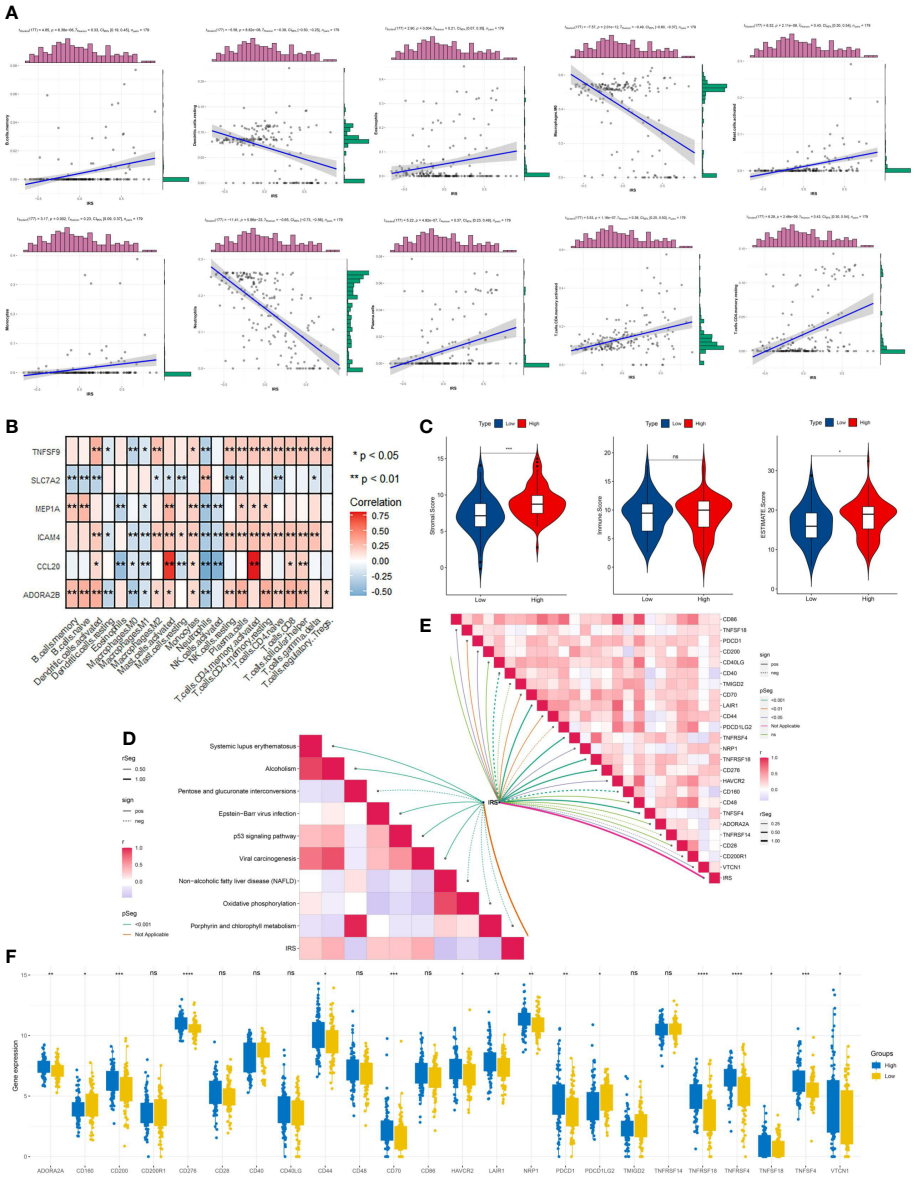

FIGURE 7
Immune signatures of different risk groups. **(A)** Correlations between IRG and immune cell types. **(B)** The correlations of immune cell infiltration and the hub six genes in the risk model. **(C)** Comparison of immune-related scores between low-risk and high-risk groups. **(D)** the association between IRG and the enrichment scores of immunotherapy response-related gene signatures or **(E)** IRG and the expression of many immune checkpoints. **(F)** The differentially expressed immune checkpoint-related genes between the high- and low risk groups. *p < 0.05, **p < 0.01, ***p < 0.001, ****p < 0.0001, ns, not significant.

Dasatinib, Docetaxel, MG-132, Nilotinib, Obatoclax Mesylate, Paclitaxel, PHA-665752, Sunitinib, Vinblastine, Vorinostat, and VX-680 yielded advantageous effectiveness for low-risk patients (Figure 9C).

3.11 Validation of the expression levels of hub genes *in vitro* experiment

qRT-PCR was applied to verify the mRNA expression levels of six hub genes in plasma samples from 58 virus-related HCC patients and 50 normal people. The unpaired t-test was performed to compute the differences between the virus-related HCC plasma samples and normal plasma samples. And plasma samples validated that the significant differences existed in the expression levels of CCL20, and SLC7A2 between HCC and normal tissues, that is, CCL20 was highly expressed in most HCC plasma samples while the expression of SLC7A2 was significantly higher in normal plasma samples than in virus-related HCC plasma samples (Figure 10A). Subsequently, we extracted total RNA from different tumor cell lines (SMMC7721, Huh7, HepG2, and HCCLM3) and the normal liver cell lines (WLR68, and LO2) to measure the mRNA expression levels of CCL20, and SLC7A2. qRT-PCR assays were implemented and the results showed that the

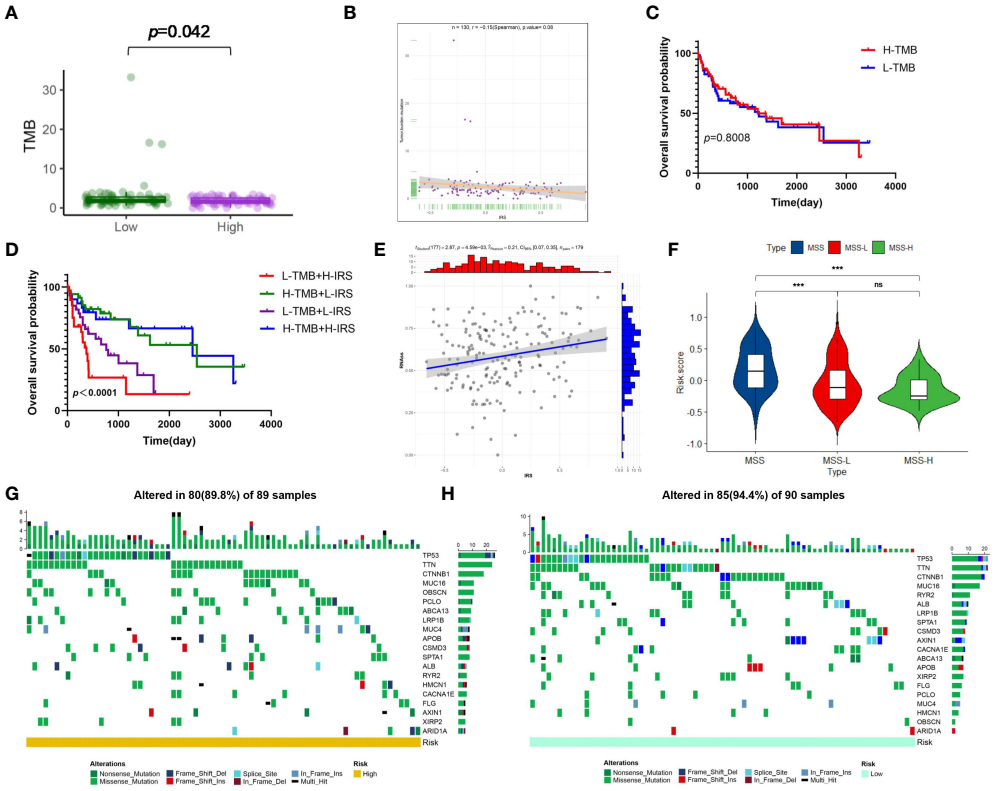

FIGURE 8
Risk signature-based tumor mutation burden (TMB), microsatellite instability (MSI), stemness analyses, and somatic mutation features. **(A)** The difference in TMB between the high- and low-risk groups. **(B)** Spearman's correlation analyses between IRG and TMB. **(C)** Kaplan–Meier analysis of the OS between the low- and high-TMB groups. **(D)** The comparison of OS among four subgroups stratified by both TMB and IRG score. **(E)** Correlation between IRG and mRNAsi scores (RNAss). **(F)** Relationships between IRG and MSI. The waterfall plot showing the differences in somatic genomic mutation between **(G)** the high- and **(H)** low-risk groups. *p < 0.05, **p < 0.01, ***p < 0.001, ns, not significant.

mRNA expression levels of CCL20 were significantly higher in liver cancer cells, like SMMC7721, Huh7, HepG2, and HCCLM3, than in normal cells, such as WLR68, and LO2. However, the consequence for SLC7A2 expression level was adverse (Figures 10B, C).

3.12 CCL20 knockdown combined with SLC7A2 overexpression inhibited tumor growth *in vivo*

To observe the function of CCL20 and SLC7A2 during hepatocarcinogenesis, CCL20 was silenced by transfection with shCCL20 in SMMC7721 cells. In addition, SLC7A2 was further overexpressed based on the SMMC7721 cells with silence of CCL20. First, we successfully constructed two lentiviral vectors harboring shRNA-CCL20-1, and shRNA-CCL20-2, respectively, and established two stable knockdown cell lines in SMMC-7721. The two different shRNAs, especially shRNA-CCL20-2, effectively knocked down the expression of CCL20. Also, SLC7A2 overexpression was indicated *in vitro* (Figures 10D, E). Afterwards, we examined the effect of shCCL20, overSLC7A2, and shCCL20/overSLC7A2 on the morphology of SMMC7721 cells. Compared with control cells, shCCL20 cells, and overSLC7A2 cells, showing a spindle-like shape with scattered growth, cells with knockdown of CCL20 combined with SLC7A2 overexpression induced a cobblestone-like appearance with the significant dispersion change (Figure 10F). Furthermore, the study established nude mouse tumor xenograft models injected by SMMC7721 cells that were transfected with shCtrl or shCCL20/overSLC7A2. Tumor volume was measured every 3 days (Figure 10G). We found that CCL20 knockdown combined with SLC7A2 overexpression significantly lessened the tumor volume (Figure 10H). After 30 days, we measured the tumor weight and observed that tumor weight was distinctly lowered by CCL20 knockdown combined with SLC7A2 overexpression (Figures 10I, J).

4 Discussion

Due to several factors, like vaccination policies and migration, virus infection sustains a health problem publicly and globally with changing epidemiology (44). Presently, virus infection has been documented by an incremental risk of developing chronic HBV infection (CHB), progression to liver fibrosis and end-stage liver disease (ESLD) and evolution of HCC (45). Despite great improvements in the matter of HCC treatment, tumor recidivation triggered by metastasis and drug resistance are still unamiable to HCC sufferers (46, 47). Thus, if we could make early

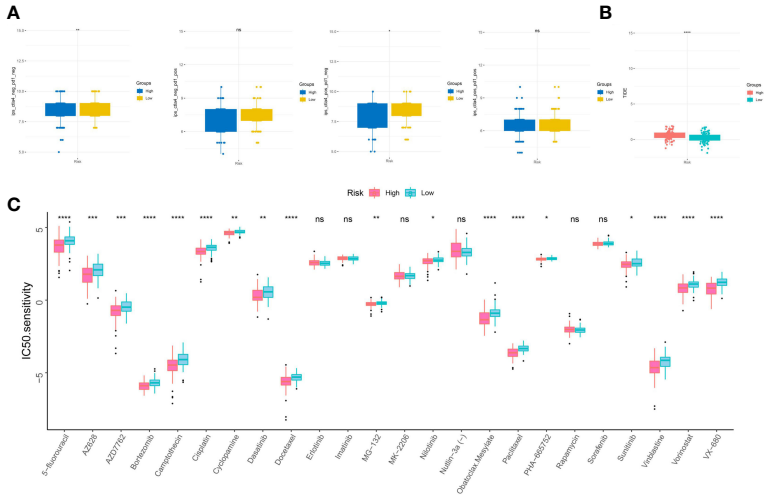

FIGURE 9
Sensitivity to drugs in virus-related HCC patients with different inflammation-related risk score subgroups. **(A)** immunophenotype score (IPS) and **(B)** tumor immune dysfunction and exclusion (TIDE) in different IRG score groups. **(C)** Relationships between IRG and chemotherapeutic sensitivity. *p < 0.05, **p < 0.01, ***p < 0.001, ****p < 0.0001, ns, not significant.

diagnosis and predict the therapeutic effect with a small number of biomarkers, the HCC sufferers would benefit a lot from the risk warning. Previous studies indicated that serum biomarkers, including circulating tumor cells or nucleic acids, and the combination of retinol and retinal panel had preeminent accuracy for HCC prognosis (48, 49). Also, inflammatory response-associated biomarkers in serum, such as medium-granulocyte ratio, platelet-lymphoid ratio and lymphoid-monocyte ratio, have an excellent performance to predict HCC prognosis (50). Accumulative evidence has testified the inevitable relationship between inflammation and intrinsic immunity (51), illustrating that inflammation targeting may serve a vital role to facilitate tumor immunotherapy. However, numerous reports have only emphasized a single inflammatory-related marker or a specific immune cell subtype. Besides, few studies concentrated on the association between inflammation and virus-related HCC. Hence, it is indispensable to clarify the holistic impact and TME infiltration characters regulated by the combinatorial action of disparate IRGs. All the IRGs based on Molecular Signatures Database (MSigDB) were accumulated and several HCC datasets, were applied systematically and comprehensively to filtrate the hub IRG DEGs to establish an inflammation-related model, for probing the distinction of risk models in immune cell infiltration, immune checkpoints, and drug sensitivity to offer clinical prognostic information and guide treatment for virus-related HCC patients.

In this study, 47 inflammation-related signatures were identified and analyzed in TCGA-LIHC database. The candidates were mainly enriched in immune response, IL-17 signaling pathway, TNF signaling pathway, and NF-kappa B signaling pathway. Consistent with other studies (52–55), Chronic inflammation and the presence of inflammatory cells (mainly macrophages) at the tumor site are highly correlated with specific malignancies. Also, cytokines, incorporating tumor necrosis factor (TNF) and Interleukins (IL), can regulate host responses to infection, immune, inflammation, and trauma. Besides, nuclear factor-kappa B (NF-kappa B) comprised of a series of transcription factors regulate the expression of numerous genes included in inflammation and cell proliferation. The results explain that inflammation converts not only inflammatory cells but also alters cytokines to act in collaboration with specific cytokine inhibitors and soluble cytokine receptors to regulate the immune response. Based on these signatures, consensus clustering analysis proved that patients could be divided into three clusters, and there were significant distinctions in the OS among them. The findings revealed that inflammation in virus-related HCC is heterogeneous and sufferers with diverse inflammatory patterns have disparate prognoses.

Subsequently, through the combination of univariable Cox regression analysis, GMM, and LASSO Cox regression analysis, we screened 6 survival-related key signatures, including Meprin A Alpha (MEP1A), CC chemokine ligand 2 (CCL2), Adenosine A2b receptor subtype (ADORA2B), Tumor necrosis factor superfamily member 9 (TNFSF9), Intracellular adhesion molecule 4 (ICAM4), and Solute carrier family 7 member 2 (SLC7A2). They all had been reported to be involved in inflammation or HCC progression previously (56–61). MEP1A, a zinc metalloprotease, was reported to participate in the regulation of inflammatory response and fibrosis. Further analyses verified that MEP1A played a crucial role to regulate cytoskeletal events and accelerated HCC cell proliferation, migration, and invasion (62). Also, In HCC patients, CCL2 was highly expressed and regarded as a prognostic factor. Farther blockade of CCL2/CCR2 signaling restrained liver tumour growth *via* stimulating T cell antitumor immune response (63). ADORA2B functioned as an endogenous feedback loop to dominate hypoxia-relevant inflammation, which was transcriptionally induced under hypoxia or inflammation by hypoxia-inducible transcription factor HIF1A (64). Furthermore, ADORA2B expression was negatively associated with OS of HCC patients. Accordingly, compared with control groups, mice treated with sorafenib in combination with ADORA2B blockage reagents emerged evident inhibition of tumor progression (65). TNFSF9, also known as

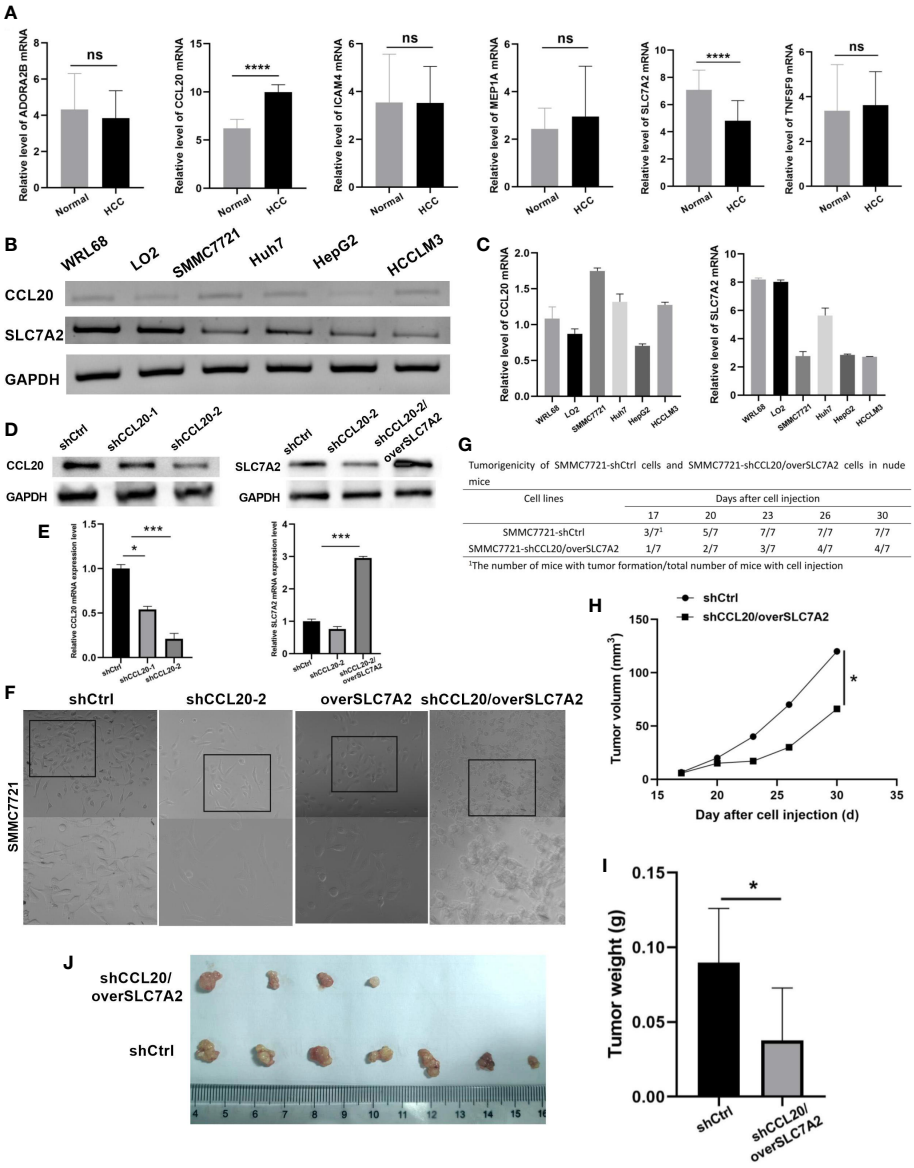

FIGURE 10
Validation of expression and tumorigenicity of hub genes. **(A)** qRT-PCR validation of MEP1A, CCL20, ADORA2B, TNFSF9, ICAM4, and SLC7A2 in HCC and normal plasmas. **(B, C)** The mRNA expression level of CCL20 and SLC7A2 in HCC cell lines (SMMC7721, Huh7, HepG2, and HCCLM3) and the normal liver cell lines (WLR68, and LO2) was indicated by qRT-PCR assays. **(D)** The protein and **(E)** mRNA expression of CCL20 and SLC7A2 was analyzed by western blotting and RT-PCR in stable SMMC-7721 cells expressing-shRNA against luciferase or CCL20 and over SLC7A2. **(F)** Morphology of HCC cells after knockdown of CCL20 and overexpression of SLC7A2. **(G)** Tumorigenicity of SMMC7721-shCtrl cells and SMMC7721-shCCL20/overSLC7A2 cells in nude mice. **(H)** Tumor volume was measured every 3 days after tumor formation in nude mice injected with SMMC7721 cells transfected with shCtrl or shCCL20/overSLC7A2. **(I, J)** Tumor weight was measured in nude mice injected with SMMC7721 cells transfected with shCtrl or shCCL20/overSLC7A2 after 30 days. *p < 0.05; **p < 0.01; ***p < 0.005; ****p < 0.0001, ns, not significant.

CD137L and 4-1BBL, had been exhibited in cancer immunotherapy in virtue of the role as a T-cell co-stimulator. Shen YL, et al. considered that TNFSF9 expression was downregulated in roughly 70% of HCC tissues. Thus, TNFSF9 may be a tumor suppressor, deemed as a therapeutic target for HCC (59). As for ICAM4, the studies uncovered that it was vital for immune synapse formation between NK cells and HCC cells to advance NK-mediated immunotherapeutic effects (60). SLC7A2, a member of the solute carrier family, was an independent risk factor for the prognosis of HCC patients if reduced. SLC7A2 Upregulation reduced HCC invasion and metastasis, whereas its downregulation boosted invasion and metastasis. Hence, SLC7A2 may offer novel mechanistic insight into the cancer-promoting property of HCC patients (61). The concrete mechanisms about the signatures in inflammation, immunotherapy, and drug reactivity of virus-related HCC sustained vague, which was one of the limitations of the study. We would continue to study them further in the future.

Based on the six genes, IRG score was calculated to construct a prognostic model for prediction of virus-related HCC patients. IRG score was obviously relevant to clinicopathological features of virus-related HCC. After confounding parameters were controlled, the results attested that IRG score was an independent predictor for virus-related HCC patients' prognosis. ROCs further showed its

prediction robustness for 1-, 3-, and 5-year OS. Thus, IRG score may generate a reliable capacity to make prediction for sufferers' prognoses. The accumulation of gene mutations leaded to carcinogenesis and was interrelated with inflammation (66). Our findings demonstrated that an apparent difference existed between low and high IRG score in terms of genomic alterations. Huo J, et al. confirmed that preferable prognosis originated from HCC patients with higher TMB (67). Although it is not imperfectly consistent with our findings to some extent, the prognostic benefit in the high-TMB group was eliminated by IRG score after combining TMB and IRG score for survival analysis. These findings further demonstrated the prognostic robustness of IRG score in virus-related HCC patients. Some clinicopathological characteristics, such as TNM stage, was also identified as an independent negative prognostic factor for patients. Therefore, we further constructed a nomogram using IRG score combined with TNM stage to better predict the survival of patients.

Current reports have ascertained crosstalk between cellular metabolic writing and TME remodeling (68, 69). Although numerous HCC patients produced a poor response to immunotherapy, the improvement of immune response efficiency had been the emphasis of immune research (70). In the present study, we quantified tumor inflammation through the calculated IGR score based on the construction of the IRM, objectively displaying the relationship between the inflammation reprogramming and immune microenvironment, aimed at conducting the distinct treatment methods of the two groups. For instance, CD4+, CD8+, B cells, and macrophage cells were infiltrated in the high-IRG subgroup. Also, immune interactions were pivotal characteristics of carcinogenesis and therapeutic target for HCC. In the TME, stromal cells and immune cells were the essential elements, which scores were connected with clinical characteristics and prognosis of HCC sufferers (71). We calculated these scores with the ESTIMATE algorithm and found that a high IRG score cluster significantly showed higher ESTIMATE and stromal scores than a low IRG score cluster. The results suggested that inflammation could be associated with the involvement of TME, thus regulating neoplastic occurrence and development. Therefore, to make quantification of tumor inflammation *via* the IRM may be beneficial to forecast immune responses and avert immunosuppressive therapy in sufferers, who do not respond immunologically.

HCC arises on the background of chronic liver disease. Despite the development of effective anti-viral therapeutics, HCC is continuing to rise. Thus, many patients present with advanced disease out with the criteria for transplant, resection or even locoregional therapy. For patients who are not candidates of curative treatments, locoregional therapies such as transarterial chemoembolization (TACE), transarterial radioembolization (TARE), and stereotactic body radiation (SBRT) can improve survival and quality of life. Sorafenib, a multi-kinase VEGF inhibitor, is the most widely used systemic chemotherapy approved as a first-line agent for unresectable or advanced HCC. Whilst checkpoint inhibitors are at the forefront of this revolution, other therapeutics such as inhibitory cytokine blockade, oncolytic viruses, adoptive cellular therapies and vaccines are emerging (72, 73). This study identified the potential sensitive drugs for patients in different IRG score groups, and the combination of these drugs and targeting angiogenesis may contribute to alleviating drug resistance and improving clinical outcomes. Furthermore, the effectiveness of immunotherapy requires specific biomarkers as a predictive pattern. TIDE and IPS signatures have been created to evaluate ICIs response. Accordingly, we observed that virus-related HCC patients with low IRG scores displayed low TIDE scores. All the above results demonstrate IRGs is an advantageously predictive tool in precision immunotherapy for virus-related HCC patients.

5 Conclusion

In conclusion, we have summarized the prognostic role of inflammation-related regulatory genes in virus-related HCC patients and then constructed a prognostic model based on IRGs involving six genes, which can accurately and stably predict survival and guide individualized treatment decisions in virus-related HCC patients. We further found that alterations in TME characteristics may be a potential mechanism of this model to predict the prognosis of virus-related HCC patients. Although we verified the stability of the risk model from multiple aspects, there are still some limitations. First, further studies with a large sample size are required to draw definitive conclusions. Furthermore, extensive prospective studies are necessary to gain insight into the relationship between risk scores and TME *in vivo* and vitro models.

Data availability statement

The original contributions presented in the study are included in the article/Supplementary Material. Further inquiries can be directed to the corresponding author.

Ethics statement

The studies involving human participants were reviewed and approved by the Ethical Committee of Chengdu Medical College approved the present study. Written informed consent was obtained from each participant by the institutional guidelines. The patients/participants provided their written informed consent to participate in this study. The animal study was reviewed and approved by the Ethical Committee of Chengdu Medical College approved the present study.

Author contributions

YH designed the study, performed bioinformatics and experiments. Y-jG analyzed the data and prepared the figures. YH wrote the manuscript. S-rL revised the manuscript. All of the authors read and approved the final manuscript.

Funding

This work is supported by the grants from The Special Project of Liyan Workshop Aesthetic Medicine Research Center of Chengdu Medical College (20YM008) and Chengdu Medical

College Foundation (CYZYB20-04), and Innovation and entrepreneurship training program for Sichuan Province College Students, Chengdu Medical College (S202013705095).

Acknowledgments

We thank all the participants of the laboratory for their kindness and help.

Conflict of interest

The authors declare that the research was conducted in the absence of any commercial or financial relationships that could be construed as a potential conflict of interest.

Publisher's note

All claims expressed in this article are solely those of the authors and do not necessarily represent those of their affiliated organizations, or those of the publisher, the editors and the reviewers. Any product that may be evaluated in this article, or claim that may be made by its manufacturer, is not guaranteed or endorsed by the publisher.

Supplementary material

The Supplementary Material for this article can be found online at: https://www.frontiersin.org/articles/10.3389/fonc.2023.1118152/full#supplementary-material

SUPPLEMENTARY FIGURE 1
Validation of prognostic models for six inflammation-related signatures. **(A–C)** risk score distribution, survival status, the expression level of hub genes, Principal component analysis, and Kaplan-Meier curves at different risk groups from ICGA database **(A)** and GSE84337 database **(B)**. *p < 0.05.

SUPPLEMENTARY FIGURE 2
The correlation analysis of IRG and clinicopathological variables and corresponding stratification analysis in virus-related HCCs. The correlation between IRG and **(A)** Age, **(B)** Alcohol consumption, **(C)** Gender, **(D)** TNM stage, **(E)** Fetoprotein, and **(F)** Radiation therapy and its corresponding OS analysis. *p < 0.05, **p < 0.01, ***p < 0.001.

SUPPLEMENTARY FIGURE 3
Correlations between IRG and immune cell types.

References

1. Tsai WL, Chung RT. Viral hepatocarcinogenesis. *Oncogene* (2010) 29(16):2309–24. doi: 10.1038/onc.2010.36

2. Ringelhan M, McKeating Jane A, Protzer U. Viral hepatitis and liver cancer. *Philos Trans R Soc Lond B Biol Sci* (2017) 372(1732):20160274. doi: 10.1098/rstb.2016.0274

3. Loureiro D, Tout I, Narguet S, et al. miRNAs as potential biomarkers for viral hepatitis b and c. *Viruses* (2020) 12(12):1440. doi: 10.3390/v12121440

4. Sadri Nahand J, Bokharaei-Salim F, Salmaninejad A, Nesaei A, Mohajeri F, Moshtzan A, et al. microRNAs: Key players in virus-associated hepatocellular carcinoma. *J Cell Physiol* (2019) 234(8):12188–225. doi: 10.1002/jcp.27956

5. Shlomai A, Jong YD, Rice CM. Virus associated malignancies: The role of viral hepatitis in hepatocellular carcinoma. *Semin Cancer Biol* (2014) 26:78–88. doi: 10.1016/j.semcancer.2014.01.004

6. Lee J, Tsai K-N, James OuJ-H. Mechanisms of hepatitis b virus-induced hepatocarcinogenesis. *Recent Results Cancer Res* (2021) 217:47–70. doi: 10.1007/978-3-030-57362-1_3

7. Stanislas P, Sylvie, et al. The remarkable history of the hepatitis c virus. *Genes Immun* (2019) 20(5):436–46. doi: 10.1038/s41435-019-0066-z

8. Okusaka T, Ikeda M, Morizane C, et al. Chemotherapy for hepatocellular carcinoma: Current status and future perspectives. *Jpn J Clin Oncol* (2018) 48(2):103–14. doi: 10.1093/jjco/hyx180

9. Zhao Y, Zhang YN, Wang KT, et al. Lenvatinib for hepatocellular carcinoma: From preclinical mechanisms to anti-cancer therapy. *Biochim Biophys Acta (BBA) - Rev Cancer* (2020) 1874(1):188391. doi: 10.1016/j.bbcan.2020.188391

10. Demir T, Lee SS, Kaseb AO. Systemic therapy of liver cancer. *Adv Cancer Res* (2021) 149:257–94. doi: 10.1016/bs.acr.2020.12.001

11. PJohnston M, Khakoo S. Immunotherapy for hepatocellular carcinoma: Current and future. *World J Gastroenterol* (2019) 25(24):2977–89. doi: 10.3748/wjg.v25.i24.2977

12. Keenan BP, Fong L, Kelley RK. Immunotherapy in hepatocellular carcinoma: the complex interface between inflammation, fibrosis, and the immune response. *J Immunotherapy Cancer* (2019) 7(1):267. doi: 10.1186/s40425-019-0749-z

13. Oura K, Morishita A, Tani J, Masaki T. Tumor immune microenvironment and immunosuppressive therapy in hepatocellular carcinoma: A review. *Int J Mol Sci* (2021) 22(11):5801. doi: 10.3390/ijms22115801

14. Nakatsu G. Toward a postbiotic era of microbiome science: Opportunities to advance immunotherapies for hepatocellular carcinoma. *J Gastroenterol Hepatol* (2022) 37(1):34–8. doi: 10.1111/jgh.15715

15. Woller N, Kühnel F. Virus infection, inflammation and prevention of cancer. *Rev Recent Results Cancer Res* (2014) 193:33–58. doi: 10.1007/978-3-642-38965-8_3

16. Read SA, Douglas MW. Virus induced inflammation and cancer development. *Cancer Lett* (2014) 345(2):174–81. doi: 10.1016/j.canlet.2013.07.030

17. J m C, Chew V. Impact of viral etiologies on the development of novel immunotherapy for hepatocellular carcinoma. *Semin Liver Dis* (2019) 40(2):131–42. doi: 10.1055/s-0039-3399534

18. Yang Y, Kim S, Seki E. Inflammation and liver cancer: Molecular mechanisms and therapeutic targets. *Semin Liver Dis* (2019) 39(1):26–42. doi: 10.1055/s-0038-1676806

19. Marc R, Dominik P, Tracy O, et al. The immunology of hepatocellular carcinoma. *Nat Immunol* (2018) 19(3):222–32. doi: 10.1038/s41590-018-0044-z

20. Demaria S, ikarsky E, Karin M, Eli P, Mathias H. Cancer and inflammation: Promise for biologic therapy. *J Immunotherapy* (2010) 3(4):335. doi: 10.1097/CJI.0b013e3181d32e74

21. Mathai AM, Alexander J, Kuo FY, Torbenson M, Swanson PE, Yeh MM. Type II ground-glass hepatocytes as a marker of hepatocellular carcinoma in chronic hepatitis b. *Hum Pathol* (2013) 44(8):1665–71. doi: 10.1016/j.humpath.2013.01.020

22. Prieto J. Inflammation, HCC and sex: IL-6 in the centre of the triangle. *J Hepatol* (2008) 48(2):380–1. doi: 10.1016/j.jhep.2007.11.007

23. Kumar RA, Biju P, Balasubramaniyan V. Increased systemic zonula occludens 1 associated with inflammation and independent biomarker in patients with hepatocellular carcinoma. *BMC Cancer* (2018) 18(1):572–. doi: 10.1186/s12885-018-4484-5

24. Reghupaty SC, Mendoza R, Sarkar D. AEG-1 targeting for inhibiting inflammation: potential anti-HCC strategy. *Oncotarget* (2019) 10(6):629–30. doi: 10.18632/oncotarget.26602

25. Esparza-Baquer A, Labiano I, Sharif O, Oakley F, Hijona E, Jimenez-Aguero R, et al. The anti-inflammatory receptor TREM2 halts the generation of HCC in mice through the inhibition of liver inflammation and hepatocyte proliferative responses. *J Hepatol* (2018) 68:S675–6. doi: 10.1016/S0168-8278(18)31610-6

26. Yu S, Wang Y, Jing L. Autophagy in the "inflammation-carcinogenesis" pathway of liver and HCC immunotherapy. *Cancer Lett* (2017) 411:82–9. doi: 10.1016/j.canlet.2017.09.049

27. Miao L, Zhang Z, Ren Z. Application of immunotherapy in hepatocellular carcinoma. *Front Oncol* (2021) 11:699060. doi: 10.3389/fonc.2021.699060

28. Linderman GC, Steinerberger S. Clustering with t-SNE. *J Mach Learn Res* (2019) 1(2):313–32. doi: 10.1137/18M1216134

29. Monti S, Tamayo P, Mesirov JP, Golub TR. Consensus clustering: A resampling-based method for class discovery and visualization of gene expression microarray data. (2003) 52(1-2):91–118. doi: 10.1023/A:1023949509487

30. Meng Z, Ren D, Zhang K, Wu H. Using ESTIMATE algorithm to establish an 8-mRNA signature prognosis prediction system and identify immunocyte infiltration-related genes in pancreatic adenocarcinoma. *Aging* (2020) 12(6):5048–70. doi: 10.18632/aging.102931

31. Wang Y, Hou H, Lin C, Kuo Y, Yao C, Hsu C, et al. A CIBERSORTx-based immune cell scoring system could independently predict the prognosis of patients with myelodysplastic syndromes. *Blood Adv* (2021) 5(22):4535–48. doi: 10.1182/bloodadvances.2021005141

32. Hu X, Shen F, Zhao Z, Qu X, Ye J. An individualized gait pattern prediction model based on the least absolute shrinkage and selection operator regression. *J Biomechanics* (2020) 112(16):110052. doi: 10.1016/j.jbiomech.2020.110052

33. Hui HQ, Ding LX, University W. Rapid robust clustering algorithm for Gaussian finite mixture model. *Comput Sci* (2013). doi: 10.1016/j.patcog.2006.09.012

34. Vickers AJ, Elkin EB. Decision curve analysis: A novel method for evaluating prediction models. *Med Decision Making* (2006) 26(6):565–74. doi: 10.1177/0272989X06295361

35. Mayakonda A, Lin DC, Assenov Y, Plass C, Koeffler HP. Maftools: Efficient and comprehensive analysis of somatic variants in cancer. *Genome Res* (2018) 28(11). doi: 10.1101/gr.239244.118

36. Paul G, Nancy C, Huang RS. pRRophetic: An r package for prediction of clinical chemotherapeutic response from tumor gene expression levels. *PLoS One* (2014) 9(9): e107468–e107468. doi: 10.1371/journal.pone.0107468

37. Munir T. Microscopic-observation drug-susceptibility assay for the diagnosis of TB. *New Engl J Med* (2006) 355(15):1539.

38. Samstein RM, Lee CH, Shoushtari AN. Tumor mutational load predicts survival after immunotherapy across multiple cancer types. *Nat Genet* (2019) 51(2):202–6. doi: 10.1038/s41588-018-0312-8

39. Sahin IH, Akce M, Alese O. Immune checkpoint inhibitors for the treatment of MSI-H/MMR-D colorectal cancer and a perspective on resistance mechanisms. *Br J Cancer* (2019) 121(10):809–18. doi: 10.1038/s41416-019-0599-y

40. Xu Q, Xu H, Chen S, Zhu Y, Huang W. Immunological value of prognostic signature based on cancer stem cell characteristics in hepatocellular carcinoma. *Front Cell Dev Biol* (2021) 9:710207. doi: 10.3389/fcell.2021.710207

41. Nishino K, Umezawa A. *Induced pluripotent stem cells from human extra-embryonic amnion cells: Role of DNA methylation in maintaining stemness*. Springer Netherlands (2012) 4:59–65.

42. Fu J, Li K, Zhang W. Large-Scale public data reuse to model immunotherapy response and resistance. *Genome Med* (2020) 12(1):21. doi: 10.1186/s13073-020-0721-z

43. Charoentong P, Finotello F, Angelova M, Mayer C, Efremova M, Rieder D, et al. Pan-cancer immunogenomic analyses reveal genotype-immunophenotype relationships and predictors of response to checkpoint blockade. *Cell Rep* (2017) 18 (1):248–62. doi: 10.1016/j.celrep.2016.12.019

44. Lampertico P, Agarwal K, Berg T, et al. Clinical practice guidelines on the management of hepatitis b virus infection. *J Hepatol* (2017) 67(2):370–98. doi: 10.1016/j.jhep.2017.03.021

45. Sarmati L, Malagnino V. HBV infection in HIV-driven immune suppression. *Viruses* (2019) 11(11):1077. doi: 10.3390/v11111077

46. Tang W, Chen Z, Zhang W, Cheng Y, Wang X. The mechanisms of sorafenib resistance in hepatocellular carcinoma: Theoretical basis and therapeutic aspects. *Signal Transduct Target Ther* (2020) 5(1):87.

47. Qin S, Bi F, Gu S, et al. Donafenib versus sorafenib in first-line treatment of unresectable or metastatic hepatocellular carcinoma: A randomized, open-label, parallel-controlled phase II-III trial. *J Clin Oncol* (2021) 39(27):3002–11. doi: 10.1200/JCO.21.00163

48. Tsuchiya N, Yu S, Endo I, Saito K, Uemura Y, Nakatsura T. Biomarkers for the early diagnosis of hepatocellular carcinoma. *World J Gastroenterol* (2015) 21 (37):10573–83. doi: 10.3748/wjg.v21.i37.10573

49. Han J, Han M-l, Xing H, et al. Tissue and serum metabolomic phenotyping for diagnosis and prognosis of hepatocellular carcinoma. *Int J Cancer* (2020) 146(6):1741–53. doi: 10.1002/ijc.32599

50. Yu JI, Park HC, Yoo GS, Paik SW, Nam H. Clinical significance of systemic inflammation markers in newly diagnosed, previously untreated hepatocellular carcinoma. *Cancers* (2020) 12(5):1300. doi: 10.3390/cancers12051300

51. Lin W-W, Karin M. Cytokine-mediated link between innate immunity, inflammation, and cancer. *J Clin Invest* (2007) 117(5):1175–83. doi: 10.1172/JCI31537

52. Ben-Baruch A. Inflammation-associated immune suppression in cancer: The roles played by cytokines, chemokines and additional mediators. *Semin Cancer Biol* (2006) 16(1):38–52. doi: 10.1016/j.semcancer.2005.07.006

53. Tanaka T, Narazaki M, Kishimoto T. IL-6 in inflammation, immunity, and disease. *Cold Spring Harbor Perspect Biol* (2014) 6(10):a016295. doi: 10.1101/cshperspect.a016295

54. Guijarro C, Egido J. Transcription factor-kappa b (NF-kappa b) and renal disease. *Kidney Int* (2001) 59(2):415–24. doi: 10.1046/j.1523-1755.2001.059002415.x

55. Dinarello CA. Proinflammatory cytokines. *Chest* (2000) 118(2):503–8. doi: 10.1378/chest.118.2.503

56. Ge W, Hou C, Zhang W, Guo X, Gao P, Song X, et al. Mep1a contributes to ang II-induced cardiac remodeling by promoting cardiac hypertrophy, fibrosis and inflammation. *J Mol Cell Cardiol* (2021) 152(5):52–68. doi: 10.1016/j.yjmcc.2020.11.015

57. Wang XM, Hamza M, Wu TX, Dionne RA. Upregulation of IL-6, IL-8 and CCL2 gene expression after acute inflammation: Correlation to clinical pain. *Pain* (2009) 142(3):275–83. doi: 10.1016/j.pain.2009.02.001

58. Ehrentraut H, A Westrich J, K Eltzschig H, Clambey ET, Tobias E. Adora2b adenosine receptor engagement enhances regulatory T cell abundance during endotoxin-induced pulmonary inflammation. *PLoS One* (2012) 7(2):e32416. doi: 10.1371/journal.pone.0032416

59. Yu LS, Yu G, Hai FG, et al. TNFSF9 exerts an inhibitory effect on hepatocellular carcinoma. *J Dig Dis* (2017) 18(7):395–403.

60. Miok K, Seon-Jin L, Sangsu S. Novel natural killer cell-mediated cancer immunotherapeutic activity of anisomycin against hepatocellular carcinoma cells. *Sci Rep* (2018) 8(1):10668–. doi: 10.1038/s41598-018-29048-8

61. Xia S, Wu J, Zhou W, Zhang M, Liao J. SLC7A2 deficiency promotes hepatocellular carcinoma progression by enhancing recruitment of myeloid-derived suppressors cells. *Cell Death Disease.Cell Death Dis* (2021) 12(6):570. doi: 10.1038/s41419-021-03853-y

62. Han-Yue O, Jing X, Luo J, Ru-Hai Zou Chen K, Le Y. MEP1A contributes to tumor progression and predicts poor clinical outcome in human hepatocellular carcinoma. *Hepatology* (2016) 63(4):1227–39. doi: 10.1002/hep.28397

63. Li XG, Yao WB, Yuan Y, Chen P, Li B, Li J, et al. Targeting of tumour-infiltrating macrophages *via* CCL2/CCR2 signalling as a therapeutic strategy against hepatocellular carcinoma. *Gut* (2017) 66(1):157–67. doi: 10.1136/gutjnl-2015-310514

64. Yuan XY, Mills TT, Doursout MF, Evans SE, Vidal Melo MF, Eltzschig HK, et al. Alternative adenosine receptor activation: The netrin-Adora2b link. *Front Pharmacol* (2022) 13:944994. doi: 10.3389/fphar.2022.944994

65. Liao J, Zeng DN, Li JZ, Hua QM, Xiao Z, He C, et al. Targeting adenosinergic pathway enhances the anti-tumor efficacy of sorafenib in hepatocellular carcinoma. *Hepatol Int* (2020) 14(1):80–95. doi: 10.1007/s12072-019-10003-2

66. Kay JE, Thadhani E, Samson LD, et al. Inflammation-induced DNA damage, mutations and cancer. *DNA Repair* (2019) 83:102673. doi: 10.1016/j.dnarep.2019.102673

67. Huo J, Wu L, Zang Y. A prognostic model of 15 immune-related gene pairs associated with tumor mutation burden for hepatocellular carcinoma. *Front Mol Biosci* (2020) 7:581354. doi: 10.3389/fmolb.2020.581354

68. Grawitz PB. Inflammation and cancer. *Nature* (2015) 420(6917):860–7.

69. Greten FR, Grivennikov SI. Inflammation and cancer: Triggers, mechanisms, and consequences. *Immunity* (2019) 51(1):27–41. doi: 10.1016/j.immuni.2019.06.025

70. Liu ZY, Liu X, Liang JX, et al. Immunotherapy for hepatocellular carcinoma: Current status and future prospects. *Front Immunol* (2021) 12:765101. doi: 10.3389/fimmu.2021.765101

71. Zhuang W, Zhang Z, Zhang S, et al. An immunogenomic signature for molecular classification in hepatocellular carcinoma. *Mol Therapy-Nucleic Acids* (2021) 25:105–15. doi: 10.1016/j.omtn.2021.06.024

72. Couri T, Pillai A. Goals and targets for personalized therapy for HCC. *Hepatol Int* (2019) 13(2):125–37. doi: 10.1007/s12072-018-9919-1

73. Foerster F, Gairing SJ, Müller L, et al. NAFLD-driven HCC: Safety and efficacy of current and emerging treatment options. *J Hepatol* (2022) 76(2):446–57. doi: 10.1016/j.jhep.2021.09.007

frontiers | Frontiers in Oncology

TYPE Original Research
PUBLISHED 22 March 2023
DOI 10.3389/fonc.2023.1142661

OPEN ACCESS

EDITED BY
Lujun Shen,
Sun Yat-sen University Cancer Center (SYSUCC), China

REVIEWED BY
Wen Chun-yong,
Sun Yat-sen University Cancer Center (SYSUCC), China
Jiacheng Lin,
Fujian Medical University, China

*CORRESPONDENCE
Pil Soo Sung
pssung@catholic.ac.kr

†These authors have contributed equally to this work

SPECIALTY SECTION
This article was submitted to Gastrointestinal Cancers: Hepato Pancreatic Biliary Cancers, a section of the journal Frontiers in Oncology

RECEIVED 11 January 2023
ACCEPTED 13 March 2023
PUBLISHED 22 March 2023

CITATION
Kwon MJ, Chang S, Kim JH, Han JW, Jang JW, Choi JY, Yoon SK and Sung PS (2023) Factors associated with the survival outcomes of patients with untreated hepatocellular carcinoma: An analysis of nationwide data.
Front. Oncol. 13:1142661.
doi: 10.3389/fonc.2023.1142661

Factors associated with the survival outcomes of patients with untreated hepatocellular carcinoma: An analysis of nationwide data

Min Jung Kwon[1†], Soy Chang[1†], Ji Hoon Kim[1†], Ji Won Han[1,2], Jeong Won Jang[1,2], Jong Young Choi[1,2], Seung Kew Yoon[1,2] and Pil Soo Sung[1,2*]

[1]Division of Gastroenterology and Hepatology, Department of Internal Medicine, College of Medicine, The Catholic University of Korea, Seoul, Republic of Korea, [2]The Catholic University Liver Research Center, College of Medicine, The Catholic University of Korea, Seoul, Republic of Korea

Introduction: In this study, we examined the natural course of untreated hepatocellular carcinoma (HCC) and identified predictors of survival in an area where hepatitis B is the predominant cause of HCC.

Methods: We identified 1,045 patients with HCC who did not receive HCC treatment and were registered in the Korean Primary Liver Cancer Registry between 2008 and 2014, and were followed-up up to December 2018. Thereafter, we analyzed the clinical characteristics of patients who survived for <12 or ≥12 months. A Cox proportional regression model was used to identify the variables associated with patient survival.

Results and discussion: The mean age of the untreated patients at HCC diagnosis was 59.6 years, and 52.1% of patients had hepatitis B. Most untreated patients (94.2%) died during the observation period. The median survival times for each Barcelona Clinic Liver Cancer (BCLC) stage were as follows: 31.0 months for stage 0/A (n = 123), 10.0 months for stage B (n = 96), 3.0 months for stage C (n = 599), and 1.0 month for stage D (n = 227). Multivariate Cox regression analysis demonstrated that BCLC stage D (hazard ratio, 4.282; P < 0.001), model for end-stage liver disease (MELD) score ≥10 (HR, 1.484; P < 0.001), and serum alpha-fetoprotein (AFP) level ≥1,000 ng/mL (HR, 1.506; P < 0.001) were associated with poor survival outcomes in patients with untreated HCC. In untreated patients with HCC, advanced stage BCLC, serum AFP level ≥1,000 ng/mL, and MELD score ≥10 were significantly associated with overall survival.

KEYWORDS

hepatocellular carcinoma, tumor stage, MELD score, fetoprotein (AFP), survival & prognosis

1 Introduction

Primary liver cancer is the sixth most commonly diagnosed cancer and the third leading cause of cancer-related deaths worldwide (1). Hepatocellular carcinoma (HCC) accounts for 75–85% of primary liver cancers and is a major healthcare issue (1, 2). The average crude incidence rate of HCC in Korea over the past 10 years was 22.4/100,000 person-years (3). Among patients in Korea, hepatitis B virus (HBV) infection is the leading cause of HCC (65%), followed by hepatitis C virus (HCV) (10%), and other causes (25%) (3–5). Despite advances in the diagnosis and treatment of HCC, prognoses following tumor development remain poor, with 5-year survival rates of 33.6% in the Republic of Korea and 18.1% in other Asian countries (3). Recent advances in immune-based therapies have enabled survival in patients with advanced HCC (6, 7).

To date, a considerable number of patients with HCC have remained untreated. A recent Korean study has addressed this issue. According to the results of a National Health Insurance Service database study in Korea, 27.6% of patients with HCC were left untreated between 2008 and 2013. In this study, the risk of mortality was higher for untreated patients in every subgroup, and the fully-adjusted hazard ratio (HR) for all-cause mortality comparing untreated to treated patients was 3.11 (95% confidence interval, 3.04–3.18) (8). However, this study employed an administrative claims dataset that lacked data pertaining to important clinical variables, such as performance status, Barcelona Clinic Liver Cancer (BCLC) stage, and tumor markers (8). Further research regarding clinical variables is necessary to determine the natural course of untreated HCC.

In an analysis of 128 hospitals by the United States (US) Veterans Administration, 24% of patients with HCC were untreated, and the median overall survival (OS) time was 3.6 months. This study also identified a model for end-stage liver disease (MELD) scores and alpha-fetoprotein (AFP) levels as prognostic factors in untreated patients, independent of the BCLC stage (9). Similarly, an analysis of an Italian liver cancer database that utilized data from 21 medical institutions showed that 11.7% of untreated patients had a median OS of 9 months (10). This study showed that female patients and those diagnosed with ascites or multinodular HCC were more likely to have advanced untreated HCC (10). However, it should be noted that both studies were performed with a largely HCV-positive cohort.

In this nationwide, multicenter, retrospective cohort study, we aimed to determine the natural course of untreated HCC in South Korea where HBV is the primary cause of HCC, and to identify predictors of survival in patients with untreated HCC. Data were obtained from a large, representative national cancer registry database that was based on random patient sampling and contained clinically important variables, such as laboratory findings, BCLC stage, and performance status.

2 Methods

2.1 Patients and study design

We used the KPLCR database, which contains hospital-based data from a randomly selected representative subset of patients with newly diagnosed HCC in Korea. The KPLCR contains data from approximately 15% of patients who were newly diagnosed with primary liver cancer and registered in the KCCR, a nationwide cancer registry that includes more than 95% of all cancer cases in Korea. Patients in the KPLCR were randomly selected from the KCCR using a probability proportional to size method after stratification by region within each year (11–13).

A total of 10,742 patients with HCC were identified using the KPLCR registry between 2008 and 2014. We excluded 29 patients with incomplete or missing data that were required for HCC diagnosis. We also excluded 4,038 patients with incomplete or missing data regarding major clinical parameters, such as BCLC stage and Child–Pugh class. Of the remaining patients, 5,630 had received at least one HCC-specific treatment and 1,045 had never received any HCC-specific treatment (Figure 1). We obtained data on the following characteristics of the 1,045 eligible patients from the KPLCR database: age, sex, BCLC stage, HCC etiology, Child–Pugh class, Eastern Cooperative Oncology Group (ECOG) performance status, initial serum AFP level, tumor count, tumor size, MELD score, portal vein invasion, encephalopathy, and ascites. HCC etiology was categorized as HBV, HCV, HBV and HCV co-infection, alcohol use, and others. HBV infection was confirmed by HBsAg positivity, HCV infection was confirmed by the presence of anti-HCV antibody (Ab) positivity, and HBV+HCV infection was confirmed by both HBsAg and anti-HCV Ab positivity. The initial serum AFP levels were dichotomized into ≥1000 ng/mL and <1000 ng/mL based on a previous study regarding factors predictive of "advanced" HCC (14–16). KPLCR is based on a national cancer registry program, in which all registered patients' dates of death are recorded. Therefore, it is certain that patients without a date of death were in fact alive at the end of follow-up. Survival time was defined as the time (in months) from HCC diagnosis to death or end of follow-up (31 December 2018).

2.2 Statistical analysis

Data are presented as numbers with percentages for categorical variables and as means or medians (interquartile range) for continuous variables. Comparisons of categorical variables between groups were performed using Pearson's chi-squared test. OS was calculated using the Kaplan–Meier method, and univariate analysis was performed using the log-rank test. Factors significantly associated with overall survival in the univariate analyses were considered potential input variables for the multivariate Cox proportional hazards regression analysis. We selected variables likely to be independent of one another concerning clinical interactions, followed by multivariate analysis to identify those that remained reliable predictors of survival in untreated patients with HCC. The results are presented as HRs with 95% confidence intervals. Statistical significance was set at $P < 0.05$. All statistical analyses were performed using SPSS software version 24.0 (SPSS Inc., Chicago, IL, USA).

3 Results

3.1 Baseline characteristics

Of the 6,675 patients with HCC, 1,045 did not receive any HCC-specific treatments, including resection, ablation, chemoembolization,

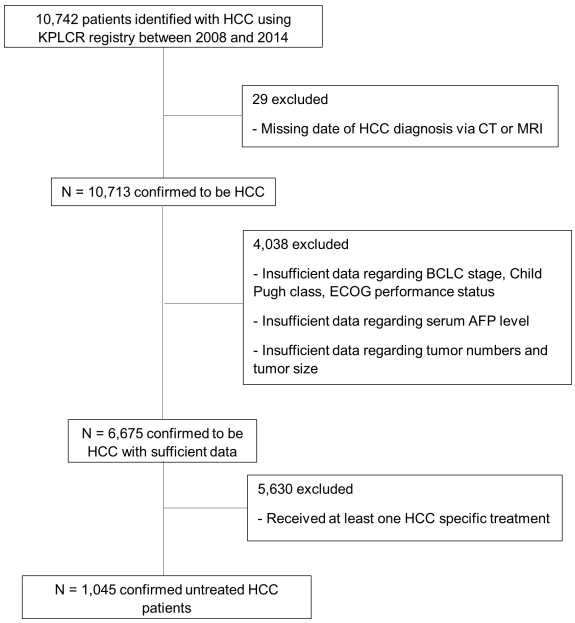

FIGURE 1
Flowchart showing the enrolment of study patients.

chemotherapy, or liver transplantation; the remaining 5,630 received at least one HCC-specific treatment (Figure 1). The study cohort consisted of the 1,045 untreated patients with HCC. The mean age at HCC diagnosis was 59.55 years, and 80.2% of patients were male. In total, 123 (11.7%) patients had BCLC stage 0/A, 96 (9.2%) had stage B, 599 (57.3%) had stage C, and 227 (21.7%) had stage D disease at the time of diagnosis (Table 1). Compared with patients with HCC who had received treatment, the untreated group was older and had a more advanced BCLC stage, higher Child–Pugh class, higher MELD score, and poorer performance status at diagnosis ($P < 0.001$; Table 1). The untreated group also had higher serum AFP levels, higher tumor counts, larger tumors, and greater portal vein invasion at diagnosis ($P < 0.001$; Table 1). The most common etiology of HCC was HBV infection in both the treated (n = 3598, 63.9%) and untreated (n = 544, 52.1%; Table 1) groups.

Most untreated patients died within the observation period, with a median survival time of 3.0 months. The median survival times for each BCLC stage were as follows: 31.0 months for stage 0/A (n = 123), 10.0 months for stage B (n = 96), 3.0 months for stage C (n = 599), and 1.0 month for stage D (n = 227).

Considering that we extracted information from a nationwide database maintained by the government, the registry did not provide information regarding why some patients did not receive treatment for HCC. Therefore, we categorized the baseline characteristics of untreated patients as BCLC stage 0/A, B, and C/D, to explore reasons untreated patients did not receive the treatments, especially in the early stages (0/A and B) (Supplementary Table 1). The early-stage group (stage 0/A and B) included more patients over 60 years old, which may have influenced their decision on whether to receive treatment.

3.2 Factors affecting 12-month survival and OS

A chi-squared test comparing groups of patients who survived for <12 months and those who survived for ≥12 months showed that the following characteristics were associated with decreased 12-month survival rates ($P < 0.001$; Table 2): BCLC stage D disease classification, Child–Pugh class C, MELD score ≥10, serum AFP level ≥1000 ng/mL, poor performance status, moderate-to-severe ascites, multiple tumors, large tumor size (≥5 cm), and portal vein invasion.

3.3 Univariate analysis for predictors of OS in untreated patients with HCC

According to the log-rank test, more advanced BCLC stage (A), more advanced Child–Pugh class (B), higher MELD score (C), higher serum AFP level (D), worse ECOG performance status (E), presence of ascites, history of encephalopathy, greater number of tumors (F), larger tumor size (G), and portal vein invasion (H) were reliable predictors of unfavorable OS ($P < 0.001$). However, the age (I), sex (J), and etiology (K) of HCC were not significantly associated with OS in patients with untreated HCC (Figure 2).

3.4 Multivariate analysis for predictors of OS in untreated patients with HCC

Two different multivariate analysis models were constructed based on a combination of factors that reliably predicted OS in the univariate analysis. Multivariate analysis model 1 (variables: BCLC

10.3389/fonc.2023.1142661

TABLE 1 Characteristics of HCC patients who received and did not receive any treatment.

	Received no treatment, n = 1045 (%)	Received treatment, n = 5630 (%)	*P* value
Age, y			< .0001
<60	457 (43.7)	2948 (52.4)	
≥60	588 (56.3)	2682 (47.6)	
Sex			0.309
Male	838 (80.2)	4433 (78.7)	
Female	207 (19.8)	1197 (21.3)	
BCLC stage			
0/A (very early, early)	123 (11.7)	2965 (52.6)	< .0001
B (intermediate)	96 (9.2)	681 (12.1)	
C (advanced)	599 (57.3)	1860 (33.0)	
D (end stage)	227 (21.7)	124 (2.2)	
Etiology			< .0001
HBV	544 (52.1)	3598 (63.9)	
HCV	102 (9.8)	608 (10.8)	
HBV+HCV	24 (2.3)	71 (1.3)	
Alcohol use	155 (14.8)	600 (10.7)	
Others	220 (21.1)	753 (13.4)	
Child-Pugh class			< .0001
A	469 (44.9)	4803 (85.3)	
B	428 (41.0)	748 (13.3)	
C	148 (14.2)	79 (1.4)	
ECOG performance status			< .0001
0	550 (52.6)	4547 (80.8)	
1	265 (25.4)	898 (16.0)	
2	119 (11.4)	131 (2.3)	
3	65 (6.2)	34 (0.6)	
4	46 (4.4)	20 (0.4)	
Serum AFP level (ng/ml)			< .0001
<1000	610 (58.4)	4565 (81.1)	
≥1000	435 (41.6)	1065 (18.9)	
Tumor no.			< .0001
Single	439 (42.0)	3639 (64.6)	
Multiple	606 (58.0)	1991 (35.4)	
Tumor size			< .0001
< 5cm	279 (26.7)	3734 (66.3)	
≥ 5cm	766 (73.3)	1896 (33.7)	
MELD score	(n = 984, missing = 61)	(n = 5471, missing = 159)	< .0001
<10	401 (40.8)	3945 (72.1)	
≥10	583 (59.2)	1526 (27.9)	
Portal vein invasion	517 (49.5)	4639 (82.4)	< .0001
No	528 (50.5)	991 (17.6)	
Yes			

stage, MELD score, and serum AFP) showed that BCLC stage D (HR, 4.282; $P < 0.001$), MELD score ≥10 (HR, 1.484; $P < 0.001$), and serum AFP level ≥1,000 ng/mL (HR, 1.506; $P < 0.001$) were associated with worse survival outcomes in untreated patients with HCC (Table 3). Multivariate analysis model 2 (variables: BCLC stage, serum AFP, and age) showed that BCLC stage D (HR = 5.155, $P < 0.001$) and serum AFP level ≥ 1,000 ng/mL (HR, 1.532; $P < 0.001$) were associated with worse survival outcomes in untreated patients with HCC (Table 3). Additionally, because of the increasing importance and correlation between metabolic syndrome and HCC, we also calculated hazard ratios of body mass index (BMI) and diabetes mellitus as variables associated with the prognosis of patients with untreated HCC. A BMI ≥ 25 kg/m^2 was also associated with better prognosis (Table 4).

10.3389/fonc.2023.1142661

TABLE 2 Potential determinants of survival among 1045 patients with untreated HCC.

	Total, N=1045	Survival <12 months, n = 810 (%)	Survival ≥12 months, n = 235 (%)	Mean survival months	*P* value
Age, y	457	368 (80.5)	89 (19.5)	12.77	0.047
<60	588	442 (75.2)	146 (24.8)	12.38	
≥60					
BCLC stage					< .0001
0/A (very early, early)	123	35 (28.5)	88 (71.5)	41.33	
B (intermediate)	96	50 (52.1)	46 (47.9)	22.08	
C (advanced)	599	505 (84.3)	94 (15.7)	8.87	
D (end stage)	227	220 (96.9)	7 (3.1)	2.64	
Etiology					0.001
HBV	544	446 (82.0)	98 (18.0)	11.57	
HCV	102	70 (68.6)	32 (31.4)	12.74	
HBV+HCV	24	18 (75.0)	6 (25.0)	10.42	
Alcohol use	155	106 (68.4)	49 (31.6)	16.5	
Others	220	170 (77.3)	50 (22.7)	12.37	
Child-Pugh class					< .0001
A	469	291 (62.0)	178 (38.0)	20.53	
B	428	376 (87.9)	52 (12.1)	7.26	
C	148	143 (96.6)	5 (3.4)	2.6	
MELD score	401	261 (65.1)	140 (34.9)	18.42	< .0001
(n = 984, missing = 61)	583	513 (88.0)	70 (12.0)	7.4	
<10					
≥10					
Serum AFP level (ng/ml)	610	417 (68.4)	193 (31.6)	17.25	< .0001
<1000	435	393 (90.3)	42 (9.7)	5.97	
≥1000					
ECOG performance status					< .0001
0	550	374 (68.0)	176 (32.0)	17.31	
1	265	220 (83.0)	45 (17.0)	9.49	
2	119	107 (89.9)	12 (10.1)	6.92	
3	65	64 (98.5)	1 (1.5)	2.57	
4	46	45 (97.8)	1 (2.2)	1.98	
Encephalopathy					0.015
(n = 1042, missing = 3)					
None	1006	773 (76.8)	233 (23.2)	12.85	
Mild (confusion)	27	26 (96.3)	1 (3.7)	4.41	
Severe (Stupor or coma)	9	9 (100.0)	0 (0.0)	1.44	
Ascites					< .0001
(n = 1037, missing = 8)					
None	523	339 (64.8)	184 (35.2)	19.64	
Mild	297	257 (86.5)	40 (13.5)	7.04	
Moderate to severe	217	208 (95.9)	9 (4.1)	3.28	
Tumor no.					< .0001
Single	439	297 (67.7)	142 (32.3)	18.48	
Multiple	606	513 (84.7)	93 (15.3)	8.26	
Tumor size					< .0001
< 5cm	279	148 (53.0)	131 (47.0)	15.84	
≥ 5cm	766	662 (86.4)	104 (13.6)	6.07	
Portal vein invasion	517	315 (61.0)	202 (39.0)	21.13	< .0001
No	528	495 (94.0)	33 (6.0)	4.16	
Yes					

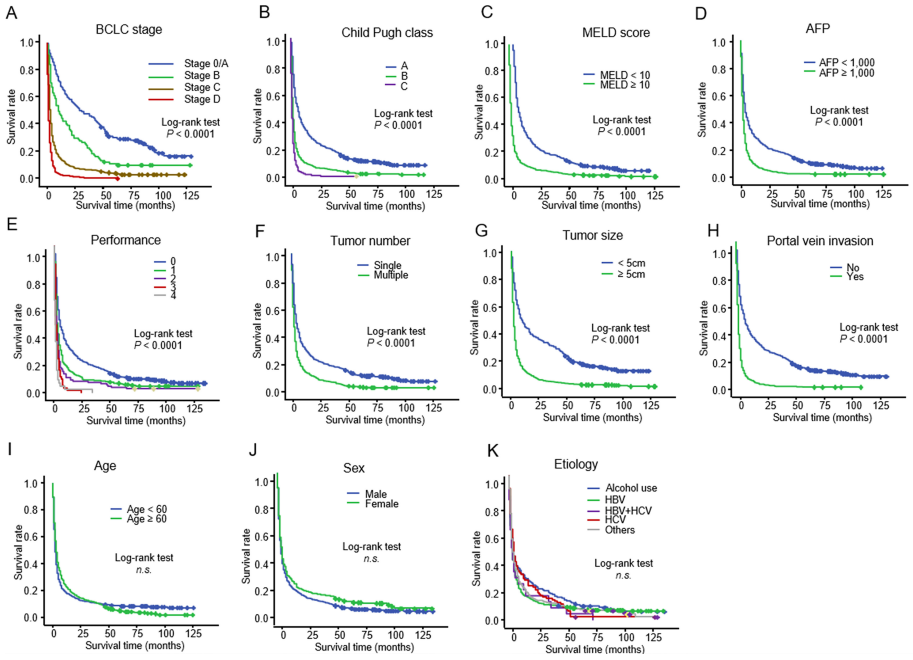

FIGURE 2
Kaplan–Meier curve showing the overall survival in 1,045 patients with untreated HCC stratified according to **(A)** BCLC stage: **(B)** Child–Pugh class: **(C)** MELD score: **(D)** serum AFP level: **(E)** ECOG performance score: **(F)** tumor number: **(G)** tumor size: **(H)** portal vein invasion: **(I)** age **(J)** sex: and **(K)** etiology HCC, hepatocellular carcinoma; BCLC, Barcelona Clinic Liver Cancer; MELD, model for end-stage liver disease; AFP, alpha-fetoprotein; ECOG, Eastern Cooperative Oncology Group.

4 Discussion

Investigating the natural course of untreated HCC is essential to determine the factors that affect prognosis and the role of HCC screening with respect to lead-time bias (17). To our knowledge, this is the largest study to use a nationwide cohort of more than 1,000 untreated patients with HCC with detailed clinical information. Multivariate Cox regression analysis showed that advanced stage BCLC, serum AFP level, MELD score, and lower BMI were significantly associated with poor survival outcomes in untreated patients with HCC.

Previously, a meta-analysis reviewed 68 articles regarding prognostic factors of untreated patients with HCC and found that ECOG performance score, Child–Pugh B-C classes, presence of portal vein thrombosis, and presence of ascites were associated with poor survival in intermediate/advanced BCLC stages. However, in many of the studies included in the meta-analysis, the causes of HCC were missing; HCV status was missing in 11 of the 30 randomized controlled trial (RCTs) reviewed, HBV status was missing in six RCTs, and the proportion of alcohol consumption was not reported in 13 RCTs (18). Another study conducted in the US between 2004 and 2011 (n = 518) demonstrated that in untreated patients with HCC, advanced BCLC stage (A vs. D), MELD score (10–19 vs. <10, ≥20 vs. <10), and AFP level (≥1000 vs. <10 ng/mL) were predictive of 12-month mortality (17). In this study, a high percentage of patients had HCV infection, which is the major cause of HCC in the US.

In our study, a large proportion of patients had HBV infection, which is the major cause of HCC in Korea. As mentioned above, HBV is the leading cause of HCC (65%), followed by HCV (10%) and other causes (25%) in Korea (3, 4, 19). This aspect is notable since the study mentioned above was conducted in US veterans between 2004 and 2011, and consisted of a population in which a majority (60.6%) of the HCC study population had HCV infection (17). The median OS in their study was 3.6 months, whereas the median OS observed in this study was 3.0 months (17). Moreover, a study by Sinn et al. suggested differences in the clinical characteristics of HCC according to etiology including HBV-driven HCCs and HCV-driven HCCs. According to the study, the median age of diagnosis of HCC was higher in HCV-driven HCCs and the tumor size larger; furthermore, the presence of portal vein invasion was more frequent in HBV-driven HCCs than in HCV-driven HCCs (20). Unfortunately, because the KCCR is an anonymous nation-wide database, the data we extracted from the KPLCR was limited by several drawbacks, including the antiviral treatment history of patients with HBV and HCV, and the period of alcohol abstinence etiology.

Several factors may explain why the untreated patients with HCC in our study chose not to be treated. First, untreated patients with HCC are older and thus may have been less prone to aggressive treatment. Second, compared to treated patients with HCC whose percentage of HBV infection is 63.5%, the proportion of HBV infection is of a smaller degree (53.5%), and the cause of carcinogenesis is more concentrated on alcoholism and others, such as non-alcoholic steatohepatitis (NASH) or autoimmune hepatitis. This may also be because compared with younger patients, older patients are more prone to NASH-induced liver cirrhosis. Moreover, patients with alcoholic liver diseases are less

10.3389/fonc.2023.1142661

TABLE 3 Multivariate Cox Proportional Hazards Regression Models of Factors Associated with Mortality in 1045 Patients With Untreated HCC.

#1	Overall mortality	
Variable	HR (95% CI)	*P* value
BCLC stage	Ref.	0.023
0/A	1.428 (1.050-1.942)	< .0001
B	2.561 (2.026-3.238)	< .0001
C	4.282 (3.272-5.604)	
D		
MELD score	Ref.	< .0001
<10	1.484 (1.289-1.708)	
≥10		
Serum AFP level (ng/ml)	Ref.	< .0001
<1000	1.506 (1.316-1.723)	
≥1000		
#2	Overall mortality	
Variable	HR (95% CI)	*P* value
BCLC stage	Ref.	0.023
0/A	1.429 (1.051-1.944)	< .0001
B	2.691 (2.130-3.399)	< .0001
C	5.155 (3.961-6.711)	
D		
Serum AFP level (ng/ml)	Ref.	< .0001
<1000	1.532 (1.338-1.754)	
≥1000		
Age, y	Ref.	0.078
<60	1.126 (0.987-1.284)	
≥60		

TABLE 4 Multivariate cox proportional hazards regression models of factors associated with mortality in 806 patients with untreated HCC with information on BMI and diabetes.

#1	Overall mortality	
Variable	HR (95% CI)	*P* value
BCLC stage	Ref.	0.142
0/A	1.293 (0.917-1.824)	< .0001
B	2.441 (1.879-3.172)	< .0001
C	3.878 (2.861-5.257)	
D		
MELD score	Ref.	< .0001
<10	1.538 (1.315-1.799)	
≥10		
Serum AFP level (ng/ml)	Ref.	< .0001
<1000	1.453 (1.249-1.690)	
≥1000		
BMI (kg/m^2)		
<25	Ref.	
≥25	0.750 (0.636-0.886)	0.001
Diabetes		
No	Ref.	
Yes	0.972 (0.826-1.143)	0.731

(Continued)

TABLE 4 Continued

#2	Overall mortality	
Variable	HR (95% CI)	*P* value
BCLC stage 0/A B C D	Ref. 1.322 (0.938-1.865) 2.566 (1.975-3.334) 4.789 (3.548-6.464)	0.111 < .0001 < .0001
Serum AFP level (ng/ml) <1000 ≥1000	Ref. 1.498 (1.287-1.743)	< .0001
Age, y <60 ≥60	Ref. 1.126 (0.971-1.307)	0.117
BMI (kg/m^2)		
<25	Ref.	
≥25	0.802 (0.678-0.949)	0.010
Diabetes		
No	Ref.	
Yes	0.964 (0.818-1.136)	0.660

compliant with treatment and surveillance than non-alcoholics, and alcoholics' socioeconomic status tends to be on the downside, and they tend to be diagnosed with progressive HCC when it is too late for treatment. Moreover, in South Korea, there is a single-payer system and the National Health Insurance Service covers the entire population; hence, the treatment rates are higher than those in other nations. However, even with the single-payer system in place, treatment availability has been shown to vary according to income. These factors may explain why our pool of patients chose not to be treated but considering our retrospective characteristic of our study, it in an inevitable limitation. In South Korea, a nationwide cancer screening program has been implemented and credited with enhancing the outcomes of patients with HCC over the last two decades (21, 22). This program has shown that HBV-induced HCC is highly prevalent, yet compliance with the screening program has been suboptimal (23). Targeted screening programs for high-risk cohorts could increase the treatment rates and enhance the outlook of individuals with HCC.

This study had some limitations. As data were gathered retrospectively, the HCC stages and some prognostic covariates may have been misclassified. We also do not know whether untreated patients received any etiology-specific treatment (e.g., antiviral therapy), which may have confounded the patients' liver function and overall survival. Our study is also biased towards the Korean population and further multinational studies will be needed, considering the differences that may exist, especially in the etiological origins of HCC.

5 Conclusion

For physicians treating patients with HCC, understanding the natural course of the disease is crucial. Using data from the Korean Primary Liver Cancer Registry of untreated patients with HCC from 2008 to 2014, we investigated those factors associated with prognosis. Overall, our study used a nationwide HCC registry to demonstrate that advanced BCLC stage, serum AFP level ≥1,000 ng/mL,MELD score ≥10, and higher BMI (≥25 kg/m^2) were significantly associated with overall survival in untreated patients with HCC. Further multinational studies will reveal the natural history of HCC in populations where HBV is not the main cause of HCC.

Data availability statement

Publicly available datasets were analyzed in this study. This data can be found here: Korean Primary Liver Cancer Registry.

Ethics statement

The studies involving human participants were reviewed and approved by Institutional Review Board of St. Mary's Hospital in Seoul. Written informed consent for participation was not required for this study in accordance with the national legislation and the institutional requirements.

Author contributions

JK, MK, and SC contributed in the study concept, study design, interpretation of data, writing up of the first draft of the paper, critical revision of the manuscript for important intellectual content. JW and JJ contributed in study design, data analysis, interpretation of data, critical revision of the manuscript for important intellectual content. JC and SY contributed in the study design, data analysis, interpretation of data, critical revision of the manuscript for important intellectual content. PS conceived the idea for this study and participated in the study concept, study design, interpretation of data, critical revision of the manuscript for important intellectual content. All authors contributed to the article and approved the submitted version.

Funding

This study was supported by the research fund of the Seoul St. Mary's hospital. This study was also supported by the Basic Science Research Program supported this research through the National Research Foundation of Korea (NRF) funded by the Korean government (MSIT; 2021R1C1C1005844 to PS).

Conflict of interest

The authors declare that the research was conducted in the absence of any commercial or financial relationships that could be construed as a potential conflict of interest.

Publisher's note

All claims expressed in this article are solely those of the authors and do not necessarily represent those of their affiliated organizations, or those of the publisher, the editors and the reviewers. Any product that may be evaluated in this article, or claim that may be made by its manufacturer, is not guaranteed or endorsed by the publisher.

Supplementary material

The Supplementary Material for this article can be found online at: https://www.frontiersin.org/articles/10.3389/fonc.2023.1142661/full#supplementary-material

References

1. Sung H, Ferlay J, Siegel RL, Laversanne M, Soerjomataram I, Jemal A, et al. Global cancer statistics 2020: GLOBOCAN estimates of incidence and mortality worldwide for 36 cancers in 185 countries. *CA Cancer J Clin* (2021) 71:209–49. doi: 10.3322/caac.21660

2. Reig M, Forner A, Rimola J, Ferrer-Fabrega J, Burrel M, Garcia-Criado A, et al. BCLC strategy for prognosis prediction and treatment recommendation: The 2022 update. *J Hepatol* (2022) 76:681–93. doi: 10.1016/j.jhep.2021.11.018

3. Chon YE, Jeong SW, Jun DW. Hepatocellular carcinoma statistics in South Korea. *Clin Mol Hepatol* (2021) 27:512–4. doi: 10.3350/cmh.2021.0171

4. Torimura T, Iwamoto H. Optimizing the management of intermediate-stage hepatocellular carcinoma: Current trends and prospects. *Clin Mol Hepatol* (2021) 27:236–45. doi: 10.3350/cmh.2020.0204

5. Sung PS. Crosstalk between tumor-associated macrophages and neighboring cells in hepatocellular carcinoma. *Clin Mol Hepatol* (2022) 28:333–50. doi: 10.3350/cmh.2021.0308

6. Baretti M, Kim AK, Anders RA. Expanding the immunotherapy roadmap for hepatocellular carcinoma. *Cancer Cell* (2022) 40:252–4. doi: 10.1016/j.ccell.2022.02.017

7. Trifylli EM, Koustas E, Papadopoulos N, Sarantis P, Aloizos G, Damaskos C, et al. An insight into the novel immunotherapy and targeted therapeutic strategies for hepatocellular carcinoma and cholangiocarcinoma. *Life (Basel)* (2022) 12:665. doi: 10.3390/life12050665

8. Kim YA, Kang D, Moon H, Sinn D, Kang M, Woo SM, et al. Survival in untreated hepatocellular carcinoma: A national cohort study. *PloS One* (2021) 16:e0246143. doi: 10.1371/journal.pone.0246143

9. Serper M, Taddei TH, Mehta R, D'Addeo K, Dai F, Aytaman A, et al. Association of provider specialty and multidisciplinary care with hepatocellular carcinoma treatment and mortality. *Gastroenterology* (2017) 152:1954–64. doi: 10.1053/j.gastro.2017.02.040

10. Giannini EG, Farinati F, Ciccarese F, Pecorelli A, Rapaccini GL, Di Marco M, et al. Prognosis of untreated hepatocellular carcinoma. *Hepatology* (2015) 61:184–90. doi: 10.1002/hep.27443

11. Lee JS, Cho IR, Lee HW, Jeon MY, Lim TS, Baatarkhuu O, et al. Conditional survival estimates improve over time for patients with hepatocellular carcinoma: An analysis for nationwide Korea cancer registry database. *Cancer Res Treat* (2019) 51:1347–56. doi: 10.4143/crt.2018.477

12. Yoon JS, Lee HA, Kim HY, Sinn DH, Lee DH, Hong SK, et al. Hepatocellular carcinoma in Korea: An analysis of the 2015 Korean nationwide cancer registry. *J Liver Cancer* (2021) 21:58–70. doi: 10.17998/jlc.21.1.58

13. Chon YE, Lee HA, Yoon JS, Park JY, Kim BH, Lee IJ, et al. Hepatocellular carcinoma in Korea between 2012 and 2014: An analysis of data from the Korean nationwide cancer registry. *J Liver Cancer* (2020) 20:135–47. doi: 10.17998/jlc.20.2.135

14. Lee J, Han JW, Sung PS, Lee SK, Yang H, Nam HC, et al. Comparative analysis of lenvatinib and hepatic arterial infusion chemotherapy in unresectable hepatocellular carcinoma: A multi-center, propensity score study. *J Clin Med* (2021) 10:4045. doi: 10.3390/jcm10184045

15. Sung PS, Jang JW, Lee J, Lee SK, Lee HL, Yang H, et al. Real-world outcomes of nivolumab in patients with unresectable hepatocellular carcinoma in an endemic area of hepatitis b virus infection. *Front Oncol* (2020) 10:1043. doi: 10.3389/fonc.2020.01043

16. Sung PS, Choi MH, Yang H, Lee SK, Chun HJ, Jang JW, et al. Diffusion-weighted magnetic resonance imaging in hepatocellular carcinoma as a predictor of a response to cisplatin-based hepatic arterial infusion chemotherapy. *Front Oncol* (2020) 10:600233. doi: 10.3389/fonc.2020.600233

17. Khalaf N, Ying J, Mittal S, Temple S, Kanwal F, Davila J, et al. Natural history of untreated hepatocellular carcinoma in a US cohort and the role of cancer surveillance. *Clin Gastroenterol Hepatol* (2017) 15:273–81.e1. doi: 10.1016/j.cgh.2016.07.033

18. Cabibbo G, Enea M, Attanasio M, Bruix J, Craxi A, Camma C. A meta-analysis of survival rates of untreated patients in randomized clinical trials of hepatocellular carcinoma. *Hepatology* (2010) 51:1274–83. doi: 10.1002/hep.23485

19. Sung PS, Park DJ, Roh PR, Mun KD, Cho SW, Lee GW, et al. Intrahepatic inflammatory IgA(+)PD-L1(high) monocytes in hepatocellular carcinoma development and immunotherapy. *J Immunother Cancer* (2022) 10:e003618. doi: 10.1136/jitc-2021-003618

20. Sinn DH, Gwak GY, Cho J, Paik SW, Yoo BC. Comparison of clinical manifestations and outcomes between hepatitis b virus- and hepatitis c virus-related hepatocellular carcinoma: Analysis of a nationwide cohort. *PloS One* (2014) 9:e112184. doi: 10.1371/journal.pone.0112184

21. Yim SY, Seo YS, Jung CH, Kim TH, Lee JM, Kim ES, et al. The management and prognosis of patients with hepatocellular carcinoma: What has changed in 20 years? *Liver Int* (2016) 36:445–53. doi: 10.1111/liv.12960

22. Im S, Jang ES, Lee JH, Lee CS, Kim BH, Chung JW, et al. Surveillance rate and its impact on survival of hepatocellular carcinoma patients in south Korea: A cohort study. *Cancer Res Treat* (2019) 51:1357–69. doi: 10.4143/crt.2018.430

23. The Korean Association for the Study of the Liver (KASL). KSL clinical practice guidelines for management of chronic hepatitis B. *Clin Mol Hepatol* (2022) 28:276–331. doi: 10.3350/cmh.2022.0084

frontiers | Frontiers in Oncology

TYPE Original Research
PUBLISHED 27 March 2023
DOI 10.3389/fonc.2023.1145380

OPEN ACCESS

EDITED BY
Lujun Shen,
Sun Yat-sen University Cancer Center (SYSUCC), China

REVIEWED BY
Qiao Zhou,
Sichuan Academy of Medical Sciences and Sichuan Provincial People's Hospital, China
Weijie Sun,
Anhui Medical University, China

*CORRESPONDENCE
Xiaochun Zhang
zxc9670@qdu.edu.cn

†These authors contributed equally to this work and share first authorship.

SPECIALTY SECTION
This article was submitted to Gastrointestinal Cancers: Hepato Pancreatic Biliary Cancers, a section of the journal Frontiers in Oncology

RECEIVED 16 January 2023
ACCEPTED 15 March 2023
PUBLISHED 27 March 2023

CITATION
Zhu J, Xu X, Jiang M, Yang F, Mei Y and Zhang X (2023) Comprehensive characterization of ferroptosis in hepatocellular carcinoma revealing the association with prognosis and tumor immune microenvironment. *Front. Oncol.* 13:1145380. doi: 10.3389/fonc.2023.1145380

Comprehensive characterization of ferroptosis in hepatocellular carcinoma revealing the association with prognosis and tumor immune microenvironment

Jingjuan Zhu[1,2†], Xiao Xu[1,2†], Man Jiang[1], Fangfang Yang[2], Yingying Mei[2] and Xiaochun Zhang[1*]

[1]Cancer Precision Medical Center, The Affiliated Hospital of Qingdao University, Qingdao University, Qingdao, China, [2]Qingdao Medical College, Qingdao University, Qingdao, China

Background: Ferroptosis is a type of regulatory cell death (RCD) mode that depends on iron-mediated oxidative damage. It has the potential to improve the efficacy of tumor immunotherapy by modulating the tumor microenvironment (TME). Currently, immunotherapy has significantly improved the overall treatment strategy for advanced hepatocellular carcinoma (HCC), but the distinct immune microenvironment and high tolerance to the immune make massive differences in the immunotherapy effect of HCC patients. As a result, it is imperative to classify HCC patients who may benefit from immune checkpoint therapy. Simultaneously, the predictive value of ferroptosis in HCC and its potential role in TME immune cell infiltration also need to be further clarified.

Methods: Three ferroptosis molecular models were built on the basis of mRNA expression profiles of ferroptosis-related genes (FRGs), with notable variations in immunocyte infiltration, biological function, and survival prediction. In order to further investigate the predictive impact of immunotherapy response in HCC patients, the ferroptosis score was constructed using the principal component analysis (PCA) algorithm to quantify the ferroptosis molecular models of individual tumors.

Results: In HCC, there were three totally different ferroptosis molecular models. The ferroptosis score can be used to assess genetic variation, immunotherapy response, TME characteristics, and prognosis. Notably, tumors with low ferroptosis scores have extensive tumor mutations and immune exhaustion, which are associated with a poor prognosis and enhanced immunotherapy response.

Conclusions: Our study indicates that ferroptosis plays an indispensable role in the regulation of the tumor immune microenvironment. For HCC, the ferroptosis

score is an independent prognostic indicator. Assessing the molecular model of ferroptosis in individual tumors will assist us in better understanding the characteristics of TME, predicting the effect of immunotherapy in HCC patients, and thus guiding a more reasonable immunotherapy program.

KEYWORDS

hepatocellular carcinoma, ferroptosis, molecular typing, prognosis, tumor microenvironment, immunotherapy

1 Introduction

Hepatic cancer, especially hepatocellular carcinoma (HCC), which accounts for more than 90% of primary hepatic tumors, is the third leading cause of tumor-related deaths worldwide (1). In recent years, immunotherapy such as immune checkpoint inhibitors (ICIs) has completely replaced systematic chemotherapy as the first-line treatment method for advanced HCC (2, 3). The adoption of the Atezolizumab-Bevacizumab protocol as standard treatment, in particular, heralds the beginning of a revolutionary age (4). However, the complex pathophysiology, distinctive heterogeneity, and high immunological tolerance of HCC contribute significantly to variation in the therapeutic impact of immunotherapy in patients (5, 6). Numerous mechanisms, including immune evasion, dysfunction of effector T lymphocytes, immunosuppression, and poor tumor antigen expression, are present in the microenvironment of HCC (6). Any of these potential processes could be a formidable impediment to immunotherapy. The occurrence and development of HCC are thought to be a multi-step process, and the precise molecular processes leading to the formation of HCC have traditionally been the focus of HCC research. In the past, many researchers have discussed it from different perspectives. For instance, the cholangiocarcinoma-like (CCL) signature (7), the hepatoblastoma 16 gene (HB16) signature (8), the NCI proliferation (NCIP) signature (9), the hepatic stem cells (HS) signature (10), the 65 genes recurrence risk score (RS65 score) (11), the Seoul National University recurrence (SNUR) signature (12), the Hippo pathway signature (13), and the Hoshida signature (14). These molecular typing based on multi-omic data elaborated the genetic and immunological characteristics of HCC patients from different perspectives, which is the cornerstone for directing accurate treatment. Therefore, it is essential to perform molecular classification of HCC patients who may benefit from immune checkpoint therapy.

Ferroptosis is distinct from cell necrosis, apoptosis, and autophagy (15, 16). Iron metabolism disruption and reactive oxygen species (ROS) buildup resulting in lipid peroxidation are the main factors contributing to ferroptosis (17). Induction of ferroptosis has emerged as a promising cancer treatment option in recent years, especially for refractory malignant tumors (18, 19). Ferroptosis-related lipid peroxides encourage dendritic cells to identify, phagocytose, and handle tumor antigens before presenting them to CD8+T lymphocytes as a recognition signal. CD8+T cells release IFN-γ, which inhibits the cystine absorption of tumor cells and activates cytotoxic T lymphocytes, hence enhancing tumor immunotherapy (20–22). These findings suggest that ferroptosis has a profound impact on TME and immunotherapy. Ferroptosis provides an innovative idea for the development of new candidate drugs for the treatment of refractory cancers. After acquired resistance to EGFR-TKIs, EGFR-mutated lung cancer cells showed increased sensitivity to ferroptosis inducers (23). Jiang et al. reported that TYRO3 can promote the development of the tumor microenvironment by reducing the ratio of M1/M2 macrophages while inhibiting TYRO3 can promote tumor ferroptosis and make drug-resistant tumors sensitive to PD-1 therapy (24). A recent study found that the small molecule MMRi62 can induce ferroptosis in pancreatic ductal adenocarcinoma (PDAC) cells carrying KRAS and/or p53 gene mutations, thus inhibiting tumor growth and preventing metastasis (25). These recent studies indicate that the induction of ferroptosis may overcome the drug resistance of targeting and immunotherapy. When transforming ferroptosis into clinical application, it will be particularly important to develop specific therapies that can induce ferroptosis in cancer cells while avoiding systemic adverse reactions. In this regard, nanoparticle ferroptosis inducers provide unique advantages (26). In 2021, the scientific research team led by Jianlin Shi proposed a non-ferrous ferroptosis-like strategy based on a hybrid CoMoO4-phosphomolybdic acid nanosheet (CPMNS). The ferroptosis-like cell death process is triggered by increasing ROS, depleting GSH (glutathione), and regulating GPX4 activity. Both *in vitro* and *in vivo* results have proved significant anticancer efficacy, indicating that this ferroptosis-like death strategy supported by CPMNS extends the applicability of the concept of ferroptosis to the process of ferroptosis-like death induced by non-ferrous metals, which will contribute to future progress in the field of cancer treatment programs (27). Last but not least, we currently lack biomarkers to mark ferroptosis in the body. The exploration of suitable biomarkers will facilitate the development of further *in vivo* research and clinical surveillance (28, 29).

The inflammatory state of TME has been proven to be essential for the occurrence, development, invasion, and metastasis of almost all solid tumors (30). In most cases, HCC is the result of chronic liver inflammation that leads to the formation of a complex TME composed of immune cells and stromal cells. TME involves the development of metastasis and drug resistance. This has become a challenge in the treatment of HCC patients because it influences the response to targeted and immunotherapy (31). In the past decade,

immunotherapy has developed rapidly and has been recognized as a key strategy for controlling the progression of malignant tumors. PD-1/PD-L1 inhibitors have been approved for many solid tumors and hematological malignancies, including non-small cell lung cancer, melanoma, urothelial carcinoma, esophageal carcinoma, renal cell carcinoma, and Hodgkin's lymphoma (32). According to the results of the IMbrave150 study, Atezolizumab combined with bevacizumab has been approved for the first-line treatment of unresectable locally advanced or metastatic hepatocellular carcinoma (33). Another promising immune checkpoint inhibitor treatment strategy is the combination of Durvalumab (PD-L1 inhibitor) and Tremelimumab (CTLA-4 inhibitor). PD-L1 and CTLA-4 are both inhibitory molecules expressed in T cells. Treatment with these two antibodies recently showed promising results in the phase III HIMALAYA clinical trial (NCT03298451). Their effectiveness in improving the survival of HCC patients highlights the role of T cells in the treatment of HCC (34). Chimeric antigen receptor T cell (CAR-T) therapy is an innovative type of tumor immunotherapy. Through genetic engineering technology, T cells can specifically recognize tumor-related antigens, thus exerting anti-tumor effects (35). To date, five CAR-T cell therapies have been approved for hematological malignancies. Several CAR-T therapies are currently undergoing clinical trials for HCC targeting a variety of surface and intracellular antigens (36). It is noteworthy that the characteristics of hypoxia and nutrient deprivation of TME have seriously weakened the adaptability and efficacy of CAR-T cells, emphasizing the need for more complex engineering strategies (36). Another new option for HCC immunotherapy is adaptive T cell transfer of gamma-delta T cells (γδ T cells). Low infiltration of γδ T cells in peritumoral liver tissue is associated with a higher recurrence rate of HCC and predicts postoperative recurrence (37). Adoptive transfer of allogeneic-γδ T cells in combination with local interventional therapy has an encouraging clinical effect against HCC and intrahepatic cholangiocarcinoma (ICC) (38). At present, many drugs targeting the tumor microenvironment are under development, including synthetic drugs, biotherapeutics, and vaccines. Personalized treatment regimens will be needed to achieve maximum clinical benefits for patients.

Epithelial-mesenchymal transformation (EMT) in TME was originally thought to primarily be associated with invasive metastasis of cancer cells, but new research has revealed that EMT is an important mechanism of tumor treatment resistance (39–41). Previous research has demonstrated that tumor microenvironment (such as hypoxia), numerous growth factors, and carcinogenic-associated signaling pathways (such as TGF-β, Notch, MAPK, and KRAS signaling pathways), can activate the EMT process (42–44). Mariathasan et al. gathered a set of EMT marker genes, including EMT1 (breast cancer) (45), EMT2 (urothelial carcinoma) (46), EMT3 (metastatic melanoma) (47), angiogenesis indicators (48), and WNT targets (49). They studied a large number of patients with urothelial carcinoma who were taking an anti-PD-L1 medication and discovered that a favorable immune response was connected to CD8+T effector cell phenotype and tumor mutation burden (TMB) (50). Schreiber et al. found that inhibition of glutathione peroxidase 4 (GPX4) induced ferroptosis in mesenchymal resistant cancer cells (51). Similar to GPX4-dependent mesenchymal resistant cancer cells, persistently drug-resistant cancer cells are also highly sensitive to ferroptosis (52). As a result, further understanding the role of ferroptosis in the tumor microenvironment and EMT regulation would aid in the investigation of tumor drug resistance mechanisms.

In this study, we screened three hub genes and performed pan-cancer analysis. The expression verification and survival analysis were carried out in the validation queue of our hospital. We structured three ferroptosis molecular patterns and found that their prognosis and TME characteristics were significantly different. Then we identified the ferroptosis scoring system, which can accurately predict the effect of immunotherapy, suggesting that ferroptosis has a significant impact on the treatment of advanced HCC.

2 Material and methods

2.1 Data collection

This study analyzed mRNA expression data and clinical information of 371 members in the TCGA-LIHC cohort available in The Cancer Genome Atlas (TCGA, https://portal.gdc.cancer.gov/repository) database. Additionally, 167 samples from the GSE76427 cohort were obtained from the Gene Expression Omnibus (GEO) database (https://www.ncbi.nlm.nih.gov/geo). To further validate the results, we analyzed the mRNA expression data of 240 samples from the International Cancer Genome Consortium (ICGC, https://dcc.icgc.org/) database.

The TCGA-LIHC copy number variation (CNV) information is derived from the UCSC Xena database (https://xena.ucsc.edu/). The TCGA-LIHC clinical information is derived from the UCSC Xena database and research published by the TCGA team in *Cell* (53). Afterward, FRGs were obtained from FerrDb, which consists of a database of ferroptosis regulators, markers, and associations between ferroptosis and various diseases (54). After removing duplicate genes, in all, 258 FRGs were available for analysis (Supplementary Table 1). In addition, the data contained in TCGA, GEO, ICGC, and FerrDb is publicly available. TCGA, GEO, and ICGC policies and guidelines for data acquisition and publication were strictly followed in the conduct of this study.

2.2 FRGs screening and protein-protein interaction network construction

The RNA high-throughput sequencing data in FPKM form was converted to TPM using the "TCGAbiolinks" (version, 2.26.0) R package (55). The "limma" (version, 3.54.0) package was used to analyze 373 HCC samples and 49 paracancerous tissues from the TCGA-LIHC cohort (56). Thus, differentially expressed FRGs were identified (FDR<0.01, |logFC|>1). Univariate Cox regression analysis was performed among FRGs, and p<0.01 was used as a screening condition to identify potential prognostic genes affecting overall survival (OS). Based on these FRGs, the PPI between proteins were generated by the STRING database. Following this,

hub genes were identified *via* Cytoscape (version, 3.9.0). The confidence score was set as a score<0.4.

2.3 Pan-cancer analysis

To analyze the differential expression and survival prediction of hub genes in 33 cancers, we collected gene expression information and relevant clinical data from the TCGA database for 33 tumor types.

2.4 Immunohistochemical analysis of clinical validation cohort

We obtained 69 surgical specimens of hepatocellular carcinoma and 41 matched paracancerous tissues from the Affiliated Hospital of Qingdao University (hereinafter referred to as our hospital), as well as the corresponding clinical information. To assess the expression levels of hub genes (HRAS, SLC7A11, and SLC2A1), immunohistochemistry (IHC) was accomplished by GTVisionTM III Detection Systems (Genetech, Shanghai, China) and antibodies (18295-1-AP, ab115730, ab37185) according to the manufacturer's instructions. The immunohistochemical staining was assessed by two pathologists who were uninformed of the clinical information. When their assessments differ, the third pathologist will undertake an independent examination. For each pathological section, we observed ten optical fields under a high-power lens (× 400). We took the IHC staining score as the final staining judged criteria. IHC staining score = staining area score × staining intensity score. The staining area score was estimated on a scale of 0-4 (0, ≤10%; 1, 11-25%; 2, 26-50%; 3, 51-75%; 4, ≥75%); the staining intensity score was classified as 0 (negative), 1 (weak), 2 (moderate), or 3 (strong). We grouped the IHC staining score to demonstrate the relationship between hub gene expression and patient survival. The IHC staining score below six was defined as low expression group, while the score over six was defined as high expression group. Moreover, the differences in IHC staining scores of hub genes between tumors and adjacent normal tissues were performed using the Wilcoxon rank sum test.

2.5 Identification of the ferroptosis molecular patterns

We recognized the ferroptosis molecular patterns on the basis of FRGs mRNA expression profiles by using the "ConsensusClusterPlus" package (57). The patients from the TCGA-LIHC and GSE 76427 were then classified for further investigation. The consensus clustering algorithm calculated the number and stability of clusters.

2.6 Enrichment of functional properties and TME immune infiltration in ferroptosis

In order to search for potential biological behaviors between ferroptosis molecular patterns, the GO and KEGG functional analyses were performed by "clusterProfiler" (version, 4.6.0) package (FDR<0.05).

From the MSigDB database, we obtained the gene set "c2.cp.kegg.v7.4.symbols" for our GSVA analysis by "GSVA" (version, 1.46.0) packages (FDR<0.05). In general, GSVA is an unsupervised, nonparametric approach for estimating the levels of variation within biological pathways and processes in expression datasets.

The mechanism of TME features generation was then investigated using a Single Sample Gene Set Enrichment Analysis (ssGSEA) (58). According to the expression of a set of tumor-infiltrating immune cells (TIICs) and immune function marker genes obtained from Bindea et al., the TIICs enrichment score and immune function of each HCC sample were quantitatively assessed. Mariathasan et al. identified and characterized a series of gene sets that relate to the following biological processes: antigen processing machinery; epithelial-mesenchymal transition (EMT) markers consisting of EMT1, EMT2, and EMT3; angiogenesis signature; Pan-fibroblast TGF-β response signature (Pan-FTBRS); WNT targets; FGFR3 related genes (Supplementary Table 2) (50). We retrieved associated gene sets from the MSigDB database, to further illuminate the processes by which ferroptosis influences the tumor immune microenvironment including the following: TGF-EMT down-regulation signal pathways; TGF-EMT up-regulation signal pathways; MAPK signal pathways; NOTCH signal pathways; KRAS up-regulation signal pathways; KRAS down-regulation signal pathways; hallmark-hypoxia; HIF-1 signal pathways to increase oxygen delivery; HIF-1 signal pathways to decrease oxygen consumption.

2.7 The ferroptosis score

We identified differentially expressed genes (DEGs) associated with the ferroptosis pattern through the "limma" package and screened prognostic genes using Univariate Cox regression models (p<0.05). We used principal component analysis (PCA) to quantify the ferroptosis molecular models of individual tumors and constructed a scoring system, which was termed the ferroptosis score. We defined the ferroptosis score as follows: Ferroptosis score =Σ (PC1i + PC2i), where i denotes the expression of prognostic DEGs associated with ferroptosis molecular models (59, 60). Patients were divided into low and high ferroptosis score groups in accordance with the threshold of -23.27889 established by "Survminer".

The independent prognostic value of the ferroptosis score was determined with Univariate and Multivariate Cox analysis. Next, a prediction model was constructed by integrating the ferroptosis score and other independent clinical risk factors according to the prognostic multivariate profile. A nomogram plot was used to visualize the relationship between the variables in the prediction model by following a certain scale in the same plane. A prognostic calibration plot was used for fit analysis of the model to the actual situation and to determine predictive efficacy.

2.8 Assessment of tumor mutation burden and immunotherapy response

Based on the MAF files, somatic mutation data was visualized using the "maftools" (version, 2.14.0) package (61). We calculated

the TMB of each patient as follows: TMB= (total count of variants)/(total length of exons).

In addition, Jiang et al. proposed TIDE method in order to simulate immune escape mechanisms in cancer, including T cell dysfunction and T cell rejection (62). In this study, TIDE was used to assess response to immunotherapy. A higher TIDE score not only indicates that the tumor has an immune avoidance phenotype, but also predicts a poor response to ICIs in cancer patients.

2.9 Chemotherapeutic drug sensitivity prediction

The sensitivity of ferroptosis to chemotherapeutic agents was assessed by the Genomics of Drug Sensitivity in Cancer (GDSC; https://www.cancerrxgene.org/) database (63). The half maximum inhibitory concentration (IC_{50}) was calculated by the "pRRophetic" (64).

2.10 Statistical analysis

We used Wilcoxon rank-sum tests for comparing the two groups and Kruskal-Wallis tests for assessing multiple comparisons. Based on the output from the "survminer" package, a dividing point was determined for each subgroup. In order to analyze the survival times of different subgroups, Kaplan-Meier curves and log-rank tests were used.

3 Results

3.1 The landscape of genetic variation of FRGs in hepatic cancer

A total of 258 ferroptosis-related genes (FRGs) were included in the analysis. We found that in the TCGA-LIHC cohort, 30.6% of FRGs (79/258), was differentially expressed in HCC tissues and non-tumor para-cancer tissues (FDR<0.01, |logFC|>1; Supplementary Table 3). As a result of a subsequent Univariate Cox regression analysis, 58 FRGs were correlated with overall survival (OS) (p<0.01; Supplementary Table 4). By cross-overlapping 79 differentially expressed FRGs and prognostic related genes, we obtained 32 differentially expressed prognostic related FRGs (Figure 1A). The forest map displayed the Hazard ratios of the 32 FRGs in the single-factor Cox regression analysis (Figure 1B). The heat map showed that the expression levels of 32 FRGs were significantly different between tumor tissues and normal tissues. FRGs were significantly enriched in tumor tissues (Figure 1C). We also examined the incidence of somatic mutations and copy number variations (CNVs) for FRGs. According to the position of the 32 FRGs on the chromosome, the CNV changes are shown in Figure 1D. As a result of the CNV variation frequency analysis, CNV variation was very common in FRGs, most of which focused on copy number amplification (Figure 1E). We found that CDKN2A had the highest frequency of mutation in HCC samples, followed by NARS (Figure 1F). The above analysis presented that the expression of FRGs in normal liver tissue and HCC tissue was highly heterogeneous, suggesting that the modifications in the expression of FRGs may contribute significantly to the occurrence and development of hepatocellular carcinoma.

3.2 Hub gene screening and Pan-cancer analysis

We generated a protein-protein interaction network (PPI) for FRGs and identified three hub genes *via* Cytoscape, including HARS, SLC7A11, and SLC2A1 (Figure 2A, Supplementary Figure 1A). These three FRGs showed significant differential expression in matched samples of cancer and Normal paracancerous tissue in TCGA-LIHC cohort (Figure 2B). Pan-cancer analysis demonstrated that these three FRGs were significant differential expression in most cancers (Figures 2C–E). The survival analysis of these three genes also showed their potential role in survival prediction (Figures 2F–H).

3.3 Clinical cohort verification

In order to evaluate the expression level of hub genes (HRAS, SLC7A11 and SLC2A1) in hepatocellular carcinoma, we conducted immunohistochemical (IHC) analysis. The expression of HRAS, SLC2A1, and SLC7A11 was positive in the majority of specimens from the validation cohort in our hospital. Among them, SLC7A11 has strongly stained in 38 (55.1%) specimens, HRAS was strongly stained in 41 (59.4%) specimens, and SLC2A1 was strongly stained in 32 (46.4%) specimens (Figure 3A; Supplementary Table 5). Finally, the Kaplan-Meier curve showed that patients with high gene expression had a shorter survival than patients with low gene expression (Figure 3B).

3.4 Ferroptosis molecular patterns with different TME features and function

According to the expression of the three FRGs in the TCGA-LIHC and GSE76427 cohorts, HCC patients were subdivided into three molecular patterns by unsupervised cluster analysis, termed ferroptosis clusters A, B, and C (A: n=194, B: n=107, C: n=236; Supplementary Figure 1B). It was demonstrated by the principal component analysis (PCA) that the three subtypes were entirely separate (Figure 4A). Among the three molecular patterns, the three FRGs were significantly highly expressed in cluster B, and appreciably low expressed in cluster A (Figure 4B). Prognostic analysis revealed an exceedingly favorable outcome in ferroptosis cluster A, whereas cluster B had the most detrimental prognosis (p<0.001; Figure 4C).

Afterward, we evaluated the correlation among these patterns and TME features. Immune cell infiltration varied greatly between the three molecular patterns, especially for ferroptosis cluster A, which was

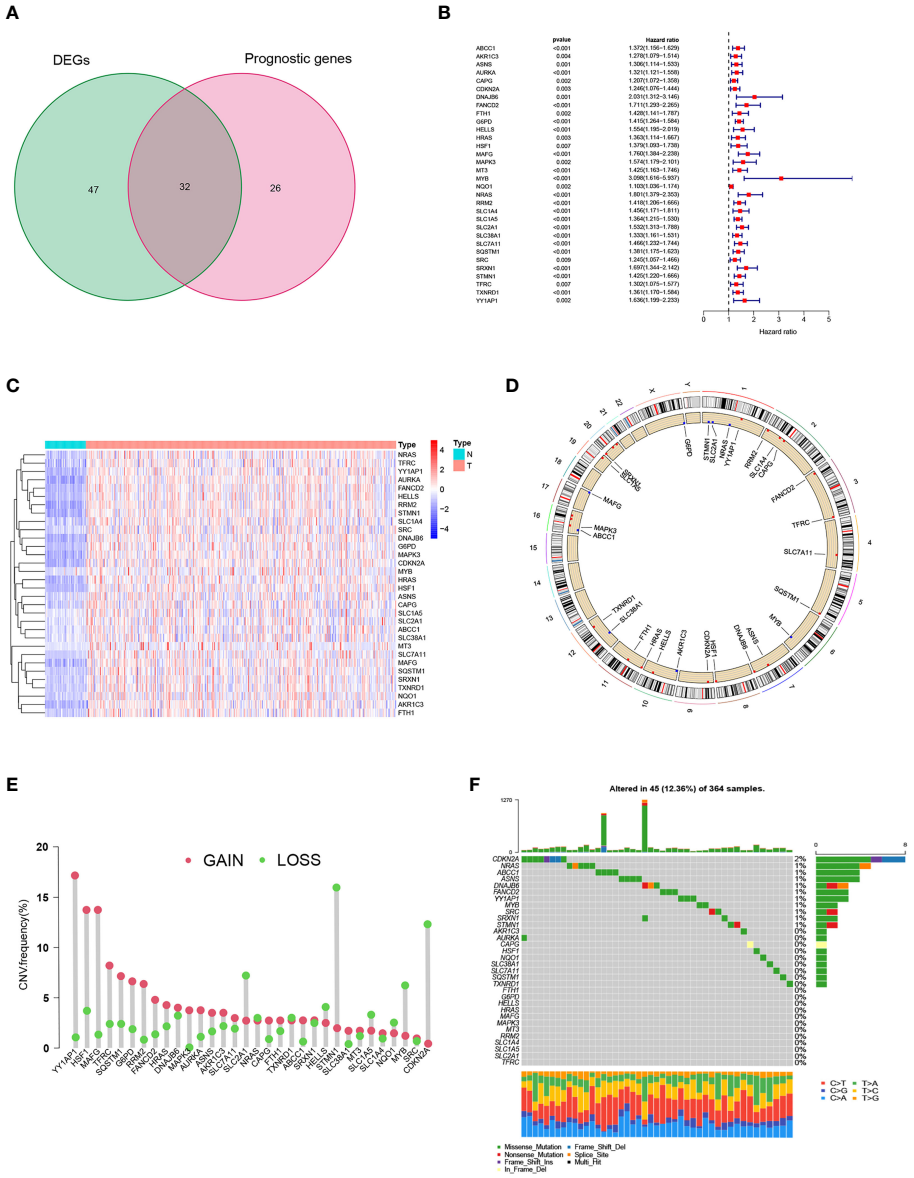

FIGURE 1
Prognostic ferroptosis-related gene (FRGs) differentially expressed in TCGA. **(A)** Venn graph showing the intersection of prognostic genes and differentially expressed genes. **(B)** Forest plots illustrating the Univariate Cox regression analysis of overlapping genes. **(C)** Expression of overlapping genes in tumor tissue. **(D)** CNV alteration locations for 32 FRGs. **(E)** The frequency of CNV variation of 32 FRGs. Alteration frequency was represented by the height of the column. Green dots indicating deletions; red dots indicating amplifications. **(F)** The mutation frequency of 32 FRGs in 364 patients with HCC. One patient was represented by each column. The upper bar plot indicated the extent of tumor mutations. Numbers on the right indicated the frequency of mutations in each gene. The right bar plot showed the proportions of the different types of variants. Stacked bar plot of each sample was able to show the fraction of conversions.

remarkably rich in NK cells and type-II IFN (IFN-γ) response. Ferroptosis cluster B was abounding in activated dendritic cells (aDCs), antigen-presenting cells (APCs), check-point, human leukocyte antigen (HLA), macrophages, regulatory T cells (Tregs), major histocompatibility complex (MHC) class I (Figure 4D). We also explored the relationship between ferroptosis clusters and various biological processes. The results manifested that EMT2, EMT3, antigen processing machinery, and WNT targets scored the highest in ferroptosis cluster B, as well as angiogenesis signature, which was significantly enriched in ferroptosis cluster A (Figure 4E). In particular, ferroptosis cluster B was found to be significantly enriched in hypoxia-related signaling pathways and EMT-related signaling pathways (such as TGF-β, MAPK, and KRAS signaling pathway) (Figure 4F). We further assessed the hypoxia status of the three ferroptosis molecular patterns using the Buffa Hypoxia Score and found equally significant differences (Supplementary Figure 1C) (65). Hypoxia and EMT are two important tumor microenvironmental biological processes that significantly affect the prognosis of HCC patients, which makes it necessary to pay attention to their relationship with ferroptosis. Their interaction may be an important clue to observing the effect of ferroptosis on immunotherapy and the prognosis of hepatocellular carcinoma.

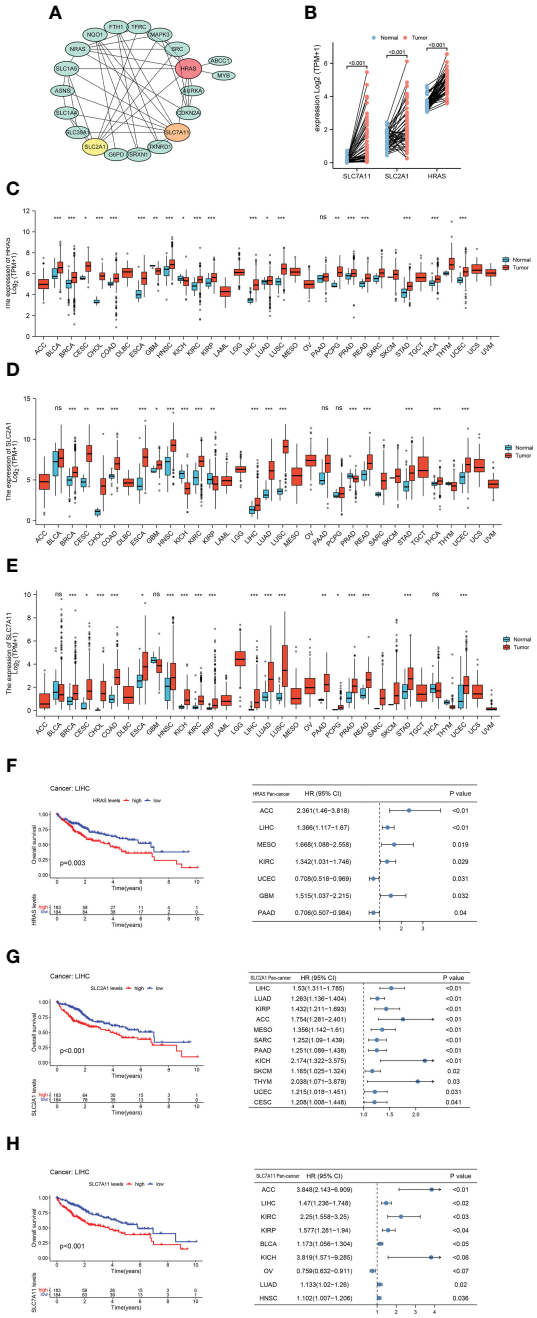

FIGURE 2
Hub Gene Screening and Pan-carcinoma Analysis. **(A)** Identified PPI hub genes. **(B)** Differential expression of HRAS, SLC2A1, and SLC7A11 in HCC paired samples. **(C)** Differential expression of HRAS in 33 cancers. ns, not significant; *p<0.05; **p<0.01; ***p<0.001. **(D)** Differential expression of SLC2A1 in 33 cancers. ns: not significant; *p<0.05; **p<0.01; ***p<0.001. **(E)** Differential expression of SLC7A11 in 33 cancers. ns: not significant; *p<0.05; **p<0.01; ***p<0.001. **(F)** Kaplan-Meier survival curve of HRAS and pan-carcinoma Univariate Cox regression analysis. **(G)** Kaplan-Meier survival curve of SLC2A1 and pan-carcinoma Univariate Cox regression analysis. **(H)** Kaplan-Meier survival curve of SLC7A11 and pan-carcinoma Univariate Cox regression analysis.

Subsequently, we explored the differences in ferroptosis molecular patterns in biological signaling pathways. As shown in Figure 4G, ferroptosis cluster A was markedly enriched in fatty acid metabolism, adipocytokine signaling pathway, glycolysis and gluconeogenesis, and PPAR signaling pathways. The ferroptosis cluster B presented enrichment pathways prominently related to the p53 signaling pathway, T cell receptor signaling pathway, adherens junction, mTOR signaling pathway, Oocyte meiosis, ubiquitin-mediated proteolysis, cell cycle, and DNA damage repair. Therefore, it is reasonable to speculate that cluster B may be associated with invasive HCC, while cluster A may be associated with metabolic disorders.

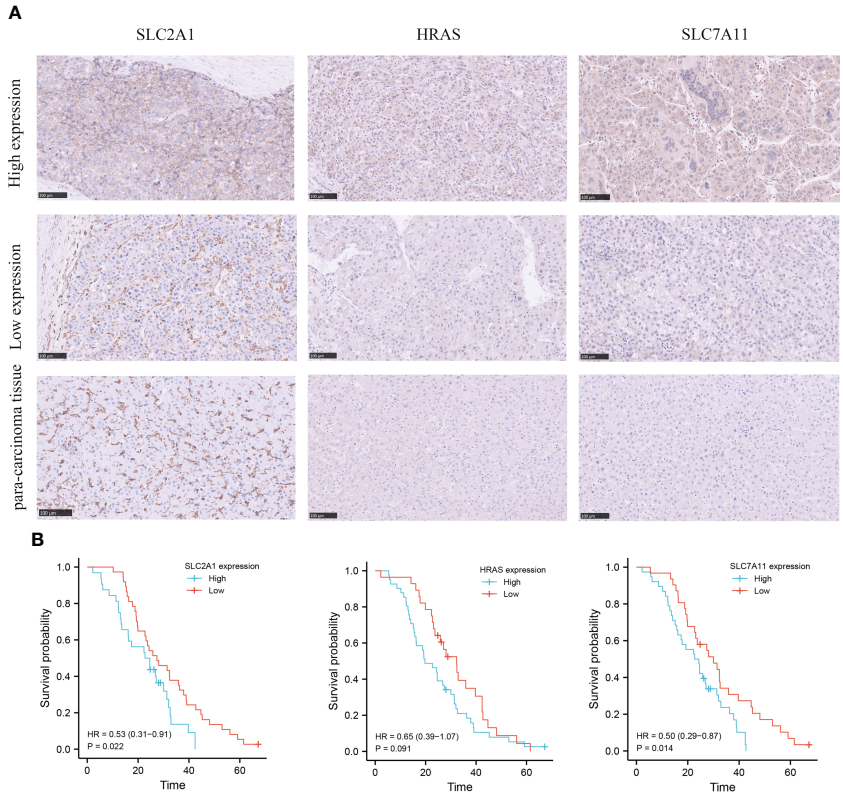

FIGURE 3
Immunohistochemical (IHC) analysis of clinical validation cohort. **(A)** Comparison of SLC2A1, HRAS, and SLC7A11 expression in HCC tissues and adjacent tissues. **(B)** Survival curves of HCC patients with high and low SLC2A1, HRAS, and SLC7A11 expression.

3.5 Generation of ferroptosis-related genomic patterns

As a means of further detecting potential biological processes among the ferroptosis molecular patterns, we determined 1139 DEGs related to ferroptosis molecular patterns, then performed GO and KEGG enrichment analysis (Figures 5A, B). As expected, DEGs were enriched in a number of molecular functions related to cell-substrate junction, focal adhesion, ficolin-1-rich granule, regulation of telomerase RNA localization to Cajal body, Fc epsilon RI signaling pathway, Cholesterol metabolism, which confirmed again that ferroptosis molecular patterns played an effective role in tumor immune activation, invasion and proliferation, and metabolic disorder.

In order to further verify the regulatory mechanism, the Univariate Cox analysis was conducted on these DEGs and screened out 794 prognostic DEGs (p<0.05). On the basis of these prognostic DEGs, we conducted an unsupervised cluster analysis, the TCGA-LIHC and GSE76427 patients were classified into three ferroptosis genomic patterns and we named them gene clusters A, B, and C (A: n=214, B: n=84, and C: n=239; Supplementary Figure 1D). Further investigation was carried out on the prognostic implications of ferroptosis gene clusters. In general, it was found that subjects in gene cluster A recorded a longer OS, whereas those in gene cluster B exhibited a more pessimistic outlook (p<0.001; Figure 5C). The expression of HRAS, SLC2A1, and SLC7A11 differed significantly between the three gene clusters, which also matched the expected outcomes of the ferroptosis molecular patterns (Figure 5D). The heatmap showed that ferroptosis-related genomic patterns were almost identical to the ferroptosis molecular patterns (Supplementary Figure 1E).

3.6 Construction of ferroptosis scoring system

However, our previous studies were based on patient populations. Considering individual heterogeneity and the complex mechanisms of HCC, we developed a PCA-based scoring algorithm to quantify the ferroptosis molecular pattern in individual patients, which we call the ferroptosis score. The ferroptosis scores in the ferroptosis clusters, as well as the gene clusters, were substantially different (p<0.01; Figures 5E, F). Ferroptosis cluster B patients had the poorest prognosis and the lowest ferroptosis score, as predicted, whereas cluster A patients had the opposite features (Figure 5E). The gene cluster produced the expected result in the ferroptosis score (Figure 5F).

3.7 Development of an independent prognostic model for HCC based on ferroptosis

We investigated the significance of the ferroptosis score in forecasting survival. Afterward, they were categorized into two groups: high ferroptosis and low ferroptosis (high group: n=423,

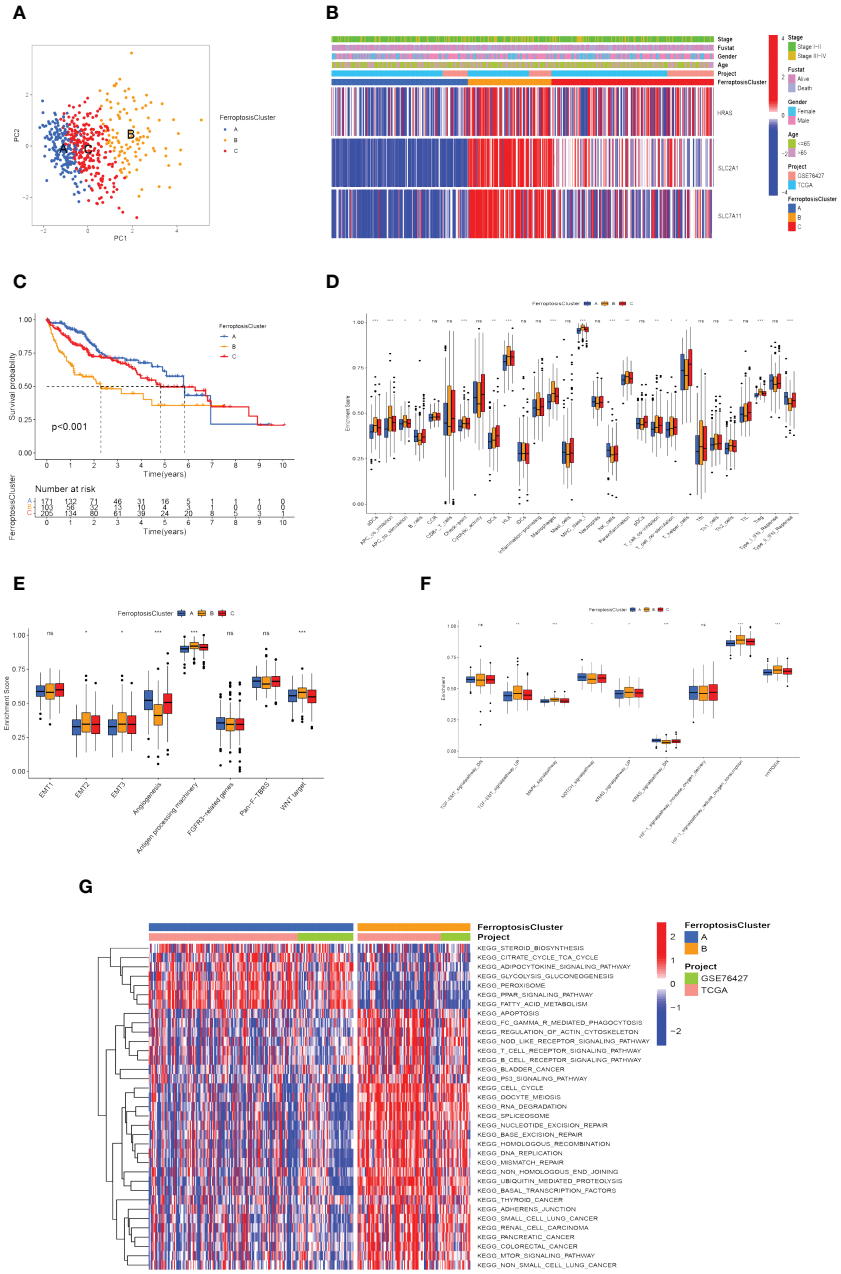

FIGURE 4
Recognition of ferroptosis molecular patterns with specific TME features and functional enrichment analysis. **(A)** Principal component analysis of hub gene expression profiles distinguished three ferroptosis clusters, A (blue), B (yellow), and C (red). **(B)** Heat map displaying the correlation between the hub genes expression and ferroptosis clusters. **(C)** Kaplan-Meier curves for the three molecular patterns of HCC patients. **(D)** Box plots displayed the levels of immune infiltration in the three patterns. ns, not significant; *p<0.05; **p<0.01; ***p<0.001. **(E, F)** Differences in stromal activation pathway **(E)** and carcinogenesis-related pathways **(F)** in the three ferroptosis clusters. ns, not significant; *p<0.05; **p<0.01; ***p<0.001. **(G)** GSVA analysis revealed distinct activations of biological pathways in ferroptosis clusters. Blue represented the inhibition pathway and red represented the activation pathway.

low group: n=61). Consistent with our previous research, TCGA and GEO samples with low ferroptosis scores implied a more adverse prognosis than those with high ferroptosis scores (p<0.001; Figure 6A). We also used the ICGC cohort for validation and obtained consistent results (p<0.001; Figure 6B). Ferroptosis score also showed good predictive power in other indicators of clinical benefit, for example, disease special survival (DSS), disease-free survival (DFS), and progression-free survival (PFS) (p<0.001; Figures 6C–H). In the univariate and multivariate cox regression analysis, the ferroptosis score showed significantly superior survival prediction ability compared with other molecular classifications in previous studies (Supplementary Figure 1F).

We further established a nomogram plot to verify the accuracy of the prediction of the ferroptosis score in HCC (Figure 6I). We assigned a risk score to each clinical risk variable, including stage, age, gender, and ferroptosis score. Compared with other clinical features, the highest number of risk points was contributed by the ferroptosis score (from -60 to 50). The calibration curve of 1-, 2-, and 3-year

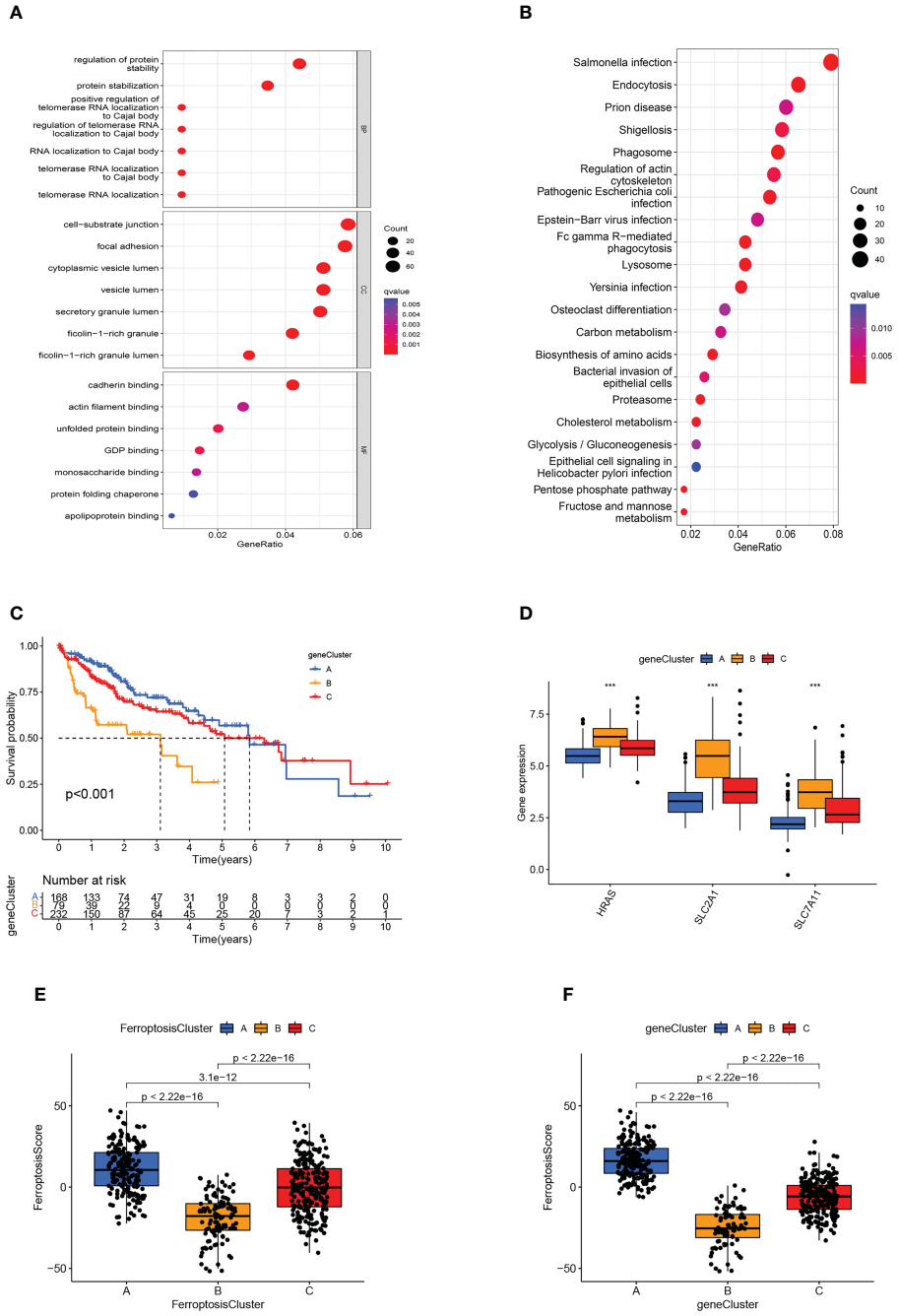

FIGURE 5
Generation of ferroptosis-related genomic patterns and the ferroptosis score. **(A, B)** GO **(A)** and KEGG **(B)** analysis based on differentially expressed genes. **(C)** Kaplan-Meier curves for the three gene clusters of HCC patients. **(D)** Box plots showed hub gene expression in the three gene clusters. ***p<0.001. **(E, F)** Box plots displayed the differences in ferroptosis scores among the three ferroptosis clusters **(E)** and the three gene clusters **(F)**.

OS was illustrated in Figure 6J. When compared to the actual situation, the predicted 1-year survival rate, 3-year survival rate, and 5-year survival rate of the model are close to the diagonal, indicating that the ferroptosis scoring model has a strong fitting effect.

3.8 Correlation between ferroptosis score and clinical features

We explored the relationship between clinical characteristics, molecular characteristics in previous studies and ferroptosis score group (Supplementary Table 6). Patients in the high score group have clinical features related to good prognosis (such as relatively low Child-Pugh classification, Stage, Grade, AFP). The median BMI of patients in the low ferroptosis score group was 22.80, while that in the high ferroptosis score group was 24.98. The Wilcoxon rank sum test showed statistically significant differences between the two groups (p=0.011).

We discovered that low score group patients had significant aggressive features and embryonic stem cell-like expression traits (ES signature), including CCL subtype (CCL feature), HB16 cluster

2, SOH subtype (HIPPO), HS subtype (NCIHS), high RS65 score, and NCIP cluster A (Supplementary Table 6). This indirectly confirmed that the ferroptosis molecular patterns may represent different developmental stages of HCC origin cells or different transformation mechanisms.

3.9 TMB characteristic of ferroptosis score

The waterfall plots showed the 20 genes with the highest mutation frequency in the somatic mutation data of patients in the TCGA-LIHC cohort. We compared the differences in mutation

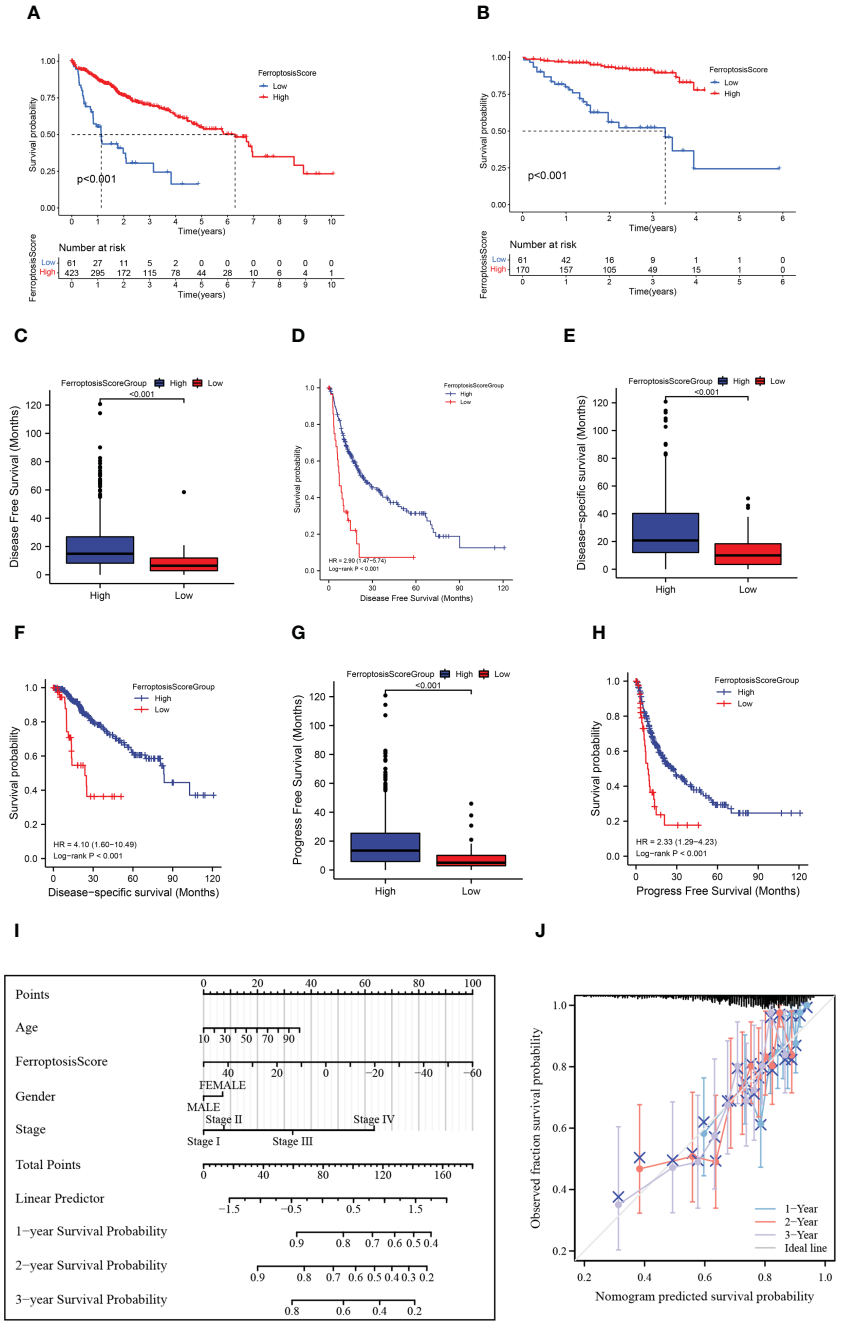

FIGURE 6
HCC prognosis based on the ferroptosis score. **(A, B)** Kaplan-Meier survival curves for the ferroptosis score groups in TCGA+GEO **(A)** and ICGC **(B)**. **(C)** Box plots showed the differences in disease-free survival (DFS) between ferroptosis score groups. **(D)** Kaplan-Meier curves for the ferroptosis score groups in disease-free survival (DFS). **(E)** Box plots showed the differences in disease special survival (DSS) between ferroptosis score groups. **(F)** Kaplan-Meier curves for the ferroptosis score groups in disease special survival (DSS). **(G)** Box plots showed the differences in progression-free survival (PFS) between ferroptosis score groups. **(H)** Kaplan-Meier curves for the ferroptosis score groups in progression-free survival (PFS). **(I)** Nomogram plot of prognostic multivariate regression model. **(J)** Prognostic Calibration plot evaluating the fit analysis of the model to the actual situation.

landscape between the two ferroptosis score groups. Figures 7A, B demonstrated that patients with low ferroptosis scores suffered from a greater tumor mutation burden than patients with high ferroptosis scores. It should be noted that the mutation frequency of TP53 in the low ferroptosis score group was significantly increased, and the ferroptosis score of TP53 mutant samples was also significantly lower than that of wild-type samples (p<0.01; Figure 7C). The association of TP53 mutations with poor prognosis is well known in many cancer types. In order to more accurately evaluate p53 functional status, the TCGA team developed a p53 signature (53). HCC patients with low p53 expression displayed a significantly reduced OS relative to their high p53 signature counterparts. We found that higher ferroptosis scores also had significantly elevated p53 signatures (Figure 7D).

The quantification analysis of TMB confirmed that low ferroptosis tumors had higher TMB levels (p=0.028; Figure 7E). The ferroptosis score and TMB were negatively correlated (p=0.019; Figure 7F). Further evidence showed that poor prognosis was strongly associated with high TMB and low ferroptosis scores (p<0.001; Figure 7G). Considering the synergistic effect of TMB and ferroptosis scores on the prognosis, we conducted a hierarchical prognostic analysis. We found that patients with high ferroptosis score and low TMB had a great survival advantage (p<0.001; Figure 7H). These data indicate that ferroptosis score combined with TMB can further improve the prognosis of patients.

3.10 Ferroptosis score, TME features, and response to immunotherapy

The single sample Gene Set Enrichment Analysis (ssGSEA) results showed that the ferroptosis score was significantly correlated with hypoxia, NOTCH, KRAS, and TGF-EMT signaling pathways (Figure 8A). An immune correlation analysis conducted in Figure 8B revealed a significant positive relationship between ferroptosis score and NK cells, T helper cells, type-I, and type-II IFN responses, and negatively correlated with immunosuppressive cell Tregs. Based on these findings, it was again confirmed that ferroptosis could affect tumor growth and progression by regulating the tumor microenvironment.

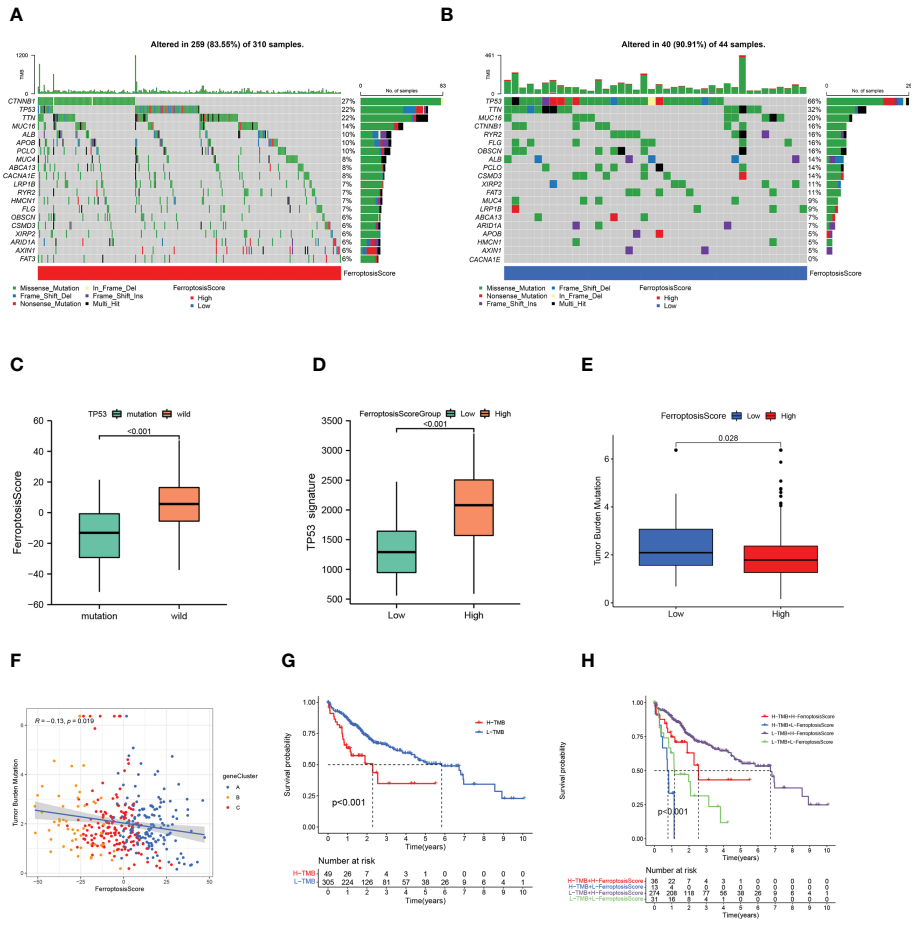

FIGURE 7
Ferroptosis score and tumor mutation burden. **(A, B)** Tumor somatic mutation waterfall plots established for those with high ferroptosis scores **(A)** and low ferroptosis scores **(B)**. **(C)** Box plot illustrated the difference of ferroptosis score between the TP53 mutation status. **(D)** Box plot illustrated the difference of p53 signature between the ferroptosis score groups. **(E)** Box plot illustrated the differences between the ferroptosis score groups in tumor mutation burden. **(F)** Relationships among ferroptosis score, tumor mutation burden, and gene clusters. **(G)** Kaplan-Meier curves of high and low tumor mutation burden patients. **(H)** Kaplan-Meier curves based on both the ferroptosis score and tumor mutation burden.

Basic research and clinical trials to exploring the predictive efficacy of immunotherapy biomarkers remain limited. To analyze the immunological response and tolerance to immunotherapy in HCC patients, we chose CD274, CTLA4, LAG3, HAVCR2, IDO1, and PDCD1 as immune checkpoint-related signatures and CD8A, CXCL10, GZMA, CXCL9, GZMB, GZMA, IFNG, PRF1, TBX2, and TNF as immunological activity-related signatures. The majority of immunological checkpoints and immunoreactive-related markers were found to be significantly overexpressed in the group with poor ferroptosis scores (Figure 8C).

In the process of DNA replication, the base mismatch loses its repair function and causes accumulation, which causes microsatellite instability (MSI), thus increasing the risk of tumor occurrence. Pabolizumab has been approved for use in MSI-H/dMMR solid tumors. This is also the first drug approved by the Food and Drug Administration (FDA) based on molecular markers rather than tumor tissue sources. Therefore, the changes in MSI-H/dMMR status and related molecules in tumor patients have important implications. We evaluated the MSI MANTIS score and microsatellite instability sensor (MSIsensor) score among the ferroptosis scoring groups (p<0.01; Figures 8D, E). The MSI MANTIS score has a positive correlation with the probability of MSI-H status (66, 67), and MSIsensor is an effective tool to obtain MSI status from standard tumor normal paired sequence data (68). Not surprisingly, both MSI scores were e higher in the low ferroptosis score group.

The Tumor Immune Dysfunction and Exclusion (TIDE) algorithm was used to evaluate the TCGA-LIHC cohort. The TIDE score of the high ferroptosis group was significantly higher than that of the low ferroptosis group, and the ferroptosis score of the ICIs-response group was significantly lower than that of the non-response group (p<0.01; Figures 8F, G). Together, this evidence

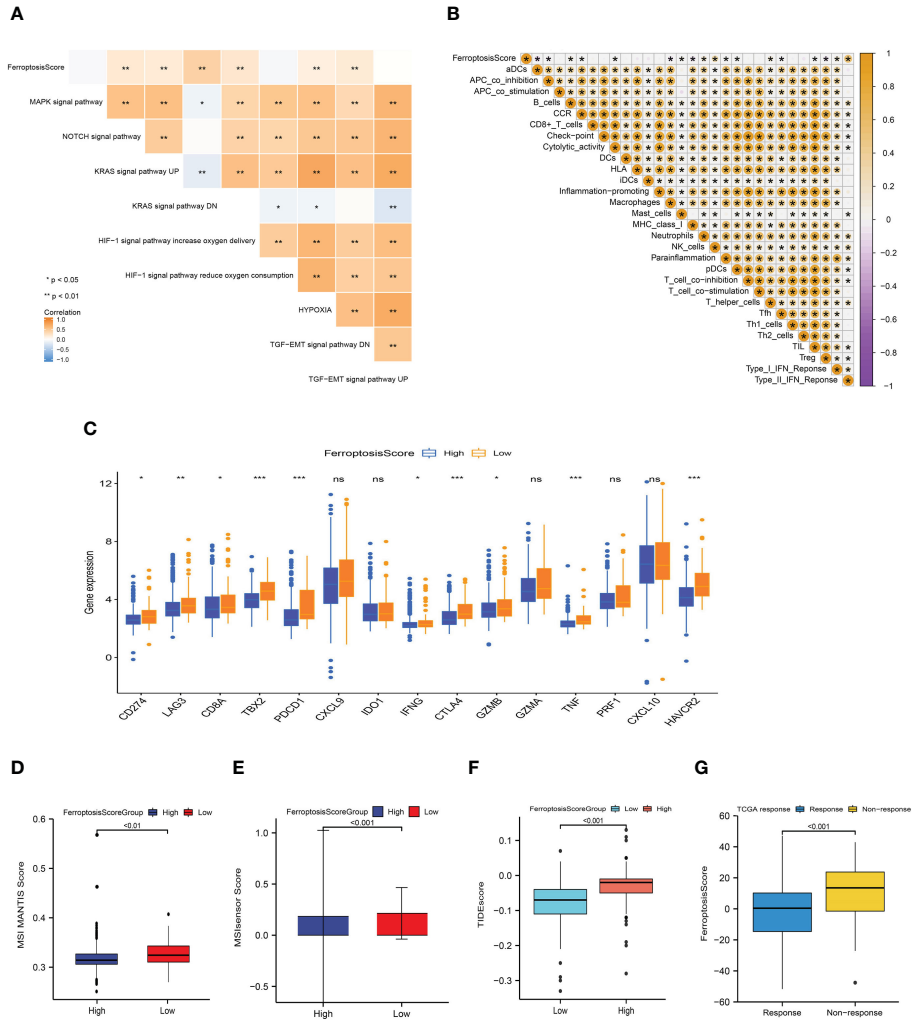

FIGURE 8
Ferroptosis score correlated with immunotherapy efficacy and response to immunotherapy. **(A, B)** Heat maps of the correlation between ferroptosis score and carcinogenic related signaling pathways **(A)** and immune cell infiltration **(B)**. *p<0.05; **p<0.01; ***p<0.001. **(C)** Box plot depicting the differences between the ferroptosis score groups in the relative expression of checkpoints. ns: not significant; *p<0.05; **p<0.01; ***p<0.001. **(D, E)** Differences between ferroptosis score groups and MSI MANTIS score **(D)** and MSIsensor score **(E)**. **(F)** Box plot depicting the differences between the ferroptosis score groups in the TIDE score. **(G)** Box plot depicting the differences of ferroptosis score between the immunotherapy response groups.

strongly supports the effect of ferroptosis scores in predicting immunotherapy outcomes.

3.11 Differences in chemotherapy drug sensitivity between ferroptosis score groups

We examined the relationship between the ferroptosis score and the half-maximum inhibitory concentration (IC_{50}) of chemotherapy drugs. Many drugs, including 5-fluorouracil, Dasatinib, Gemcitabine, and a variety of receptor tyrosine kinases (RTK), were significantly associated with the ferroptosis score. Compared with the low ferroptosis score group, the high ferroptosis score group has a higher estimated value of IC_{50} (Figure 9). The relationship between ferroptosis score and the semi-maximum inhibitory concentration (IC_{50}) of other chemotherapy drugs were shown in the Supplementary Figure 2. In conclusion, the high ferroptosis score indicates that HCC patients were more sensitive to these therapeutic drugs.

4 Discussion

In recent years, with the tremendous advancement of ICIs monotherapy in the treatment of solid tumors, clinical researchers have conducted extensive research into hepatocellular carcinoma. In 2017, Nivolumab was approved by the FDA to treat Sorafenib treated HCC patients, and became the first immunotherapy drug approved for advanced HCC (2). But the subsequent Checkmate-459 did not meet the primary endpoint, implying that PD-1 inhibitors are effective in hepatocellular carcinoma, but the single-agent efficacy of PD-1 inhibitors still does not fulfill therapeutic needs (69). Subsequently, the combination of PD-L1 inhibitor (Atelizumab) and Bevacizumab ("T+A" scheme for short) in the phase III clinical trial (IMbrave150) for the treatment of advanced hepatocellular carcinoma significantly improved the survival period and quality of life of patients (4, 70, 71). Consequently, with the diversification of systematic treatment schemes for advanced hepatocellular carcinoma, how to accurately select multi-target inhibitors and appropriate immunotherapy schemes has emerged as a hot research topic. Therefore, the key to the treatment of advanced liver cancer in the future is to subdivide patients and find personalized, highly effective, and minimally invasive whole-course treatment strategies to improve long-term survival. Exploring the biomarkers of immunotherapy and molecular targeted therapy based on molecular typing can accurately screen patients who will benefit from immunotherapy and predict the efficacy and prognosis of drugs.

In this study, we identified 32 FRGs that displayed differential expression and a significant correlation with survival in HCC tissues and nearby non-tumor tissues. These FRGs play a vital role in the occurrence, proliferation, metastasis, and even drug resistance of malignant tumors. Then we screened three hub genes (HRAS, SLC7A11, and SLC2A1). We discovered that the high expression of the three hub genes predicted a poor prognosis for patients with liver cancer through the survival analysis of the TCGA cohort, GEO cohort, and the validation cohort of the Affiliated Hospital of Qingdao University. And consistent conclusions were obtained in pan-cancer analysis. Consequently, we identified three molecular subtypes of ferroptosis based on the mRNA expression profiles of FRGs. These three subtypes differ significantly in terms of prognosis, molecular function, immune infiltration microenvironment, and response to immunotherapy. The findings demonstrated a considerable enrichment of NK cell and type II interferon (IFN-γ) response, as well as a particularly pronounced survival advantage for ferroptosis cluster A. It has been proved that NK cells directly kill tumor cells through cytolytic granules and act synergistically with other immune cells through proinflammatory cytokines and chemokines, which is closely related to the prognosis of cancer patients (72–74). At the same time, ferroptosis cluster B was considerably abundant in Tregs and other immunosuppressive cells. Several hypoxia-related and EMT-related signaling pathways (including the TGF-β, MAPK, and KRAS signaling pathways) were also substantially expressed in ferroptosis cluster B. These mechanisms are thought to inhibit T lymphocytes.

The transcriptome differentially expressed genes (DEGs) among different ferroptosis molecular subtypes were particularly enriched for biological processes related to energy metabolism, proliferation, DNA repair, and immune activation. Based on these DEGs, which are considered the characteristic genes related to ferroptosis subtypes, we identified three gene clusters. We found that the ferroptosis-associated genomic patterns almost overlap with the ferroptosis molecular patterns. This implied that there were specific molecular patterns of ferroptosis in HCC. Therefore, a comprehensive assessment of the molecular patterns of ferroptosis is essential to gain insight into HCC. Considering the heterogeneity of HCC, we evaluated each patient ferroptosis molecular patterns by PCA, established ferroptosis scores, and divided HCC patients into groups with high and low ferroptosis scores. Ferroptosis cluster B and gene cluster B had the lowest survival rate and the lowest ferroptosis score, suggesting that a low ferroptosis score may predict unfavorable survival. By combining ferroptosis scores with other independent clinical risk variables, we constructed prognostic multivariate regression models. When compared to other clinical traits, the ferroptosis score contributes the greatest risk factors and has a good prediction efficiency for the outcome of HCC patients. Further investigation into the association between ferroptosis score and clinical characteristics of hepatocellular carcinoma revealed that low ferroptosis score group was significantly related to the features of patients with poor prognosis (such as increased AFP, advanced stage, and poor differentiation). As a result, it was proven that the ferroptosis score was a reliable index for evaluating patient survival.

The prevalence of obesity has reached epidemic proportions and has increased dramatically in recent decades. In addition to causing metabolic and cardiovascular diseases, obesity is also an established risk factor for several gastrointestinal cancers and is strongly associated with pancreatic and liver cancers in particular (75). Therefore, the hepatic molecular mechanisms involving

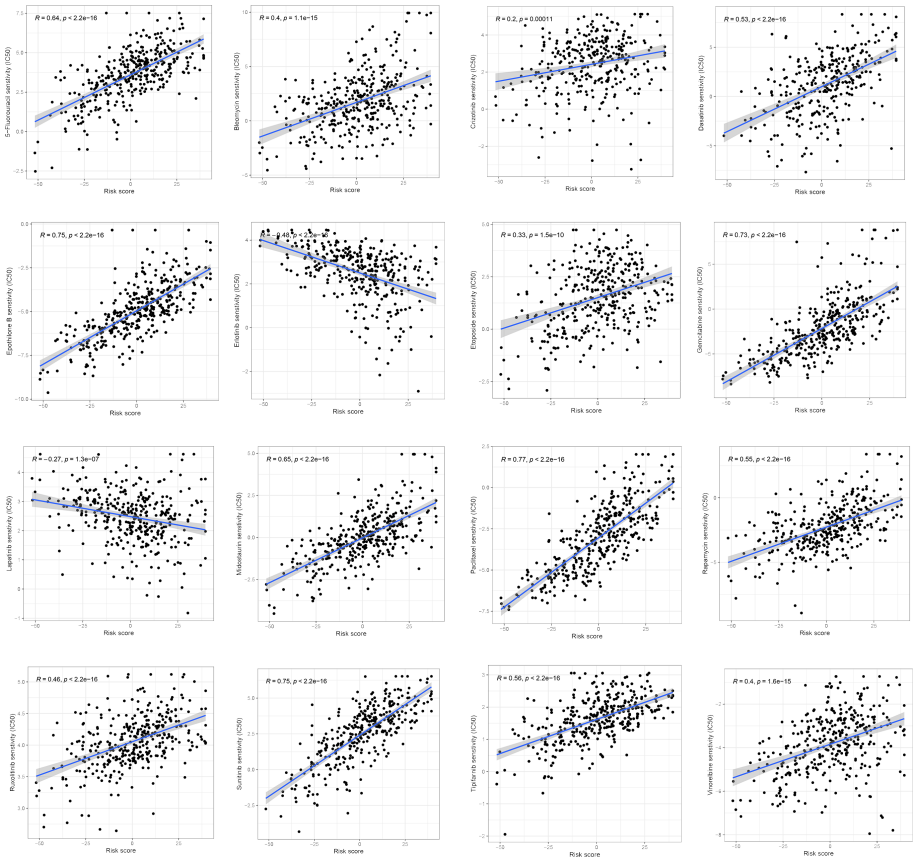

FIGURE 9
Correlation of ferroptosis scores with chemotherapeutic drug sensitivity.

obesity and NAFLD induced hepatocarcinogenesis and potential early markers of HCC are being extensively studied (76). Body mass index (BMI) is a commonly used international standard to measure the degree of obesity and health (77). We investigated the difference in BMI between ferroptosis score groups in patients with hepatocellular carcinoma. The results showed that there was a positive correlation between ferroptosis score and BMI. It has been found that obesity is closely related to the disturbance of iron metabolism, mainly characterized by high ferritin levels (78). Ferroptosis caused by iron accumulation is accompanied by elevated ROS, decreased GSH and inflammatory reactions, insulin resistance and mitochondrial dysfunction, leading to metabolic disorders and the development of obesity (79–81). In terms of immunity, obesity may lead to ferroptosis in Tregs and B1 cells by reducing the levels of NRF2, GPX4 and GCH1 (80, 82). In our previous study, biological processes such as fatty acid and glucose metabolism were also enriched in ferroptosis cluster A. Therefore, it is reasonable to speculate that the occurrence or development mechanism of this subset of HCC patients is related to metabolism.

Several studies have shown that HCC subtypes with poor prognosis may arise from hepatic progenitor cells. The diverse cell origins of HCC may play an important role in the heterogeneous course of HCC. Therefore, we also explored the link between ferroptosis scoring systems and previously developed molecular models. These molecular models focus on the exploration of the tissue origin of HCC and the mechanism between molecular and clinical pathology and clinical behavior. We discovered that the low ferroptosis score group was closely connected to hepatic stem cell origin subtype (CCL subtype, HB16 cluster 2, SOH subtype, HS subtype, and NCIP cluster A) and early recurrence subtype (RS65, SNUR). These subtypes are characterized by a high degree of malignancy, an abundance of hepatic progenitor cell markers (such as cytokeratin 19 and Ep-CAM), a low level of differentiation, increased vascular invasion, and satellite lesions (known risk factors for early recurrence).

Jiang et al. discovered that p53 may inhibit Cys absorption and trigger ferroptosis by preventing SLC7A11 gene expression, thereby inhibiting the growth of tumor cells (83). Woo et al. constructed the p53 signature to evaluate the expression functional status of p53 and found that it was significantly associated with reduced OS. Tumors with low p53 expression were significantly associated with increased copy number instability, increased pathological grading, decreased expression of marker genes in mature hepatocytes, increased risk of tumor recurrence (53, 84, 85). All of these results confirm that the formation of cancers with invasive characteristics is significantly influenced by TP53. In our study, TP53 mutations and p53 signatures were evaluated to determine the functional status and activity of p53. We found that p53 signatures were significantly reduced in the low ferroptosis score group, consistent with the conclusions of Woo et al.

As the main components of tumor microenvironment, immune cells and stromal cells play a crucial role in the regulation of tumor genesis and development. Additionally, immune cell phenotypic and function will be directly impacted by ferroptosis. Our study found that the immune exhaustion subtypes characterized by low ferroptosis score have significant tumor promoting signals (such as activated stroma, T cell exhaustion and immunosuppressive components). Immune dysfunction may be caused by immunosuppressive cells (such as Tregs). The overexpression of immune checkpoint molecules (PD-1, PD-L1, CTLA4, LAG3, and TIM3) in the low ferroptosis score group also indicated T cell exhaustion.

At present, there is no recognized biomarker to accurately predict the efficacy of immunotherapy for HCC. PD-L1 expression, TMB, MSI are the most commonly used indicators to predict the efficacy of ICIs, but their predictive value in HCC lacks the support of high-level clinical evidence (6). The pan-cancer study by Yarchoan et al. demonstrated that patients with high PD-L1 expression and TMB at the same time had the best ICIs efficacy (86). If the PD-L1 level reflects the degree of immune escape from the tumor, TMB represents the immunogenicity of the tumor itself. These are two different dimensions of whether immunotherapy is working. TMB has been found to be inversely associated with survival outcomes in HCC patients, but patients with higher TMB are more likely to respond to checkpoint therapy (87). In contrast to patients with microsatellite instability-low (MSI-L) cancers, those with MSI-high (MSI-H) tumors had a higher response rate to ICIs (88). Therefore, we comprehensively evaluated the immune checkpoint expression, TMB and MSI in HCC patients. We found that there were significant statistical differences among the three indicators in different ferroptosis score groups. Low ferroptosis score was associated with better immunotherapeutic response in all three indicators. Our study also showed that the ferroptosis score combined with TMB could further improve the survival prediction of patients. Additionally, the TIDE score was applied to the TCGA cohort to forecast immunotherapy, which again verified the predictive value of the ferroptosis score for immunotherapy response. According to our analysis of drug sensitivity, the half maximal inhibitory concentration (IC_{50}) of several drugs, including 5-fluorouracil, Dasatinib, Gemcitabine, and a variety of receptor tyrosine kinases (RTK), showed a significant positive correlation with the ferroptosis score. The ferroptosis scoring system can stratify patients, screen sensitive patients, and find new methods to overcome the problems related to chemotherapy resistance. These drug sensitivity analyses provide a potential direction for future treatment work.

Overall, our study has a comprehensive exploration of predictive efficacy, clinical characteristics linkage, immune microenvironment, and immunotherapy. We believe that rigorous multifaceted validation analysis will help improve our understanding of this field. However, due to limited time and experimental conditions, there are some unavoidable flaws in our research that cannot be avoided. The specific molecular and biological regulation mechanism of ferroptosis affecting the prognosis of hepatocellular carcinoma has not been verified by experiments. It is hoped that in future studies, we will be able to determine the role of ferroptosis and its related pathways in the development and progression of hepatocellular carcinoma and clarify its signaling mechanisms, which will ultimately help clinicians evaluate the prognosis of hepatocellular carcinoma in order to guide patients to better receive individualized treatment and select appropriate drugs. We hope these studies can provide some valuable clues for future scientific research and clinical practice.

5 Conclusions

In this study, we systematically evaluated the ferroptosis molecular patterns in HCC. In order to quantify the ferroptosis status of each patient, we also developed an ferroptosis score. The results showed that ferroptosis score plays a non-negligible role in evaluating the origin of tumor tissue, TME landscape, survival prognosis and predicting the effect of immunotherapy. These results suggested that ferroptosis score might serve as a basis for molecular classification of HCC in order to develop effective targeted therapies and scientifically designed clinical trials.

Data availability statement

The original contributions presented in the study are included in the article/Supplementary material. Further inquiries can be directed to the corresponding author.

Ethics statement

The studies involving human participants were reviewed and approved by Institutional Review Board of The Affiliated Hospital of Qingdao University. The patients/participants provided their written informed consent to participate in this study.

Author contributions

Administrative support (JZ), study conception and design (XX), provision of study materials and patients (FY), data collection and assembly (YM), data analysis and interpretation, manuscript writing, final approval of the manuscript (XX, JZ, MJ, XZ). All authors contributed to the article and approved the submitted version.

Funding

Funding for this research was provided by the Qingdao Key Discipline Foundation; Shandong Health Science and technology development foundation (202102040497).

Conflict of interest

The authors declare that the research was conducted in the absence of any commercial or financial relationships that could be construed as a potential conflict of interest.

Publisher's note

All claims expressed in this article are solely those of the authors and do not necessarily represent those of their affiliated organizations, or those of the publisher, the editors and the reviewers. Any product that may be evaluated in this article, or claim that may be made by its manufacturer, is not guaranteed or endorsed by the publisher.

Supplementary material

The Supplementary Material for this article can be found online at: https://www.frontiersin.org/articles/10.3389/fonc.2023.1145380/full#supplementary-material

References

1. Sung H, Ferlay J, Siegel RL, Laversanne M, Soerjomataram I, Jemal A, et al. Global cancer statistics 2020: Globocan estimates of incidence and mortality worldwide for 36 cancers in 185 countries. *CA Cancer J Clin* (2021) 71(3):209–49. doi: 10.3322/caac.21660

2. El-Khoueiry AB, Sangro B, Yau T, Crocenzi TS, Kudo M, Hsu C, et al. Nivolumab in patients with advanced hepatocellular carcinoma (Checkmate 040): An open-label, non-comparative, phase 1/2 dose escalation and expansion trial. *Lancet* (2017) 389 (10088):2492–502. doi: 10.1016/s0140-6736(17)31046-2

3. Sharma P, Siddiqui BA, Anandhan S, Yadav SS, Subudhi SK, Gao J, et al. The next decade of immune checkpoint therapy. *Cancer Discovery* (2021) 11(4):838–57. doi: 10.1158/2159-8290.Cd-20-1680

4. Finn RS, Qin S, Ikeda M, Galle PR, Ducreux M, Kim TY, et al. Atezolizumab plus bevacizumab in unresectable hepatocellular carcinoma. *N Engl J Med* (2020) 382 (20):1894–905. doi: 10.1056/NEJMoa1915745

5. Nishida N, Kudo M. Immune checkpoint blockade for the treatment of human hepatocellular carcinoma. *Hepatol Res* (2018) 48(8):622–34. doi: 10.1111/hepr.13191

6. Cheng AL, Hsu C, Chan SL, Choo SP, Kudo M. Challenges of combination therapy with immune checkpoint inhibitors for hepatocellular carcinoma. *J Hepatol* (2020) 72(2):307–19. doi: 10.1016/j.jhep.2019.09.025

7. Woo HG, Lee JH, Yoon JH, Kim CY, Lee HS, Jang JJ, et al. Identification of a cholangiocarcinoma-like gene expression trait in hepatocellular carcinoma. *Cancer Res* (2010) 70(8):3034–41. doi: 10.1158/0008-5472.Can-09-2823

8. Cairo S, Armengol C, De Reyniès A, Wei Y, Thomas E, Renard CA, et al. Hepatic stem-like phenotype and interplay of Wnt/Beta-catenin and myc signaling in aggressive childhood liver cancer. *Cancer Cell* (2008) 14(6):471–84. doi: 10.1016/j.ccr.2008.11.002

9. Lee JS, Chu IS, Heo J, Calvisi DF, Sun Z, Roskams T, et al. Classification and prediction of survival in hepatocellular carcinoma by gene expression profiling. *Hepatology* (2004) 40(3):667–76. doi: 10.1002/hep.20375

10. Lee JS, Heo J, Libbrecht L, Chu IS, Kaposi-Novak P, Calvisi DF, et al. A novel prognostic subtype of human hepatocellular carcinoma derived from hepatic progenitor cells. *Nat Med* (2006) 12(4):410–6. doi: 10.1038/nm1377

11. Borger DR, Tanabe KK, Fan KC, Lopez HU, Fantin VR, Straley KS, et al. Frequent mutation of isocitrate dehydrogenase (Idh)1 and Idh2 in cholangiocarcinoma identified through broad-based tumor genotyping. *Oncologist* (2012) 17(1):72–9. doi: 10.1634/theoncologist.2011-0386

12. Woo HG, Park ES, Cheon JH, Kim JH, Lee JS, Park BJ, et al. Gene expression-based recurrence prediction of hepatitis b virus-related human hepatocellular carcinoma. *Clin Cancer Res* (2008) 14(7):2056–64. doi: 10.1158/1078-0432.Ccr-07-1473

13. Sohn BH, Shim JJ, Kim SB, Jang KY, Kim SM, Kim JH, et al. Inactivation of hippo pathway is significantly associated with poor prognosis in hepatocellular carcinoma. *Clin Cancer Res* (2016) 22(5):1256–64. doi: 10.1158/1078-0432.Ccr-15-1447

14. Hoshida Y, Nijman SM, Kobayashi M, Chan JA, Brunet JP, Chiang DY, et al. Integrative transcriptome analysis reveals common molecular subclasses of human hepatocellular carcinoma. *Cancer Res* (2009) 69(18):7385–92. doi: 10.1158/0008-5472.Can-09-1089

15. Chen X, Li J, Kang R, Klionsky DJ, Tang D. Ferroptosis: Machinery and regulation. *Autophagy* (2021) 17(9):2054–81. doi: 10.1080/15548627.2020.1810918

16. Jiang X, Stockwell B, Conrad M. Ferroptosis: Mechanisms, biology and role in disease. *Nat Rev Mol Cell Biol* (2021) 22(4):266–82. doi: 10.1038/s41580-020-00324-8

17. Stockwell B, Friedmann Angeli J, Bayir H, Bush A, Conrad M, Dixon S, et al. Ferroptosis: A regulated cell death nexus linking metabolism, redox biology, and disease. *Cell* (2017) 171(2):273–85. doi: 10.1016/j.cell.2017.09.021

18. Hassannia B, Vandenabeele P, Vanden Berghe T. Targeting ferroptosis to iron out cancer. *Cancer Cell* (2019) 35(6):830–49. doi: 10.1016/j.ccell.2019.04.002

19. Guo J, Xu B, Han Q, Zhou H, Xia Y, Gong C, et al. Ferroptosis: A novel anti-tumor action for cisplatin. *Cancer Res Treat* (2018) 50(2):445–60. doi: 10.4143/crt.2016.572

20. Lang X, Green MD, Wang W, Yu J, Choi JE, Jiang L, et al. Radiotherapy and immunotherapy promote tumoral lipid oxidation and ferroptosis *Via* synergistic repression of Slc7a11. *Cancer Discovery* (2019) 9(12):1673–85. doi: 10.1158/2159-8290.Cd-19-0338

21. Wang W, Green M, Choi JE, Gijón M, Kennedy PD, Johnson JK, et al. Cd8(+) T cells regulate tumour ferroptosis during cancer immunotherapy. *Nature* (2019) 569 (7755):270–4. doi: 10.1038/s41586-019-1170-y

22. Zitvogel L, Kroemer G. Interferon-Γ induces cancer cell ferroptosis. *Cell Res* (2019) 29(9):692–3. doi: 10.1038/s41422-019-0186-z

23. Zhang T, Sun B, Zhong C, Xu K, Wang Z, Hofman P, et al. Targeting histone deacetylase enhances the therapeutic effect of erastin-induced ferroptosis in egfr-activating mutant lung adenocarcinoma. *Transl Lung Cancer Res* (2021) 10(4):1857–72. doi: 10.21037/tlcr-21-303

24. Jiang Z, Lim SO, Yan M, Hsu JL, Yao J, Wei Y, et al. Tyro3 induces anti-Pd-1/Pd-L1 therapy resistance by limiting innate immunity and tumoral ferroptosis. *J Clin Invest* (2021) 131(8). doi: 10.1172/jci139434

25. Li J, Lama R, Galster SL, Inigo JR, Wu J, Chandra D, et al. Small-molecule Mmri62 induces ferroptosis and inhibits metastasis in pancreatic cancer *Via* degradation of ferritin heavy chain and mutant P53. *Mol Cancer Ther* (2022) 21 (4):535–45. doi: 10.1158/1535-7163.Mct-21-0728

26. Liang C, Zhang X, Yang M, Dong X. Recent progress in ferroptosis inducers for cancer therapy. *Adv Mater* (2019) 31(51):e1904197. doi: 10.1002/adma.201904197

27. Wu C, Liu Z, Chen Z, Xu D, Chen L, Lin H, et al. A nonferrous ferroptosis-like strategy for antioxidant inhibition-synergized nanocatalytic tumor therapeutics. *Sci Adv* (2021) 7(39):eabj8833. doi: 10.1126/sciadv.abj8833

28. Stockwell BR. Ferroptosis turns 10: Emerging mechanisms, physiological functions, and therapeutic applications. *Cell* (2022) 185(14):2401–21. doi: 10.1016/j.cell.2022.06.003

29. Zhang C, Liu X, Jin S, Chen Y, Guo R. Ferroptosis in cancer therapy: A novel approach to reversing drug resistance. *Mol Cancer* (2022) 21(1):47. doi: 10.1186/s12943-022-01530-y

30. Zhang Y, Zhang Z. The history and advances in cancer immunotherapy: Understanding the characteristics of tumor-infiltrating immune cells and their therapeutic implications. *Cell Mol Immunol* (2020) 17(8):807–21. doi: 10.1038/s41423-020-0488-6

31. Sas Z, Cendrowicz E, Weinhäuser I, Rygiel TP. Tumor microenvironment of hepatocellular carcinoma: Challenges and opportunities for new treatment options. *Int J Mol Sci* (2022) 23(7). doi: 10.3390/ijms23073778

32. Chen Y, Pei Y, Luo J, Huang Z, Yu J, Meng X. Looking for the optimal pd-1/Pd-L1 inhibitor in cancer treatment: A comparison in basic structure, function, and clinical practice. *Front Immunol* (2020) 11:1088. doi: 10.3389/fimmu.2020.01088

33. Casak SJ, Donoghue M, Fashoyin-Aje L, Jiang X, Rodriguez L, Shen YL, et al. Fda approval summary: Atezolizumab plus bevacizumab for the treatment of patients with advanced unresectable or metastatic hepatocellular carcinoma. *Clin Cancer Res* (2021) 27(7):1836–41. doi: 10.1158/1078-0432.Ccr-20-3407

34. Qin S, Xu L, Yi M, Yu S, Wu K, Luo S. Novel immune checkpoint targets: Moving beyond pd-1 and ctla-4. *Mol Cancer* (2019) 18(1):155. doi: 10.1186/s12943-019-1091-2

35. Brudno JN, Kochenderfer JN. Recent advances in car T-cell toxicity: Mechanisms, manifestations and management. *Blood Rev* (2019) 34:45–55. doi: 10.1016/j.blre.2018.11.002

36. Guo J, Tang Q. Recent updates on chimeric antigen receptor T cell therapy for hepatocellular carcinoma. *Cancer Gene Ther* (2021) 28(10-11):1075–87. doi: 10.1038/s41417-020-00259-4

37. Cai XY, Wang JX, Yi Y, He HW, Ni XC, Zhou J, et al. Low counts of Γδ T cells in peritumoral liver tissue are related to more frequent recurrence in patients with hepatocellular carcinoma after curative resection. *Asian Pac J Cancer Prev* (2014) 15 (2):775–80. doi: 10.7314/apjcp.2014.15.2.775

38. Zhang T, Chen J, Niu L, Liu Y, Ye G, Jiang M, et al. Clinical safety and efficacy of locoregional therapy combined with adoptive transfer of allogeneic Γδ T cells for advanced hepatocellular carcinoma and intrahepatic cholangiocarcinoma. *J Vasc Interv Radiol* (2022) 33(1):19–27.e3. doi: 10.1016/j.jvir.2021.09.012

39. Fuchs BC, Fujii T, Dorfman JD, Goodwin JM, Zhu AX, Lanuti M, et al. Epithelial-to-Mesenchymal transition and integrin-linked kinase mediate sensitivity to epidermal growth factor receptor inhibition in human hepatoma cells. *Cancer Res* (2008) 68(7):2391–9. doi: 10.1158/0008-5472.Can-07-2460

40. McConkey DJ, Choi W, Marquis L, Martin F, Williams MB, Shah J, et al. Role of epithelial-to-Mesenchymal transition (Emt) in drug sensitivity and metastasis in bladder cancer. *Cancer Metastasis Rev* (2009) 28(3-4):335–44. doi: 10.1007/s10555-009-9194-7

41. Saxena M, Stephens MA, Pathak H, Rangarajan A. Transcription factors that mediate epithelial-mesenchymal transition lead to multidrug resistance by upregulating abc transporters. *Cell Death Dis* (2011) 2(7):e179. doi: 10.1038/cddis.2011.61

42. Foroutan M, Cursons J, Hediyeh-Zadeh S, Thompson EW, Davis MJ. A. Transcriptional program for detecting tgfβ-induced emt in cancer. *Mol Cancer Res* (2017) 15(5):619–31. doi: 10.1158/1541-7786.Mcr-16-0313

43. Xu Z, Feng J, Li Y, Guan D, Chen H, Zhai X, et al. The vicious cycle between ferritinophagy and ros production triggered emt inhibition of gastric cancer cells was through P53/Akt/Mtor pathway. *Chem Biol Interact* (2020) 328:109196. doi: 10.1016/j.cbi.2020.109196

44. Yuan X, Wu H, Han N, Xu H, Chu Q, Yu S, et al. Notch signaling and emt in non-small cell lung cancer: Biological significance and therapeutic application. *J Hematol Oncol* (2014) 7:87. doi: 10.1186/s13045-014-0087-z

45. Damrauer JS, Hoadley KA, Chism DD, Fan C, Tiganelli CJ, Wobker SE, et al. Intrinsic subtypes of high-grade bladder cancer reflect the hallmarks of breast cancer biology. *Proc Natl Acad Sci U.S.A.* (2014) 111(8):3110–5. doi: 10.1073/pnas.1318376111

46. Hedegaard J, Lamy P, Nordentoft I, Algaba F, Høyer S, Ulhøi BP, et al. Comprehensive transcriptional analysis of early-stage urothelial carcinoma. *Cancer Cell* (2016) 30(1):27–42. doi: 10.1016/j.ccell.2016.05.004

47. Hugo W, Zaretsky JM, Sun L, Song C, Moreno BH, Hu-Lieskovan S, et al. Genomic and transcriptomic features of response to anti-Pd-1 therapy in metastatic melanoma. *Cell* (2016) 165(1):35–44. doi: 10.1016/j.cell.2016.02.065

48. Sjödahl G, Lauss M, Lövgren K, Chebil G, Gudjonsson S, Veerla S, et al. A molecular taxonomy for urothelial carcinoma. *Clin Cancer Res* (2012) 18(12):3377–86. doi: 10.1158/1078-0432.Ccr-12-0077-t

49. Spranger S, Bao R, Gajewski TF. Melanoma-intrinsic B-catenin signalling prevents anti-tumour immunity. *Nature* (2015) 523(7559):231–5. doi: 10.1038/nature14404

50. Mariathasan S, Turley SJ, Nickles D, Castiglioni A, Yuen K, Wang Y, et al. Tgfβ attenuates tumour response to pd-L1 blockade by contributing to exclusion of T cells. *Nature* (2018) 554(7693):544–8. doi: 10.1038/nature25501

51. Viswanathan VS, Ryan MJ, Dhruv HD, Gill S, Eichhoff OM, Seashore-Ludlow B, et al. Dependency of a therapy-resistant state of cancer cells on a lipid peroxidase pathway. *Nature* (2017) 547(7664):453–7. doi: 10.1038/nature23007

52. Lei G, Zhuang L, Gan B. Targeting ferroptosis as a vulnerability in cancer. *Nat Rev Cancer* (2022) 22(7):381–96. doi: 10.1038/s41568-022-00459-0

53. Cancer Genome Atlas Research Network. Comprehensive and integrative genomic characterization of hepatocellular carcinoma. *Cell* (2017) 169(7):1327–41.e23. doi: 10.1016/j.cell.2017.05.046

54. Zhou N, Bao J. Ferrdb: A manually curated resource for regulators and markers of ferroptosis and ferroptosis-disease associations. *Database (Oxford)* (2020) 2020: baaa021. doi: 10.1093/database/baaa021

55. Colaprico A, Silva TC, Olsen C, Garofano L, Cava C, Garolini D, et al. Tcgabiolinks: An R/Bioconductor package for integrative analysis of tcga data. *Nucleic Acids Res* (2016) 44(8):e71. doi: 10.1093/nar/gkv1507

56. Ritchie ME, Phipson B, Wu D, Hu Y, Law CW, Shi W, et al. Limma powers differential expression analyses for rna-sequencing and microarray studies. *Nucleic Acids Res* (2015) 43(7):e47. doi: 10.1093/nar/gkv007

57. Wilkerson MD, Hayes DN. Consensusclusterplus: A class discovery tool with confidence assessments and item tracking. *Bioinformatics* (2010) 26(12):1572–3. doi: 10.1093/bioinformatics/btq170

58. Bindea G, Mlecnik B, Tosolini M, Kirilovsky A, Waldner M, Obenauf AC, et al. Spatiotemporal dynamics of intratumoral immune cells reveal the immune landscape in human cancer. *Immunity* (2013) 39(4):782–95. doi: 10.1016/j.immuni.2013.10.003

59. Sotiriou C, Wirapati P, Loi S, Harris A, Fox S, Smeds J, et al. Gene expression profiling in breast cancer: Understanding the molecular basis of histologic grade to improve prognosis. *J Natl Cancer Inst* (2006) 98(4):262–72. doi: 10.1093/jnci/djj052

60. Zhang X, Shi M, Chen T, Zhang B. Characterization of the immune cell infiltration landscape in head and neck squamous cell carcinoma to aid immunotherapy. *Mol Ther Nucleic Acids* (2020) 22:298–309. doi: 10.1016/j.omtn.2020.08.030

61. Mayakonda A, Lin DC, Assenov Y, Plass C, Koeffler HP. Maftools: Efficient and comprehensive analysis of somatic variants in cancer. *Genome Res* (2018) 28(11):1747–56. doi: 10.1101/gr.239244.118

62. Kim ST, Cristescu R, Bass AJ, Kim KM, Odegaard JI, Kim K, et al. Comprehensive molecular characterization of clinical responses to pd-1 inhibition in metastatic gastric cancer. *Nat Med* (2018) 24(9):1449–58. doi: 10.1038/s41591-018-0101-z

63. Yang W, Soares J, Greninger P, Edelman EJ, Lightfoot H, Forbes S, et al. Genomics of drug sensitivity in cancer (Gdsc): A resource for therapeutic biomarker discovery in cancer cells. *Nucleic Acids Res* (2013) 41(Database issue):D955–61. doi: 10.1093/nar/gks1111

64. Geeleher P, Cox N, Huang RS. Prrophetic: An r package for prediction of clinical chemotherapeutic response from tumor gene expression levels. *PloS One* (2014) 9(9): e107468. doi: 10.1371/journal.pone.0107468

65. Buffa FM, Harris AL, West CM, Miller CJ. Large Meta-analysis of multiple cancers reveals a common, compact and highly prognostic hypoxia metagene. *Br J Cancer* (2010) 102(2):428–35. doi: 10.1038/sj.bjc.6605450

66. Bonneville R, Krook MA, Kautto EA, Miya J, Wing MR, Chen HZ, et al. Landscape of microsatellite instability across 39 cancer types. *JCO Precis Oncol* (2017) 2017:PO.17.00073. doi: 10.1200/po.17.00073

67. Lu M, Zhao B, Liu M, Wu L, Li Y, Zhai Y, et al. Pan-cancer analysis of Setd2 mutation and its association with the efficacy of immunotherapy. *NPJ Precis Oncol* (2021) 5(1):51. doi: 10.1038/s41698-021-00193-0

68. Niu B, Ye K, Zhang Q, Lu C, Xie M, McLellan MD, et al. Msisensor: Microsatellite instability detection using paired tumor-normal sequence data. *Bioinformatics* (2014) 30(7):1015–6. doi: 10.1093/bioinformatics/btt755

69. Yau T, Park JW, Finn RS, Cheng AL, Mathurin P, Edeline J, et al. Nivolumab versus sorafenib in advanced hepatocellular carcinoma (Checkmate 459): A randomised, multicentre, open-label, phase 3 trial. *Lancet Oncol* (2022) 23(1):77–90. doi: 10.1016/s1470-2045(21)00604-5

70. Galle PR, Finn RS, Qin S, Ikeda M, Zhu AX, Kim TY, et al. Patient-reported outcomes with atezolizumab plus bevacizumab versus sorafenib in patients with unresectable hepatocellular carcinoma (Imbrave150): An open-label, randomised, phase 3 trial. *Lancet Oncol* (2021) 22(7):991–1001. doi: 10.1016/s1470-2045(21)00151-0

71. Cheng AL, Qin S, Ikeda M, Galle PR, Ducreux M, Kim TY, et al. Updated efficacy and safety data from Imbrave150: Atezolizumab plus bevacizumab vs. sorafenib for unresectable hepatocellular carcinoma. *J Hepatol* (2022) 76(4):862–73. doi: 10.1016/j.jhep.2021.11.030

72. Pang YL, Zhang HG, Peng JR, Pang XW, Yu S, Xing Q, et al. The immunosuppressive tumor microenvironment in hepatocellular carcinoma. *Cancer Immunol Immunother* (2009) 58(6):877–86. doi: 10.1007/s00262-008-0603-5

73. Chew V, Chen J, Lee D, Loh E, Lee J, Lim KH, et al. Chemokine-driven lymphocyte infiltration: An early intratumoural event determining long-term survival in resectable hepatocellular carcinoma. *Gut* (2012) 61(3):427–38. doi: 10.1136/gutjnl-2011-300509

74. Wada Y, Nakashima O, Kutami R, Yamamoto O, Kojiro M. Clinicopathological study on hepatocellular carcinoma with lymphocytic infiltration. *Hepatology* (1998) 27 (2):407–14. doi: 10.1002/hep.510270214

75. Calle EE, Rodriguez C, Walker-Thurmond K, Thun MJ. Overweight, obesity, and mortality from cancer in a prospectively studied cohort of U.S. adults. *N Engl J Med* (2003) 348(17):1625–38. doi: 10.1056/NEJMoa021423

76. Marengo A, Rosso C, Bugianesi E. Liver cancer: Connections with obesity, fatty liver, and cirrhosis. *Annu Rev Med* (2016) 67:103–17. doi: 10.1146/annurev-med-090514-013832

77. Chooi YC, Ding C, Magkos F. The epidemiology of obesity. *Metabolism* (2019) 92:6–10. doi: 10.1016/j.metabol.2018.09.005

78. González-Domínguez Á, Visiedo-García FM, Domínguez-Riscart J, González-Domínguez R, Mateos RM, Lechuga-Sancho AM. Iron metabolism in obesity and metabolic syndrome. *Int J Mol Sci* (2020) 21(15). doi: 10.3390/ijms21155529

79. Zhang S, Sun Z, Jiang X, Lu Z, Ding L, Li C, et al. Ferroptosis Increases Obesity: Crosstalk between Adipocytes and the Neuroimmune System. *Front Immunol* (2022) 13:1049936. doi: 10.3389/fimmu.2022.1049936

80. Hoy AJ, Nagarajan SR, Butler LM. Tumour fatty acid metabolism in the context of therapy resistance and obesity. *Nat Rev Cancer* (2021) 21(12):753–66. doi: 10.1038/s41568-021-00388-4

81. Zhu J, Thompson CB. Metabolic regulation of cell growth and proliferation. *Nat Rev Mol Cell Biol* (2019) 20(7):436–50. doi: 10.1038/s41580-019-0123-5

82. Zhang S, Sun Z, Jiang X, Lu Z, Ding L, Li C, et al. Ferroptosis increases obesity: Crosstalk between adipocytes and the neuroimmune system. *Front Immunol* (2022) 13:1049936. doi: 10.3389/fimmu.2022.1049936

83. Jiang L, Kon N, Li T, Wang SJ, Su T, Hibshoosh H, et al. Ferroptosis as a P53-mediated activity during tumour suppression. *Nature* (2015) 520(7545):57–62. doi: 10.1038/nature14344

84. Rashid A, Wang JS, Qian GS, Lu BX, Hamilton SR, Groopman JD. Genetic alterations in hepatocellular carcinomas: Association between loss of chromosome 4q and P53 gene mutations. *Br J Cancer* (1999) 80(1-2):59–66. doi: 10.1038/sj.bjc.6690321

85. Donehower LA, Soussi T, Korkut A, Liu Y, Schultz A, Cardenas M, et al. Integrated analysis of Tp53 gene and pathway alterations in the cancer genome atlas. *Cell Rep* (2019) 28(11):3010. doi: 10.1016/j.celrep.2019.08.061

86. Yarchoan M, Albacker LA, Hopkins AC, Montesion M, Murugesan K, Vithayathil TT, et al. Pd-L1 expression and tumor mutational burden are independent biomarkers in most cancers. *JCI Insight* (2019) 4(6). doi: 10.1172/jci.insight.126908

87. Gok Yavuz B, Hasanov E, Lee SS, Mohamed YI, Curran MA, Koay EJ, et al. Current Landscape and Future Directions of Biomarkers for Immunotherapy in Hepatocellular Carcinoma. *J Hepatocell Carcinoma* (2021) 8:1195-207. doi: 10.2147/jhc.S322289

88. Asaoka Y, Ijichi H, Koike K. Pd-1 blockade in tumors with mismatch-repair deficiency. *N Engl J Med* (2015) 373(20):1979. doi: 10.1056/NEJMc1510353

Frontiers in Oncology

Advances knowledge of carcinogenesis and tumor progression for better treatment and management

The third most-cited oncology journal, which highlights research in carcinogenesis and tumor progression, bridging the gap between basic research and applications to imrpove diagnosis, therapeutics and management strategies.

Discover the latest Research Topics

See more →

Frontiers

Avenue du Tribunal-Fédéral 34
1005 Lausanne, Switzerland
frontiersin.org

Contact us

+41 (0)21 510 17 00
frontiersin.org/about/contact